DEVELOPMENT OF A PROCEDURE FOR AUTOMATING THERMAL ZONING FOR BUILDING ENERGY SIMULATION

A Dissertation

by

MINJAE SHIN

Submitted to the Office of Graduate and Professional Studies of
Texas A&M University
in partial fulfillment of the requirements for the degree of

DOCTOR OF PHILOSOPHY

Chair of Committee,	Jeff S. Haberl
Committee Members,	Juan-Carlos Baltazar
	Wei Yan
	Michael B. Pate
Head of Department,	Robert Warden

August 2018

Major Subject: Architecture

ABSTRACT

Although several of today's Building Information Modeling (BIM) tools automatically produce default building thermal zoning in the required Building Energy Simulation (BES) electronic formats, these same models do not provide detailed documentation about how their algorithm(s) work or any guidance about how to create and evaluate the building thermal zones in the BES during the early stages of the design of buildings, relying instead on the user to select the thermal zones. Therefore, there is a need to develop a well-documented, accurate thermal zoning method that can assist designers with their building energy simulation.

The purpose of this study is to develop a method to automatically or semi-automatically divide a commercial building into HVAC thermal zones for a building energy simulation that provides feedback to the user regarding how the resultant zones provide comfortable indoor conditions.

This study accomplishes a number of objectives, which include: 1) development of a new thermal zoning method to automatically, or semi-automatically create a building thermal zone in simulation models; 2) development of a simplified, commercial base-case model based on the information from the NREL commercial building model, "Run 3A" DOE-2 simulation model, and ASHRAE Standard 90.1-2013; 3) parametric studies of different configurations of thermal zones to evaluate several influential parameters on the developed new thermal zoning method.

DEDICATION

To my mother, father, and brother for making me feel special and loved.

ACKNOWLEDGEMENTS

This dissertation was accomplished with the support and encouragement from many people. First of all, I would like to express my sincere gratitude to Prof. Jeff Haberl for guiding me as my committee chair. He has continuously provided me with the necessary guidance with his patience for all the years that I have studied at Texas A&M University, and has supported and encouraged me to accomplish my doctoral study. I would also like to thank Prof. Juan-Carlos Baltazar for his support and encouragement, and Prof. Wei Yan, and Prof. Michael Pate for giving their valuable advice on my dissertation as my committee members.

I would also like to extend my appreciation to all the members at the Energy Systems Laboratory who have supported me during my doctoral studies with funding throughout the Texas Emissions Reduction Program (TERP), and my funding support from the Fort Hood Energy Office.

Finally, I am deeply grateful to my mother, father, and brother. They have always encouraged me to continue and accomplish my goal.

CONTRIBUTORS AND FUNDING SOURCES

This work was supervised by a dissertation committee consisting of Professors Jeff S. Haberl, Juan-Carlos Baltazar, and Wei Yan of the Department of Architecture and Professor Michael B. Pate of the Department of Mechanical Engineering. All work for the dissertation was completed independently by the student.

Graduate study was supported by a Graduate Research Assistantship from Energy Systems Laboratory, which is a branch of Texas A&M Engineering Experiment Station within The Texas A&M University System. In addition, this study was funded by the American Society of Heating, Refrigerating and Air-conditioning Engineers (ASHRAE) Graduate Student Grant-In-Aid, which is a fund allocated to the Research Program for the Society's Fiscal Year 2014-2015.

TABLE OF CONTENTS

Page

LIST OF FIGURES

Page

LIST OF TABLES

Page

CHAPTER I

INTRODUCTION

1.1. Background

Today, it is widely recognized that one of the largest energy consumer sectors worldwide is the buildings sector. In the United States, buildings account for approximately 40% of the nationwide source energy use if one includes the thermal waste from non-renewable electricity generation (DOE 2012). A recent article also showed that energy consumption in buildings, particularly related to Heating, Ventilation and Air-Conditioning (HVAC) systems, is growing significantly. Currently, the HVAC-related energy use represents 50% of building energy consumption and 20% of total energy consumption in the USA (Perez-Lombard et al. 2008).

In the construction sector today it is a conventional practice to provide a final product (i.e., the building) without fully testing the product (Bazjanac 2005). In general, under current practice when the building construction is completed, the building ownership and operation are transferred to the owner after commissioning, sometimes without feedback from the operational performance measurement (Bordass et al. 2001). This can be a critical problem, since there are no perfect systems or products in the building sector. Therefore, there needs to be a quality improvement process and enhancement at the product design stage with constant feedback to the product designers about whether or not the product performs as expected. Consequently, in order to design and produce a higher quality product, feedback from building operational performance

measurement is needed to predict the accuracy of the performance of the building at the design stage. During the building design and construction process, hourly, whole-building energy simulation modeling offers one of the few opportunities to test the performance of a building envelope and HVAC system prior to the completion of the building. Therefore, such building energy performance simulation programs can be useful tools to evaluate building energy performance during the building's life-cycle, both at the design and operation stages (Maile et al. 2007).

Simulating the energy usage of buildings has become a key strategy in designing high performance buildings that can better meet the needs of society. In addition, the automated exchange of data between the architect's design software and the energy consultant's building energy simulation software is an important feature for the future of the building design process. Several leading Computer-Aided Design (CAD) vendors offer Building Information Modeling (BIM) software that they claim is capable of accurately simulating building energy use, even automatically generating the HVAC thermal zones in a proposed design. For instance, one of the commercially available schematic design tools in the building design process, Autodesk Vasari (Autodesk 2013), has a feature that can automatically divide a building geometry into perimeter and core zones at each floor based on the ASHRAE 90.1-2013, Appendix G (ASHRAE 2013). However, Autodesk has not released the details of the zoning algorithm, or provided a discussion of how the procedure works in their software. Therefore, how can HVAC design engineers know if it is accurately representing their designs? Furthermore, the American Society of Heating, Refrigerating and Air-Conditioning Engineers (ASHRAE)

does not provide a complete set of instructions that defines the methods of producing a complete thermal model from printed floor plans, CAD models, or BIM applications, which includes instructions about thermal zoning.

In the literature, there has been significant progress towards the development of integrated design tools motivated by the large software providers who are developing new software or adapting existing software programs (Hetherington et al. 2012). Unfortunately, these new tools still contain simplification when it comes to specifying the inputs for the Building Energy Simulation (BES). ASHRAE Research Project 1468 (Clayton et al. 2012) has made several significant contributions regarding the interoperability from BIM to BES software. To accomplish this the RP-1468 project conducted empirical sensitivity tests of multiple options for different envelope components of the BES models. These tests showed how to solve some difficult modeling problems, for example with curved surfaces and window shading. Based on the results of this project, a conceptual BIM thermal model was able to generate instructions for creating an input file for the BES from the BIM with high accuracy. However, this project did not provide specific advice about building thermal zoning issues, which is an important feature in today's buildings that can have a significant impact on a building's thermal behavior and energy consumption. Although, as previously mentioned several of today's BIM tools automatically produce default building thermal zoning in the required BES electronic formats, these same models do not provide detailed documentation about how their algorithm(s) work or any guidance about how to create and evaluate the building thermal zones in the BES during the early

stages of the design of buildings, relying instead on the user to select the thermal zones. Therefore, there is a need to develop a well-documented, accurate thermal zoning method that can assist designers with their building energy simulation.

1.2. Purpose and Objectives

The purpose of this study is to develop a method to automatically or semi-automatically divided a commercial building into HVAC thermal zones for a building energy simulation that provides feedback to the user regarding how the resultant zones provide comfortable indoor conditions. To achieve the goal of this study, the following objectives are proposed:

1) To investigate and review the relevant literature about the selection of building thermal zoning in terms of building energy simulation looking especially for features, methods or procedures that can be used in the current work;
2) To develop a method to automatically, or semi-automatically create a building thermal zone that provides feedback about comfort conditions;
3) To identify building features that are most likely to have the greatest impact on the results;
4) To demonstrate the method by creating thermal zoning models for a selection of reference buildings using simulations of these models.

1.3. Organization of the Dissertation

The dissertation is organized in six chapters, which include: 1) Introduction, 2) Literature Review; 3) Significance of the Study; 4) Methodology; 5) Results of Parametric Study on Thermal Zoning; and 6) Summary and Future Work.

Chapter I provides the background, purpose and objectives of this research. Chapter II contains the literature review of the previous research and information related to this study, including a review of: building energy simulation tools; definition of building thermal zones; thermal zoning in terms of HVAC design and building energy simulation; and previous studies on building thermal zoning method for building energy simulation. Chapter III discusses the importance of this study as well as the scope and limitations of the research. Chapter IV describes the overall methodology to conduct this study, including: development of thermal zoning method for building energy simulation; tests of the proposed thermal zoning method, development of simplified commercial base-case model; analysis of the application of the new method to a case-study office building, which includes as-built and calibrated simulations. In Chapter V presents the results of the parametric study on thermal zoning. Chapter VI summarizes the results of the study, and proposes recommendations for future study.

CHAPTER II

LITERATURE REVIEW

This chapter examines the previous literature regarding the concept of building thermal zoning in terms of the design, construction, and operation of buildings, with a specific focus on Building Energy Simulation (BES). The literature reviewed includes: building energy simulation tools; thermal zoning in design and simulation; and previous studies about thermal zoning in simulation.

2.1. Building Energy Simulation Tools

During the past four decades, hourly building energy performance simulation tools have been used to predict the peak energy demand and energy consumption of new buildings, which includes the design and proper sizing of the HVAC systems. BES tools have also been used to evaluate energy savings from energy conservation retrofits to existing buildings (Gaasch et al. 2014). These calculations are typically performed based on the physical properties of the building and its mechanical systems, which are exposed to dynamic inputs such as weather, occupancy, lighting and equipment loads (Coakley et al. 2014). In addition, the calculations are generally performed over the course of a full year. The most widely-used tools, including: DOE-2.1e, DOE-2.2/eQUEST, EnergyPlus, and TRNSYS are described below.

2.1.1. DOE-2.1e

DOE-2.1e is a building energy simulation tool that predicts the hourly energy use and energy cost of a building given hourly weather information, a building geometric and HVAC description, and the utility rate structure. DOE-2.1e (LBNL 1993a) is an hourly fixed-schematic, whole-building, energy simulation program that uses one sub-program for the translation of inputs (i.e., the Building Design Language (BDL) Processor) and four simulation sub-programs (LOADS, SYSTEMS, PLANT and ECONOMICS) that execute in sequence to perform the simulation. DOE-2.1e uses: a) the response factor method to calculate the dynamic heat transfer through multi-layered wall, and b) the ASHRAE weighting factor method, for calculating overall heat transfer within each thermal zone (LBNL 1982, 1984, 1993b). DOE-2.1e has been widely used for evaluating the energy performance of buildings, and offers a great capability for simulating a wide range of design features. It has been extensively validated for accuracy and consistency (Judkoff and Neymark 1995; Haberl and Cho 2004).

2.1.2. DOE-2.2/eQUEST

The Quick Energy Simulation Tool (eQUEST) is an easy-to-use building energy simulation program that is based on the DOE-2.2 calculation engine (Hirsch 2015). In contrast to DOE-2.1e, this program provides a Graphical User Interface (GUI) that includes a building creation wizard and Energy Efficiency Measure (EEM) wizard. The building input wizard option enables users to quickly specify building details without the

need for an exclusive knowledge of building energy simulation and the detailed input information. In addition, using the EEM wizard, users are able to quickly walk through the process of evaluating the building energy savings and specific design decisions.

2.1.3. EnergyPlus

This computer program is a new, more advanced whole-building energy simulation tool that incorporates the best features of DOE-2 in a new platform (Crawley et al. 2001; Crawley et al. 2008). EnergyPlus also uses the response factor method for the transient heat transfer through multi-layered walls. In difference to DOE-2 the transient heat conduction through the walls is integrated with a heat balance based zone simulation. The input and output data structures are tailored to facilitate third party interface development. EnergyPlus allows user-specified time steps of less than an hour, and performs load calculations and simulations of the response of the systems and plant at each time step. EnergyPlus provides more accurate space temperature predictions, which is crucial for system and plant sizing, occupant comfort and occupant health calculations (Crawley et al. 2008). It also allows users to evaluate realistic system controls, moisture adsorption and desorption in selected building elements, radiant heating and cooling systems, and inter-zone air flow, photovoltaic systems and fuel cells.

2.1.4. TRNSYS

TRNSYS (TRaNsient SYstem Simulation Program) was developed by the Solar Energy Laboratory at the University of Wisconsin, primarily as a program for simulating

solar thermal systems (Klein 1976), which was later incorporated into general HVAC system simulations. It is a transient system simulation program with a modular structure that allows for the simulation of complex energy systems by configuring and assembling a series of smaller components (Klein et al. 2004). TRNSYS subroutines representing the physical components are combined and solved simultaneously with the building envelope thermal balance and the air network module at each time step. The TRNSYS library includes: components for a multi-zone building models, low-energy buildings, HVAC systems, renewable energy systems, including passive solar, active solar thermal and photovoltaic systems, wind energy, fuel cells and cogeneration, etc. Furthermore, the modular nature of TRNSYS facilitates the addition of new mathematical models to the program (Klein et al. 2010), which cannot be easily incorporated with DOE-2.1e or eQUEST.

2.1.5. Summary of Building Energy Simulation Tools

The four building energy simulation tools reviewed in the previous section represent the most widely-used programs in the building design process, which are used for the optimization of new buildings, and in research. However, there are many other building energy simulation tools that have similar features and capabilities (Crawley et al. 2008; Zhu 2013; Nguyen et al. 2014). Therefore, users need to be careful when considering an appropriate simulation tool to make sure they meet the simulation needs for their purpose.

In this study, the DOE-2.1e program will be used to develop an automated procedure for automated thermal zoning for building energy simulation.

2.2. Building Thermal Zoning

2.2.1. Definition of Building Thermal Zone

In the previous literature, building thermal zones have been called by different names such as thermal zones (ASHRAE 2013), thermal blocks (COMNET 2010), or HVAC zones (COMNET 2010). However, all these different terms indicate the same idea and concept. In ASHRAE Standard 90.1-2013 (ASHRAE 2013, p. 12), an HVAC zone is clearly defined as "a space or group of spaces within a building with heating and cooling requirements that are sufficiently similar so that desired conditions (e.g., temperature) can be maintained throughout using a single sensor (e.g., thermostat or temperature sensor)". To be specific, COMNET (The Commercial Energy Services Network) commercial buildings energy modeling guidelines and procedures (COMNET 2010, pp. 2-2) provides the following definitions of thermal blocks, and HVAC zones:

- An HVAC zone is "…a physical space within the building that has its own thermostat and zonal HVAC system for maintaining thermal comfort." (COMNET 2010, pp. 2-2). HVAC zones are usually identified on the HVAC plans for a new building. An HVAC zone should not be split between different thermal blocks. However, a thermal block may include more than one HVAC zone.

- A thermal block is "…a space or collection of spaces within a building having sufficiently similar space-conditioning requirements so that those conditions could be maintained with a single thermal controlling device such as a thermostat." (COMNET 2010, pp. 2-2). In addition, a thermal block is a heat transfer concept and not always a geometric concept: therefore, spaces need not be contiguous to be combined within a single thermal block. However, they are controlled by one thermostat.

In summary, a building thermal block or thermal zone is controlled and maintained by a single thermostat sensor that has its own set-point and schedule. In addition, all the HVAC zones in that thermal block should maintain the same temperature over the period of the day. However, in reality not all spaces in a thermal zone maintain the same temperature. Also, the concept of thermal zoning can be separated in terms of HVAC design, and building energy simulation, since both are required to analyze the building. Therefore, the importance of the distinction of thermal zoning in HVAC design versus thermal zoning in building energy simulation will be discussed.

2.2.2. Thermal Zoning in HVAC Design

In addition to temperature, there are several other parameters that should be maintained in a single thermal zone such as humidity, outside air ventilation, operating periods, freeze protection, pressurization, etc. However, the most common reason for variations in thermal zoning in HVAC design is due to variations in thermal loads

(McDowall 2006). Therefore, HVAC engineers need to determine whether an individual space or groups of adjacent indoor spaces in the building have similar thermal loads prior to the selection of a HVAC system for the building (Grondzik and Kwok 2014). In this section, the relevant literature on building thermal zoning in the HVAC design is reviewed included: Gay and Fawcett (1935), Bovay (1981) Kreider (2001), Bachman (2003), McDowall (2006), Price (2011), and Grondzik and Kwok (2014).

The term "Zoning" or "Thermal Zone" can be found in the HVAC design literature as early as the 1930s. For example, Gay and Fawcett (1935) mentioned thermal zone control strategies for small and large commercial buildings. They pointed out that buildings may be divided into thermal zones for greater accuracy of HVAC control, since various indoor environmental conditions can exist in the building, which include: (1) exposure to prevailing winds and solar radiation and the degree of shelter from surroundings; (2) occupancy depending upon the activities and hours of the occupants; and (3) various methods of construction in different sections producing unequal heating requirements.

Bovay (1981) introduced a thermal zoning procedure for large commercial buildings. This is needed because HVAC system must be capable of satisfying ever-changing loads every day of the year. In the procedure, each space in an exposure has its own individual requirements. Furthermore, it was recommended that a load profile be developed for any desired zone or space as a function of outdoor temperature. The procedure provided a visual picture of the load requirements that must be met by the HVAC system over a wide range of conditions. Unfortunately, the procedure stated that

the exterior zone had wide fluctuations in cooling requirements due to variable lighting and occupancy by people; the diurnal variations of outdoor dry-bulb temperature; sun and cloud cover; as well as shading from adjacent buildings impose a large and continually varying load on exterior zones. Bovay's procedure also stated that the interior zones are usually isolated from variable loads caused by the outdoor weather, except for outdoor air supplied for ventilation, which is treated by specialized equipment that is not in the space itself. Therefore, the primary loads are the heat from: lights, business machines, and people. The interior zone loads also experiences very little variation; quite often these loads are constant.

Kreider (2001) also contains information about thermal zoning. He pointed out that even when the entire building is kept at the same temperature, a multi-zone analysis becomes necessary if the spatial distribution of heat gains in different zone is non-uniform; for example such would be the case if the facades of the building faced different orientation (N, S, E, W). For example, consider a single-zone building with large windows on the north and south sides, during a sunny winter day when the gains just balance the total heat loss, then neither heating nor cooling would be required for the entire building, according to a one-zone simulation analysis. However, how can the heat from the south facing window migrate to the north side of the zone unless some form of mixing is present? In addition, he stated that the basic criterion for zoning is the ability to control the comfort conditions. Therefore, in choosing the zones for a multi-zone analysis, the designer should try to match the distribution of heat gains and losses. The most common and important division is between interior and perimeter zones, because

the interior of a building is not exposed to the changing environment. In addition, different facades of the perimeter should be considered separately for cooling load calculations, since solar heat gain can vary by orientation depending on the time of day.

Bachman (2003) also contained advice about thermal zoning. He suggested five characteristics in order for thermal zoning to satisfy thermal loads and times of peak gain in all rooms in a zone with any degree of uniformity as follows:

1) *Similar solar exposure and orientation*: East-facing rooms and west-facing rooms will have vastly different schedules of thermal needs, just as rooms with large window areas will have different needs than rooms with smaller windows.
2) *Similar envelope exposure*: Perimeter rooms with exposure to the outdoor environment through the exterior envelope will have different heating and cooling needs than rooms in the core of the building, which always need cooling in all but extreme cold climates because they have no direct means of heat gain/loss to the exterior of the building.
3) *Similar occupancy type and density*: Zones such as libraries and auditoriums should be grouped in different thermal zones because they have significantly different 24-hour profiles for internal loads. Likewise, adjacent private offices and large class rooms should also not share a thermostat since these two, different zones can have very different internal loads and ventilation requirements.
4) *Similar schedules*: For example, weekday classrooms in a church school would not be in the same thermal zone as the Sunday congregational assembly space. In

a similar fashion, offices with weekend use where cooling systems may be activated for the comfort of a few workers should not be zoned together with large lobby spaces, where there are no workers on the weekend.

5) *Shared incremental capacity*: Where multiple, modular HVAC systems are used, it is common engineering practice to select small package units and distribute them as needed across the different thermal zones of the building. Retail buildings typically use modular rooftop HVAC units of about 8 to 10 tons cooling capacity and divide the retail floor area into thermal zones of an appropriate size.

McDowall (2006) also covered thermal zoning design considerations in terms of thermal variations as follows:

1) *Solar gain*: Solar gain through windows can create a significant difference in cooling loads, or the need for heating, at varying times of the day according to window orientation, season, and the prevailing weather condition.
2) *Wall or roof heat gains or heat losses*: Thermal zones directly under the roof in a multi-floor building will experience more heat gain in the summer, and heat loss in the winter, than similar thermal zone, directly below the upper floor.
3) *Occupancy*: The use of multiple zones and the importance of maintaining good temperature control will influence how critical thermal zoning is.
4) *Equipment and associated heat loads*: Equipment that gives off significant heat may require a separate thermal zone in order to maintain a reasonable temperature for the occupants. For example, a row of private offices may have

worked well as a single thermal zone, but the addition of a significant number of computers in one of those offices might make it very warm compared to the other offices. Therefore, the office could now require a separate thermal zone.

5) *Freeze protection in cold climates*: In a cold climate, the perimeter walls and roof lose heat to the outside. Therefore, it is often advantageous to designate perimeter thermal zones as separate thermal zones from those in the core of the building.

Price (2011) also showed the impact of solar loading on the operation of a building. According to Price, solar loading is an important aspect of the operation of a building. As the sun travels across the sky during the day, the amount of solar energy that is absorbed on each of the exterior thermal zones varies throughout the day. In addition, South-facing side of the building will see different amounts of solar energy at different times of the year because of the seasonal variation of the sun's path across the sky. A typical floor in a multistory building in the mid-summer was shown in this book to show that only an interior thermal zone would use a constant volume of air for a constant occupancy load.

Finally, Grondzik and Kwok (2014) also provided advice about thermal zoning. In their book they offered three influencing factors on thermal zoning as follows:

1) *Function*: Particularly important because of the variations in internal heat gains between different functions for a thermal zone. A zone function may also influence the thermal zoning organization of a building.

2) *Schedule*: Closely related to zone function, scheduling can influence both the envelope and the support system. If one activity has operating hours different from those of the remainder of the building, a separate mechanical system should be provided for the thermal zone(s) that have different activities. Otherwise, the large equipment required to serve the whole building would be oversized, and could be inefficient at providing heating or cooling for only one thermal zone.
3) *Orientation*: The book states that the degree of exposure to daylight, direct sun, and wind are also important to thermal zoning. In the book a single floor in a square multi-story office building is used as an example. On a cold, sunny, and windy day, the book states the perimeter spaces with direct sun through the windows may gain more heat than is lost and thus need cooling. Although the required cooling might be accomplished by the opening windows in the zone, too much cold air may make occupants near the windows uncomfortable. In addition, perimeter spaces on the same floor without direct sun may have a net heat loss due to the heat loss through the walls, glass, infiltration, and possibly the lack of electric lighting (i.e., internal load). Therefore, the book recommended that under certain condition, such spaces would need heat from a mechanical system during the same day that an adjacent perimeter zone on the same floor requires cooling. Finally, interior spaces are often overheated by the heat gain from electric lighting because they do not lose heat directly to the exterior. Therefore, these spaces may also need cooling from the mechanical system, sometimes when it is

cold outside (i.e., outside air temperatures are well below the thermostat set-point temperature).

In summary, the literature regarding thermal zoning in HVAC system design provided selected criteria for the division of thermal zones, which included: (a) solar gains, (b) orientation, (c) occupancy, (d) schedule, and (e) space function. Using these factors, the concept of building thermal zones in the HVAC design process can be clearly described. However, all of the criteria reviewed only discussed qualitative attributes of thermal zoning in HVAC system design. None of the previous literature provide a general purpose quantitative method for selection thermal zones.

2.2.3. Thermal Zoning in Whole-Building Energy Simulation

Whole-Building energy simulation programs (e.g., DOE-2.1e, DOE-2.2/eQUEST, EnergyPlus, TRNSYS, etc.) are widely used to evaluate the building energy performance during the early design phase. During the modeling process, a large number of input parameters must be determined by the user of the software. One of the important inputs to produce accurate and reliable results from the analysis is thermal zoning. However, currently, although thermal zoning strategies based on rules-of-thumb exist (DOE 2015), there is no well-documented, standard method of thermal zoning for all types of building to be analyzed by a whole-building energy simulation program.

One example of a rule-of-thumb thermal zoning strategy is Appendix G of ASHRAE Standard 90.1-2013 (ASHRAE 2013), which provides general thermal zoning

guidelines for generic HVAC systems in a building. In Appendix G, the basic rules for thermal zoning for the whole-building energy simulation includes:

- *Separate interior and perimeter spaces*: Assign separate thermal blocks to interior spaces located more than 15 feet from an exterior wall and to perimeter spaces within 15 feet of the exterior.
- *Separate orientations with significant amounts of glazing*: Glazed exterior walls should be assigned to different perimeter thermal blocks for each major orientation (i.e., North, East, South, and West). Glazed orientations within 45 degrees of each other may be combined. Spaces with two or more glazed orientations, such as corner offices, should be separated from glazed thermal zones having the different orientations.
- *Separate top, bottom, and middle floors*: Spaces exposed to ambient conditions, such as the top floor or an overhanging floor, and spaces in contact with the ground, such as the ground floor, should be separately zoned from thermal zones that are exposed to ambient conditions, such as intermediate floors in a multi-story building.

The International Building Performance Simulation Association (IBPSA) also provides a few simple criteria regarding thermal zoning when a building energy simulation model is created (IBPSA 2012). The criteria for thermal zoning provided by IBPSA include: usage, temperature control, solar gains, perimeter or interior location, HVAC distribution system type, and separate interior and perimeter thermal zones:

- *Usage*: Any rooms that are combined into a single thermal zone should have similar internal loads (i.e., people, lights, and equipment) and usage schedules. For example, it would not be appropriate to put a high density, variable occupancy conference room on the same zone as a regular, moderate density office space that has constant occupancy.
- *Temperature Control*: Any rooms that are combined into a single thermal zone should have the same heating and cooling set-points and the same thermostat schedules. Since a thermal zone is controlled by one thermostat, it is imperative that all rooms in that thermal zone have the same temperature set-points.
- *Solar Gains*: Any rooms that are combined into a single thermal zone should have similar solar gains. Shading should also be considered when determining thermal zoning according to solar exposure. At a minimum, for perimeter zones with glazed openings, there should be at least one thermal zone for each compass direction. For additional accuracy include a thermal zone for any fenestration that varies by 45 degrees or more. Unglazed exterior zones can be combined if the other criteria are satisfied.
- *Perimeter or Interior Location*: Perimeter areas should be separately thermally zoned from interior spaces, with the depth of perimeter thermal zoning typically 12-15 feet from the exterior wall. This is important as the heating and cooling requirements can vary greatly – perimeter thermal zones can require winter heating while core thermal zones in the same building with no exterior exposure can require year-round cooling.

- *HVAC Distribution System Type*: In a building energy model, you cannot combined thermal zones if they are served by different HVAC distribution system types (i.e., a radiant floor versus a fan coil unit). Since the entire thermal zone would be assigned to one HVAC system type, you can only combine thermal zones that will be served by the same type of HVAC system.
- *Separate Interior and Perimeter Thermal Zones*: Assign separate thermal blocks to interior thermal zones located more than 15 feet from an exterior wall and to perimeter thermal zones within 15 feet of the exterior.

Finally, the Chartered Institution of Building Services Engineers (CIBSE) Applications Manual AM11 (CIBSE 1998) also provides guidance on thermal zoning for the building energy simulation. The manual states the primary purpose of thermal zoning is to avoid undue complexity. Therefore, thermal zones in a building can be grouped together into one thermal zone if:

- They are likely to perform similarly without environmental controls.
- They have similar heating and cooling equipment and thermostat set-points.
- The internal gains from occupants, lighting and equipment are similar.
- The solar gains are similar.

In addition, thermal zones should be split into more than one thermal zone if:

- Variations in environmental conditions within the thermal zone are of importance.
- There is likely to be temperature stratification.

- Solar or internal gains differ significantly throughout the space and mixing of the air is limited.

In addition, the CIBSE manual states that the boundary between such thermal zones should not be assigned thermal mass and should not impede radiative heat transfer. Also, the geometry should be simplified but care should be taken to conserve areas, volumes and orientation.

In summary, the standards and guidelines related to building energy simulation modeling commonly stated that the interior space of a simulated building needed to be separated into core and perimeter thermal zones, and divided by orientations. In addition, the spaces that have similar internal loads, occupancy, and schedules could be aggregated into one thermal zone in the simulation model.

2.3. Previous Studies about Building Thermal Zoning for Building Energy Simulation

Over the past four decades, during the time when the building energy simulation programs were being developed, only a few studies focused on the impact of thermal zoning strategies during the building energy modeling process. This section examines the concept of thermal zoning from the previous studies, as well as published thermal zoning procedures for building energy simulation proposed by various authors. The sources of literature include the publications from: the proceedings, journals and handbooks from ASHRAE; the published proceedings from the 1970 through 2015 building energy simulation conferences of the International Building Performance

Simulation Association (IBPSA); the Energy and Buildings Journal; the Journal of Building Performance Simulation; the Architectural Science Review; the Renewable and Sustainable Energy Review, and various theses and dissertations. The relevant studies on building thermal zoning in the building energy simulation reviewed included: Lokmanhekim (1971), Heidell and Taylor (1985), Goldberg (1985), Hinchey (1991), Samuels et al. (1993), Pan et al. (2007), Musau and Steemers (2007), Musau and Steemers (2008), Tian and Love (2009), Smith et al. (2011), Raftery (2011), O'Brien et al. (2011), Smith (2012), Georgescu et al. (2012), Bleil De Souza and Alsaadani (2012), Jones et al. (2013), Dogan et al. (2014, 2015), and Yi (2015).

In 1971, during the time when building energy simulation programs were first being developed, the U.S. Post Office sponsored the development of a computer simulation program for analyzing the energy consumption of the U.S. Post Office facilities across the U.S. (USPS 1971), which is commonly referred to as the Post Office program. This building energy simulation program is considered to be the first public domain program for whole-building simulation that calculated hourly cooling and heating loads, HVAC system energy use, plant energy use, and was capable of performing an hourly economic analysis (USPS 1971; Haberl and Cho 2004). Lokmanhekim (1971) described the basic structure of the program that consisted of four main sub-programs, which ran in sequence: 1) The Load Calculation Sub-program; 2) A Thermal Loads Plot Sub-program; 3) A Systems Simulation Sub-program; and 4) An Economic Analysis program. In addition, the report by Lokmanhekim provided the definition of space and thermal zoning to perform the thermal zoning in the simulation

program. In this procedure it was recommended that the thermal zoning for a simulation utilize interior temperature plots for the spaces that could be compared to determine compatible grouping of spaces into thermal zones. However, this study did not provide any details about the procedure for the thermal zoning for an hourly simulation. In addition, the simple thermal zoning selection statement in this study was only mentioned once and was not demonstrated and/or verified through testing in case study simulations.

Heidell and Taylor (1985) were some of the first to examine how well a DOE-2 simulation was calibrated for a large office building, by matching the actual end-use energy consumption of the building. In this study, measured data were compared with the simulation results, including end-use energy consumption, heating and cooling loads by thermal zone and the results presented for monthly energy use, and monthly peak demand. This study recommended that the simulation model have the same thermal zones as the actual building's thermal zones. In addition, the study showed the building schedules were also important variables to be considered for a well-calibrated simulation model. However, the study did not explain how the actual thermal zones in the building were used to create the thermostatic zones in the simulation model.

Goldberg (1985) evaluated five building energy simulation programs in terms of experimental, long-term, and transient energy usage data for two residential houses. The two-step validation methodology he employed utilized a constrained optimization approach involving a parametric variation of individual building envelope features. The results illustrated the viability of the parametric variation methodology and showed the importance of earth-contact, heat transfer modeling in heating dominated climates. In the

study, the computation time[1] for an annual simulation period was reduced from 7.25 hours for 10 zones to 2.78 hours for 4 zones, which is a 62% decrease. However, this study also did not explain how the actual thermal zones in the building should be created for the simulation model.

Hinchey (1991) tested how sensitive DOE-2 results were to assumptions about the number of thermal zones for a large commercial office building. In her study, the different thermal zoning assumptions were compared to one another by inspecting graphical output from the simulation program versus measured data. One-zone, five-zone, and eighteen-zone building energy models for the same building were developed, and the results showed that a difference of only 3.5% of total energy consumption was found between the different models. However, although a typical and traditional thermal zoning approach (i.e., core and perimeter method) was applied in this study, it did not consider other ways to zone the building. In addition, this study tested only one specific building and HVAC system type and only considered one thermostat setting for all zones. Therefore, the results from the study may not apply to other building types with varying thermostat temperature. In addition, it is not clear if variations in exterior window areas were considered in the study.

Samuels et al. (1993) studied problems with current Australian energy efficient design guides regarding thermal zoning in solar efficient designs that had living rooms with a northerly orientation (i.e., toward the equator, which would be similar to southern

[1] The type of the computer that used in this simulation was Apple II Plus with 64 kBytes of Ram.

exposures). Their survey showed that occupants prefer to have winter sunlight and daylight penetration into their bedrooms as well as their living room. However, this study suggested only alternative thermal zoning principles, not thermal zoning selection methods or numerical procedures. In addition, the object of this study was residential buildings especially passive house designs, so the results may not apply to other building types.

Pan et al. (2007) developed a method for calibrating a computer simulation on the basis of guidelines published in the previous literature. Their model calibration was conducted by comparing simulation output against measured energy use. In their study, the simulation model was divided into one internal zone and four perimeter zones facing north, south, east, and west with the depth of 13.8 ft (4.2 m) from the external wall. However, although a typical and traditional thermal zoning approach (i.e., core and perimeter method) was applied to this study, they did not consider other ways to zone the building.

Musau and Steemers (2007) investigated energy use in laboratory buildings. They showed it may be influenced by interior space planning and/or the ways the space was used. The results showed the percentage variations of peak winter loads with interior physical definition, activity organization and orientation were within a range of 40% except for the effect of open vs. closed floor plans, which resulted in a variation of 73% in the total peak winter loads. The summer load variations were within 50% between the open, mixed and closed layouts, and 84% between different closed plan layouts. In addition, the study showed the most significant factor regarding the

utilization of energy use was whether the laboratory plan was open or closed. However, this study considered only three common laboratory space interior layouts. In addition, the base-case model did not include variations in exterior window effects such as window sizes, windows, types, etc. Finally, it did not provide a detailed method or procedure about how to zone the spaces in the simulation.

In a separate study, Musau and Steemers (2008) investigated the impact on energy use of the different ways in which office spaces can be organized and used. The analysis indicated that the variations in the combined thermal and lighting loads were 19% and 51% of the base-case loads, respectively, during the UK peak winter and summer period, respectively. The analysis demonstrated that space planning and utilization can have significant impacts on energy use and are important in assessing energy performance. However, this study considered only five typical office space interior layouts. In addition, the base-case model did not include an evaluation of exterior window size, placement, properties, etc. Finally, it did not provide any details about a method or procedure to zone the spaces in the simulation.

Tian and Love (2009) investigated a multi-floor radiant slab cooling system in an institutional building using calibrated simulation with measured building energy use and meteorological data. This study found that core zones had smaller cooling load fluctuations and peak cooling loads per unit floor area than the perimeter zones. However, their study only used a typical and traditional thermal zoning approach (i.e., core and perimeter method) in the study. In addition, the study did not utilize a

parametric analysis, only a one-time simulation. Finally, the results did not show how changes in zoning can impact annual energy use in the simulation.

Smith et al. (2011) presented a method to automatically generate an energy model from an architect's basic massing model. In their study, a usability test was conducted with architects and students that revealed that most users of the tool could obtain a simulation of the simple model in less than 2 hours. However, only the typical and traditional thermal zoning approach (i.e., core and perimeter method) was applied to this study, which did not consider other ways to zone the building. In addition, the study did not provide a method or procedure about how to zone the spaces in the simulation. Finally, the results did not show the impact of different zoning strategies on the annual energy use in the simulation.

Raftery (2011) developed a new thermal zoning method that defined the various type of thermal zones in a model based on four major criteria: 1) The function of the space; 2) The position of the zone relative to the exterior; 3) Available measured data; and 4) The method used to condition the zone. Raftery's zone-typing method yielded a more detailed thermal zoning plan than the traditional core and perimeter zoning method. The method increased run-time from 0.7 hours to 3.6 hours, an increase of 370%. However, the zone-typing in the method did not have a numerical selection procedure. In addition, this procedure relied on a user's subjective use of a simulation program. In addition, the thermal zoning method was not verified through any test or case study. Finally, the results did not show the impact of different zoning strategies on the same building on the annual energy use in the simulation.

O'Brien et al. (2011) conducted sensitivity analyses that: 1) quantified the impact of thermal zoning and inter-zonal airflow on building performance; 2) optimized south-facing glazing area; and 3) optimized thermal comfort for passive solar houses. This study showed the relationships between thermal zoning and inter-zonal airflow rate. The results showed that passive solar buildings, in particular, can benefit from increased air circulation with a forced air system because it allows solar gains to be redistributed and thus reduces direct gain zone overheating and total energy consumption. In addition, with increased air circulation, the heating and cooling energy was reduced by a total of 16% while the magnitude of overheating is reduced by 55%. However, this study tested only for a specific building type (i.e., passive solar house) and was based on the actual thermostat zones. In addition, the thermal zoning method that was used in the study did not have a numerical procedure. Finally, this study did not verified the performance (i.e., thermal comfort) of the variations that were studied, and it does not provide a method or procedure about how to zone the spaces in the simulation.

Smith (2012) tested various thermal zoning configurations based on Appendix G of ASHRAE Standard 90.1-2007 to figure-out the impact on the building energy use. The results showed that 1-zone and 2-zone model underestimated the energy use versus a 5-zone model. It also suggest that perhaps a better default for the perimeter offset in a core and perimeter zoning configurations would be closer to sixteen feet (16 ft.) versus ten feet (10 ft.) and twenty feet (20 ft.) perimeter offsets. This study demonstrated the importance of using reasonable zoning assumptions in conceptual models, but it did not

provide a generalized method or procedure about how to zone a building in the simulation.

Georgescu et al. (2012) analyzed a detailed building energy model using an optimization method called the Koopman operator, an infinite-dimensional, linear operator that captures nonlinear, finite-dimensional dynamics without linearization, in order to identify and develop zoning approximations based on observations of zone temperature. The purpose of the approximation was to reduce the complexity of the model while minimally impacting model accuracy. In the model used in the study, the number of zones were reduced from 191 zones to 32 zones with only a 3.3% error in prediction. The paper also included guidelines to help maintain model accuracy, including: 1) When merging zones, the thermal mass of un-modeled walls should be captured; 2) Zones containing exterior surfaces should not be merged with zones that do not contain exterior surfaces; 3) Perimeter zones that are merged should have similar surface orientations and window areas; 4) Zones containing a small volume and surface area can be merged with a much larger adjacent zone with little loss of accuracy. However, a detailed model of all the zones must first be created in order to establish a baseline model to compare against. In order to use this method, unfortunately, creating a detail model of all zones takes a significant amount of time, and often implies uncertainty (i.e., when the number of parameters in the model increases). Finally, this study did not provide a generalized, step-by-step procedure about how to establish the thermal zones in a building simulation model.

Bleil De Souza and Alsaadani (2012) examined how recommended settings for internal gains and ventilation rates together with the use of different zoning strategies can produce significant variations in the predicted energy demands in office buildings. Their results showed that thermal behavior of each zone was mainly influenced by a relationship between different combinations of floor area, window area and internal gains. In addition, they showed a way to zone a building to predict ranges of heating and cooling demands by working with extremes in terms of window-to-floor area ratio combined with internal gain settings. However, they concluded that more simulations and tests were necessary to establish a set of criteria about how to set-up zoning strategies that considered various combinations of floor area, window area and internal gains. Finally, since only one climate and HVAC system was applied to this study, they suggested repeating the study for different systems in different climates.

Jones et al. (2013) described a series of five automated steps to translate geometric data from an un-zoned CAD model into a multi-zone building energy model. The study showed that if a full simulation has been run, the building may be zoned by analyzing interior temperature profiles (i.e., Koopman operator). However, the study fell short of developing a generalized method of thermal zoning. In addition, only the common and traditional thermal zoning approach (i.e., core and perimeter method) was applied to the case-study building.

Dogan et al. (2014) presented an algorithm for the automated, multi-zone building energy model production for urban and schematic designs. Their algorithm used a robust straight skeleton algorithm (Felkel and Obdrzalek 1998) with an arbitrary

building massing that was subdivided into core and perimeter thermal zones. A straight skeleton algorithm is a method of representing a polygon by a topological skeleton that is similar to the medial axis but differs in that the skeleton is composed of straight line segments, while the medial axis of a polygon may involve parabolic curves. It may be computed by simulating the shrinking process by which it is defined. Their proposed algorithm was tested with various floor plans with varying complexity. However, it only showed how to subdivide the floor volumes into thermal zones based on the traditional core and perimeter method. This study fell short of developing a procedure that automatically converts massing models into building energy models. Unfortunately, there was no consideration of indoor temperature profiles in the thermal zoning method.

Dogan et al. (2015) introduced a general algorithm to automatically convert arbitrary building massing models into multi-zone, multi-floor building energy models. In this new method, the different layouts changed the annual heating and cooling loads by up to 21%. Using this new algorithm, the test results[2] showed that for small models, the geometry was computed within milliseconds, and for larger models, for example: 184 zones require 15.5 seconds to compute. EnergyPlus simulation time ranged from 20 seconds to 5 minutes for the largest model. This study basically follows the zoning method which provided by Appendix G of ASHRAE Standard 90.1-2013 which is core and perimeter method. However, this study did not consider a method for grouping spaces into a common zone.

[2] The tests were conducted using a Macbook Pro with a 2.3 GHz Intel Core i7 chip, 8GB of RAM.

Yi (2015) developed an interface to suggest optimized thermal-zone layouts to facilitate a thermal-zoning-based space arrangement. To accomplish this, four major performance criteria were adopted for evaluation, including Energy Use Intensity (EUI); Predicted Mean Vote (PMV); daylight level; and room shading. This program allowed regrouping of thermal zones according to spatial functions. In the method, it was necessary to take external local conditions into account within the simulation as well as considering extra subdivisions for the perimeter space(s). The results showed indoor thermal conditions as well as the occupancy schedule had a large impact on the final layout. However, this thermal zoning method used in this study is entirely based on the spatial functions only. Therefore, this study did not consider any thermal parameters to group spaces into a zone. This study also relied on the user's subjective judgement to select the zones. Furthermore, the proposed method did not consider HVAC system type for thermal zoning.

Georgescu and Mezić (2015) introduced a systematic approach to creating zoning approximations in an institutional building. In a similar fashion as their previous study (Georgescu et al. 2012), utilizing the Koopman operator, the time-series output produced by a building simulation was decomposed into spatial modes that captured the thermal behavior of a building at different time-scales. The study also provided guideline to help maintain model accuracy in the study: 1) one space use classification is the same throughout the thermal zone; 2) all rooms in a thermal zone that are adjacent to glazed exterior walls face the same orientation or their orientations vary by less than 45°; and 3) separate zones should be assumed for interior and perimeter rooms. However, one

limitation of this study was that a detailed building model must first be created so that a simplified zone model can be produced.

2.4. Possible Impact Factors on Building Thermal Zoning Strategy

2.4.1. Building Shape

Building shape or form can affect both building construction cost and energy consumption significantly (Ourghi et al. 2007). Previous studies have examined correlations between building shapes and building thermal loads (i.e., building energy consumption), including: Ourghi et al. (2007), Catalina et al. (2011), and Mottahedi et al. (2015).

Ourghi et al. (2007) developed a simplified analysis model to evaluate the impact of building shape on total energy consumption for office buildings. In this study, a parametric analysis was performed to investigate the impact on the annual electricity use of different building shapes when all other aspects of the building remained the same. The results showed that a rectangular-shaped building consumed more energy than a non-rectangular-shaped building (i.e., L-shaped building) when the window-to-wall ration was 25%. In the analysis, an equation-based procedure was developed using the correlations.

Catalina et al. (2011) conducted several thermal and lighting simulations with different building shapes and glazing areas in different climates to evaluate the impact on building energy consumption in office buildings. In this study, it was found that a compact-shape building (i.e., rectangular shape) can be 6 - 10 % more energy efficient

than other shapes. In addition, it was concluded that building shape can be significant factor that affects energy consumption especially in hot climates with large amounts of solar radiation and hot outdoor temperatures.

Mottahedi et al. (2015) developed a multi-linear regression model to investigate the effect of different building shapes including: an H-shape, a T-shape, and a rectangular shape on total heating and cooling loads in two different climates (i.e., cold-dry and warm-marine). The results showed that there was a robust correlation between building shapes and the level of energy consumption. In addition, it was found that a T-shape building showed the highest total energy consumption in both climates.

2.4.2. Window-to-wall Ratio

The building envelopes can play a significant role in many aspects of the energy balance in a building. For example, it can directly affect the solar heat gain or the heat loss (i.e., energy use for cooling and heating) in the building since the building enclosure is the physical barrier between the exterior conditions and the conditioned interior of the building. Of all the building envelope elements, the windows have the most significant impact on the building energy performance because they permit exterior solar radiation to penetrate through the glazing and they conduct heat to/from the exterior. Therefore, a proper design and development of a window façade system is essential to reduce the energy consumption in buildings.

Among all the parameters related to the window façade system, the Window-to-Wall Ratio (WWR) is considered a critical factor that can significantly influence the

energy consumption in buildings (Lee et al. 2013; Shen and Tzempelikos 2013; Goia 2016). Consequently, there have been many previous efforts to determine the relationship between the WWR and building energy consumption. Previous studies have investigated correlations between the WWR and building thermal loads (i.e., building energy consumption), including: Shen and Tzempelikos (2012), Goia et al. (2013), and Goia (2016).

Shen and Tzempelikos (2012) conducted an integrated daylighting and building energy simulation analysis for private office spaces by varying windows and shading properties for different climates (i.e., Chicago and Los Angeles). The results indicated that a window façade with an automated shading system that has a WWR in the range of 30% to 50% can reduce total energy consumption versus one that has a smaller or larger WWR for most cases.

Goia et al. (2013) studied the optimal transparent percentage for a façade module for low energy office buildings located in a temperate oceanic climate in the northern hemisphere. In their study, it was observed that the ideal WWR was between 35% and 45% to attain the lowest total primary energy use regardless of the building orientations. In addition, the results showed that the north-exposed façade with inappropriate transparent percentage may have a high influence on the energy demand of the building, while the south-exposed façade has the lowest influence with the configuration.

Goia (2016) also investigated the optimal WWR to minimize building energy consumption (i.e., energy use for heating, cooling, and lighting) for different European climates and orientations. The results showed that a WWR between 30% and 45% gives

ideal values to lower total energy consumption when automated shading systems are used. In addition, it was found that if the wrong WWR configuration was implemented, the total energy consumption may be increased from 5% to 25%, compared to when the optimal WWR is used.

2.4.3. Climate Conditions

Climate conditions are one of the key driving factors of a building's total energy use (Lin and Hong 2013). In order to achieve high levels of building energy efficiency, the building design and building system operation must be considered based on the specific climate characteristics where the building is located (Heller et al. 2011). Previous studies have investigated correlations between the climate conditions and building thermal loads (i.e., building energy consumption), including: Eskin and Türkmen (2008), Yang et al. (2008), and Lin and Hong (2013).

Eskin and Türkmen (2008) studied how the energy demands in an office building vary with different conditions and control strategies in the four major climatic regions in Turkey using calibrated building energy models. In the study, the parameters that affected building energy use, such as climatic conditions (location), insulation, window systems, were investigated for each city. The various analysis results showed that it is possible to achieve 9.5% and 10% savings in annual building energy use by choosing light colors on external walls in the hot and humid climate zones of Turkey. Similarly, the study showed that a building with similar characteristics can reduce energy use by 2% and 3.6% in cold and mild climate regions of Turkey.

Yang et al. (2008) investigated the energy performance of the office building envelope designs in the five different climates in China. In this study, it was found that despite being in different climatic zones, the overall thermal heat transfer value of the building envelope for Beijing, Shanghai and Hong Kong were very similar. The study also found that some building envelopes were more likely to have more heat gain/loss than those specified by the local design/energy code. In their study recommendations were provided to improve the energy efficiency of existing buildings. In general, more insulation of the exterior walls and roofs was recommended to reduce heating energy use for buildings in cold climates.

Lin and Hong (2013) evaluated the building design and operation parameters for space-heating systems of two different office buildings in three heating-dominated U.S. climates using building energy simulation. In their study, they tried to determine the most influential parameters and their impacts on variations of space heating energy use. The results showed that variations of the space heating energy use in office buildings in three heating dominated climates can be very large. In addition, the impact of the ambient weather on space heating energy use was very consistent across office buildings in the same climate, but is significantly different across different climates.

2.5. Summary of Literature Review

This literature review presented: a review of the most widely-used, whole-building energy simulation programs in the U.S. (i.e., DOE-2.1e, DOE-2.2/eQUEST, EnergyPlus, and TRNSYS); a definition of building thermal zones; thermal zoning

methods used in the actual HVAC design process; thermal zoning methods used in building energy modeling; and an overview of the previous studies about building thermal zoning strategies for building energy simulation. The findings of the literature review are summarized below:

1) For the energy analysis of commercial buildings, four whole-building energy simulation programs were reviewed, including: DOE-2.1e, DOE-2.2/eQUEST, EnergyPlus, and TRNSYS. These programs are based on different simulation algorithms and programming structure, and have different capabilities for simulating building systems and renewable energy systems. Among these programs, DOE-2 and eQUEST are fixed-schematic programs, whereas EnergyPlus and TRNSYS are modular programs, which enables them to more readily incorporate models for simulating advanced building systems and various renewable energy systems.
2) There are several similar terms for building thermal zone such as thermal zones, thermal blocks, HVAC zones, etc. However, all these different terms indicate the same idea and concept which is: a thermal zone is a portion of a building whose HVAC system is controlled by a single sensor (i.e., thermostat).
3) Several of the previous literature on HVAC design and controls were reviewed to investigate thermal zoning procedures and methods used in the HVAC design process. These provided a consensus set of criteria for the division of thermal zones which include: (a) solar gains, (b) orientation, (c) occupancy, (d) schedule, and (e) space function. With these factors, the concept of building thermal zone

in the HVAC design process can be clearly described. However, none of the previous literature provided a set of detailed thermal zoning rules, but rather simple guidelines and factors that needed to be considered when engineers perform the job in the field. Therefore, in most designs, it appears that the thermal zoning task during the HVAC system design process tends to rely on the engineer's experiences and intuition.

4) A number of building energy modeling standards and guidelines for commercial buildings such as Appendix G of ASHRAE Standard 90.1-2013, the IBPSA Building Energy Modeling Book (BEMBook), and the CIBSE Application Manual AM11 were reviewed in terms of information about thermal zoning in building energy simulation. These standards and guidelines commonly stated that the interior space of a simulated building needed to be separated into core and perimeter thermal zones, and divided by orientations. In addition, the spaces that have similar internal loads, occupancy, and schedule could be aggregated into one zone in the simulation model. However, unfortunately, none of the previous literature provided a comprehensive, detailed thermal zoning method or detailed rules for the complete, automated thermal zoning in energy simulation modeling.
5) Although there have now been thousands of articles written about building energy simulation modeling that have documented new approaches for building energy efficiency, only a few studies have addressed how to thermally zone the building in a simulation program other than the conventional zoning process (i.e., core and perimeter method).

CHAPTER III

SIGNIFICANCE OF THE STUDY

3.1. Significance of the Study

A review of the previous literature indicated that standards and recommendations regarding building thermal zoning for building energy analysis provided only simple guidelines such as separating core from perimeter thermal zones. Furthermore, only a few studies have investigated and tested the effect of thermal zoning on a simulation model. Therefore, this study will be significant by developing and testing a detailed procedure for the thermal zoning of a building using building energy performance software programs for the purpose of calculating energy savings and improving thermal comfort for new design option.

3.2. Limitations of the Study

There are several limitations to this study which include:

1) This study has focused primarily on office buildings. Therefore, the results may not be applicable to other building types.
2) Since the base-case office building models were located in a hot and humid climate and a cold and humid climate, the application of the method to other types of buildings with different HVAC systems in different climates may lead to different conclusions.

3) This study does not consider all types building shapes. Therefore, although the proposed buildings will be based on several building shapes, other uncommon building shapes may need to be considered in a future study.
4) The study is focused on developing a procedure which has been tested using the DOE-2.1e building energy simulation program.

CHAPTER IV

METHODOLOGY

This chapter describes the methodology used to develop an automated procedure for thermal zoning for whole-building energy simulation. The chapter is divided into four sections, including: 1) Development of a new thermal zoning method for building energy simulation; 2) Development of simplified commercial base-case models to test the method; 3) Parametric study on different configurations of thermal zoning; and 4) Summary of the methodology.

4.1. Development of a New Thermal Zoning Method for Building Energy Simulation

As described earlier in Chapter II, many of the previous studies on building energy simulation have pointed out that today's building energy simulation programs contain simplified dynamic heat transfer frameworks that are used to simulate complex buildings. For example, the majority of building energy simulation programs are based on the assumption that the indoor air of every thermal zone in a building is well-mixed. In other words, the indoor temperature within a thermal zone is spatially uniform. In a similar fashion, the standards and guidelines related to building energy simulation modeling such as ASHRAE Standard 90.1, and CIBSE commonly assume that core and perimeter thermal zoning strategy can be used on most simulation models to reduce the total number of zones in the model. However, although this may or may not have a

negative impact on model accuracy, it can lead to too many thermal zones in a model, or in some cases it can lead to too few zones.

As a result, the majority of building energy simulation tools (e.g., DOE-2.2/eQUEST, EnergyPlus, etc.) usually provide two simple thermal zoning methods as a default strategy, which include a single thermal zone for each floor or a core and four perimeter zones for each floor facing roughly north, south, east, and west (N,S,E,W). The problem is that by applying these simple thermal zoning methods to a simulation model, the simulation results can become quite distorted. In one extreme example, Dogan et al. (2014) showed that the annual building thermal loads (i.e., heating/cooling loads) of the multi-thermal zone model may be up to 14% higher than a single-zone model of the same building.

4.1.1. Grid-base Thermal Zoning Method

During the early stage of architectural design process, space allocation on the given floor plan is an important task, which is used to define the requirements of the future occupants such as the right amount of space and type of space. If this process is overlooked, the space requirements might be misinterpreted, which results in cost overruns during the construction process and the building maintenance. Therefore, even in the architectural design process, spatial layout planning (i.e., thermal zoning layout in terms of HVAC design) is one of the critical tasks that can be affecting the final architectural design outcome.

A grid-base architectural floorplan layout design is one of the traditional strategies for the spatial configuration that has been widely used and accepted within architectural practice (Hillier and Connors 1966). This approach to spatial configuration is based on allocating space units over a grid-base domain. Using a set of grid squares, the available spaces are defined and a particular zone or activity is allocated by an algorithm (Michalek et al. 2002). **Error! Reference source not found.** shows an e xample of the grid-base layout design. This method has been studied and applied in various space layout and allocation research (Medjdoub 2000; Michalek and Papalambros 2002; Rodrigues et al. 2013).

The grid-base method is based on a unit space that is predefined as a square or rectangular shape. Unit spaces can be grouped into several categories based on their function (e.g., offices, restrooms, mechanical rooms, etc.) by the designer. The floor plan developed by the grid-based method can be described by a one-dimensional matrix made up of a sorted set of points, as the size and location of each unit space is defined on a given plan.

During the architectural design stages, there are many details such as the location and size of HVAC system, ducts, and pipes that may be uncertain. Accordingly, during the early stages, it is important to optimize the space layout for geometric construction. Figure 1 shows the basic concept of the grid-based layout method (i.e., 100 ft × 100 ft), in which, a designer is trying to locate certain spaces – A, B, and C within the predefined space. The grid-base method is one of the most effective ways to allocate the space during the early architectural design stage, since this method uses a planar grid. To begin

the designer needs to set the size of a unit space. In this case, the size of a unit space was defined as 10 ft × 10 ft over the given space. This set of unit spaces can be considered as a one-dimensional matrix, so we can assign a point number to each unit space as S_i (i = 1, 2, 3, ... , 100). As shown in the figure, Space A is composed of (S_{84}, S_{85}, S_{86}, S_{87}, S_{88}, S_{94}, S_{95}, S_{96}, S_{97}, S_{98}); Space B is composed of (S_{44}, S_{45}, S_{46}, S_{47}, S_{54}, S_{55}, S_{56}, S_{57}, S_{64}, S_{65}, S_{66}, S_{67}); Space C is composed of (S_1, S_2, S_3, S_4, S_5, S_6, S_{11}, S_{12}, S_{13}, S_{14}, S_{15}, S_{16}).

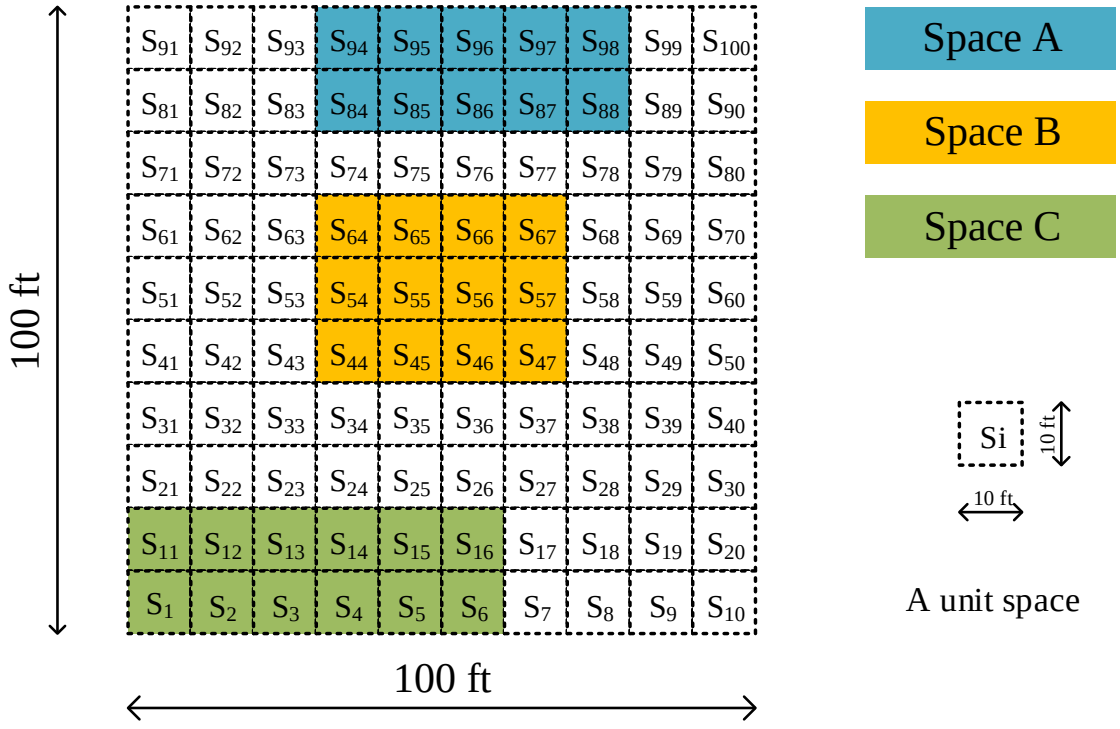

Figure 1: Representation of Geometry using Grid-base Method

4.1.2. Thermal Load Calculations for Thermal Zoning

Heat transfer in buildings is a very important phenomenon to understand for building peak thermal loads and energy calculations (Davies 2004; Moss 2007; Hensen

and Lamberts 2011). A space is mainly influenced by heat transfer through the building envelope, which is called an external thermal load (i.e., solar heat gain, infiltration/ventilation). On the other hand, the indoor environment is also influenced by internal heat generating sources such as occupants, lights, and appliances. Typically, these are called internal thermal loads. In general, the heat generation from external and internal components are not evenly balanced in a building, so HVAC systems are necessary and essential for providing a thermally comfortable environment for the occupants.

As described earlier, thermal zoning in HVAC system design is required to separate a single space or a collection of spaces into thermal zones whose thermal conditions are similar. However, in a building occupied spaces are usually maintained at a different set-point temperatures than unoccupied spaces. Therefore, in order to successfully accomplish an effective HVAC thermal zoning and provide thermal comfort indoors, it is important to group spaces having similar heating and cooling requirements (i.e., thermal load) in the early stage of the architectural design.

Typically, during the building design process building thermal loads (i.e., peak heating/cooling loads) are calculated and used to size the building HVAC systems. In addition, the thermal loads of individual zones are also necessary to calculate the air-handling unit capacity. Therefore, accurate calculation of the individual zonal thermal loads and total building loads are important. In addition, when HVAC systems are under-sized, it can have a negative impact on the occupants' thermal comfort, and/or the effectiveness of the HVAC system.

During the creation of a whole-building energy simulation, it is common practice to combine thermal zones into a single thermal zone if they have similar thermal load profiles to reduce the time and effort spent in constructing the simulation. However, grouped spaces that do not have sufficiently similar thermal characteristics can have a negative impact on the model accuracy (Georgescu 2014), which can contribute to significant difference in simulated versus actual building energy use. For example, in a single zone model that includes significant south-facing fenestration there can be localized, high thermal loads, which can be offset by a space in the same zone facing north that is less influenced by mid-day solar radiation in the winter. As a result, the calculated energy use for the entire building using a building energy simulation program averages the load over the entire zone (i.e., a well-mixed model), which may not reflect the localized loads on the north or south exposure. Consequently, when the energy demand is calculated using a building energy simulation program for single zone model, there can be load cancellation, which causes reduced energy demand for the single zone model compared to multi-zone model.

4.1.3. The Proposed New Thermal Zoning Method (Grid/Cluster Method)

Figure 2 shows the detailed procedure of the proposed new thermal zoning method for building energy simulation. In the following sections, a step-by-step description of the proposed thermal zoning method is presented in detail with related examples in the following sections.

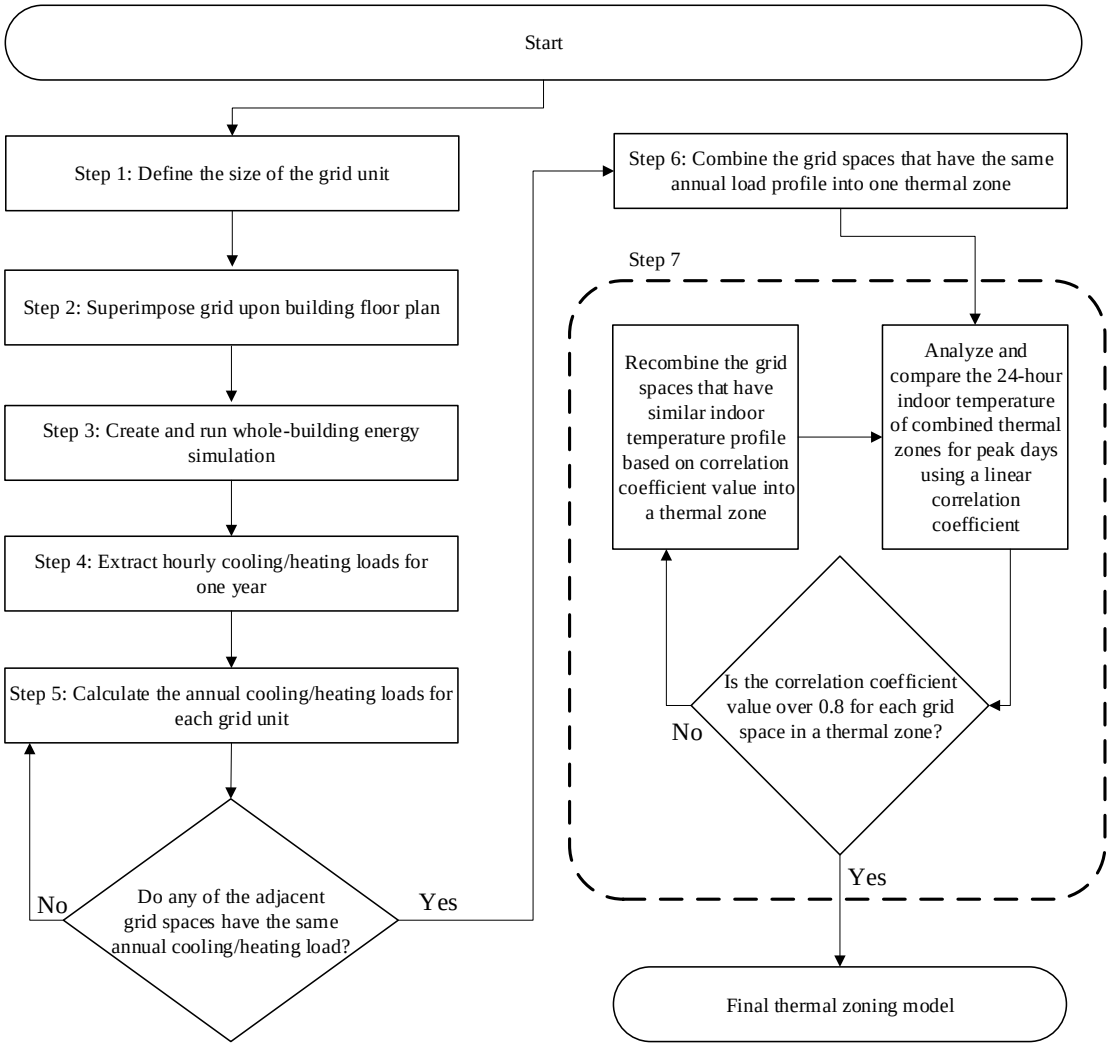

Figure 2: Procedure of the Proposed New Thermal Zoning Method

4.1.3.1. Step 1: Define grid unit

The first step in the grid/cluster thermal zoning procedure is to define the size of a grid unit. As described in Section 4.1.1, a grid unit is defined as a square or rectangular shape that can be grouped into several categories based on its function (e.g., offices, restrooms, mechanical rooms, etc.) by the designer. The most important factors that should be considered when the designer decides on the size of a grid unit is the usage of

the space and dominate activities in the space. Consequently, the minimum required size for the space based on the activities can be a grid unit size. In this study, which proposes a thermal zoning method targeting commercial buildings (i.e., office building), the size of a grid unit was set at 10 ft X 10 ft, or 100 ft^2, which is often referenced as an average-sized thermal zone for ducted air-conditioning system (Kreider et al. 2017). In general, the throw of the air diffuser must be related to the area of the space (i.e., the size of a thermal zone) to ensure that no dead airspaces exist. Other grid sizes can easily be substituted for the current assumption (i.e., 10 ft X 10 ft).

4.1.3.2. Step 2: Application of the grid unit to building floor plan

The next step is to superimpose the grid unit that was defined in the previous step upon the building floor plan. Figure 3 and Figure 4 show examples of overlaid grid units on various shapes of building floor plans that used in this portion of the study.

41	42	43	44	45	46	47	48	49	50
31	32	33	34	35	36	37	38	39	40
21	22	23	24	25	26	27	28	29	30
11	12	13	14	15	16	17	18	19	20
1	2	3	4	5	6	7	8	9	10

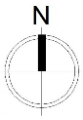

Figure 3: Example Allocation of the Grid Units on Rectangle-shape Floor Plan

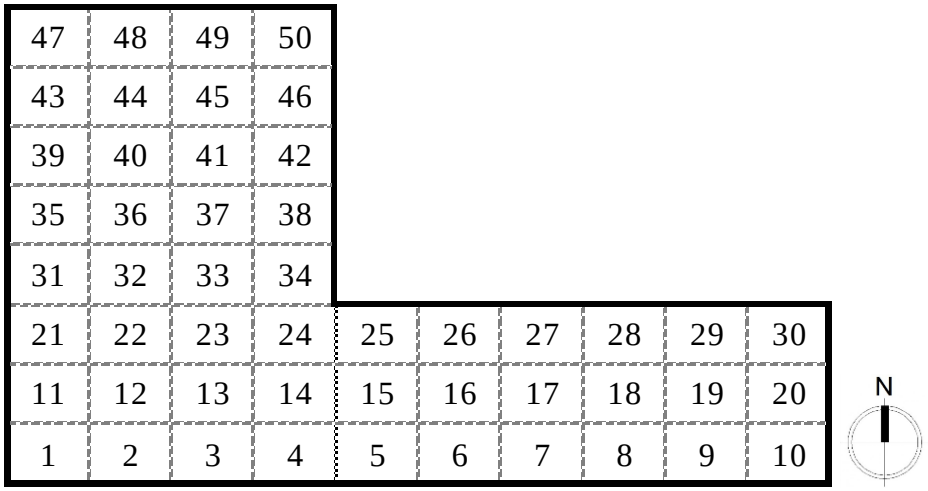

Figure 4: Example Allocation of the Grid Units on L-shape Floor Plan

4.1.3.3. Step 3: Whole-building energy simulation model

In this step, a whole-building energy simulation model was created based on the building geometry and thermal zoning information that was collected in the previous step. In this step, it is necessary that the building physical characteristics (i.e., building thermal properties) are verified against the original architectural drawings. In this study, a simplified commercial base-case model was developed and used to test the proposed new thermal zoning method. The detailed information on the base-case model is described further in Section 4.2. Figure 5 and Figure 6 show the simulation models that were used in this study.

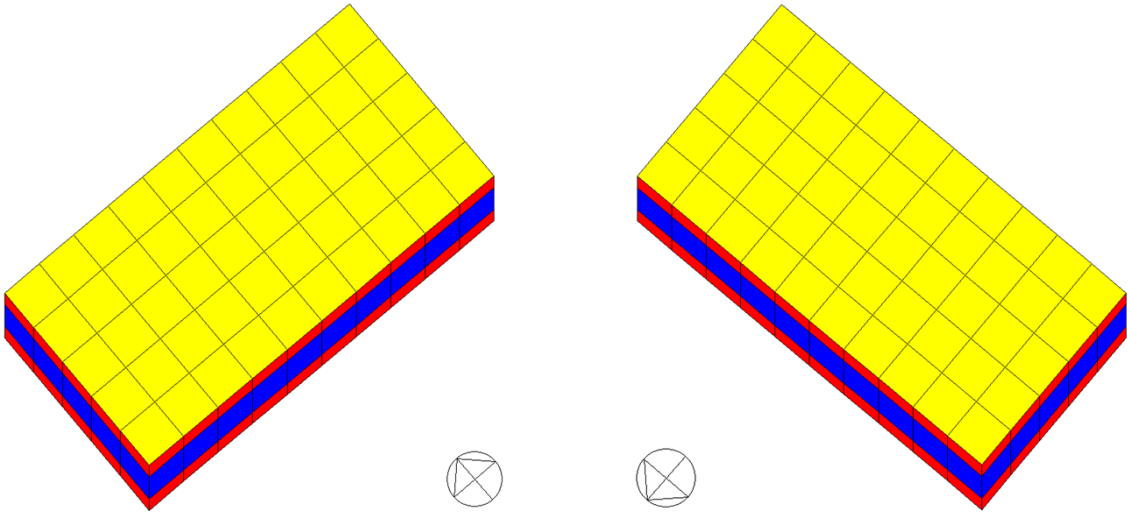

(a) Southwest View (b) Northwest View

Figure 5: 3D View of Rectangle-shape Simulation Model

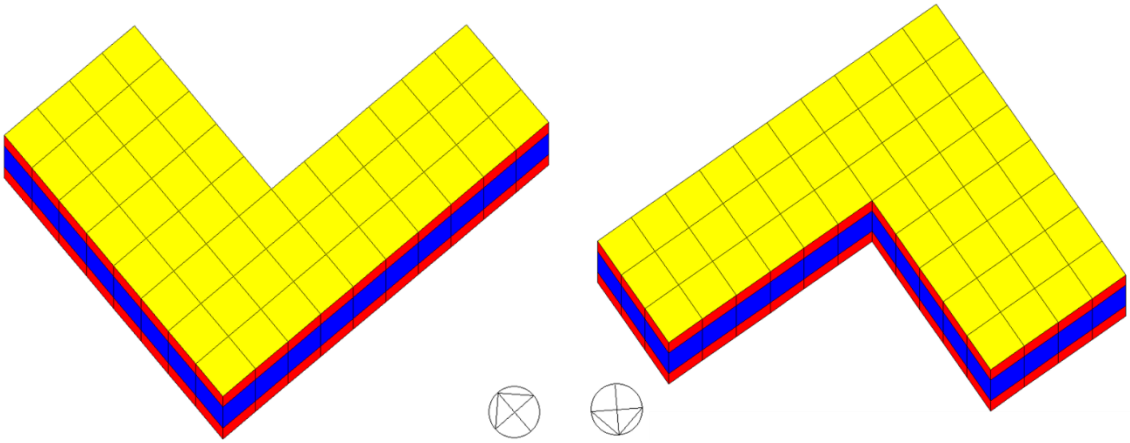

(a) Southwest View (b) Northwest View

Figure 6: 3D View of L-shape Simulation Model

4.1.3.4. Step 4: Heating/cooling loads data for each thermal zone

As described earlier, the definition of a thermal zone is that of a space or group of spaces within a building with heating and cooling requirements that are sufficiently similar. Therefore, a key parameter that is used in the proposed new thermal zoning method to merge the grid units using the heating/cooling loads data extracted from the simulation outputs. Figure 7 shows an example time series plot of hourly heating/cooling loads data for each grid unit. In this plot, it was observed that some of thermal zones were closely aligned in terms of similar annual heating/cooling loads profiles. However, it is a very time consuming process to recognize which zones are significantly related using the hourly heating/cooling loads profile data and the corresponding plots. Therefore, it was necessary to consider a more efficient statistical way to select the spaces that have closely related hourly load profiles.

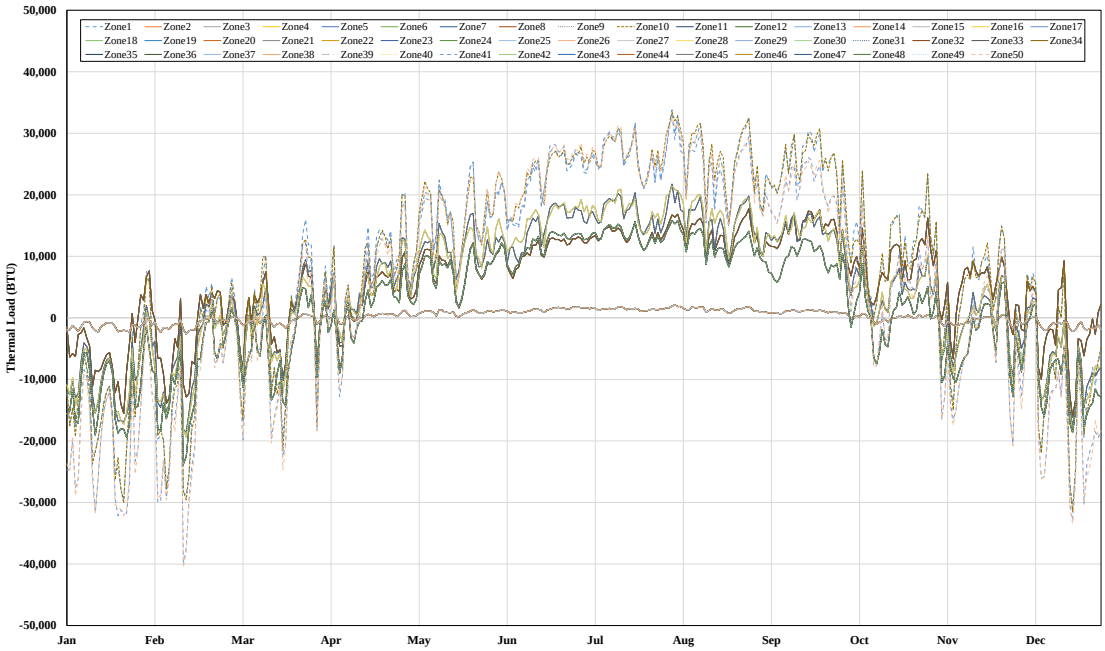

Figure 7: Example Time Series Plot of Hourly Heating/Cooling Loads for Each Grid Unit

4.1.3.5. Step 5: Annual heating/cooling loads for each grid unit

In this step, the annual heating/cooling loads for each grid space were calculated based on the hourly heating/cooling loads from the simulation outputs to identify the spaces that have similar thermal loads. Figure 9 shows an example of the simulated annual heating/cooling loads for each grid space of the model shown in Figure 8. As shown in the figure, it can be seen that identical or very similar annual heating/cooling loads exist in a number of spaces. In order to investigate the detailed differences between the cooling and heating loads for each space, total annual thermal loads were separately calculated as cooling and heating loads, which are presented in Figure 10. These plots show relative heating/cooling loads, which are expressed as percentage of the total heating/cooling loads in each space.

41	42	43	44	45	46	47	48	49	50
31	32	33	34	35	36	37	38	39	40
21	22	23	24	25	26	27	28	29	30
11	12	13	14	15	16	17	18	19	20
1	2	3	4	5	6	7	8	9	10

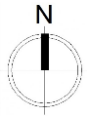

Figure 8: Example Allocation of the Grid Units on Rectangle-shape Floor Plan

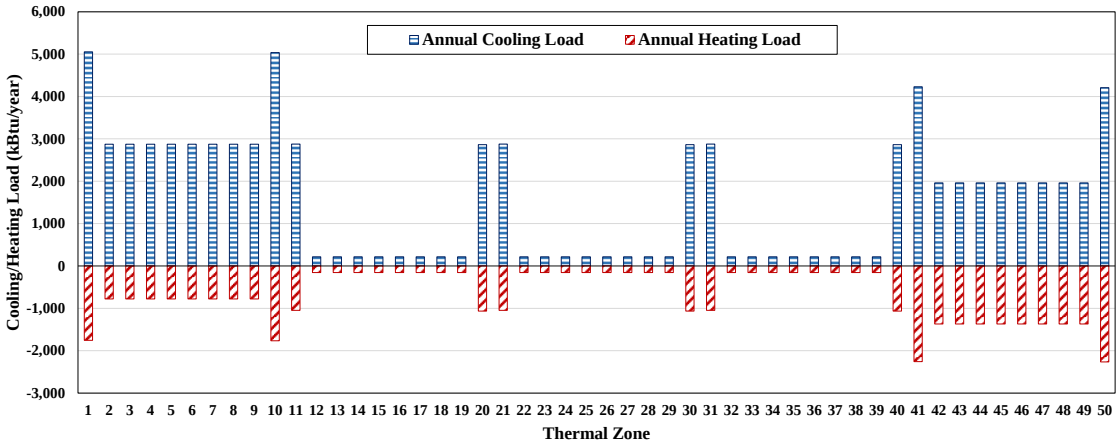

Figure 9: Example of Annual Heating/Cooling Loads for Each Space

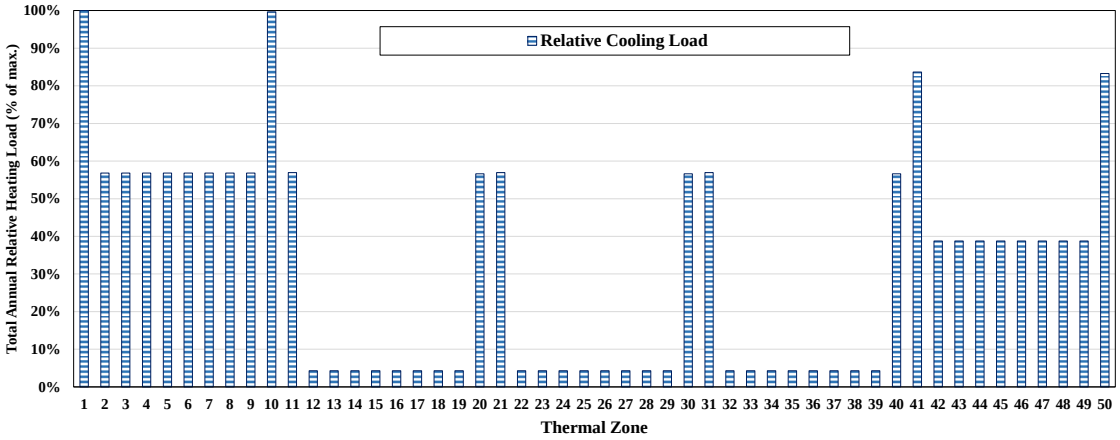

(a) Annual Total Relative Cooling Load

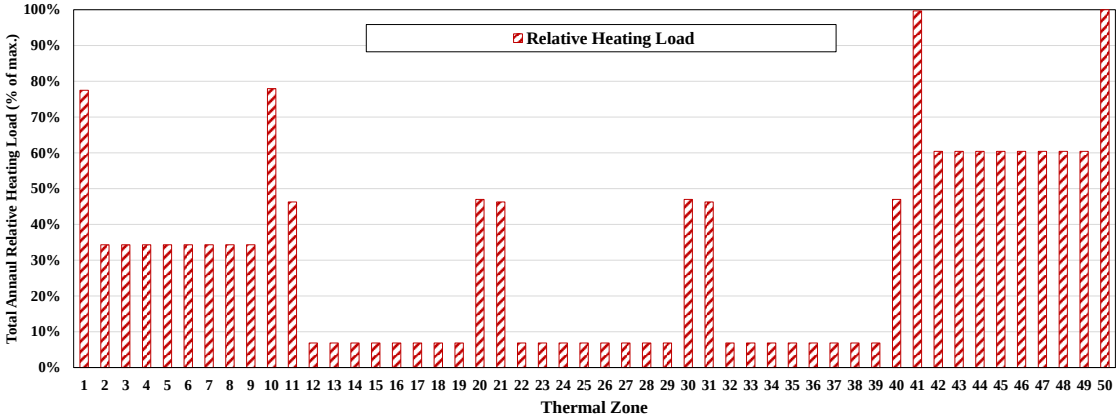

(b) Annual Total Relative Heating Load

Figure 10: Example of Annual Total Relative Heating/Cooling Loads for Each Space

4.1.3.6. Step 6: Defining thermal zones based on annual thermal load data

In this step, the grid spaces that have the same total annual thermal loads are identified and presented. Figure 11(a) shows an example of the representation of the thermal zones colored to match the office floor plan shown in Figure 11(b). As shown in the figures, the similar thermal zones can be easily identified using this method. However, it should be noted that even if the grid spaces are combined based on the same

total annual thermal load, the grid spaces must be adjacent space each other. In other words, only the adjacent grid spaces can be combined based on the total annual thermal loads. For example, Zone 1 and Zone 10 seem to have the same total annual thermal load in Figure 11. However, since those spaces are not adjacent, they cannot be combined as a thermal zone.

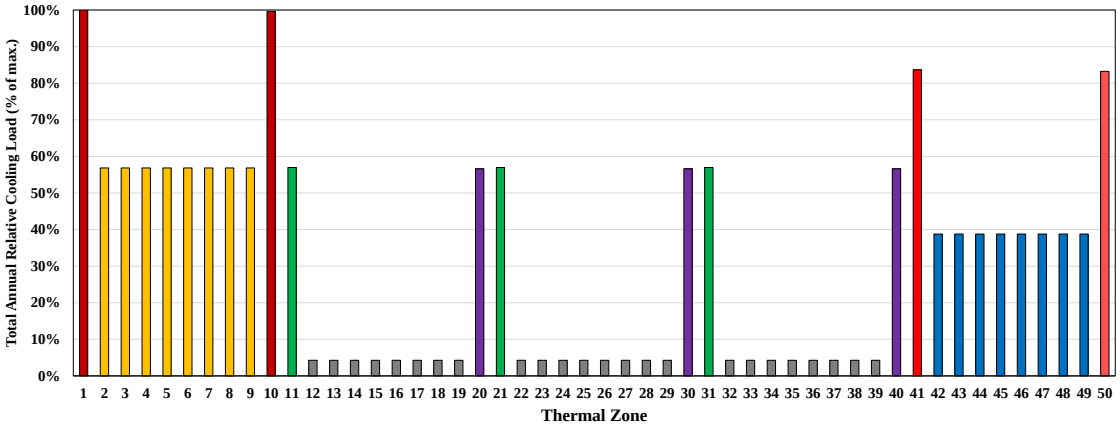

(a) Total Annual Cooling Load for Each Space

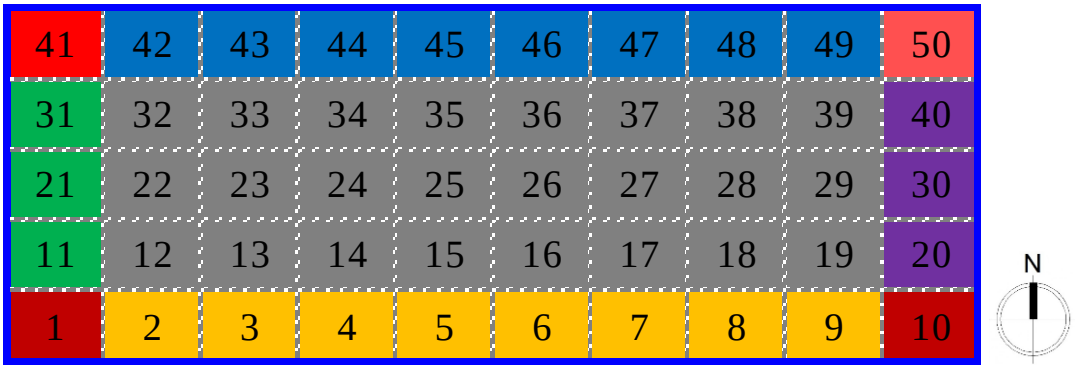

(b) Representation of Thermal Zones with Same color on the Floor Plan

Figure 11: Preliminary Thermal Zones Based on Annual Thermal Load Data

4.1.3.7. Step 7: Calibration of the combined thermal zones

Once the preliminary thermal zoning layout is defined, it is then necessary to verify that the thermal zones are combined correctly. In general, building energy and load calculation models using whole-building energy simulation programs assume that the air within a space is well-mixed. In addition, even though simulated total annual heating/cooling loads for the grid units are identical, the 24-hour profiles of the different zones can be significantly different for the peak heating/cooling days. Therefore, to verify the new thermal zoning method that uses the grid-based thermal zoning strategy, the indoor temperature profiles of the grouped thermal zones needed to be further analyzed. To accomplished this, 24-hour simulated indoor temperature profiles of the combined thermal zones for peak days (i.e., hot/cold clear days) are analyzed and compared. Figure 12 and Figure 13 show the weather conditions of the clear, peak days during the summer and winter, respectively, which are selected from the Typical Meteorological Year 3 (TMY3) weather file for Houston, TX. In addition, the same plots for Chicago, IL are shown in Figure 14 and Figure 15.

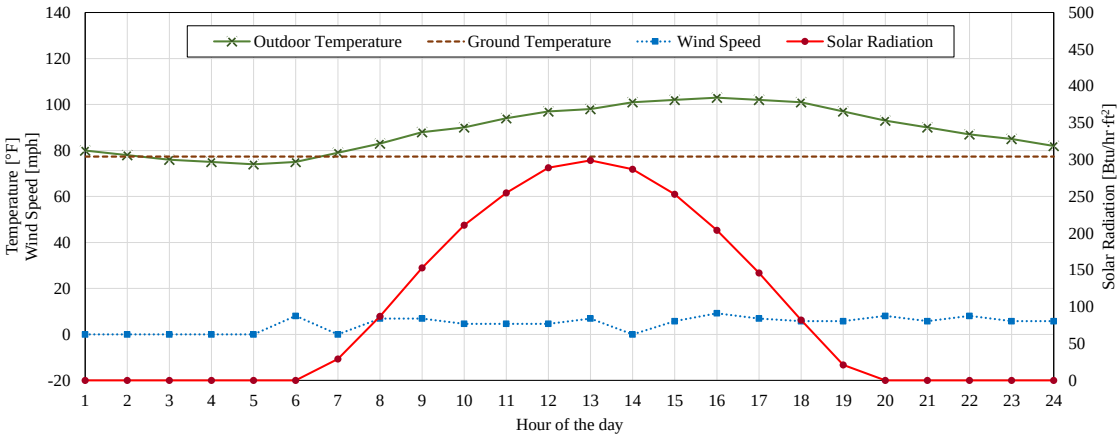

Figure 12: Weather Conditions for the Hot, Clear day (August 2) in Houston, TX

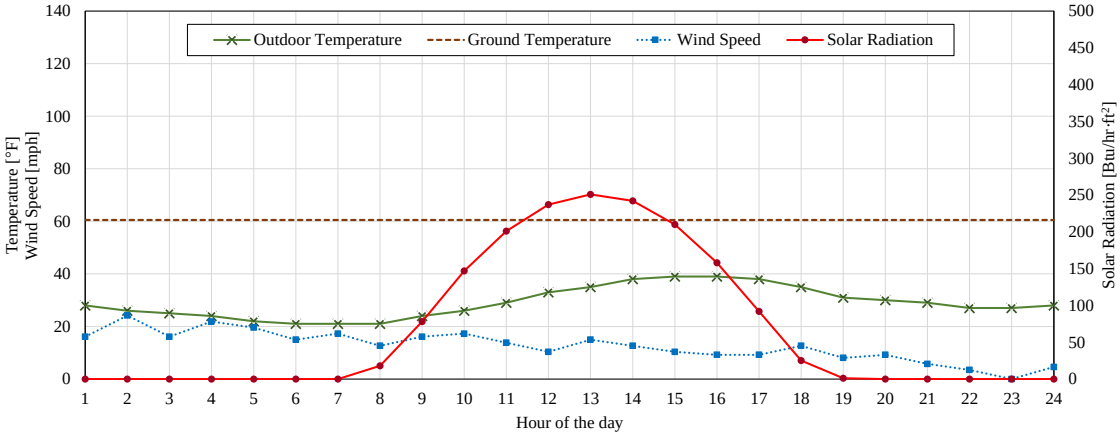

Figure 13: Weather Conditions for the Cold, Clear Day (February 11) in Houston, TX

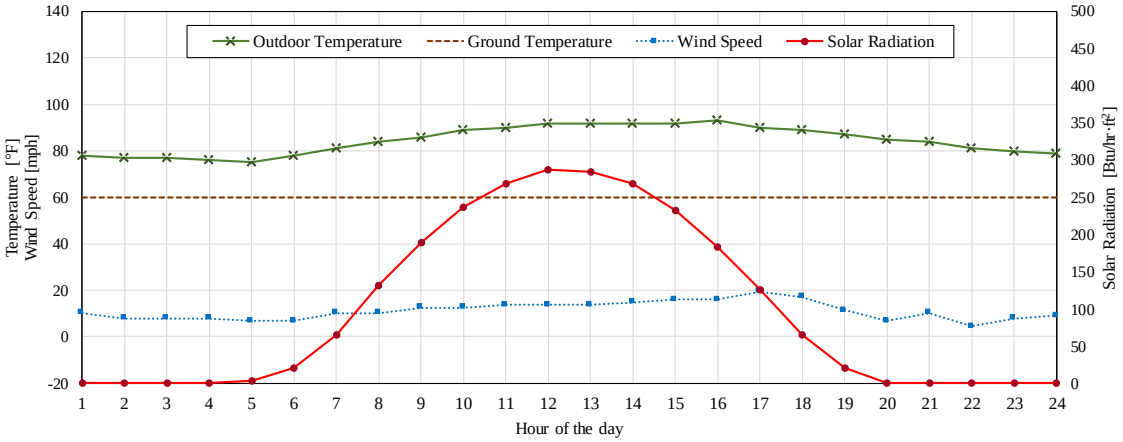

Figure 14: Weather Conditions for the Hot, Clear day (July 18) in Chicago, IL

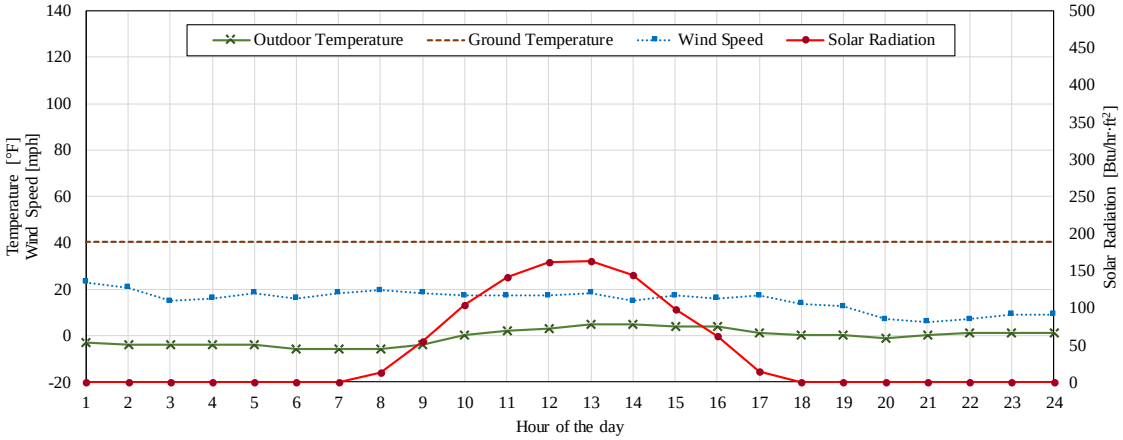

Figure 15: Weather Conditions for the Cold, Clear Day (January 27) in Chicago, IL

Once the peak days for the corresponding location are determined, the 24-hour indoor temperature profiles for the combined thermal zones can be identified from the simulation outputs. Figure 16 gives an example of the thermal zoning layout that shows the combined thermal zones colored in yellow. This grouped thermal zone was developed during the previous step based on the simulated total annual heating/cooling loads. The calculated heating/cooling loads for Zone 2 through Zone 9 are shown in

Figure 9 in the previous section. Figure 17(a) and Figure 17(b) show 24-hour indoor temperature profiles on the peak days for summer and winter, respectively. In these figures, there is only a slight difference in indoor temperature between the grouped thermal zones; about a 2.0°F difference between the hourly minimum and maximum temperature during both peak days in all eight profiles. However, this small variance between the indoor temperature profiles does not ensure that these thermal zones are grouped correctly. For example, the indoor temperature profiles can have a maximum or minimum temperature at different hours of the day, even though there is a slight variation between the profiles.

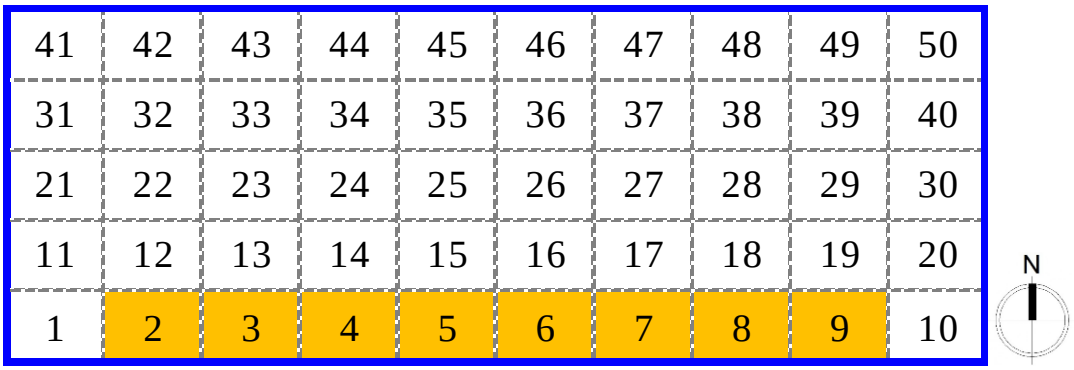

Figure 16: Example Representation of the Combined Thermal Zones

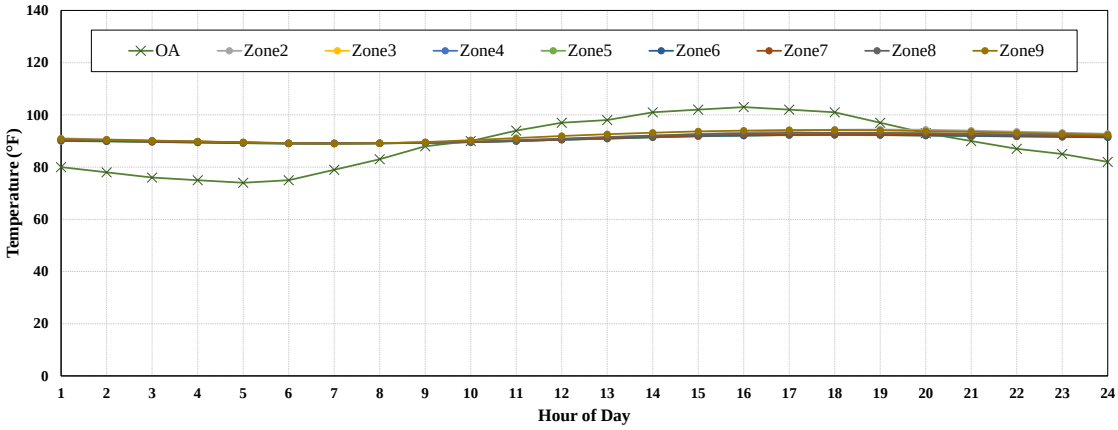

(a) Indoor Temperature Profiles on a Peak Day in the Summer

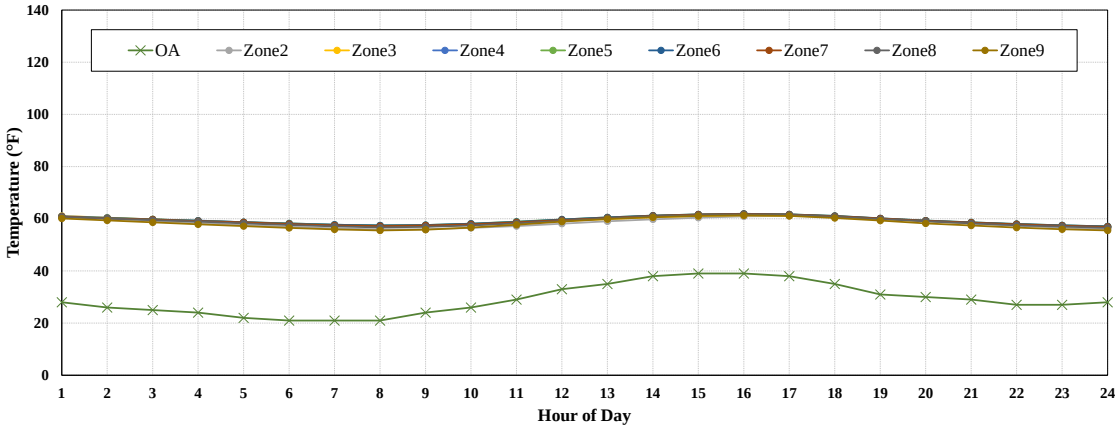

(b) Indoor Temperature Profiles on a Peak Day in the Winter

Figure 17: Indoor Temperature Profiles of a Combined Thermal Zone for Peak Days

Consequently, it is a tedious process to determine graphically how the indoor temperature profiles of each unit space in the same thermal zone are closely related each other by visually inspecting a time series plot. Therefore, a numerical criteria or measure of the strength of the relationship between the spaces was necessary for the new thermal zoning method as a supplement to a graphical display.

Fortunately, the strength of the relationship between two variables can be measured using a simple, linear correlation coefficient (Ott and Longnecker 2010). The following equation shows the variables and the algorithm used to calculate the correlation coefficient.

$$r = \frac{1}{n-1}\sum_{i=1}^{n}\left(\frac{x_i - \bar{x}}{s_x}\right)\left(\frac{y_i - \bar{y}}{s_y}\right)$$

Where:

- **n** is the sample size,
- $\boldsymbol{x_i}$, $\boldsymbol{y_i}$ are the single samples indexed with I,
- $\bar{\boldsymbol{x}}$, $\bar{\boldsymbol{y}}$ are the sample mean, and
- $\boldsymbol{s_x}$, $\boldsymbol{s_y}$ are the sample standard deviation.

The correlation coefficient, r, is a unit-free measure of the strength of a linear relationship between the variables, x and y. Therefore, the correlation coefficient can be used to determine how closely the related the 24-hour indoor temperature profiles of each unit space match another space. In general, a correlation greater than 0.8 is described as strong, whereas a correlation less than 0.5 is described as weak. In this study, once the indoor temperature profiles are calculated from the simulation outputs, the correlation coefficient for the grouped thermal zone simulated indoor temperatures for the two peak days (i.e., peak heating and peak cooling) will be calculated. Then, if the correlation is greater than 0.8, the combined thermal zone will be regarded as the final thermal zoning layout. In cases where the thermal zoning does not match

expectations, the correlation can be recalculated for the unit spaces that have correlation values less than 0.8 to search for the strongly correlated thermal zones.

Table 1 and Table 2 show the correlation coefficient for the thermal zoning cases shown in Figure 16. As shown in the tables, all the cases show correlation > 0.8, which indicates that the indoor temperature profiles of each zone have a strong positive linear correlation. Therefore, according to the criteria ($r \geq 0.8$), these unit spaces (Zone 2 through Zone 9) can be merged into a single thermal zone.

Table 1: Correlation Coefficient on a Peak Day in the Summer (Zones 2 – 9)

	Zone 2	*Zone 3*	*Zone 4*	*Zone 5*	*Zone 6*	*Zone 7*	*Zone 8*	*Zone 9*
Zone 2	1.00							
Zone 3	1.00	1.00						
Zone 4	0.99	0.99	1.00					
Zone 5	0.98	0.98	1.00	1.00				
Zone 6	0.98	0.98	1.00	1.00	1.00			
Zone 7	0.99	0.99	1.00	1.00	1.00	1.00		
Zone 8	0.99	0.99	1.00	1.00	1.00	1.00	1.00	
Zone 9	0.96	0.96	0.98	0.99	0.99	0.99	0.99	1.00

Table 2: Correlation Coefficient on a Peak Day in the Winter (Zones 2 – 9)

	Zone 2	*Zone 3*	*Zone 4*	*Zone 5*	*Zone 6*	*Zone 7*	*Zone 8*	*Zone 9*
Zone 2	1.00							
Zone 3	0.98	1.00						
Zone 4	0.97	0.99	1.00					
Zone 5	0.96	0.99	1.00	1.00				
Zone 6	0.96	0.99	1.00	1.00	1.00			
Zone 7	0.97	0.99	1.00	1.00	1.00	1.00		
Zone 8	0.97	0.99	1.00	1.00	1.00	1.00	1.00	
Zone 9	0.96	0.98	0.99	1.00	1.00	1.00	1.00	1.00

Figure 18 shows another example of thermal zoning layout based on the calculated total annual cooling load data shown in Figure 11(a). Figure 19 shows the indoor temperature profiles of each grid unit in a combined thermal zone, which is colored in grey in Figure 18. In this plot, it was observed that the indoor temperatures from some of the grid units began to increase around 10:00 a.m. This slight increase in temperatures makes a difference in the indoor temperature profiles in several of the unit spaces. However, as mentioned earlier, it is necessary to calculate the correlation coefficient for the relations between all the indoor temperature profiles from each unit space compared to all other spaces to ensure these thermal zones are combined correctly.

Table 3 shows the correlation coefficients for the thermal zoning case shown in Figure 18 and Figure 19. In this example, it was found that there are several correlations less than 0.8 (colored red), which include: Zone 19 vs. Zone 23, Zone 19 vs. 24, Zone 19 vs. Zone 25, Zone 19 vs. Zone 26, Zone 19 vs. Zone 27, Zone 23 vs. Zone 39, Zone 24 vs. Zone 29, Zone 24 vs. Zone 39, Zone 25 vs. Zone 29, Zone 25 vs. Zone 39, Zone 26 vs. Zone 29, Zone 26 vs. Zone 39, Zone 27 vs. Zone 39. Therefore, these unit spaces should be excluded from the group of thermal zones that were defined in the previous step. Also, among the excluded zones, it should be investigated if there is a possibility to recombine with the excluded unit spaces that have similar indoor temperature profile based on correlation coefficient into another thermal zone.

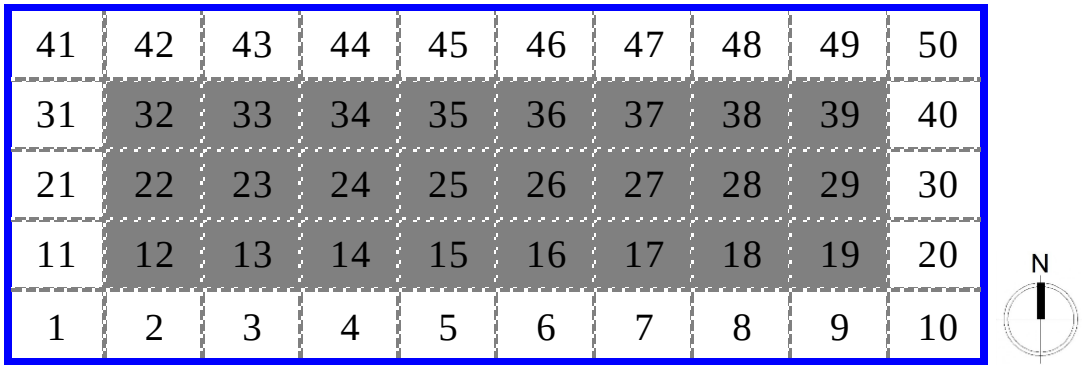

Figure 18: Example Representation of the Combined Thermal Zones

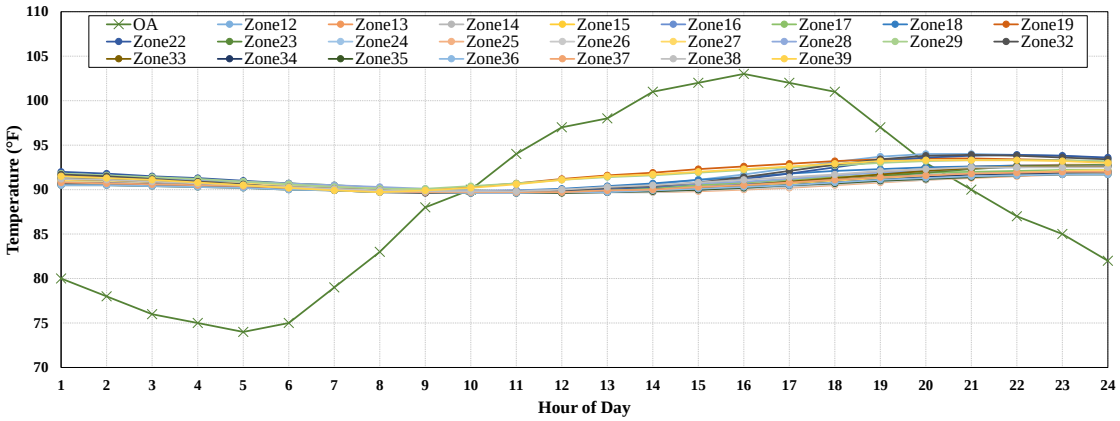

Figure 19: Indoor Temperature Profiles of a Combined Thermal Zone for a Peak Day

Table 3: Correlation Coefficient on a Peak Day in the Summer (Zones 12 – 39)

	Zone 12	Zone 13	Zone 14	Zone 15	Zone 16	Zone 17	Zone 18	Zone 19	Zone 22	Zone 23	Zone 24	Zone 25	Zone 26	Zone 27	Zone 28	Zone 29	Zone 32	Zone 33	Zone 34	Zone 35	Zone 36	Zone 37	Zone 38	Zone 39
Zone 12	1.0																							
Zone 13	1.0	1.0																						
Zone 14	1.0	1.0	1.0																					
Zone 15	1.0	1.0	1.0	1.0																				
Zone 16	1.0	1.0	1.0	1.0	1.0																			
Zone 17	1.0	1.0	1.0	1.0	1.0	1.0																		
Zone 18	1.0	1.0	1.0	1.0	1.0	1.0	1.0																	
Zone 19	0.9	0.8	0.8	0.9	0.9	0.9	0.9	1.0																
Zone 22	1.0	1.0	1.0	1.0	1.0	1.0	1.0	0.8	1.0															
Zone 23	0.9	1.0	1.0	0.9	0.9	0.9	0.9	0.7	0.9	1.0														
Zone 24	0.8	0.9	0.9	0.9	0.9	0.9	0.8	0.6	0.9	1.0	1.0													
Zone 25	0.8	0.9	0.9	0.9	0.9	0.9	0.8	0.6	0.9	1.0	1.0	1.0												
Zone 26	0.8	0.9	0.9	0.9	0.9	0.9	0.8	0.6	0.9	1.0	1.0	1.0	1.0											
Zone 27	0.9	1.0	1.0	0.9	0.9	0.9	0.9	0.7	1.0	1.0	1.0	1.0	1.0	1.0										
Zone 28	1.0	1.0	1.0	1.0	1.0	1.0	1.0	0.8	1.0	1.0	0.9	0.9	1.0	1.0	1.0									
Zone 29	1.0	0.9	0.9	0.9	0.9	0.9	1.0	1.0	0.9	0.8	0.7	0.7	0.7	0.8	0.9	1.0								
Zone 32	1.0	1.0	1.0	1.0	1.0	1.0	1.0	0.9	1.0	0.9	0.8	0.8	0.9	0.9	1.0	1.0	1.0							
Zone 33	1.0	1.0	1.0	1.0	1.0	1.0	1.0	0.8	1.0	1.0	0.9	1.0	1.0	1.0	1.0	0.9	1.0	1.0						
Zone 34	0.9	1.0	1.0	1.0	1.0	1.0	0.9	0.8	1.0	1.0	1.0	1.0	1.0	1.0	1.0	0.9	1.0	1.0	1.0					
Zone 35	1.0	1.0	1.0	1.0	1.0	1.0	1.0	0.8	1.0	1.0	0.9	1.0	1.0	1.0	1.0	0.9	1.0	1.0	1.0	1.0				
Zone 36	1.0	1.0	1.0	1.0	1.0	1.0	1.0	0.8	1.0	1.0	0.9	0.9	0.9	1.0	1.0	0.9	1.0	1.0	1.0	1.0	1.0			
Zone 37	1.0	1.0	1.0	1.0	1.0	1.0	1.0	0.8	1.0	1.0	0.9	0.9	0.9	1.0	1.0	0.9	1.0	1.0	1.0	1.0	1.0	1.0		
Zone 38	1.0	1.0	1.0	1.0	1.0	1.0	1.0	0.9	1.0	0.9	0.8	0.9	0.9	0.9	1.0	1.0	1.0	1.0	1.0	1.0	1.0	1.0	1.0	
Zone 39	0.9	0.9	0.9	0.9	0.9	0.9	0.9	1.0	0.9	0.7	0.6	0.6	0.6	0.7	0.8	1.0	0.9	0.8	0.8	0.8	0.9	0.9	0.9	1.0

Table 4 shows the correlation coefficient on a peak day in the summer between the excluded unit spaces (Zone 23 through Zone 27). As shown in the table, all the correlations indicate that there are significant correlations between those unit spaces. Therefore, these unit spaces can be combined as a single thermal zone. In addition, the correlations for the unit spaces, except the excluded ones, are shown in Table 5. These unit spaces also have correlations greater than 0.8. Consequently, the recombining of the unit spaces based on the similar indoor temperature profiles is complete. Figure 20 and Figure 21 show the indoor temperature profiles for recombined thermal zones, respectively. The final thermal zoning layout is shown in Figure 22. Two different thermal zones were created in the final version, while the initial layout had a single thermal zone.

Table 4: Correlation Coefficient on a Peak Day in the Summer

	Zone 23	*Zone 24*	*Zone 25*	*Zone 26*	*Zone 27*
Zone 23	1.00				
Zone 24	0.99	1.00			
Zone 25	0.99	1.00	1.00		
Zone 26	1.00	1.00	1.00	1.00	
Zone 27	1.00	0.99	0.99	1.00	1.00

Table 5: Correlation Coefficient on a Peak Day in the Summer

	Zone 12	*Zone 13*	*Zone 14*	*Zone 15*	*Zone 16*	*Zone 17*	*Zone 18*	*Zone 19*	*Zone 22*	*Zone 28*	*Zone 29*	*Zone 32*	*Zone 33*	*Zone 34*	*Zone 35*	*Zone 36*	*Zone 37*	*Zone 38*	*Zone 39*
Zone 12	1.0																		
Zone 13	1.0	1.0																	
Zone 14	1.0	1.0	1.0																
Zone 15	1.0	1.0	1.0	1.0															
Zone 16	1.0	1.0	1.0	1.0	1.0														
Zone 17	1.0	1.0	1.0	1.0	1.0	1.0													
Zone 18	1.0	1.0	1.0	1.0	1.0	1.0	1.0												
Zone 19	0.9	0.8	0.8	0.9	0.9	0.9	0.9	1.0											
Zone 22	1.0	1.0	1.0	1.0	1.0	1.0	1.0	0.8	1.0										
Zone 28	1.0	1.0	1.0	1.0	1.0	1.0	1.0	0.8	1.0	1.0									
Zone 29	1.0	0.9	0.9	0.9	0.9	0.9	1.0	1.0	0.9	0.9	1.0								
Zone 32	1.0	1.0	1.0	1.0	1.0	1.0	1.0	0.9	1.0	1.0	1.0	1.0							
Zone 33	1.0	1.0	1.0	1.0	1.0	1.0	1.0	0.8	1.0	1.0	0.9	1.0	1.0						
Zone 34	0.9	1.0	1.0	1.0	1.0	1.0	0.9	0.8	1.0	1.0	0.9	1.0	1.0	1.0					
Zone 35	1.0	1.0	1.0	1.0	1.0	1.0	1.0	0.8	1.0	1.0	0.9	1.0	1.0	1.0	1.0				
Zone 36	1.0	1.0	1.0	1.0	1.0	1.0	1.0	0.8	1.0	1.0	0.9	1.0	1.0	1.0	1.0	1.0			
Zone 37	1.0	1.0	1.0	1.0	1.0	1.0	1.0	0.8	1.0	1.0	0.9	1.0	1.0	1.0	1.0	1.0	1.0		
Zone 38	1.0	1.0	1.0	1.0	1.0	1.0	1.0	0.9	1.0	1.0	1.0	1.0	1.0	1.0	1.0	1.0	1.0	1.0	
Zone 39	0.9	0.9	0.9	0.9	0.9	0.9	0.9	1.0	0.9	0.8	1.0	0.9	0.8	0.8	0.8	0.9	0.9	0.9	1.0

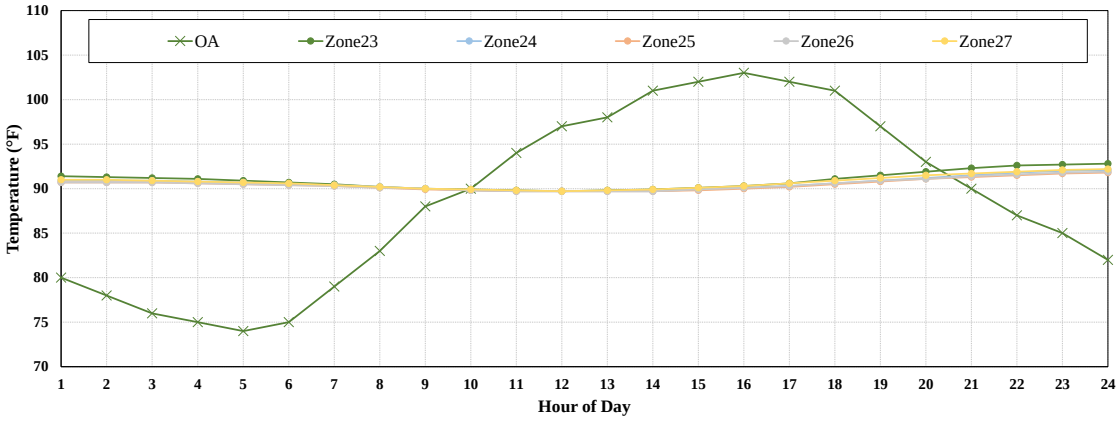

Figure 20: Indoor Temperature Profiles of a Combined Thermal Zone for a Peak Day

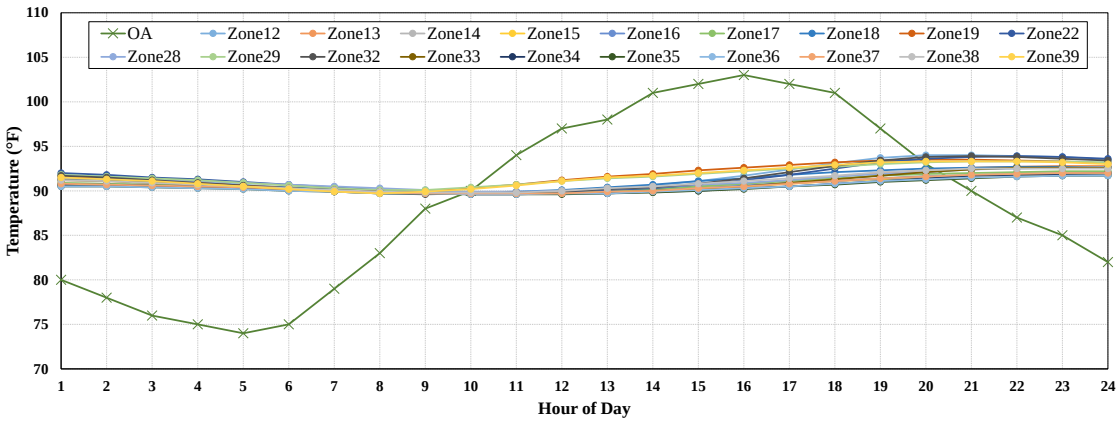

Figure 21: Indoor Temperature Profiles of a Combined Thermal Zone for a Peak Day

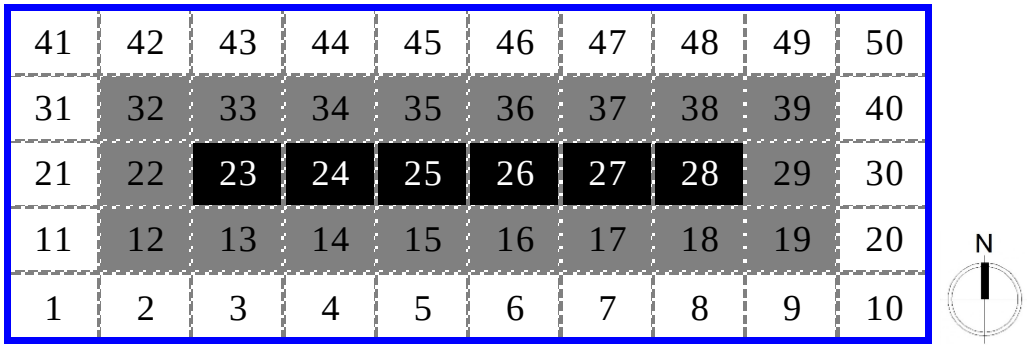

Figure 22: Final Thermal Zoning Layout

4.1.4. Variation of the Thermal Zoning Layout Based on Varying Levels of Linear Correlation Coefficients for the Simulated Zonal Temperatures

In this analysis, Linear Correlation Coefficients (LCC) of the simulated 24-hour indoor temperature profiles were determined to be useful indicators for grouping similar zones. The LCC is a measure of the strength of the relationship between variables x and y for the specific equation of a best-fit. For example, if the equation of a best fit is linear, a LCC close to 1 or -1[3] suggests that x and y have a strong linear relationship. Therefore, the correlation coefficient is always a value such that $-1 \leq r \leq 1$. The absolute value of the coefficient indicates how strong the relationship is between x and y. The closer the value is to zero, the weaker the linear relationship between x and y. The closer to the value is to 1, the stronger the linear relationship is between x and y. Using the guide that Wuensch et al. (1996) suggested for the absolute value of r:

- .00 - .19 "very weak"
- .20 - .39 "weak"
- .40 - .59 "moderate"
- .60 - .79 "strong"
- .80 – 1.0 "very strong"

In addition, we can add a verbal description of how well (or not) the 24-hour indoor temperature profiles of two zones match each other. In this study, as mentioned earlier, the LCC of 0.8 was used to search for the significantly correlated thermal zones

[3] Although a typical range of the linear correlation coefficient is -1 to 1, only the values above 1 were considered in this analysis.

in the building. This means that if there are two thermal zones that have a LCC value over 0.8, these two zones could be combined into a single thermal zone in the model. However, if the user choose a different LCC threshold, such as 0.6 or 0.7, this will impact the final thermal zoning layout, which may result in a more useful result.

Figure 23 shows a view of an example rectangle-shape simulation model (Huang 1993). This simulation model is a simplified commercial base-case model developed in this study to be used for demonstrating the thermal zoning method. The detailed information of this simulation model including input parameters is described in Section 4.2. For this building, a simulation model with 50 thermal zones was selected for a building with a 50% window-to-wall ratio for all four orientations (i.e., North, East, South, West). In this analysis, the climate chosen was the 'hot and humid', climate of Houston. Next, the proposed new thermal zoning method (i.e., Grid/Cluster thermal zoning method) was applied to the model to investigate the variation of the thermal zoning layout based on the level of the correlation coefficients.

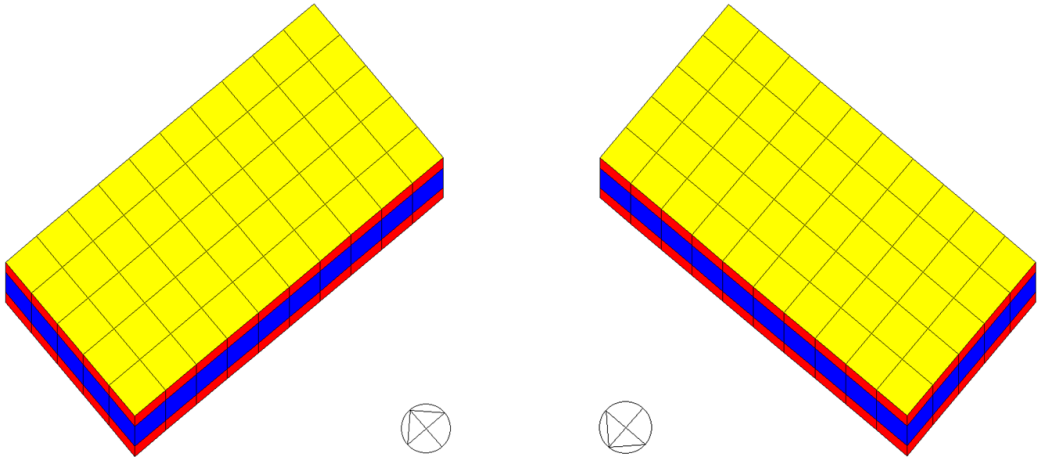

(a) Southwest View (b) Northwest View

Figure 23: View of An Example Rectangle-shape Simulation Model

Table 6 shows the resultant set of thermal zoning layouts when the grid/cluster thermal zoning method with four different LCC criteria (i.e., $r \geq 0.6$, $r \geq 0.7$, $r \geq 0.8$, $r \geq 0.9$) were applied to the example rectangle-shape simulation model. In general, regardless of the LCC values, the layouts were separated into interior and perimeter spaces, which is similar to the traditional core-perimeter zoning strategy. In addition, the perimeter spaces that are facing the same orientation were grouped as a single thermal zone. However, it was found that the thermal zoning layout starts to change for the interior spaces by varying the level of the linear correlation coefficients. When the linear correlation coefficient was set to 0.6, it yielded a similar thermal zoning layout to the traditional core-perimeter zoning layout. The layout has a single interior space and four different perimeter spaces along with each orientation. In addition, four unit spaces located at each corner of the simulation model became four unique different thermal zones. Consequently, it produced a total of nine[4] thermal zones for the simulation model. When the LCC value was increased to 0.7 or 0.8, the interior thermal zone separated into two different thermal zones. This was because only the thermal zones that had significantly similar indoor temperature profiles were grouped into the same thermal zone, which means that the grid/cluster thermal zoning method combines the thermal zones based on only slight differences in the indoor temperature profiles. In the same manner, when the LCC value was increased to 0.9, the interior thermal zone separated

[4] In general, the traditional core-perimeter thermal zoning method yields five thermal zones for a rectangular-shaped building.

into four different thermal zones. Similarly, when the grid/cluster thermal zoning method used a LCC of 0.9, 12 thermal zones resulted for the model.

Table 6: Thermal Zoning Layouts based on Different Correlation Coefficient Values for a Peak Day in the Summer in Houston, TX

Reference correlation coefficient	**Thermal zoning layout**	**Number of thermal zones**
$r \geq 0.6$	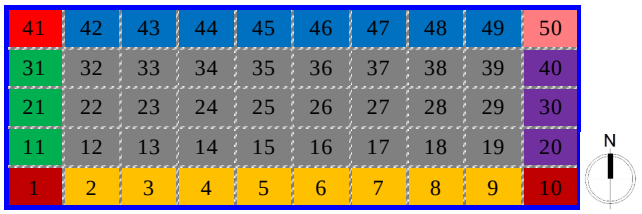	9
$r \geq 0.7$	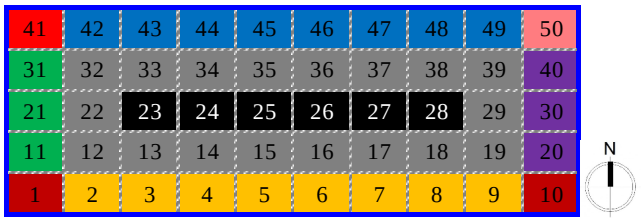	10
$r \geq 0.8$	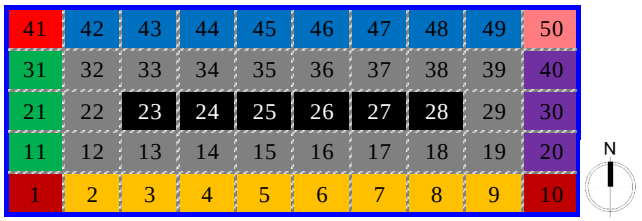	10
$r \geq 0.9$	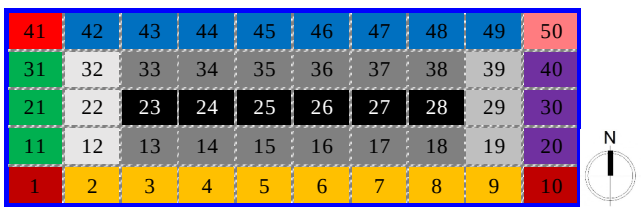	12

To investigate the differences in the indoor temperature profiles of interior thermal zones for a clear, peak day in the summer, the hourly indoor temperature profiles of the selected thermal zones (i.e., Zone 12, Zone 13, Zone 22, Zone 23) were calculated and plotted as shown in Figure 24 for the peak day cooling load (Figure 12). In addition, the LCC of the indoor temperature profiles between two corresponding thermal zones were calculated and plotted as shown in Figure 25. In the Figure 24, which is a time series plot for the selected thermal zones, by visually inspecting the patterns of the indoor temperature profile, it seems these four thermal zones are closely related to each other in terms of temperature behavior. However, it is possible to further group into two thermal zones, one for Zone 12 and Zone 13, and the other for Zone 22 and Zone 23. On the other hand, it was also found that there is about 2 °F difference between Zone 12 and Zone 23 at 08:00 pm. However, it is hard to conclude whether these differences are significant or not in the thermal zoning process. As shown in the Figure 25, the various levels of the LCCs that were calculated for all the zone combinations are a useful indicator. For example, if a user sets the linear correlation coefficient to 0.9 or higher as a numerical criteria for thermal zoning, only Zone 12 and Zone 22 could be grouped as a single thermal zone. On the contrary, if the LCC criteria was reduced to 0.6, all the selected interior zones could be considered as a single thermal zone.

Consequently, this example shows that the acceptance criteria of the LCC can significantly influence on the final layout of the thermal zoning and the total number of

thermal zones for a space. Therefore, it should be very carefully determined by the user based on the zones purpose.

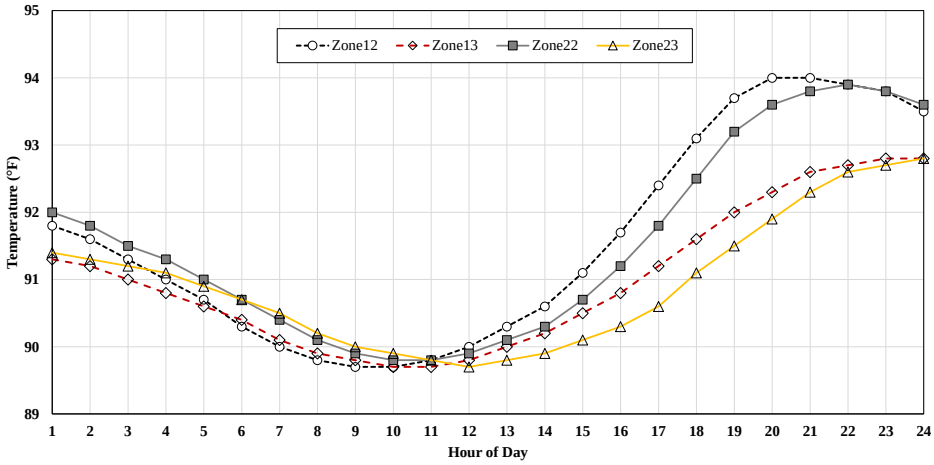

Figure 24: Indoor Temperature Profiles for Zone 12, Zone 13, Zone 22, Zone 23 for a Peak day in the Summer

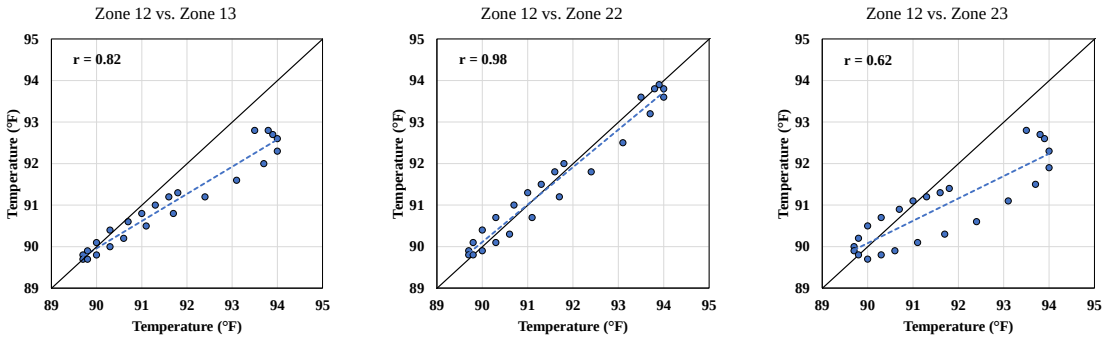

(a) Zone 12 vs. Zone 13 (b) Zone 12 vs. Zone 22 (c) Zone 12 vs. Zone 23

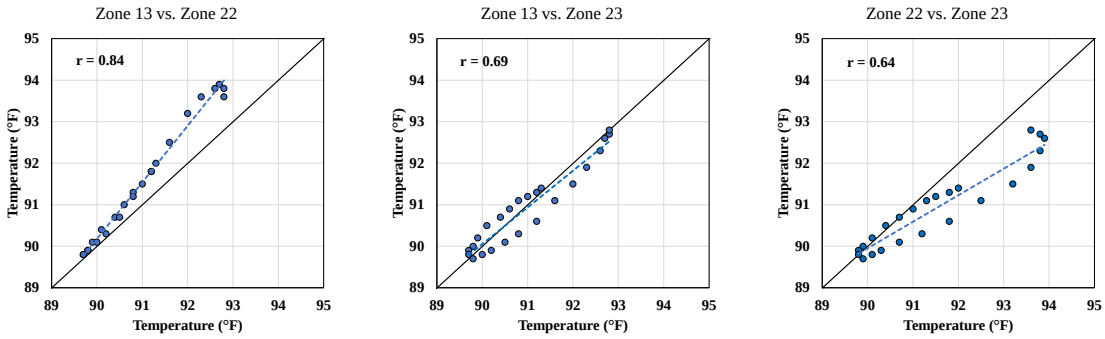

(d) Zone 13 vs. Zone 22 (e) Zone 13 vs. Zone 23 (f) Zone 22 vs. Zone 23

Figure 25: Correlation Coefficients between the Indoor Temperature Profiles of the Example Thermal Zones for a Peak day in the Summer

Table 7 shows the resultant set of thermal zoning layouts when the grid/cluster thermal zoning method with four different LCC criteria (i.e., $r \geq 0.6$, $r \geq 0.7$, $r \geq 0.8$, $r \geq 0.9$) were applied to the same example simulation model with the one that was shown in the previous analysis (Figure 23). However, this result is based on the analysis of the 24-hour indoor temperature profiles for a clear, peak day in the winter (Figure 13). In the same manner as the previous analysis, regardless of the LCC values, the layouts were separated into interior and perimeter spaces. In addition, the perimeter spaces that are facing the same orientation were grouped into a single thermal zone. For example, when the LCC set to 0.6 or 0.7, it gave a similar thermal zoning layout to that from the traditional core-perimeter zoning layout (i.e., five thermal zones). As shown in Table 7, the layout has a single interior space and four different perimeter spaces along with each orientation (i.e., $r = 0.6$ or $r = 0.7$). In addition, the four thermal zones located at each corner of the model became four different thermal zones.

If the LCC value was increased to 0.8 or 0.9, it gave two different sets of thermal zoning layouts, respectively. The shape of these two layouts were totally different with the one that was created in the previous analysis for a clear, peak day in the summer. These results indicate that the thermal zoning layout based on the 24-hour indoor temperature profile was significantly influenced by the outdoor weather condition such as the outdoor temperature and the degree of solar radiation. For example, the thermal zones in interior space for $r = 0.9$ were grouped horizontally along with the north and south walls for the winter day. In contrast, as shown in the Table 6, these thermal zones

for the interior space for the summer day were grouped into the traditional core-perimeter thermal zoning.

Table 7: Thermal Zoning Layouts Based on Different Correlation Coefficient Values for a Peak Day in the Winter in Houston, TX

Reference correlation coefficient	**Thermal zoning layout**	**Number of thermal zones**
$r \geq 0.6$	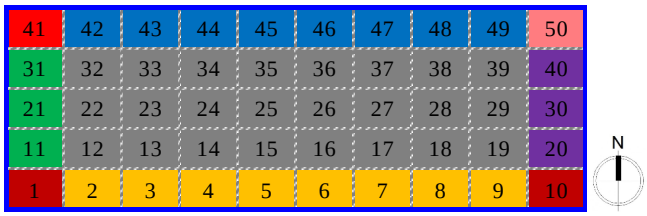	9
$r \geq 0.7$	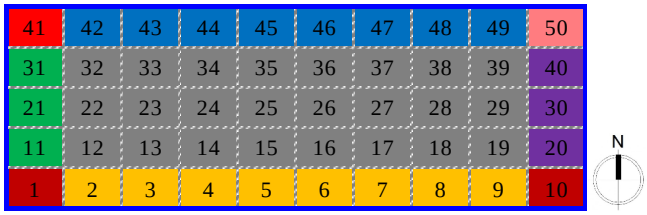	9
$r \geq 0.8$	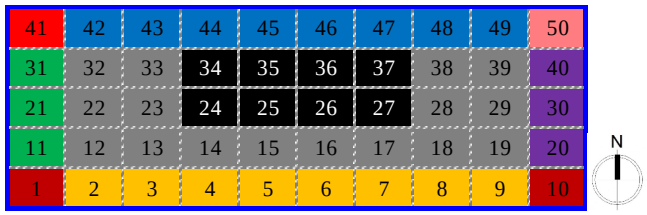	10
$r \geq 0.9$	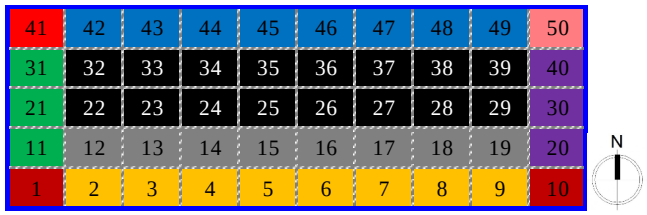	10

As same as the previous analysis, to investigate the differences in the indoor temperature profiles of interior thermal zones for a clear, peak day in the winter, the hourly indoor temperature profiles of the selected thermal zones (i.e., Zone 12, Zone 13, Zone 22, Zone 23) were calculated and plotted as shown in Figure 26. Also, the LCC of the indoor temperature profiles between the corresponding thermal zones were calculated and plotted as shown in Figure 27. In the Figure 26, which is a time series plot for the selected thermal zones, by visually inspecting the patterns of the indoor temperature profile, it seems these four unit spaces are closely related each other as same as the summer in terms of temperature behavior. Especially, it is possibly grouped into two thermal zones, one for Zone 12 and Zone 13, and the other for Zone 22 and Zone 23. On the other hand, it was also found that there is about 2.5 °F difference between Zone 13 and Zone 22 at 04:00 pm during the day. As shown in Figure 27, various levels of the LCC that were calculated for all the combinations of the selected unit spaces were presented. If a user set the LCC of 0.9 as numerical criteria for thermal zoning, Zone 12 / Zone 13 and Zone 22 / Zone 23 are supposed to be grouped as a single thermal zone, respectively. On the contrary, if the LCC is reduced to 0.6, all the selected unit spaces can be considered as a single thermal zone.

Consequently, the analysis for the example simulation model for both the summer and winter day indicates that the thermal zoning layout can be varied by season. Therefore, this should be considered when the designer decides the thermal zoning layout for the HVAC system design for the building.

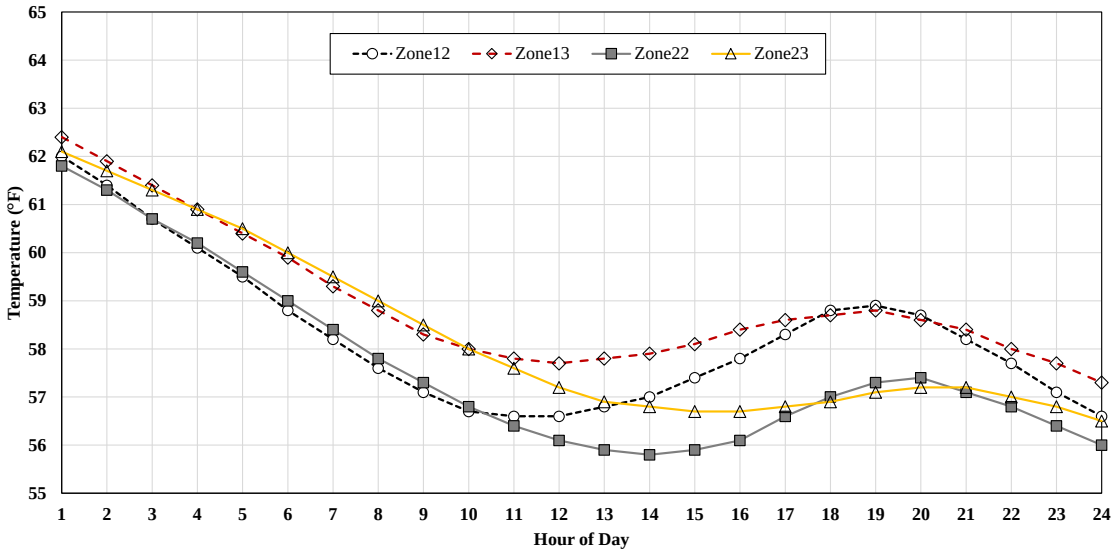

Figure 26: Indoor Temperature Profiles for Zone 12, Zone 13, Zone 22, Zone 23 for a Peak day in the Winter

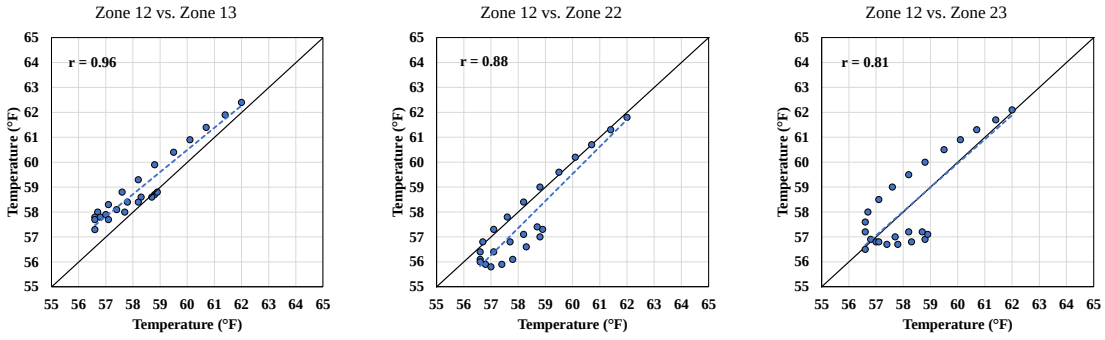

(a) Zone 12 vs. Zone 13 (b) Zone 12 vs. Zone 22 (c) Zone 12 vs. Zone 23

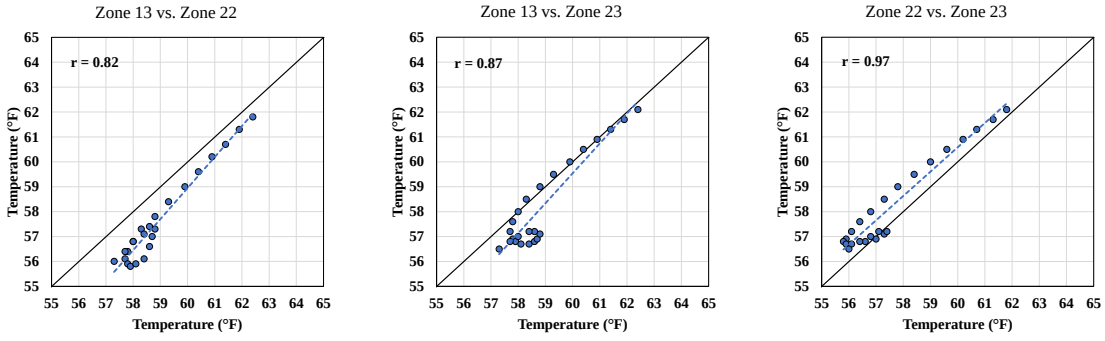

(d) Zone 13 vs. Zone 22 (e) Zone 13 vs. Zone 23 (f) Zone 22 vs. Zone 23

Figure 27: Correlation Coefficients between the Indoor Temperature Profiles of the Example Thermal Zones for a Peak day in the Winter

4.2. Development of a Simplified Commercial Base-Case Model

This section provides details about the procedure to develop the simplified commercial building base-case models used in this study. In order to investigate the validity of the new thermal zoning method for whole-building energy simulation for commercial buildings, a base-case simulation model was developed based on the minimum requirements of ASHRAE Standard 90.1-2013, which vary by climate zone.

4.2.1. Climate Conditions

In this study, hourly building envelope energy loads (i.e., heating/cooling envelope loads) were calculated using a whole-building energy simulation for several different configurations of thermal zoning layouts. In general, numerous parameters influence the thermal loads for a building such as site location, climatic condition, envelope properties, etc. One of the most important environmental factors that designers and engineers need to consider when designing a building is the building's surrounding climate. The hourly building energy loads were constructed using the grid-based, thermal zoning method, developed in this study to help group those spaces experiencing similar thermal loads.

In order to analyze the impacts of different climatic conditions on building thermal zoning strategy, two locations in the US were selected, one for a cooling dominated climate and the other for heating dominated climate, as described in Table 8. The selected sites, Houston, TX and Chicago, IL, represent 'hot and humid' and 'cold

and humid' climatic characteristic, respectively, which represent weather Zone 2A and weather Zone 5A (Baechler et al. 2010).

Table 8: Description of Selected Locations for the Simulation Models

Climate Zone	**Representative City**	**Climate Feature**	**TMY3 Weather File Location**
Zone 2A	Houston, TX	Hot and Humid	Chicago Ohare International Airport
Zone 5A	Chicago, IL	Cold and Humid	Houston George Bush International Airport

Figure 29 and Figure 30 show the hourly outdoor weather conditions of four weather variables (i.e., Dry-bulb temperature, ground temperature, wind speed, global solar radiation) for a hot/cold, clear day for Chicago, respectively. These two days were chosen as representation of the cooling and heating season to be used for the grid/thermal zoning process (See Section 4.1.3.7). The climatic information of the two selected days for Houston was shown in Figure 12 and Figure 13 in Section 4.1.3.7.

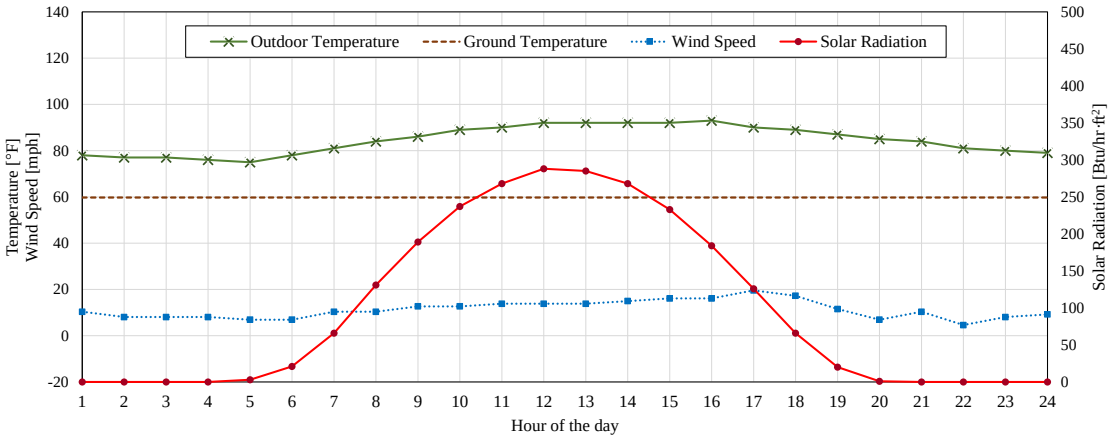

Figure 28: Weather Conditions for the Hot, Clear day (July 18) in Chicago, IL

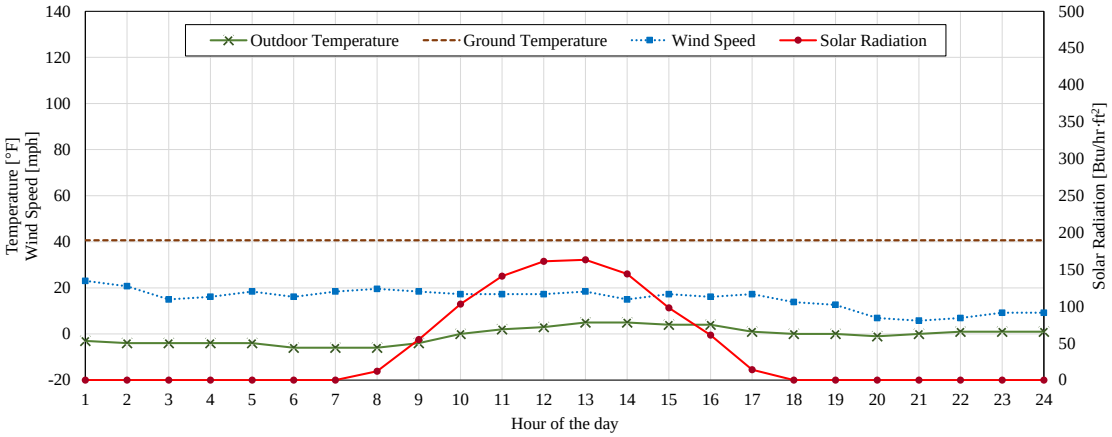

Figure 29: Weather Conditions for the Cold, Clear Day (January 27) in Chicago, IL

4.2.2. Model Description

This section provides a detailed description and procedure to develop the simplified commercial base-case model that was used for this study. In general, the base-case model was based on the "Run 3A" model, which is one of the default models that is included in the "samp1e" DOE-2.1e input file. In the analysis, the building shape and geometry of the base-case model was maintained the same as the "Run 3A" model, since

this is similar to the representative small office building model for EnegyPlus, which was developed by the National Renewable Energy Laboratory (NREL) (Deru et al. 2011).

Figure 30 and Figure 31 show the 3D view of the small office building model developed by NREL and RUN 3A model, respectively. In the NREL model and the Run 3A model have a floor area of 5,000 ft^2, with an 8 foot floor-to-ceiling height, and a 2 foot plenum height. Also, both are a single-story building. The differences between two models in terms of the geometry information, the Run 3A model has 30 degrees azimuth, while the NREL model is facing south. Also, the shape of roof for NREL model is a hip roof, and RUN 3A model has a flat roof.

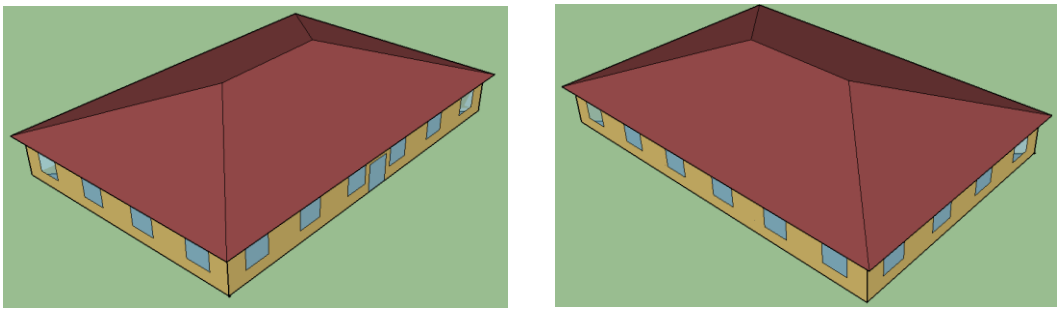

(a) Southwest View (b) Northwest View

Figure 30: View of a Small Office Building Model Developed by NREL

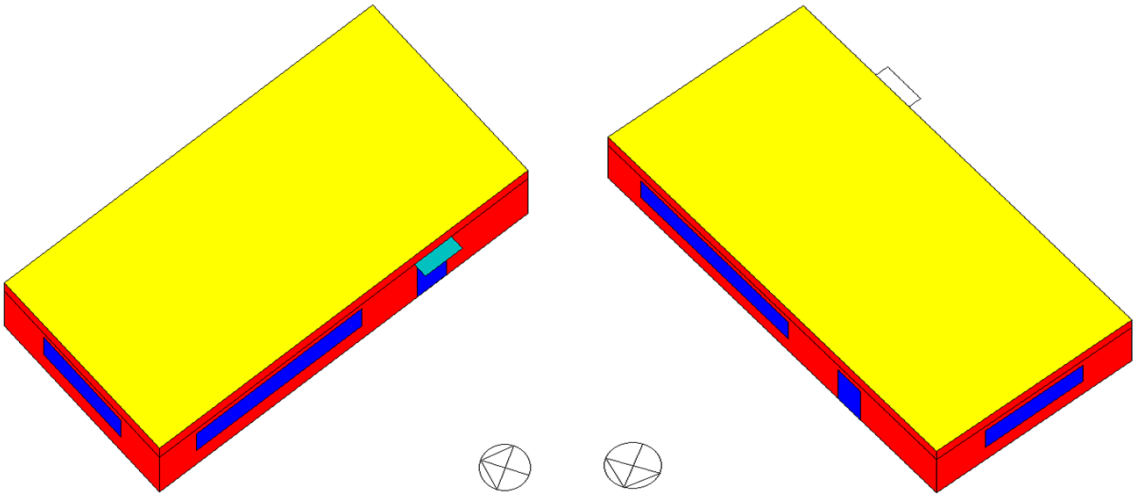

(a) Southwest View (b) Northwest View

Figure 31: View of the RUN 3A Model in the SAMPLE DOE-2 File (Huang 1993)

The base-case models were developed based on the geometric data of the RUN 3A model and the minimum requirements of building envelope required by ASHRAE Standard 90.1-2013 for Houston, TX and Chicago IL. Other input parameters that was not stated in the standard used the U.S. DOE Reference Models (Deru et al. 2011).

Specification of the base-case model input data for the two locations (i.e., Houston and Chicago) regarding the building envelope parameters are listed in Table 9. Unfortunately, ASHRAE Standard 90.1-2013 does not provide detailed inputs for all the simulation input parameters such as wall and roof construction types and layers. Therefore, it was necessary to combine information from the U.S. DOE Reference Models and the insulation requirements of the ASHRAE Standard 90.1-2013 to define all the parameters of the building envelope.

Table 9: Inputs for Building Envelop Parameters in the Base-Case Models

Simulation Input Parameters	Input Value/Attribute	
	Houston	**Chicago**
Exterior Walls	• U=0.089 Btu/hr-ft^2-°F; • Construction Layers: 1" Stucco, 5/8" Gypsum-Board, R10-Insulation, 5/8" Gypsum-Board	• U=0.051 Btu/hr-ft^2-°F; • Construction Layers: 1" Stucco, 5/8" Gypsum-Board, R16-Insulation, 5/8" Gypsum-Board
Interior Walls	• U=1.5 Btu/hr-ft^2-°F; Air Wall	• U=1.5 Btu/hr-ft^2-°F; Air Wall
Floor	• U=0.033 Btu/hr-ft^2-°F; • Slab-on-grade using Winkelmann's method; • Construction layers: A fictitious insulating layer, 1' Soil, 4" Heavy Weight Concrete	• U=0.033 Btu/hr-ft^2-°F; • Slab-on-grade using Winkelmann's method; • Construction layers: A fictitious insulating layer, 1' Soil, 4" Heavy Weight Concrete
Roof	• U=0.041 Btu/hr-ft^2-°F; • Construction layers: 0.03" Metal Surface, R25 Roof Insulation, 0.36" Built-up Roof	• U=0.021 Btu/hr-ft^2-°F; • Construction layers: 0.03" Metal Surface, R30 Roof Insulation, 0.36" Built-up Roof
Fenestration	• U=0.40 Btu/hr-ft^2-°F; • Specifications: Double pane glass, Shading-Coefficient: 0.25	• U=0.32 Btu/hr-ft^2-°F; • Specifications: Double pane glass, Shading-Coefficient: 0.40
Weather fie	• Houston-Bush Intercontinental AP 722430 (TMY3)	• Chicago-OHare Intl AP 725300 (TMY3)

In this study, the thermal loads from envelope heat transfer to each thermal zone in the base-case models were calculated and compared. All other heat generation sources were neglected. Therefore, the model does not have any ventilation or infiltration loads. In addition, the model does not contain internal heat sources such as occupants, lighting, and equipment. Finally, the system-type 'SUM' was used to simulate the energy consumption (i.e., thermal loads only) by thermal zone or group of thermal zones, which does not include any other system effects (LBNL 1984). Figure 32 shows 3D views of the base-case model that was used for this study. In addition, the plan view of the base-case model and its thermal zoning layout is shown in the Figure 33. As shown in the figure, the base-case model is composed of 50 unit spaces (i.e., thermal zones).

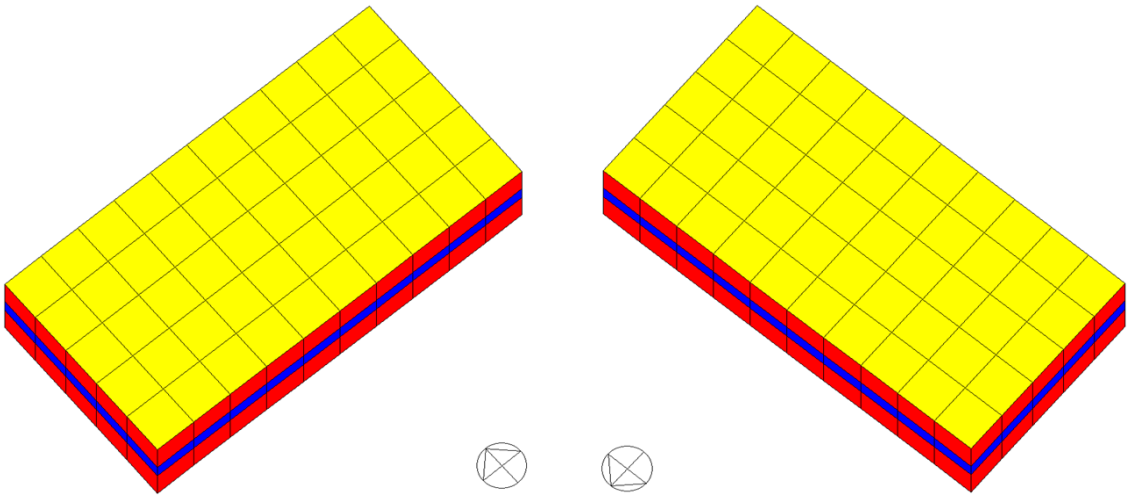

(a) Southwest View (b) Northwest View

Figure 32: View of the Simplified Commercial Base-case Model

41	42	43	44	45	46	47	48	49	50
31	32	33	34	35	36	37	38	39	40
21	22	23	24	25	26	27	28	29	30
11	12	13	14	15	16	17	18	19	20
1	2	3	4	5	6	7	8	9	10

Figure 33: Plan View of the Simplified Commercial Base-case Model

4.3.Parametric Study on Different Configurations of Thermal Zoning

The primary objective of this study is to develop and provide a detailed, automated procedure for a thermal zoning strategy of a commercial building for use with building energy simulation programs. Such a model can be used to calculate peak heating and cooling load and annual energy use, while at the same time maintaining indoor thermal comfort. In order to identify building features that are most likely to have the greatest impact on the thermal zoning approach, a parametric analysis was developed that uses a simplified commercial base-case model with varying simulation scenarios.

There are numerous parameters that may affect a thermal zoning strategy in regard to heat transfer, which include: building shape, Window-to-Wall Ratio (WWR), location or climate condition. Based on the results from the parametric study of each factor, an automatic thermal zoning procedure for building energy simulation is proposed. Figure 34 shows the overall research methodology and steps taken in this study. At first, the building parameters that may affect a thermal zoning method were considered based on the literature review, which include: climate condition, building

shape, construction type, window-to-wall ratio, and orientation of windows. This five groups of parameters have sub-parameters, respectively. For the climate condition, as described earlier, significantly different two weather conditions are considered for this study, which are Houston (Hot and Humid) and Chicago (Cold and Humid). For the building shape, the most typical commercial building shape (i.e., rectangular shape) and L-shaped building geometry were used and applied to the base-case model. These two different shaped simulation models are composed of the same size and number of the grid-base unit space, which means that two models have an identical building area and volume. For the construction type, it was assume that the heat transfer between the building and the ground may have influence on the thermal zoning strategy. Therefore, the slab-on-grade floor using "Winkelmann's ground coupling method" (Winkelmann 2002) was adopted for the simulation model. Also, the raised insulated floor, which uses the same insulation property with one that uses for the exterior wall in the model. The models that are having offset windows were used for the simulation, since this can creates the interior spaces that do not have any windows toward outside. For the window-to-wall ratio, to investigate the influence of solar radiation on the thermal zoning method, three different window-to-wall ratio were used, which include: 0%, 50%, and 80%. Furthermore, the orientation of windows can be regarded as one of the important factors that influence on the heating/cooling loads of the building. Therefore, various cases for the different location of the windows along with four orientations (i.e., North, East, South, West) were considered for the simulation model. All the parameters that were described here are shown in the Figure 35. This figure shows how the all the

different parametric test cases and the combinations of the building parameters were developed for the parametric study. A total 68 simulation cases were created based on the combinations of all these parameters. The detailed information of each parametric study cases can be found in the Appendix A. Afterward, the proposed thermal zoning method (i.e., Grid/Cluster method) was applied to all the 68 simulation cases. Using these simulation models, the hourly indoor temperature and heating/cooling loads for each model were calculated and analyzed. Based on the analysis results, the automatic thermal zoning procedure for building energy simulation was proposed.

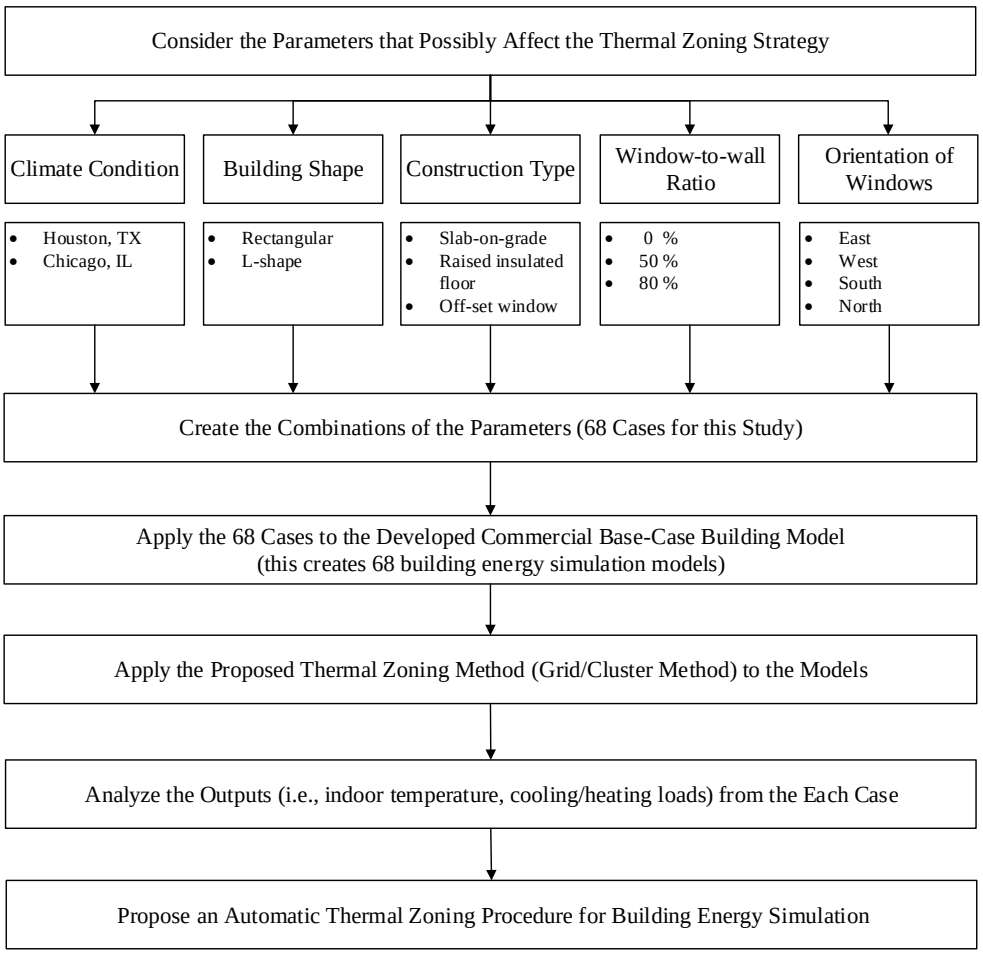

Figure 34: Overall Research Methodology

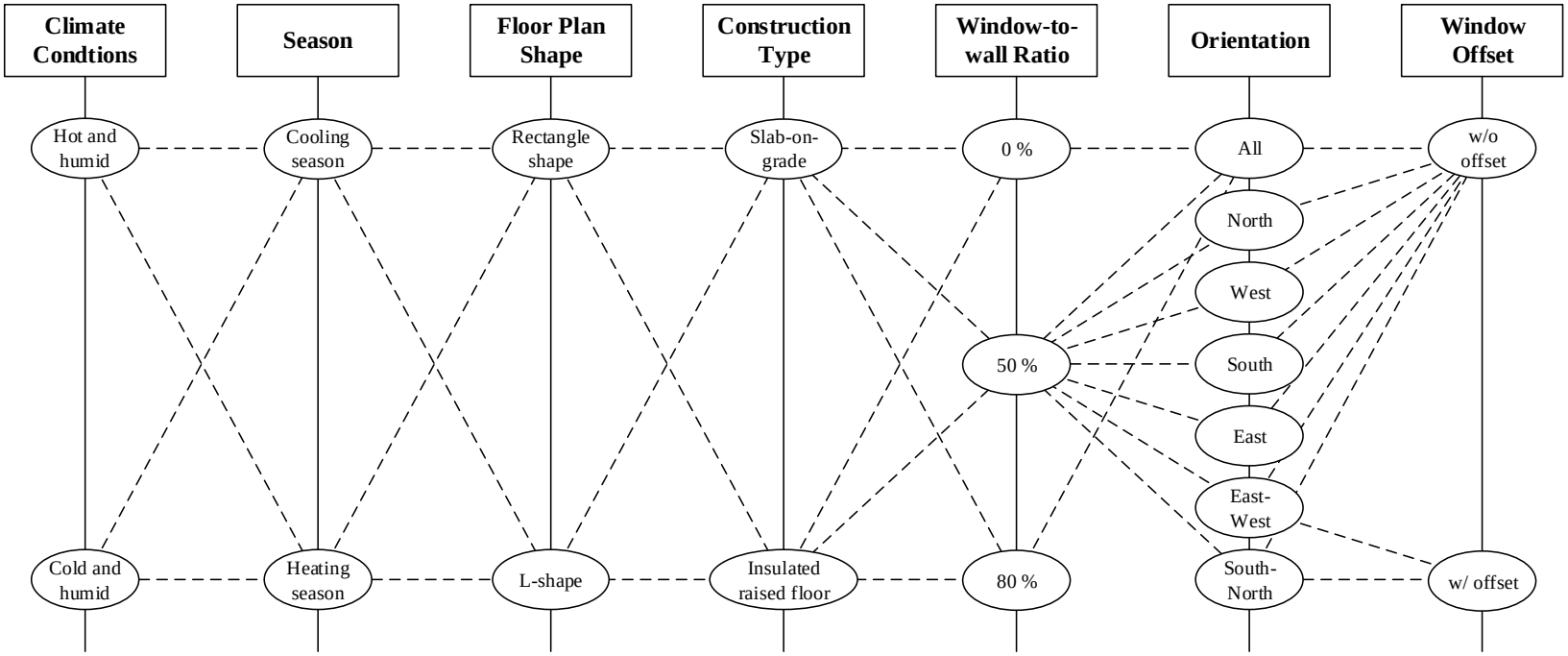

Figure 35: Parametric Study Diagram

4.3.1. Impact of Building Shape on Thermal Zoning

In this study, in order to investigate how the building shape impacts the building thermal zoning in a simulation, two different plans (i.e., rectangle-shape and L-shape) were chosen and modeled using a building energy simulation program (i.e., DOE-2.1e). As described earlier, each building shape model has an identical floor area of 5,000 ft^2. In the analysis, all the models have the same floor area (i.e., number of thermal zones), and the size of a unit thermal zone is 100 ft^2 (10 ft by 10 ft). Therefore, a total of 50 thermal zones were assigned to all models. All other parameters, except the shape of the model (i.e., model geometry), were kept the same as the base-case model. Figure 36 and Figure 37 show the 3D view of the rectangle-shape and L-shape models that were used in the analysis, respectively.

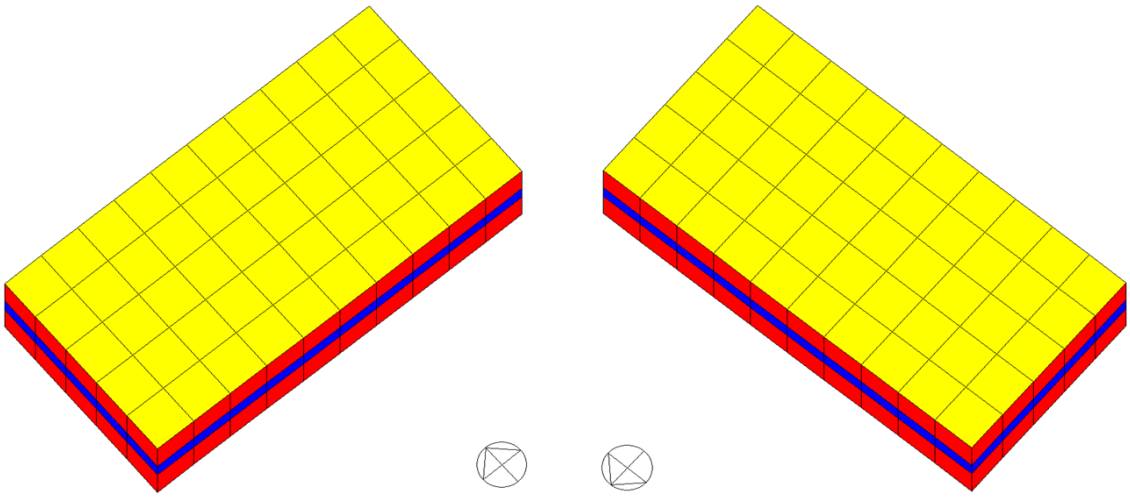

(a) Southwest View (b) Northwest View

Figure 36: View of Rectangle-shape Simulation Model

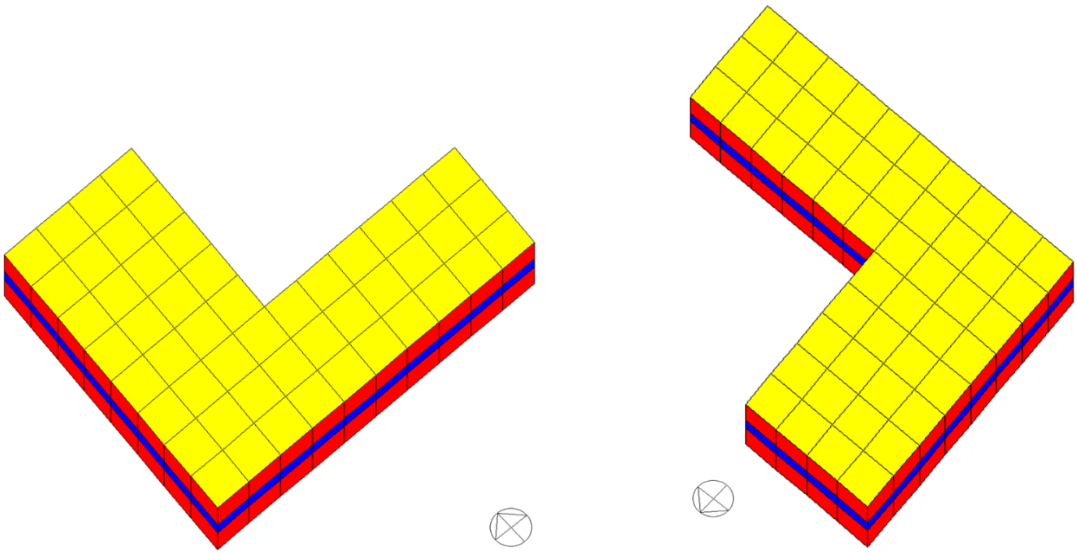

(a) Southwest View (b) Northwest View

Figure 37: 3D View of L-shape Simulation Model

For the parametric study, these two building shapes were analyzed by varying the window-to-wall ratio (0, 50%), and construction type (slab-on-grade) in two different climates (i.e., Houston and Chicago). All input values in the simulations remained the same as the base-case model, and all of the simulation models analyzed in this section are described in Table 10. At first, the grid/cluster thermal zoning method was applied to all the cases, and the building energy simulations were performed. The hourly indoor temperature and heating/cooling loads for each case were calculated and analyzed. In addition, using these output data it was investigated how the building shape has impact on the thermal zoning method and peak heating/cooling loads.

Table 10: Parametric of the Building Energy Simulation Runs on Building Shapes

Case #	Building Shape	Climate	Construction type	Window-to-wall Ratio
1	Rectangle	Houston	1-story w/ slab-on-grade	0%
2	Rectangle	Houston	1-story w/ slab-on-grade	50%
3	Rectangle	Chicago	1-story w/ slab-on-grade	0%
4	Rectangle	Chicago	1-story w/ slab-on-grade	50%
5	L-shape	Houston	1-story w/ slab-on-grade	0%
6	L-shape	Houston	1-story w/ slab-on-grade	50%
7	L-shape	Chicago	1-story w/ slab-on-grade	0%
8	L-shape	Chicago	1-story w/ slab-on-grade	50%

4.3.2. Impact of Window-to-wall Ratio on Thermal Zoning

In the current study, the implications of the WWR of the façade in each orientation of the simulation model on the building thermal zoning in simulation was investigated. Three different WWR were implemented in the simulation model: WWR = 0% , 50%, 80%. Figure 38 shows the geometric information of the façade modules that used in this study. All the different WWR façades that was shown in the figure were implemented in the simulation models. In addition, all the simulation cases used in the parametric analysis in this section are listed in Table 11. In a similar fashion with the analysis described in previous section, the grid/cluster thermal zoning method was applied to all the cases, and the building energy simulations were performed. The hourly indoor temperature and heating/cooling loads for each case were calculated and analyzed. In addition, using these output data it was investigated how the building shape has impact on the thermal zoning method and peak heating/cooling loads.

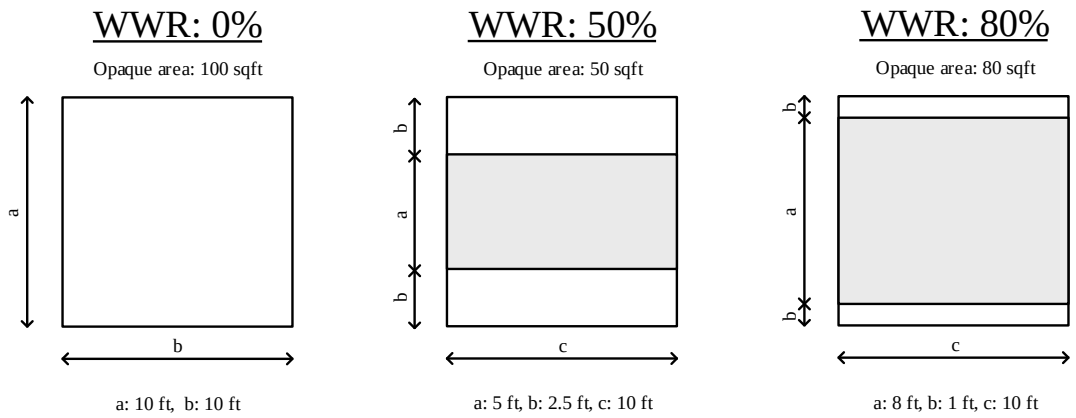

Figure 38: Geometric Characteristics of the Different WWR façades Cases

Table 11: Parametric of the Building Energy Simulation Runs on WWR

Case #	Climate	Building shape	Construction type	Window-wall ratio			
				East	West	North	South
1	Houston	Rectangle	1-story, S-O-G	0%	0%	0%	0%
2	Houston	Rectangle	1-story, S-O-G	50%	50%	50%	50%
3	Chicago	Rectangle	1-story, S-O-G	0%	0%	0%	0%
4	Chicago	Rectangle	1-story, S-O-G	50%	50%	50%	50%
9	Houston	Rectangle	1-story, S-O-G	80%	80%	80%	80%
10	Houston	Rectangle	1-story, S-O-G	50%	0%	0%	0%
11	Houston	Rectangle	1-story, S-O-G	0%	50%	0%	0%
12	Houston	Rectangle	1-story, S-O-G	0%	0%	50%	0%
13	Houston	Rectangle	1-story, S-O-G	0%	0%	0%	50%
14	Chicago	Rectangle	1-story, S-O-G	80%	80%	80%	80%
15	Chicago	Rectangle	1-story, S-O-G	50%	0%	0%	0%
16	Chicago	Rectangle	1-story, S-O-G	0%	50%	0%	0%
17	Chicago	Rectangle	1-story, S-O-G	0%	0%	50%	0%
18	Chicago	Rectangle	1-story, S-O-G	0%	0%	0%	50%
19	Houston	Rectangle	1-story, S-O-G	50%	50%	0%	0%
20*	Houston	Rectangle	1-story, S-O-G	50%	50%	0%	0%
21	Houston	Rectangle	1-story, S-O-G	0%	0%	50%	50%
22*	Houston	Rectangle	1-story, S-O-G	0%	0%	50%	50%
23	Chicago	Rectangle	1-story, S-O-G	50%	50%	0%	0%
24*	Chicago	Rectangle	1-story, S-O-G	50%	50%	0%	0%
25	Chicago	Rectangle	1-story, S-O-G	0%	0%	50%	50%
26*	Chicago	Rectangle	1-story, S-O-G	0%	0%	50%	50%

Note: S-O-G indicates slab-on-grade construction type for the floor in the model.

* The windows in this case were installed on a half of the exterior walls.

4.3.3. Impact of Climate Conditions on Thermal Zoning

As shown in the previous studies, local weather or local climate conditions are important drivers for cooling and heating loads in buildings. Consequently, this phenomenon may result in different thermal zoning strategies, according to the climate conditions.

Therefore, in this study the parametric study was carried out for two climate conditions (i.e., Chicago and Houston). A typical city representing each climate condition (i.e., hot and humid/cold and humid) was selected and its Typical Meteorological Year, 3rd generation (TMY3), weather data were used in the simulations. Table 12 shows the parameters of the building energy simulation runs for the two climate conditions. All the models used in this section has identical WWR of 50%. Two different construction types, three different building shape of models were simulated for each of the two cities.

Table 12: Parametric of the Building Energy Simulation Runs on Climate Conditions

Case	Building Shape	Climate	Construction type	Window-to-wall Ratio
2	Rectangle	Houston	1-story w/ slab-on-grade	50%
4	Rectangle	Houston	1-story w/ elevated floor	50%
7	Rectangle	Chicago	1-story w/ slab-on-grade	50%
8	Rectangle	Chicago	1-story w/ elevated floor	50%
11	L-shape	Houston	1-story w/ slab-on-grade	50%
12	L-shape	Houston	1-story w/ elevated floor	50%
15	L-shape	Chicago	1-story w/ slab-on-grade	50%
16	L-shape	Chicago	1-story w/ elevated floor	50%

4.4.Summary of the Methodology

A proposed methodology to develop an automated procedure for thermal zoning of commercial buildings for whole-building energy simulation has been described in this chapter. In order to accomplish this, the following tasks were accomplished which include:

1) A new thermal zoning method (i.e., a grid/cluster method) for building energy simulation was developed. The grid/cluster thermal zoning method is basically using simulated annual heating/cooling loads for each grid space to group the spaces that have significantly similar thermal load profiles. Once the preliminary thermal zoning layout was created, the user can select a degree of correlation coefficient for the indoor temperature profiles of each space to calibrate the thermal zoning layout.

2) A simplified, commercial base-case model was developed based on the information from the NREL commercial building model, "Run 3A" DOE-2 simulation model, and ASHRAE Standard 90.1-2013. This model was used extensively for the development of a new thermal zoning method and the parametric analysis in this study.

3) Parametric studies of different configurations of thermal zones. These parametric studies will be used to evaluate several influential parameters, including: 1) Impact of building shape on the proposed thermal zoning method; 2) Impact of window-to-wall ratio on the proposed thermal zoning method; and 3) impact of climate conditions on the proposed thermal zoning method.

The results of the parametric studies described in this chapter will be discussed in Chapter 5.

CHAPTER V

RESULTS OF PARAMETRIC STUDY ON THERMAL ZONING

This chapter presents the results of a parametric simulation study, where the proposed new thermal zoning method (i.e., grid/cluster thermal zoning method) was applied to all cases and its resultant thermal zoning layouts were compared to investigate if there were any differences between the cases. The results are presented in the following sections. In Section 5.1, an analysis of the impact of building shape on thermal zoning is presented. In Section 5.2, the analysis of the impact of window-to-wall ratio on thermal zoning is presented. Finally, in Section 5.3 the analysis of the impact of climate conditions on thermal zoning is presented. For each case, the simulated indoor temperature profiles for a clear, peak day in the summer and winter seasons were examined. In addition, the simulated annual heating/cooling loads and peak daily heating/cooling loads were compared to investigate if changes to the thermal zoning reduced the building's energy use.

5.1. Analysis of the Impact of Building Shape on Thermal Zoning

In this section, the impact of the building shape on the building thermal zoning in a simulation was examined. To accomplish this, two different building shapes (i.e., rectangle-shape and L-shape) were chosen and modeled using a building energy simulation program (i.e., DOE-2.1e Version 119). The impact of the thermal zoning layouts, which were created using the grid/cluster thermal zoning method, were

compared between the rectangle-shape and L-shape models. In the analysis other all input parameters and other conditions were identical (See Table 9 in Section 4.2.2), except the shape of the model (i.e., model geometry). In the analysis, the simulated indoor temperature profiles for the thermal zones (i.e., north, east, south, west, and interior space) were compared and examined. Finally, the calculated annual heating/cooling loads and daily peak heating/cooling loads for each case were compared for the different case to determine if any changes to the building's energy use occurred.

5.1.1. Comparison of Thermal Zoning Layout for Varying Building Shapes

In this subsection, the resultant thermal zoning layouts of four different simulation models with two different climate conditions (i.e., Hot and Humid, Cold and Humid) were examined using the grid/cluster thermal zoning method. In addition, the hourly indoor temperature profiles of each simulation case for the clear, hot/cold days in each climate were simulated and presented. In Subsection 5.1.1.1, the analysis of the rectangle-shape simulation model with only opaque walls (i.e., no exterior windows) is presented. In Section 5.1.1.2, the analysis of the rectangle-shape simulation model with exterior windows is presented. In Section 5.1.1.3, the analysis of the L-shape simulation model with only opaque walls (i.e., no exterior windows) is presented. Finally, in Section 5.1.1.4, the analysis of the L-shape simulation model with exterior windows is presented.

5.1.1.1. Thermal Zoning Layouts for Case 1 (Houston, TX) and Case 3 (Chicago, IL)

Figure 39 shows images of the building geometry for the Case 1 and Case 3 simulation models. Using the same model geometry, a Houston TMY3 weather file was used for the Case 1, while a Chicago TMY3 weather file was used for the Case 3 model.

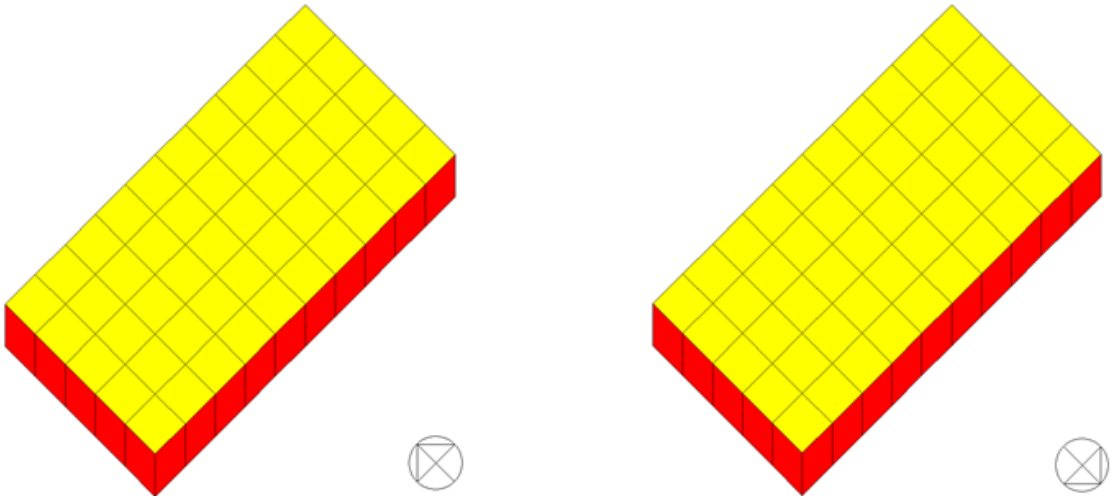

(a) Southwest View (b) Northeast View

Figure 39: View of Case 1 and Case 3 Models in the Simulation (w/o windows)

Table 13 presents the main features of the Case 1 and Case 3 simulation models. In the analysis, the Houston and Chicago TMY3 weather files were used for the simulation runs for the hot and cold climates, respectively. In the Case 1 and Case 3 simulation models the building was simulated with only opaque walls (i.e., no exterior windows). Therefore, direct solar radiation did not penetrate directly inside of the building through the windows. In each model, 50 thermal zones were simulated. Then,

the new grid/cluster thermal zoning method was applied to the models. During the thermal zoning process, a linear correlation coefficient was used to compare the interior temperature profiles. In this analysis a correlation of 0.8 or higher was used to combine the thermal zones with those that had similar indoor temperature profiles during "free-floating" conditions. The grid/cluster thermal zoning method gave a total of nine thermal zones for the Case 1 and Case 3 models for both the cooling and heating seasons.

Table 13: Main Features of the Case 1 and Case 3 Simulation Models

	Case 1 / Case 3
Building Location	Houston, TX for Case 1 Chicago, IL for Case 3
Window-to-wall Ratio	WWR: 0 % (no windows)
Floor Area	5,000 ft^2
Slab Type	Slab-on-grade
Thermal Zoning Method	The grid/cluster thermal zoning method
Linear Correlation Coefficient Used	0.8
Initial Number of Thermal Zones	50
Number of Resultant Thermal Zones	Case 1: 9 zones for heating/cooling season Case 5: 9 zones for heating/cooling season

The resultant thermal zoning layouts of the Case 1 simulation model (i.e., Houston) for the cooling and heating seasons for the building with only opaque walls are presented in Figure 40. The resultant thermal zoning layouts show that there was no difference between the thermal zoning layouts for the cooling and heating season when a

0.8 was chosen. Specifically, the grid/cluster thermal zoning method gave a similar result as the traditional core-perimeter thermal zoning method. The results show a single interior thermal zone and four different thermal zones for each orientation. In addition, the four individual zones located at each corner of the model became four different thermal zones.

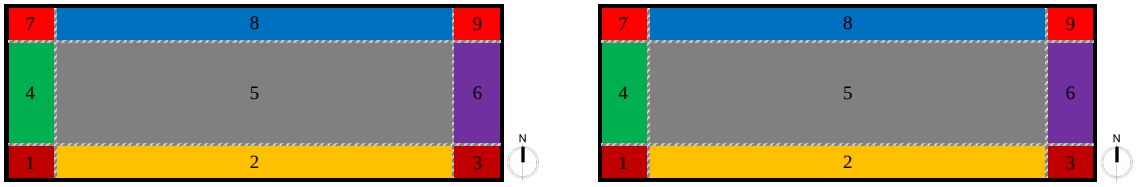

(a) For Cooling Season (b) For Heating Season

Figure 40: Resultant Thermal Zoning Layouts for Case 1 (Houston, TX)

Figure 41 shows the simulated hourly indoor temperature profiles of the resultant thermal zones for the Case 1 simulation model (i.e., no exterior windows). For a clear, hot day (i.e., August 2) in the cooling season, the results show that a maximum hourly temperature of 89.7 °F was found at 7:00 pm in Zone 7. In addition, a minimum hourly temperature of 85.7 °F was found at 8:00 am in Zone 7. The difference between a maximum and minimum hourly indoor temperatures was 4.0 °F. For a clear, cold day (i.e., February 11) in the heating season, the results show that a maximum hourly temperature of 59.0 °F was found at 1:00 am in Zone 5. In addition, a minimum hourly temperature of 55.4 °F was found at 11:00 pm in Zone 9. The difference between maximum and minimum hourly indoor temperatures for this day was 3.6 °F. In addition,

it was found that the slope of the indoor temperature profiles from 1 am through 7 am, which is before sun rise, are very similar for a clear peak summer and winter day.

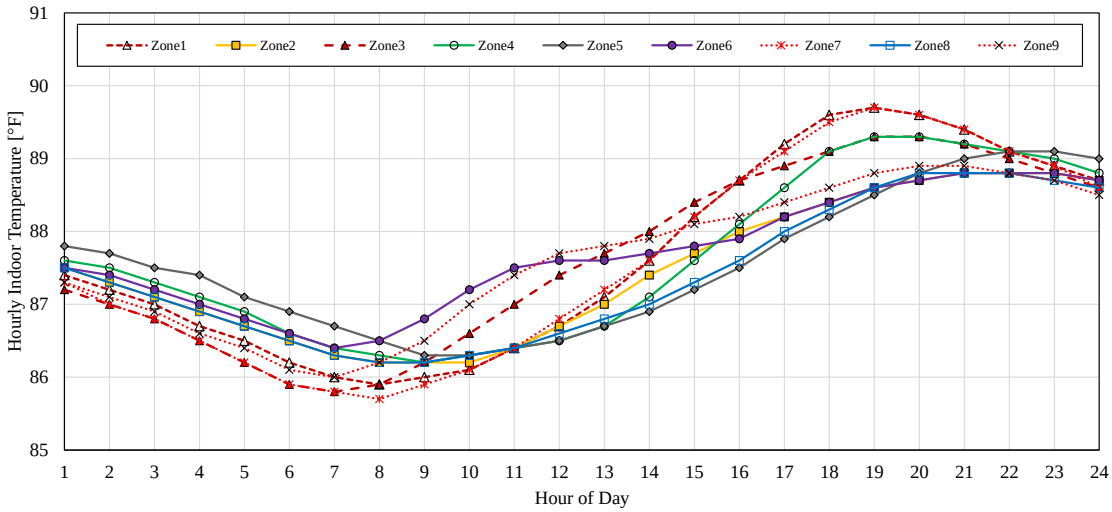

(a) For a Clear Peak Day in Cooling Season (August 2) for Houston, TX

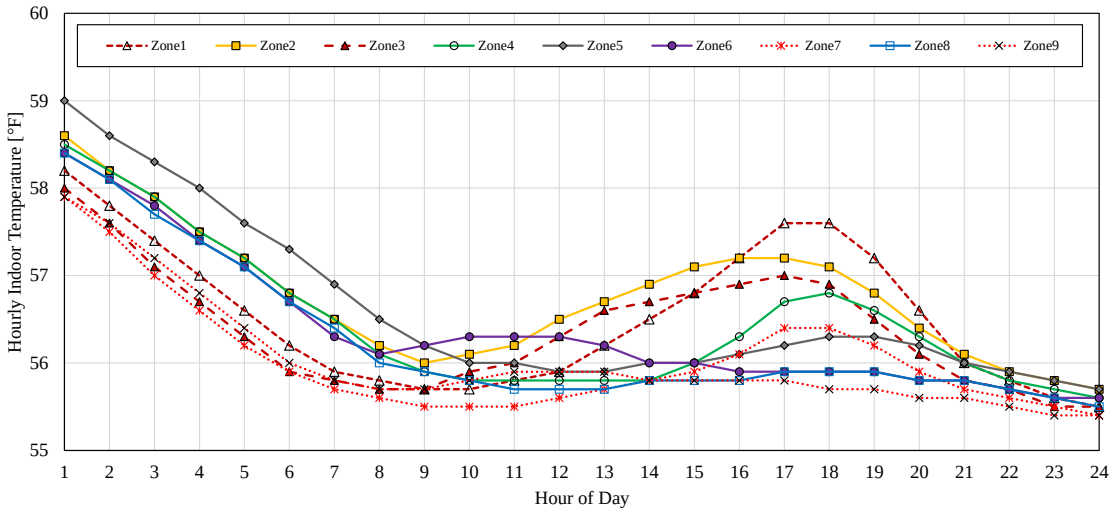

(b) For a Clear Peak Day in Heating Season (February 11) for Houston, TX

Figure 41: Indoor Temperature Profiles of Thermal Zones for Case 1 (Houston, TX)

The resultant thermal zoning layouts of the Case 3 simulation model (i.e., Chicago) for the cooling and heating seasons for the building with only opaque walls are presented in Figure 42. The resultant thermal zoning layouts show that there is no significant difference between the thermal zoning layouts for the cooling and heating season. Given these conditions the grid/cluster thermal zoning method gave similar results as the traditional core-perimeter thermal zoning method. The results show a single interior thermal zone and four different thermal zones for each orientation. For a total of five zone, one major difference between the results from the grid/cluster method and the traditional core-perimeter method is the four individual zones located at each corner of the model, which became four different thermal zones.

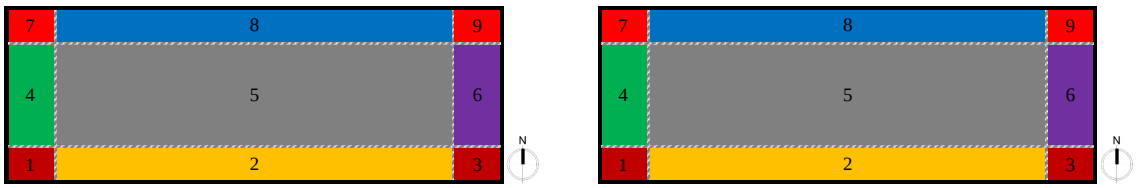

(a) For Cooling Season (b) For Heating Season

Figure 42: Resultant Thermal Zoning Layouts for Case 3 (Chicago, IL)

Figure 43 shows the simulated hourly indoor temperature profiles of the resultant thermal zones for the Case 3 simulation model (i.e., no exterior windows). For a clear, hot day (i.e., July 18) in the cooling season, the results show that a maximum hourly temperature of 76.7 °F was found at 6:00 pm in Zone 1. In addition, a minimum hourly temperature of 74.9 °F was found at 6:00 am in Zone 3 and Zone 7. The difference between the maximum and minimum hourly indoor temperatures was 1.8 °F. For a clear,

cold day (i.e., January 27) in the heating season, the results show that a maximum hourly temperature of 55.1 °F was found at 1:00 pm in Zone 2. Finally, a minimum hourly temperature of 54.7 °F was found at 03:00 am in Zone 2. The difference between maximum and minimum hourly indoor temperatures for this day was 0.4 °F.

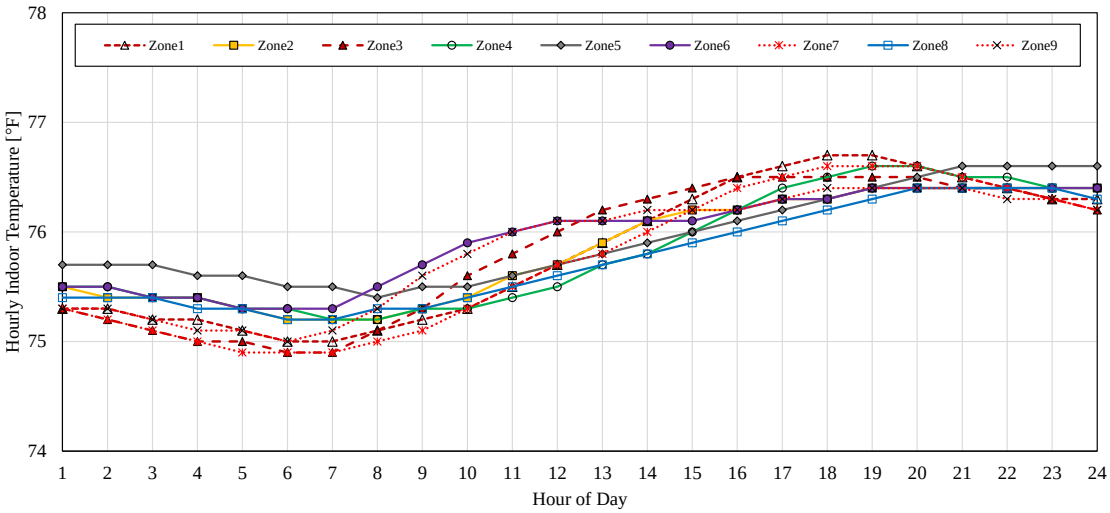

(a) For a Clear Peak Day in Cooling Season (July 18) for Chicago, IL

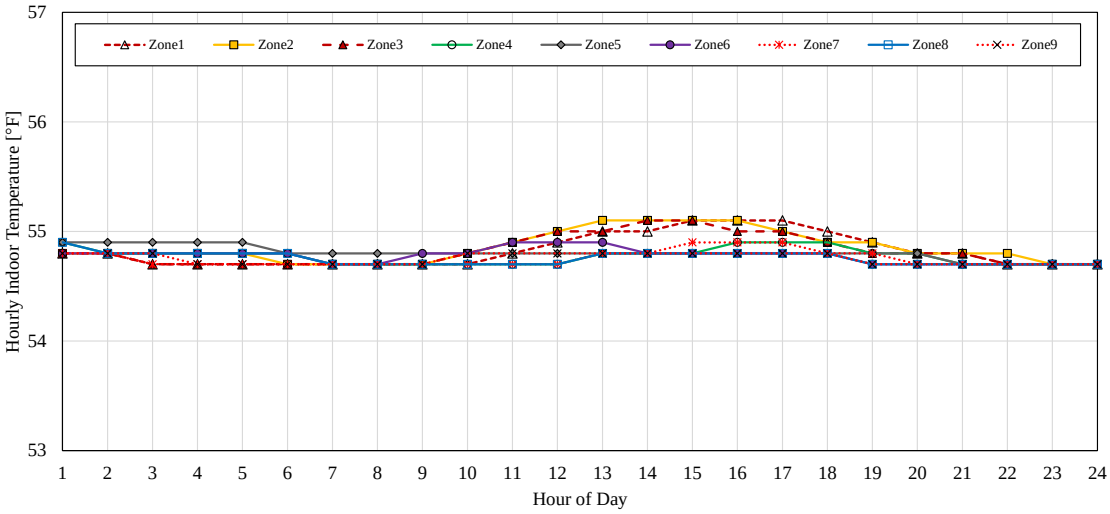

(b) For a Clear Cold Peak in Heating Season (January 27) for Chicago, IL

Figure 43: Indoor Temperature Profiles of Thermal Zones for Case 3 (Chicago, IL)

5.1.1.2. Thermal Zoning Layouts for Case 2 (Houston, TX) and Case 4 (Chicago, IL)

Figure 44 shows images of the building geometry for the Case 2 and Case 4 simulation models. Using the same model geometry, the Houston TMY3 weather file was used for the Case 2, while the Chicago TMY3 weather file was used for the Case 4 simulation model.

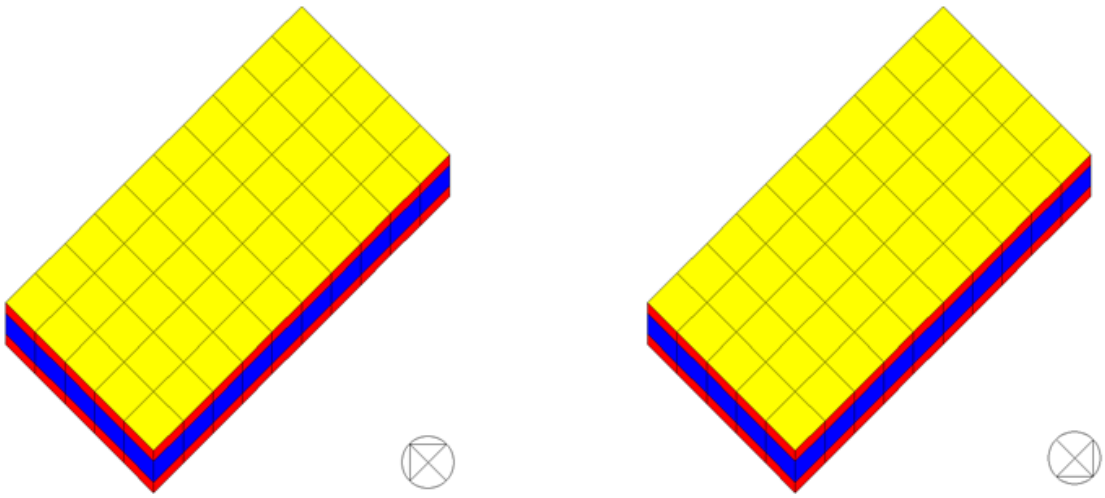

(a) Southwest View (b) Northeast View

Figure 44: View of Case 2 and Case 4 Models in the Simulation

Table 14 presents the main features of the Case 2 and Case 4 simulation models. In the analysis, the Houston and Chicago TMY3 weather files were used for the hot and cold climates, respectively. It should be noted that the Case 2 and Case 4 simulation models have a horizontal band of exterior windows with the WWR of 50%. Therefore,

solar radiation affected the thermal zoning layouts for both cases. The initial simulation models used 50 thermal zones as shown in Figure 44. The step in the new grid/cluster thermal zoning method was to test the similarity of the indoor temperature profiles of all 50 zones. During the thermal zoning process, a linear correlation coefficient of 0.8 or greater was used to combine the thermal zones into one common zone based on the results, which were previously discussed in Section 4.1.3.7. The grid/cluster thermal zoning method gave a total of 10 thermal zones for the Case 2 simulation model (Houston) for both the cooling and heating season. For the Case 4 simulation model (Chicago), the grid/cluster thermal zoning method yielded 10 thermal zones for the cooling season, and 11 thermal zones for the heating season.

Table 14: Main Features of the Case 2 and Case 4 Simulation Models

	Case 2 / Case 4
Building Location	Houston, TX for Case 2 Chicago, IL for Case 4
Window-to-wall Ratio	WWR: 50 % (all orientation)
Floor Area	5,000 ft^2
Slab Type	Slab-on-grade
Thermal Zoning Method	The grid/cluster thermal zoning method
Linear Correlation Coefficient Used	0.8
Initial Number of Thermal Zones	50
Number of Resultant Thermal Zones	Case 2: 10 zones for heating/cooling season Case 4: 10 zones for cooling season; 11 zones for heating season

The resultant thermal zoning layouts of the Case 2 simulation model for the cooling and heating seasons for the building with a horizontal band of windows with the WWR of 50% are presented in the Figure 45. In a similar fashion as Case 1 and Case 3, the thermal zoning layouts show that there was a difference between the cooling and heating season layouts. For Case 2, the grid/cluster thermal zoning method gave 10 thermal zones for both cooling and heating season layouts. However, the location and area of the Zone 6 for the cooling season (see Figure 45a) was different than results for the heating season (See Figure 45b). For the cooling season, Zone 6 was located in the exact center of the interior zone. However, for the heating season, Zone 6 was relocated toward the north-facing perimeter thermal zone without an intermediate zone. The size and location of the other thermal zones, except Zone 5 and Zone 6, were identical to Case 1 and Case 3.

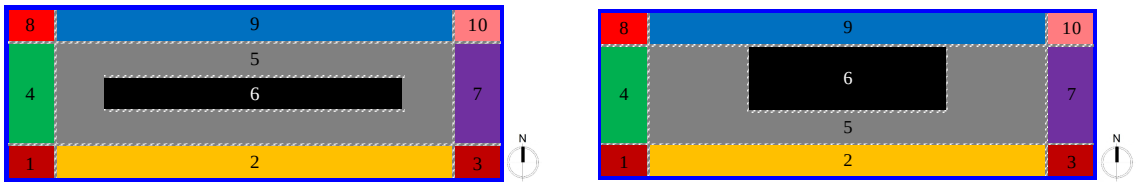

(a) For Cooling Season (b) For Heating Season

Figure 45: Resultant Thermal Zoning Layouts for Case 2 (Houston, TX)

Figure 46 shows the simulated hourly indoor temperature profiles of the resultant thermal zones for the Case 2 simulation model for Houston, TX. For a clear, hot day (i.e., August 2) in the cooling season, the results show that a maximum hourly temperature of 97.9 °F was found at 6:00 pm in Zone 1. In addition, a minimum hourly

temperature of 87.5 °F was found at 6:00 am in Zone 3. The difference between the maximum and minimum hourly indoor temperatures was 10.4 °F. For a clear, cold day (i.e., February 11) in the heating season, the results show that a maximum hourly temperature of 62.6 °F was found at 5:00 pm in Zone 1. Finally, a maximum hourly temperature of 55.1 °F was found at 7:00 am in Zone 8. The difference between maximum and minimum of the hourly indoor temperatures for this day was 7.5 °F. In addition, it was found that the slope of the indoor temperature profiles from 1 am through 7 am, which is before sun rise, are very different for a clear peak summer and winter day.

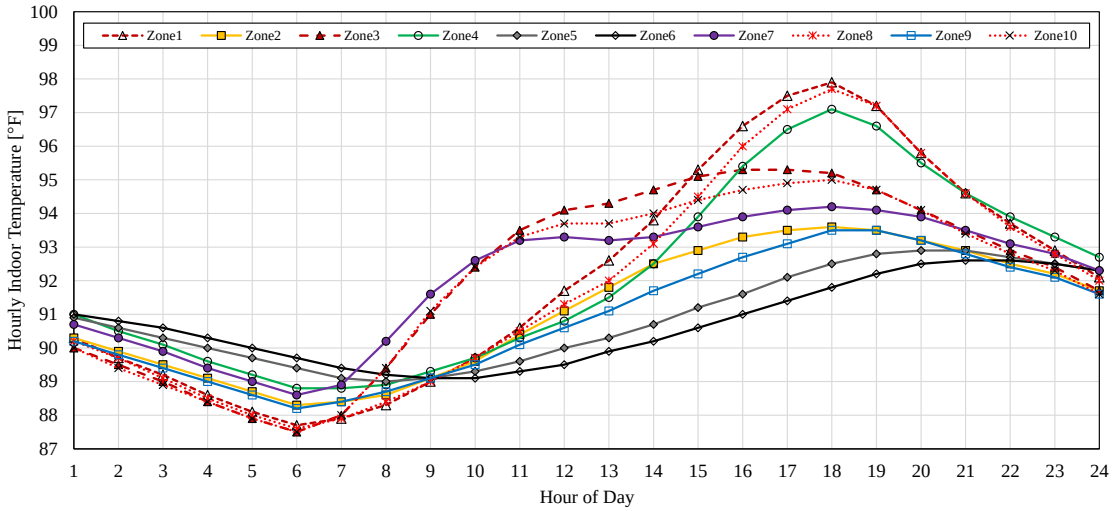

(a) For a Clear Peak Day in Cooling Season (August 2) for Houston, TX

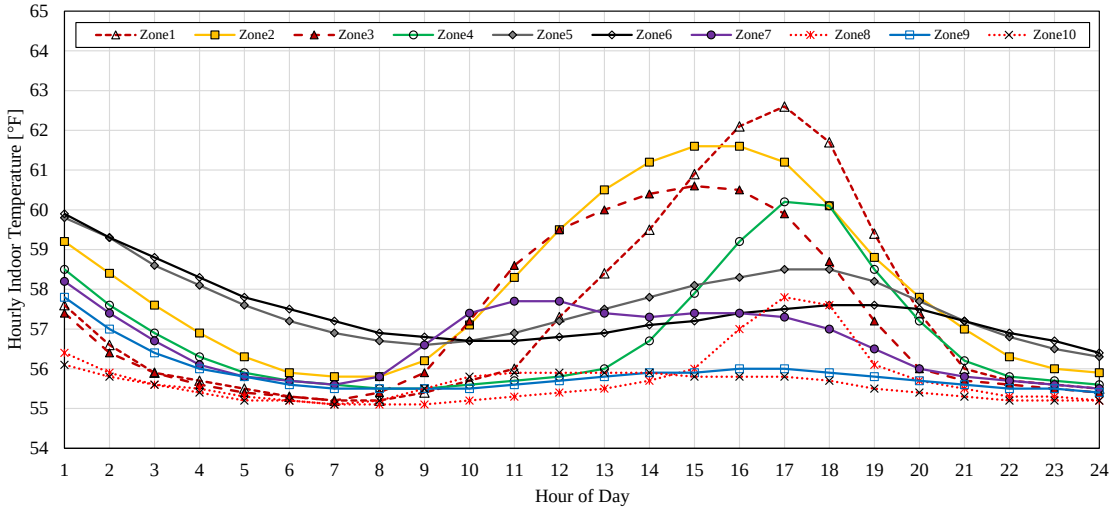

(b) For a Clear Peak Day in Heating Season (February 11) for Houston, TX

Figure 46: Indoor Temperature Profiles of Thermal Zones for Case 2 (Houston, TX)

The resultant thermal zoning layouts of the Case 4 simulation model for the cooling and heating seasons are presented in the Figure 47. In a similar fashion as the results for the Case 2 simulation model (i.e., Houston), the layouts show that there is a difference in the resultant thermal zoning between the cooling and heating season. The grid/cluster thermal zoning method yielded ten (10) thermal zones for the cooling season and eleven (11) thermal zones for heating season layout. In the result, for Chicago the location and area of the Zone 5 and Zone 6 in the layouts (see Figure 47) were different than the results for Houston. For the cooling season, Zone 6 is located in the exact center of the interior Zone 5. However, for the heating season, the interior space was divided horizontally into two separate thermal zones (i.e., Zone 5 and Zone 6). It was found that the north-south length of Zone 6 is twice longer than the one of Zone 5. Also, Zone 6 is located adjacent to Zone 10. In addition, the east-facing perimeter zone was further

divided into two different thermal zones (i.e., Zone 7 and Zone 8), which reflects the sub-division in the interior zone. In contrast, the west side of the perimeter zone of the building was not sub-divided.

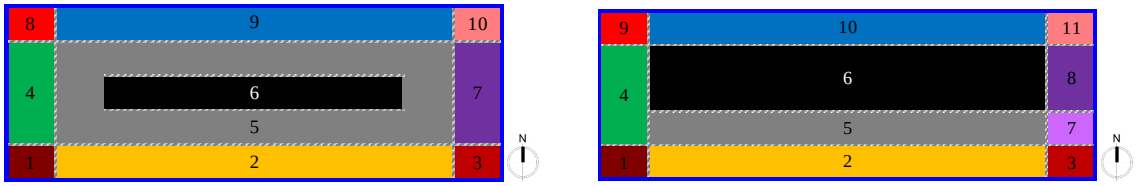

(a) For Cooling Season (b) For Heating Season

Figure 47: Resultant Thermal Zoning Layouts for Case 4 (Chicago, IL)

Figure 48 shows the simulated hourly indoor temperature profiles of the resultant thermal zones for the Case 4 simulation. For a clear, hot day (i.e., July 18) in Chicago in the cooling season, the results show that a maximum hourly temperature of 98.4 °F was found at 5:00 pm in Zone 1. In addition, a minimum hourly temperature of 88.3 °F was found at 5:00 am in Zone 10. The difference between the maximum and minimum hourly indoor temperatures was 10.1 °F. For a clear, cold day (i.e., January 27) in Chicago in the heating season, the results show that a maximum hourly temperature of 59.5 °F was found at 2:00 pm in Zone 2. Finally, a minimum hourly temperature of 54.5 °F was found at 6:00 am in Zone 1. The difference between maximum and minimum hourly indoor temperatures for this day was 5.0 °F.

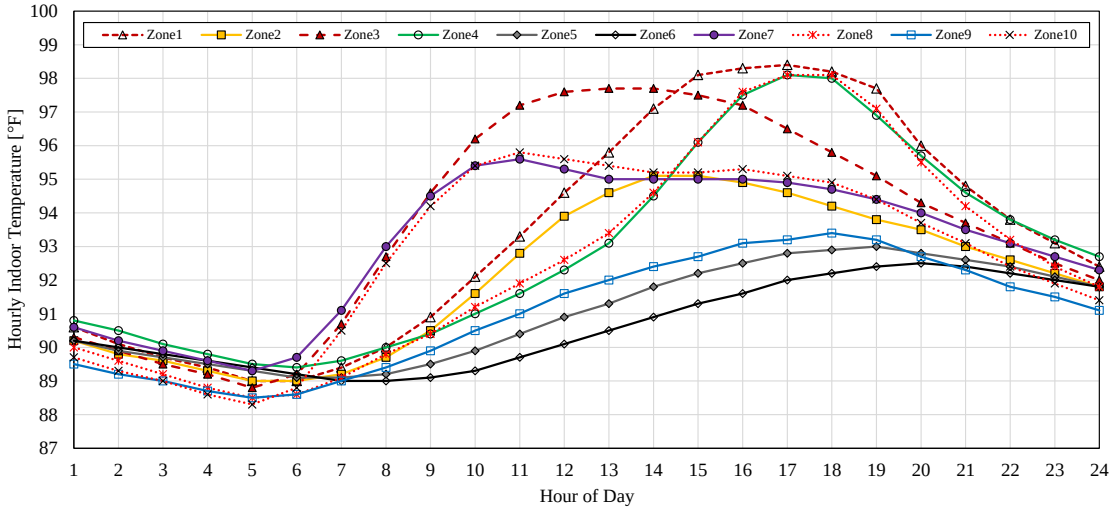

(a) For a Clear Peak Day in Cooling Season (July 18) for Chicago, IL

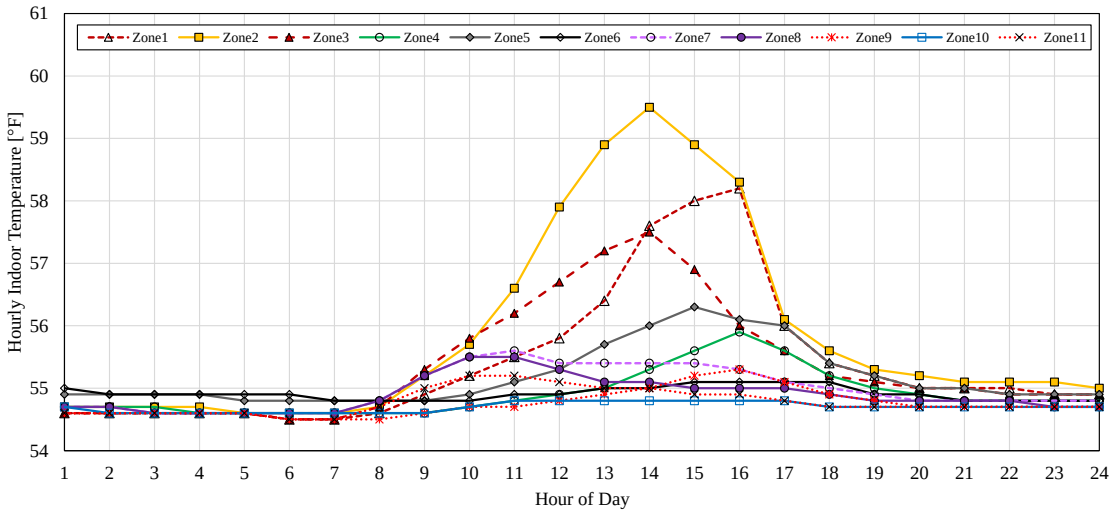

(b) For a Clear PeakDay in Heating Season (January 27) for Chicago, IL

Figure 48: Indoor Temperature Profiles of Thermal Zones for Case 4 (Chicago, IL)

5.1.1.3.Thermal Zoning Layouts for Case 5 (Houston, TX) and Case 7 (Chicago, IL)

Figure 49 shows images of the building geometry for the Case 5 and Case 7 models. Using this same model geometry, a Houston TMY3 weather file was used for the Case 5, while a Chicago TMY3 weather file was used for the Case 7 model.

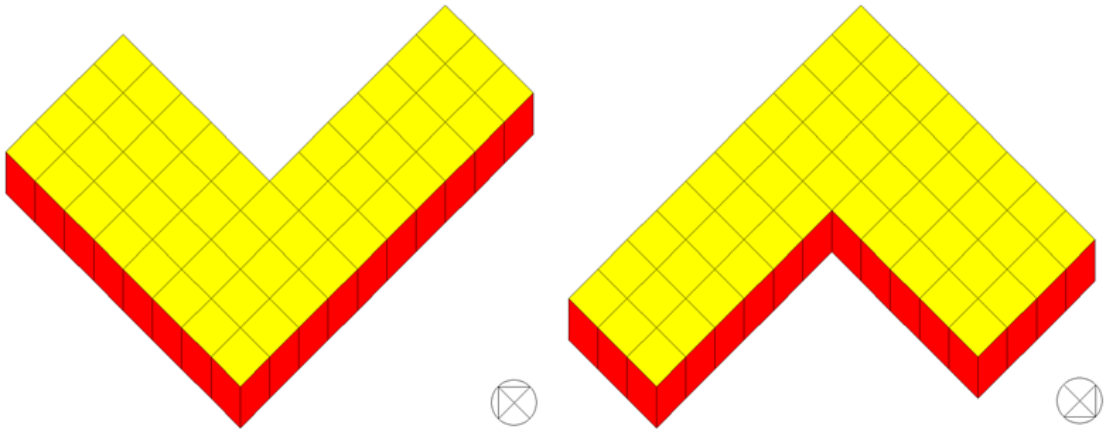

(a) Southwest View (b) Northeast View

Figure 49: View of Case 5 and Case 7 Models in the Simulation

Table 15 presents the main features of the Case 5 and Case 7 simulation models. It was supposed that this building is located in the hot and humid / cold and humid climates, so Houston/Chicago TMY3 weather files were used for the simulation runs. It should be noted that the Case 5 and Case 7 simulation models do not have exterior windows. Therefore, direct solar radiation did not penetrate directly inside of the building through the windows. In a similar fashion as the Case 1, Case 2, Case 3, and Case 4, the simulation models have 50 thermal zones initially. Then, the new grid/cluster

thermal zoning method was applied to this model after the initial simulation run. Using a similar process, during the thermal zoning process, the linear correlation coefficient of 0.8 was used to combine the thermal zones. The thermal zoning method gave a total of 12 thermal zones for the Case 5 and Case 7 models for the heating/cooling seasons.

Table 15: Main Features of the Case 5 and Case 7 Simulation Models

	Case 5 / Case 7
Building Location	Houston, TX for Case 5 Chicago, IL for Case 7
Window-to-wall Ratio	WWR: 0 % (no windows)
Floor Area	5,000 ft^2
Slab Type	Slab-on-grade
Thermal Zoning Method	The grid/cluster thermal zoning method
Linear Correlation Coefficient Used	0.8
Initial Number of Thermal Zones	50
Number of Resultant Thermal Zones	Case 5: 12 zones for heating/cooling season Case 7: 12 zones for heating/cooling season

The resultant thermal zoning layouts of the Case 5 simulation model for the cooling and heating season are presented in the Figure 50. The resultant thermal zoning layouts show that there is no significant difference between the cooling and heating season layout. The grid/cluster thermal zoning method gave a similar result as the method that follows the traditional core-perimeter thermal zoning method with exception of the corner zone as previously noted. The results show a single interior thermal zone

and five different thermal zones for each orientation. In addition, the five individual zones located at each corner of the model became five different thermal zones.

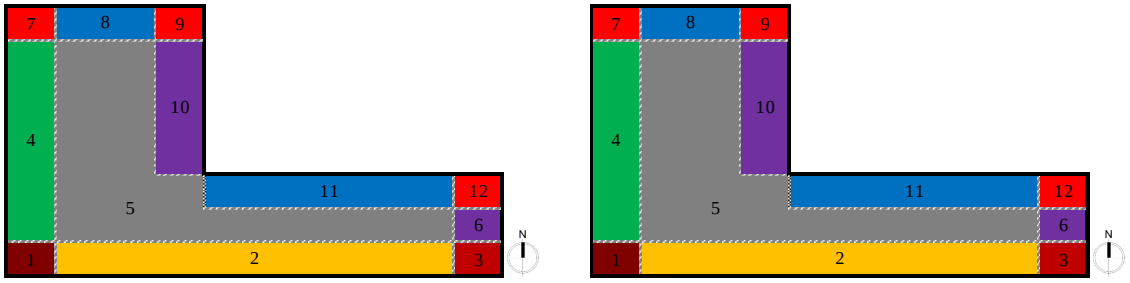

(a) For Cooling Season (b) For Heating Season

Figure 50: Resultant Thermal Zoning Layouts for Case 5 (Houston, TX)

Figure 51 shows the simulated hourly indoor temperature profiles of the resultant thermal zones for Case 5. For a clear, hot day (i.e., August 2) in the cooling season, the results show that a maximum hourly temperature of 89.9 °F was found at 7:00 pm in Zone 1. In addition, a minimum hourly temperature of 85.6 °F was found at 8:00 am in Zone 1. The difference between the maximum and minimum hourly indoor temperatures was 4.3 °F. For a clear, cold day (i.e., February 11) in the heating season, the results show that a maximum hourly temperature of 58.4 °F was found at 1:00 am in Zone 5. In addition, a minimum hourly temperature of 55.4 °F was found at 11:00 pm in Zone 9 and Zone 10. The difference between maximum and minimum hourly indoor temperatures for this day was 3.0 °F.

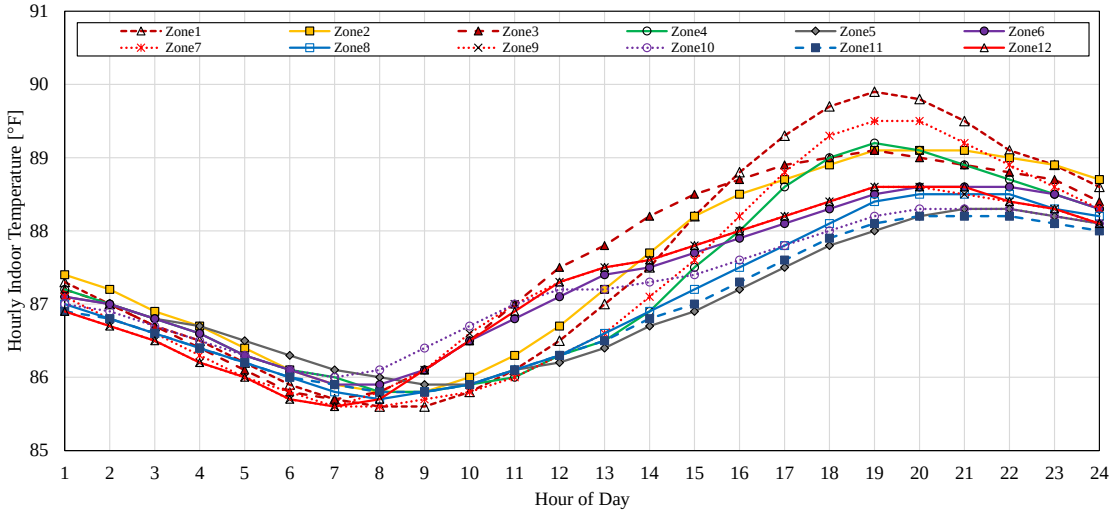

(a) For a Clear Peak Day in Cooling Season (August 2) for Houston, TX

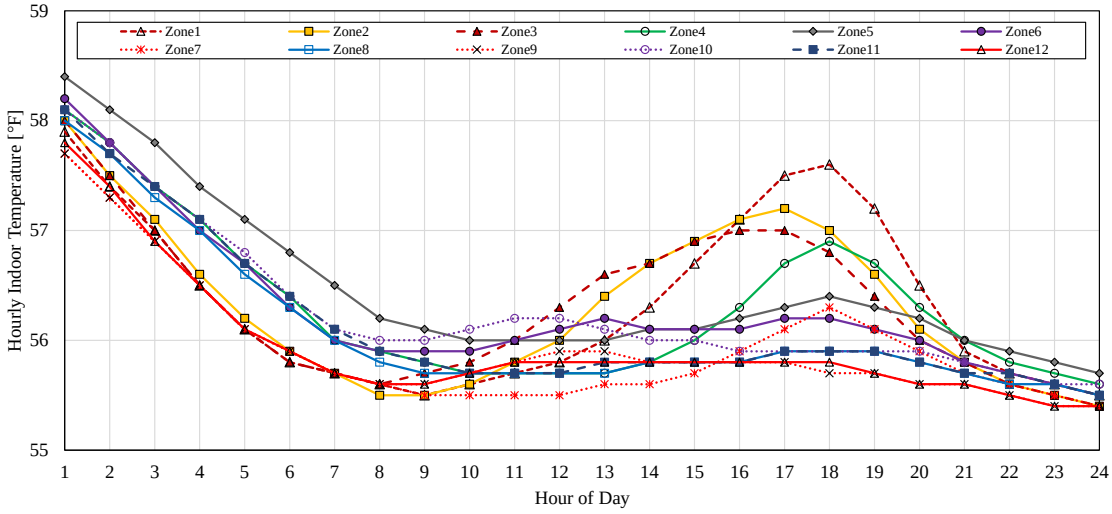

(b) For a Clear Peak Day in Heating Season (February 11) for Houston, TX

Figure 51: Indoor Temperature Profiles of Thermal Zones for Case 5 (Houston, TX)

The resultant thermal zoning layouts of the Case 7 simulation model for the cooling and heating season are presented in the Figure 52. The resultant thermal zoning layouts show that there is no difference between the cooling and heating season layout. The grid/cluster thermal zoning method gave a similar result with one that follows the

traditional core-perimeter thermal zoning method. The results show a single interior thermal zone and five different thermal zones for each orientation. In addition, the five individual zones located at each corner of the model became four different thermal zones.

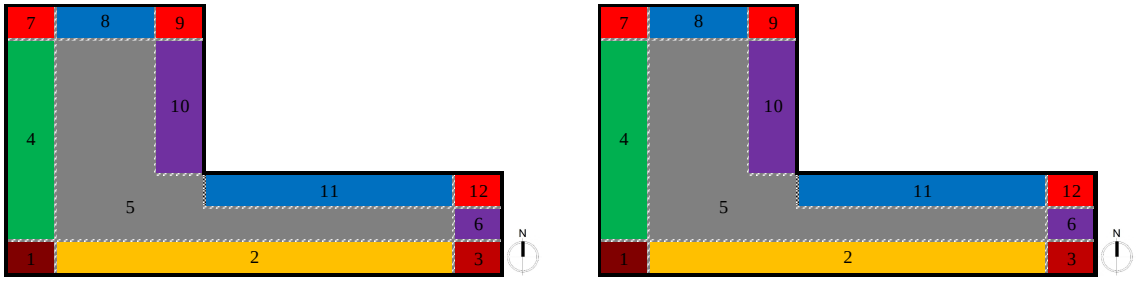

(a) For Cooling Season (b) For Heating Season

Figure 52: Resultant Thermal Zoning Layouts for Case 7 (Chicago, IL)

Figure 53 shows the simulated hourly indoor temperature profiles of the resultant thermal zones for Case 7. For a clear, hot day (i.e., July 18) in the cooling season, the results show that a maximum hourly temperature of 76.7 °F was found at 4:00 pm in Zone 1 and Zone 2. In addition, a minimum hourly temperature of 74.5 °F was found at 6:00 am in Zone 7 and Zone 9. The difference between the maximum and minimum hourly indoor temperatures was 2.2 °F. For a clear, cold day (i.e., January 27) in the heating season, the results show that a maximum hourly temperature of 55.2 °F was found at 4:00 pm in Zone 2. In addition, a minimum hourly temperature of 54.6 °F was found at 07:00 am in Zone 2. The difference between maximum and minimum hourly indoor temperatures for this day was 0.6 °F.

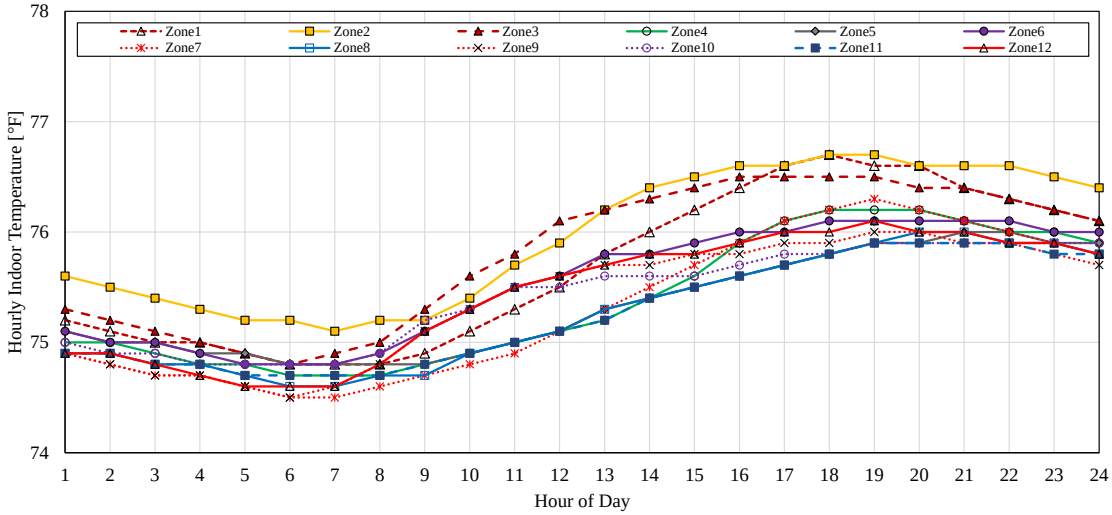

(a) For a Clear Peak Day in Cooling Season (July 18) for Chicago, IL

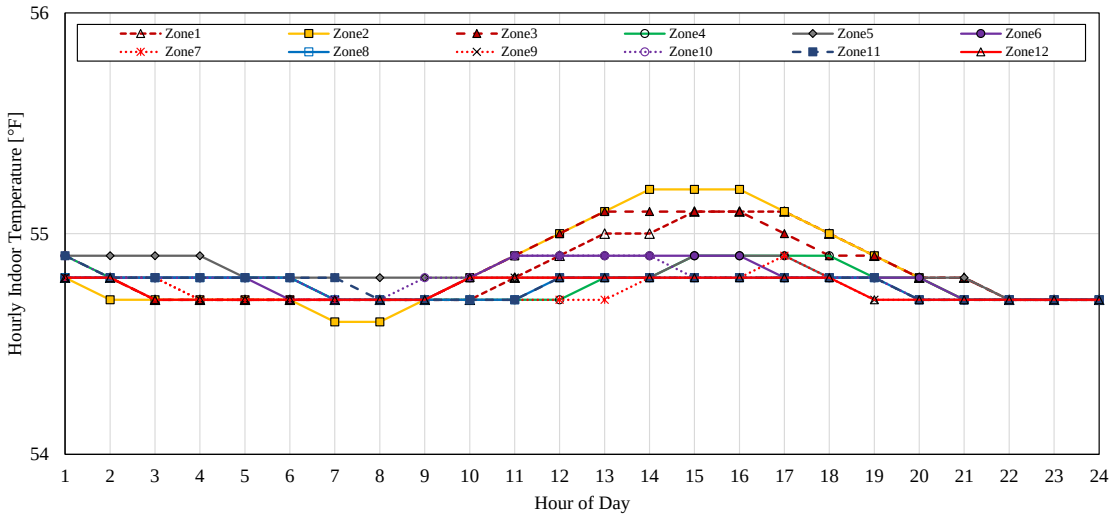

(b) For a Clear Peak Day in Heating Season (January 27) for Chicago, IL

Figure 53: Indoor Temperature Profiles of Thermal Zones for Case 7 (Chicago, IL)

5.1.1.4. Thermal Zoning Layouts for Case 6 (Houston, TX) and Case 8 (Chicago, IL)

Figure 54 shows images of the building geometry for Case 6 and Case 8 models. Using this same model geometry, Houston TMY3 weather file was used for the Case 6, while Chicago TMY3 weather file was used for the Case 8 model.

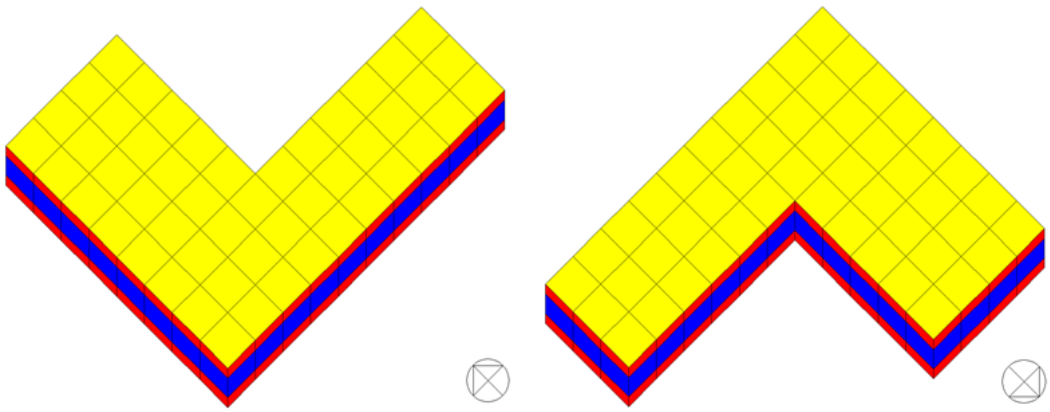

(a) Southwest View (b) Northeast View

Figure 54: View of Case 6 and Case 8 Models in the Simulation

Table 16 presents the main features of the Case 6 and Case 8 simulation models. It was supposed that this building is located in the hot and humid / cold and humid climates, so Houston/Chicago TMY3 weather files were used for the simulation runs. It should be noted that the Case 6 and Case 8 simulation models have a bended exterior window with the WWR of 50%. Therefore, solar radiation could affect creating thermal zoning layouts for both cases. The simulation models have 50 thermal zones initially, and the developed grid/cluster thermal zoning method was applied to this model after the simulation run. During the thermal zoning process, the linear correlation coefficient of

0.8 was used to combine the thermal zones. For the Case 6 simulation model, the thermal zoning method gave a total of 12 thermal zones for the cooling season, 14 thermal zones for the heating season. For the Case 8 simulation model, it gave 13 thermal zones for the cooling season, 14 thermal zones for the heating season.

Table 16: Main Features of the Case 6 and Case 8 Simulation Models

	Case 6 / Case 8
Building Location	Houston, TX for Case 6 Chicago, IL for Case 8
Window-to-wall Ratio	WWR: 50 % (all orientation)
Floor Area	5,000 ft^2
Slab Type	Slab-on-grade
Thermal Zoning Method	The grid/cluster thermal zoning method
Linear Correlation Coefficient Used	0.8
Initial Number of Thermal Zones	50
Number of Resultant Thermal Zones	Case 6: 12 zones for cooling season;14 zones for heating season Case 8: 13 zones for cooling season;14 zones for heating season

The resultant thermal zoning layouts of the Case 6 simulation model for the cooling and heating season are presented in the Figure 55. The resultant thermal zoning layouts show that there is a difference between the cooling and heating season layout. The grid/cluster thermal zoning method gave different number of total thermal zones of 12 and 14 for heating/cooling season layout, respectively. For the cooling season, the interior zone has a single thermal zone, however, for the heating season, it was divided into two different thermal zones (i.e., Zone 5 and Zone 6). In addition, the perimeter

thermal zones of the cooling season layout has 6 different thermal zones (i.e., Zone 2, Zone 4, Zone 6, Zone 8, Zone 10, Zone 11) for each orientation. However, one of the east-facing perimeter zones of the heating season layout was divided into two different thermal zones (i.e., Zone 11 and Zone 12).

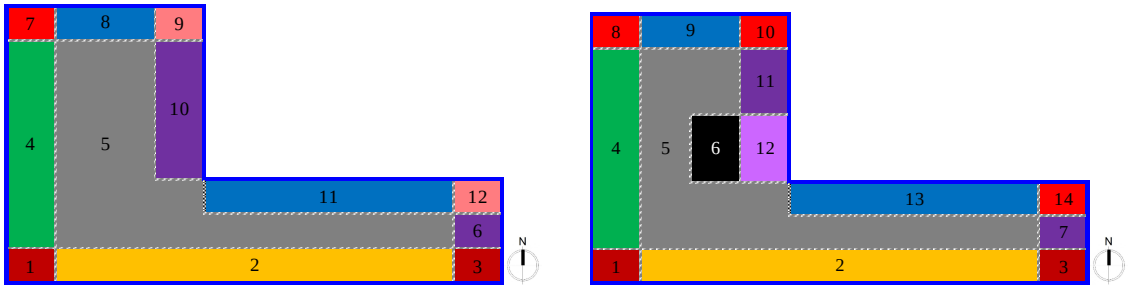

(a) For Cooling Season (b) For Heating Season

Figure 55: Resultant Thermal Zoning Layouts for Case 6 (Houston, TX)

Figure 67 shows the simulated hourly indoor temperature profiles of the resultant thermal zones for Case 6. For a clear, hot day (i.e., August 2) in the cooling season, the results show that a maximum hourly temperature of 98.3 °F was found at 6:00 pm in Zone 1. In addition, a minimum hourly temperature of 87.6 °F was found at 6:00 am in Zone 12. The difference between the maximum and minimum hourly indoor temperatures was 10.7 °F. For a clear, cold day (i.e., February 11) in the heating season, the results show that a maximum hourly temperature of 62.5 °F was found at 5:00 pm in Zone 1. In addition, a minimum hourly temperature of 55.0 °F was found at 7:00 am in Zone 8, Zone 10, and Zone 14. The difference between maximum and minimum of the hourly indoor temperatures for this day was 7.5 °F.

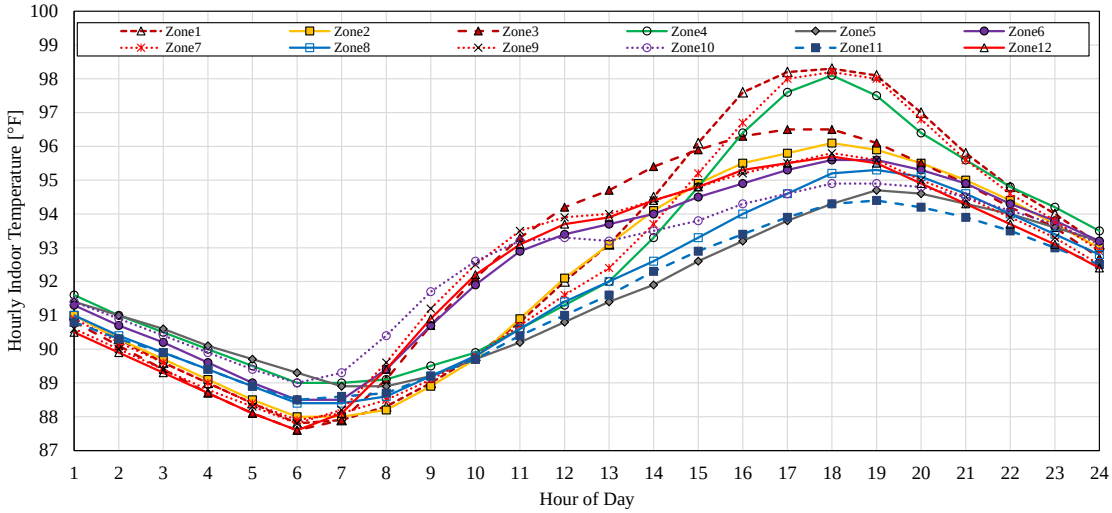

(a) For a Clear Peak Day in Cooling Season (August 2) for Houston, TX

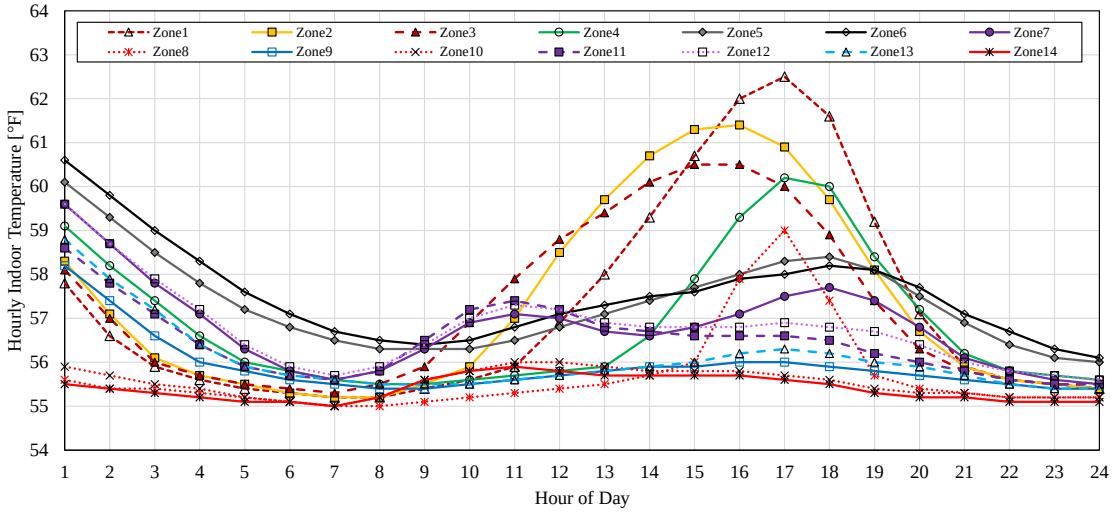

(b) For a Clear Peak Day in Heating Season (February 11) for Houston, TX

Figure 56: Indoor Temperature Profiles of Thermal Zones for Case 6 (Houston, TX)

The resultant thermal zoning layouts of the Case 8 simulation model for the cooling and heating season are presented in Figure 68. The resultant thermal zoning layouts show that there is a difference between the cooling and heating season layout. The grid/cluster thermal zoning method gave different number of total thermal zones of

13 and 14 for heating/cooling season layout, respectively. For both cooling and heating seasons, the interior zone has two different thermal zones. For the cooling season, the Zone 6 is located in the exact center of the interior zone, however, for the heating season, the interior space was divided horizontally by two separate thermal zones (i.e., Zone 6 and Zone 7). In addition, the perimeter thermal zones of the cooling season layout has 6 different thermal zones (i.e., Zone 2, Zone 4, Zone 7, Zone 9, Zone 11, Zone 12) for each orientation. However, one of the west-facing perimeter zones of the heating season layout was divided into two different thermal zones (i.e., Zone 4 and Zone 5).

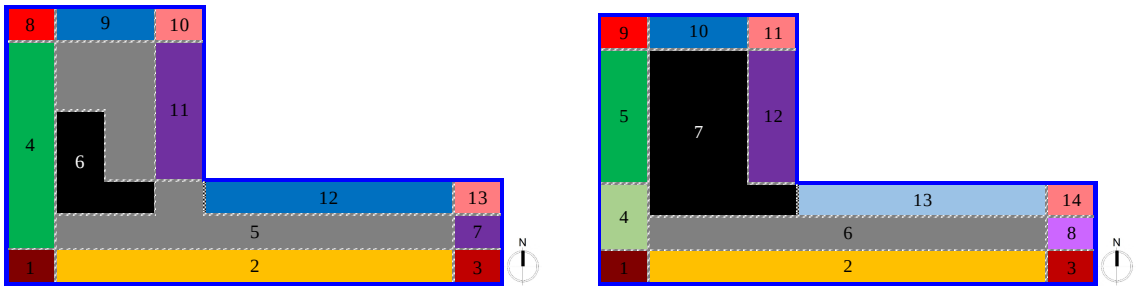

(a) For Cooling Season (b) For Heating Season

Figure 57: Resultant Thermal Zoning Layouts for Case 8 (Chicago, IL)

Figure 58 shows the simulated hourly indoor temperature profiles of the resultant thermal zones for Case 8. For a clear, hot day (i.e., July 18) in the cooling season, the results show that a maximum hourly temperature of 98.7 °F was found at 4:00 pm in Zone 1. In addition, a minimum hourly temperature of 88.8 °F was found at 5:00 am in Zone 8. The difference between the maximum and minimum hourly indoor temperatures

was 9.9 °F. For a clear, cold day (i.e., January 27) in the heating season, the results show that a maximum hourly temperature of 60.6 °F was found at 2:00 pm in Zone 2. In addition, a minimum hourly temperature of 54.5 °F was found at 04:00 am in Zone 2. The difference between maximum and minimum hourly indoor temperatures for this day was 6.1 °F.

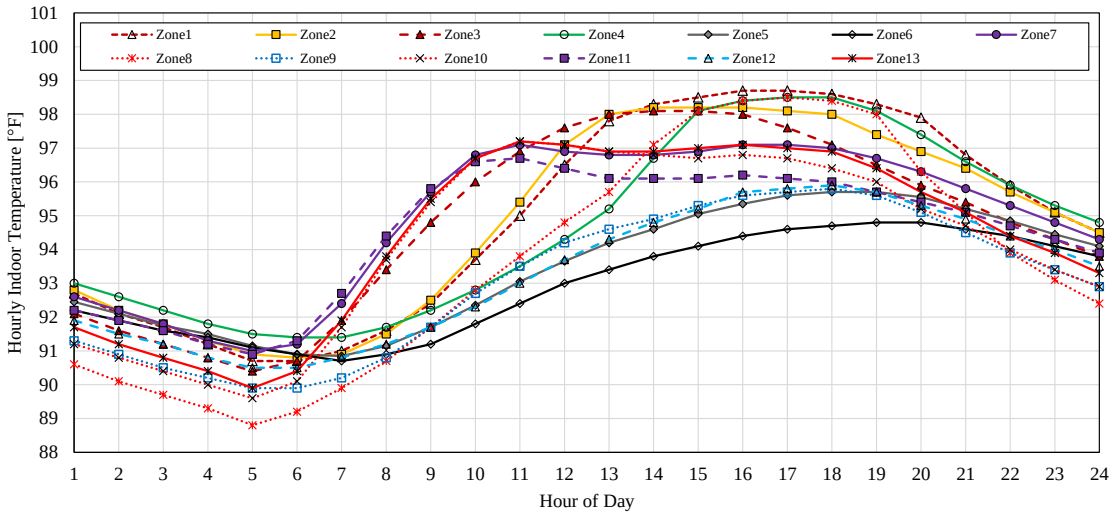

(a) For a Clear Peak Day in Cooling Season (July 18) for Chicago, IL

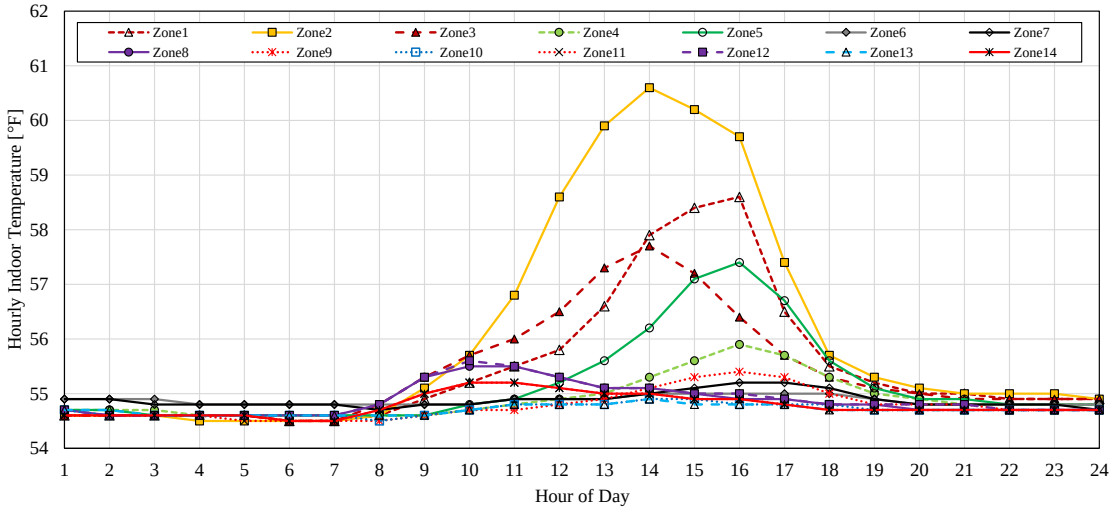

(b) For a Clear Peak Day in Heating Season (January 27) for Chicago, IL

Figure 58: Indoor Temperature Profiles of Thermal Zones for Case 8 (Chicago, IL)

5.1.2. Comparison of Heating/Cooling Loads Between Different Building Shapes

In this sub-section, the simulated annual and monthly heating/cooling loads for the rectangle-shape and L-shape simulation models, with opaque walls were compared and discussed. In this analysis, both models (i.e., the rectangle-shape and L-shape) had the same floor area. To investigate the impact of the thermal zoning strategies for the building energy simulation model on building thermal loads, a single zone thermal zoning model, using the traditional core-perimeter thermal zoning model, and a grid/cluster thermal zoning model were created for each case, and compared in regards to the heating/cooling loads. The guideline for the traditional core-perimeter thermal zoning method from the Appendix G of ASHRAE Standard 90.1-2013 (ASHRAE 2013) was used to create the core-perimeter thermal zoning models, which recommended a 12-

15 ft depth of the perimeter zone. In addition, the differences in the calculated thermal loads of the single-zone and the grid/cluster models for the rectangle-shape and L-shape models were compared to investigate if there is an impact from the building shape on the thermal zoning.

5.1.2.1. Case 1 (Rectangle-Shape Model, w/o Windows, Houston, TX) vs. Case 5 (L-Shape Model, w/o Windows, Houston, TX)

The model specification of Case 1 (i.e., a rectangle-shape model) was summarized in Table 13 in Section 5.1.1.1. This case did not have any exterior windows, and was located in Houston, TX. Figure 59 shows the thermal zoning layouts of the different zoning models (i.e., a single-zone thermal zoning model, a five-zone core-perimeter thermal zoning model, and a nine-zone grid/cluster thermal zoning model) for Case 1.

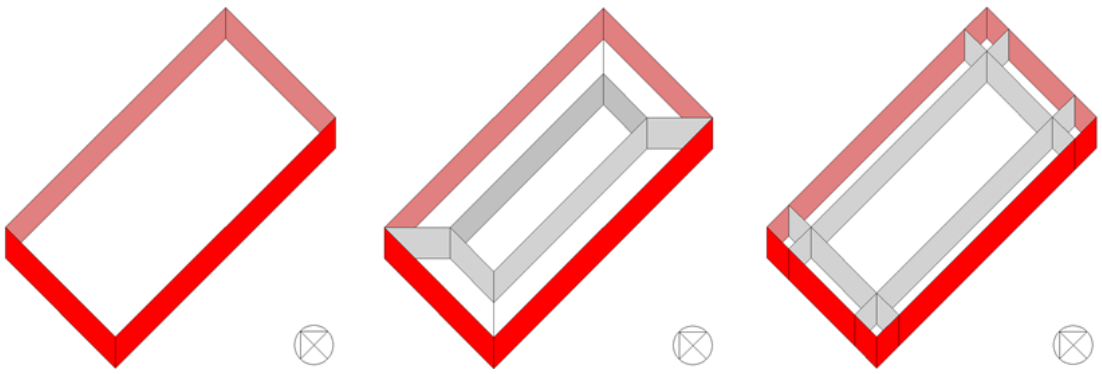

(1) 1-Zone Model (2) 5-Zone Model (3) 9-Zone Model

Figure 59: Different Zoning Models for Case 1 (Houston, TX)

Figure 60 shows the total monthly thermal loads (i.e., heating + cooling) for 1-Zone, 5-Zone, and 9-Zone thermal zoning models for Case 1 (Houston, TX), which is the rectangle-shape model with opaque walls. In addition, Figure 61 shows the total annual thermal loads (i.e., heating + cooling) for Case 1. The results show that the total monthly thermal loads of the 1-Zone model were higher than the other thermal zoning models during the heating month and cooling months. During the intermediate season (i.e., May and November), the analysis produced the opposite results of the 1-Zone model, which had the least thermal loads over the other thermal zoning models. In addition, the total monthly thermal loads of the 9-Zone model were slightly higher than 5-Zone model, which used the traditional core-perimeter zoning method. The simulated annual thermal loads of the 9-Zone model were less than the 1-Zone model.

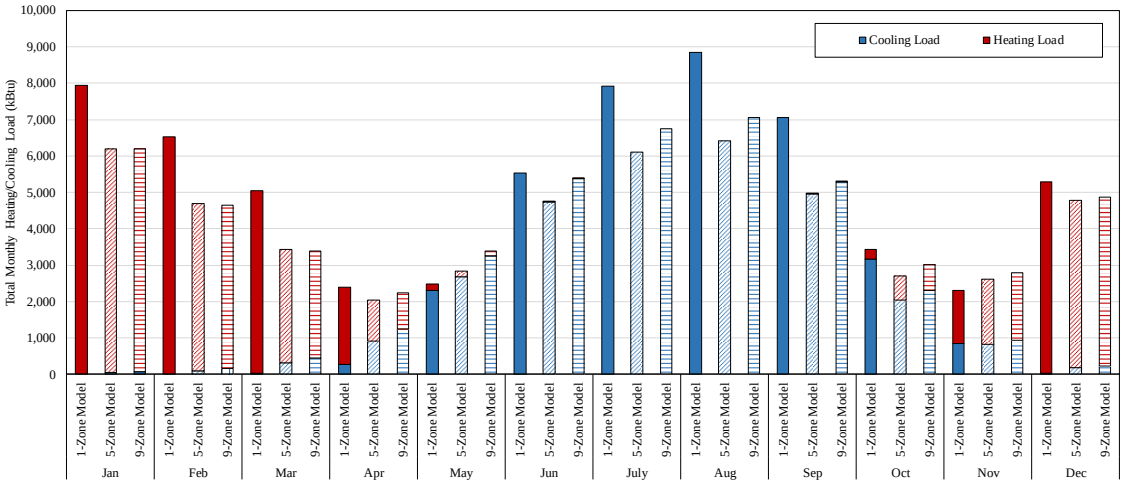

Figure 60: Total Monthly Heating/Cooling Loads for Case 1 (Houston, TX) Based on Different Thermal Zoning Methods

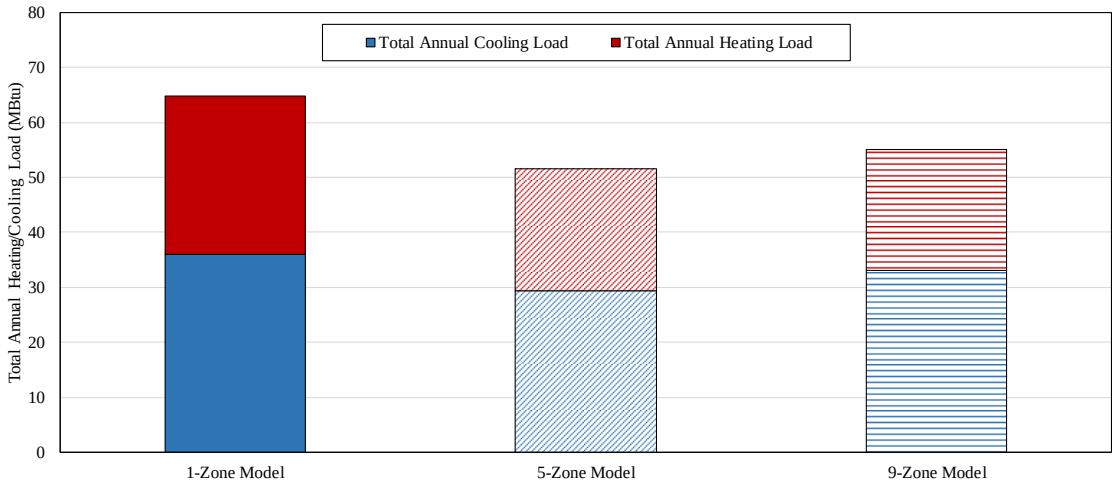

Figure 61: Total Annual Heating/Cooling Loads for Case1 (Houston, TX) Based on Different Thermal Zoning Methods

Table 17 provides a tabulated comparison of the total monthly thermal loads for the 1-Zone, 5-Zone, and 9-Zone models. Both Figure 60 and Table 17 clearly show the 1-zone model is the most consumptive of the three models.

Table 17: Comparison of Annual Thermal Loads for Case 1 (Houston, TX)

	1-Zone Model (kBtu)	**5-Zone Model (kBtu)**	**9-Zone Model (kBtu)**	**1-Zone vs. 5 Zone (kBtu)**	**1-Zone vs. 9-Zone (kBtu)**
Jan	7,936	6,206	6,198	-1,730(-22%)	-1,738(-22%)
Feb	6,536	4,695	4,639	-1,841(-28%)	-1,897(-29%)
Mar	5,044	3,439	3,439	-1,605(-32%)	-1,605(-32%)
Apr	2,402	2,033	2,244	-369(-15%)	-158(-7%)
May	2,495	2,837	3,394	341(14%)	899(36%)
Jun	5,525	4,748	5,382	-777(-14%)	-143(-3%)
Jul	7,909	6,108	6,749	-1,801(-23%)	-1,160(-15%)
Aug	8,851	6,411	7,056	-2,440(-28%)	-1,795(20%)
Sep	7,061	4,954	5,284	-2,107(-30%)	-1,777(-25%)
Oct	3,426	2,704	3,014	-721(-21%)	-412(-12%)
Nov	2,298	2,625	2,789	326(14%)	490(21%)
Dec	5,279	4,778	4,870	-501(-9%)	-409(-8%)
Total	**64,762**	**51,538**	**55,058**	**-15,135(-20%)**	**-9,704(-15%)**

The model specification of Case 5 (i.e., an L-shape model) was summarized in Table 15 in Section 5.1.1.3. This case also does not have any exterior windows, and is located in Houston, TX. Figure 62 shows the thermal zoning layouts of the different zoning models (i.e., a single-zone thermal zoning model, a seven-zone core-perimeter thermal zoning model, a twelve-zone grid/cluster thermal zoning model) for Case 5.

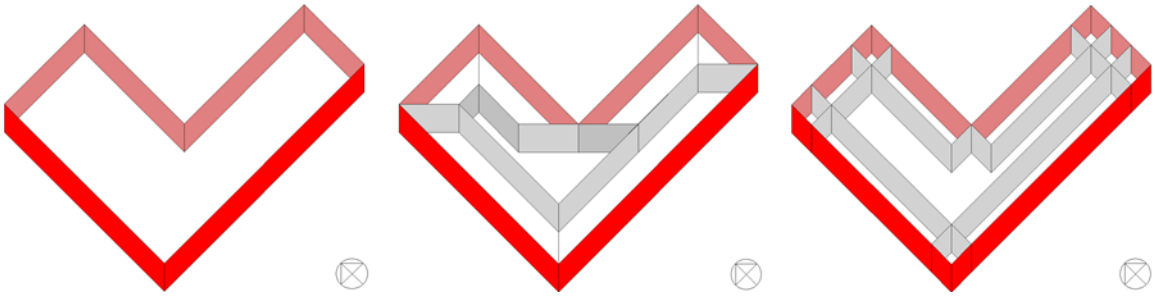

(1) 1-Zone Model (2) 7-Zone Model (3) 12-Zone Model

Figure 62: Different Zoning Models for Case 5 (Houston, TX)

Figure 63 shows the total monthly thermal loads (i.e., heating + cooling) for the 1-Zone, 7-Zone, and 12-Zone thermal zoning models for Case 5 (Houston, TX), which represents the L-shape model with opaque walls. In addition, Figure 64 shows the total annual thermal loads (i.e., heating + cooling) for Case 5. In a similar fashion as Case 1 (Houston, TX), the results showed that the total monthly thermal loads (i.e., heating + cooling) of the 1-Zone model were generally higher than the other thermal zoning models. During the intermediate season (e.g., May and November), the analysis produced the opposite results as the 1-Zone model, which had the smallest thermal loads of all three thermal zoning models. In addition, the total monthly thermal loads of the 12-Zone model were slightly higher than the 7-Zone model, which used the traditional core-perimeter zoning method. However, the simulated annual thermal loads of the 7-Zone model were less than the 1-Zone model.

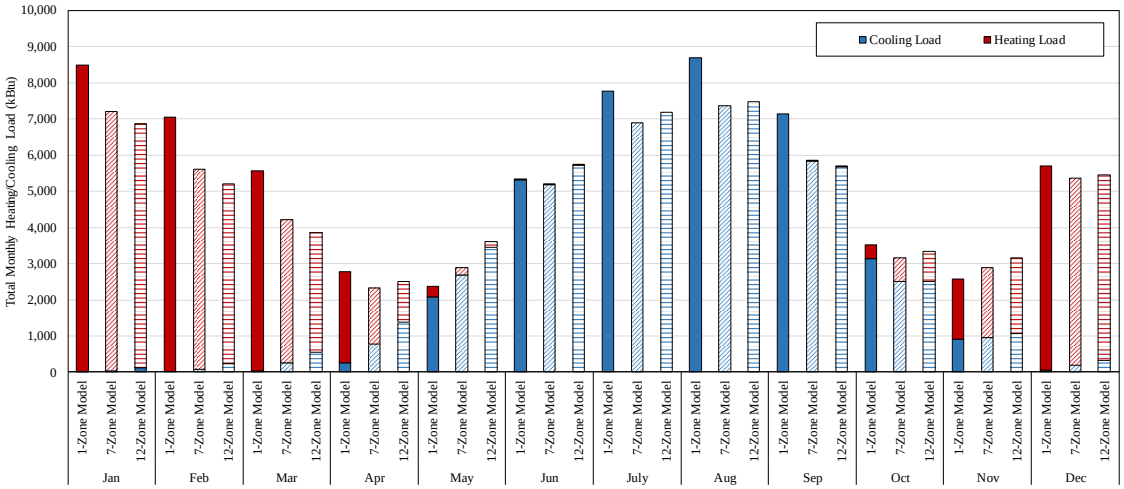

Figure 63: Total Monthly Heating/Cooling Loads for Case 5 (Houston, TX) Based on Different Thermal Zoning Methods

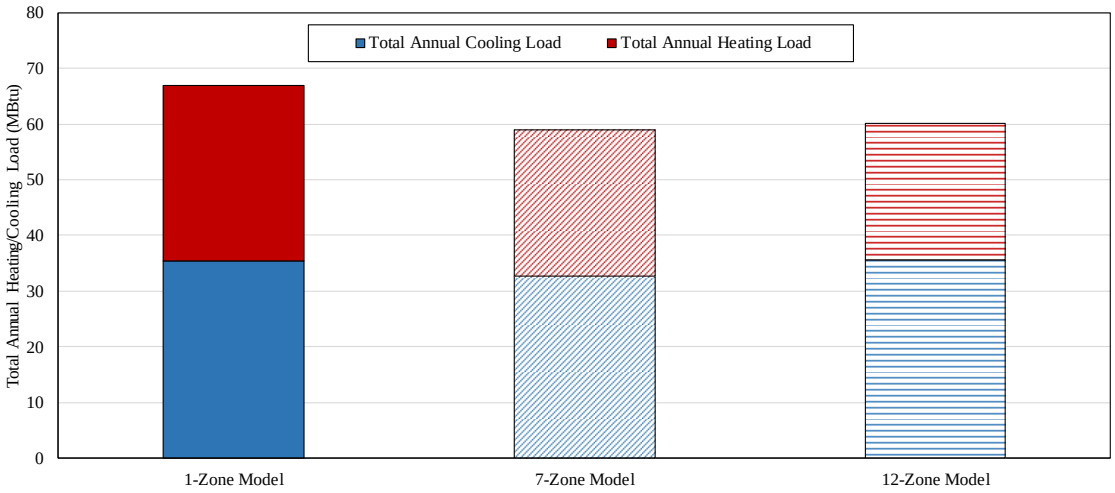

Figure 64: Total Annual Heating/Cooling Loads for Case 5 (Houston, TX) Based on Different Thermal Zoning Methods

Table 18 provides a tabulated comparison of the total monthly thermal loads for the 1-Zone, 7-Zone, and 12-Zone models. Both Figure 64 and Table 18 clearly show the 1-zone model is the most consumptive.

Table 18: Comparison of Annual Thermal Loads for Case 5 (Houston, TX)

	1-Zone Model (kBtu)	7-Zone Model (kBtu)	12-Zone Model (kBtu)	1-Zone vs. 7 Zone (kBtu)	1-Zone vs. 12-Zone (kBtu)
Jan	8,494	7,205	6,871	-1,289(-15%)	-1,623(-19%)
Feb	7,048	5,609	5,201	-1,439(-20%)	-1,847(-26%)
Mar	5,560	4,212	4,212	-1,349(-24%)	-1,349(-24%)
Apr	2,786	2,319	2,502	-468(-17%)	-285(-10%)
May	2,364	2,880	3,603	516(22%)	1,239(52%)
Jun	5,312	2,880	5,727	-138(-3%)	415(8%)
Jul	7,772	6,904	7,182	-868(-11%)	-589(-8%)
Aug	8,696	7,376	7,475	-1,320(-15%)	-1,221(-14%)
Sep	7,146	5,846	5,681	-1,300(-18%)	-1,465(-20%)
Oct	3,512	3,156	3,340	-356(-10%)	-172(-5%)
Nov	2,584	2,895	3,169	311(12%)	585(23%)
Dec	5,705	5,369	5,461	-337(-6%)	-245(-4%)
Total	**66,980**	**58,944**	**60,423**	**-8,036(-12%)**	**-6,556(-10%)**

5.1.2.2. Case 3 (Rectangle-Shape Model, w/o Windows, Chicago, IL) vs. Case 7 (L-Shape Model, w/o Windows, Chicago, IL)

The model specification for Case 3 (i.e., a rectangle-shape model) was summarized in Table 13 in Section 5.1.1.1. This case also does not have any exterior windows, and is located in Chicago, IL. Figure 65 shows the thermal zoning layouts of the different zoning models (i.e., a single-zone thermal zoning model, a five-zone core-

perimeter thermal zoning model, a nine-zone grid/cluster thermal zoning model) for Case 3.

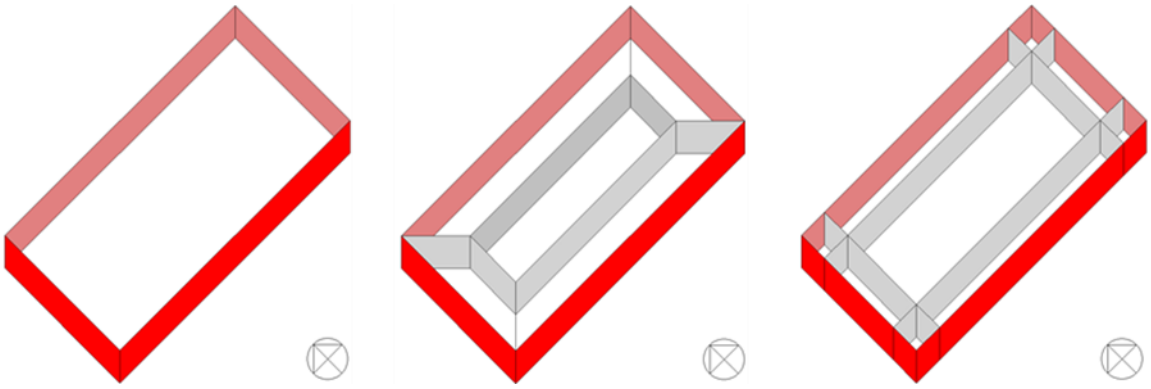

(1) 1-Zone Model (2) 5-Zone Model (3) 9-Zone Model

Figure 65: Different Zoning Models for Case 3 (Chicago, IL)

Figure 66 shows the total monthly thermal loads (i.e., heating + cooling) for the 1-Zone, 5-Zone, and 9-Zone thermal zoning models for Case 3 (Chicago, IL), which is the rectangle-shape model with opaque walls. In addition, Figure 67 shows the total annual thermal loads (i.e., heating + cooling) for Case 3. The results show that the total monthly thermal loads of the 1-Zone model were mostly higher than the other thermal zoning models. During the peak cooling period (i.e., July and August), the 1-Zone model produced the lowest thermal loads compared to the other thermal zoning models. Finally, it should be noted that the total monthly thermal loads of the 5-Zone and 9-Zone models were very similar each other throughout the year. However, the simulated annual thermal loads of the 5-Zone and 9-zone models were much less than energy use of the 1-zone model.

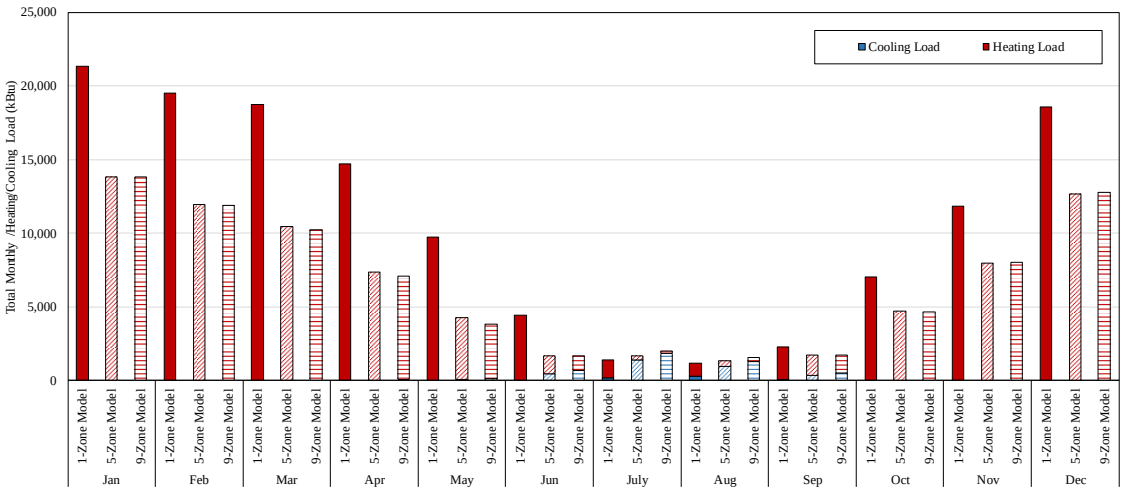

Figure 66: Total Monthly Heating/Cooling Loads for Case 3 (Chicago, IL) Based on Different Thermal Zoning Methods

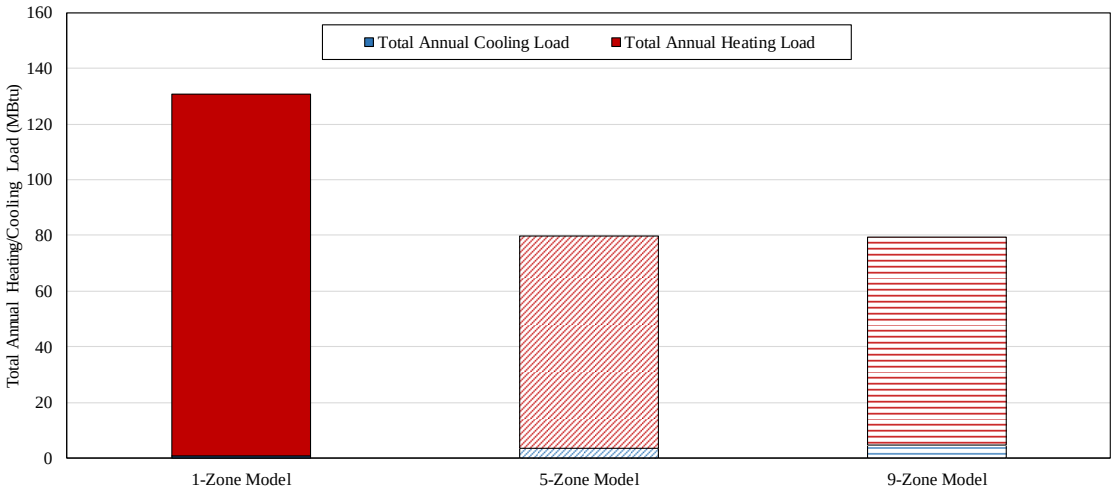

Figure 67: Total Annual Heating/Cooling Loads for Case 3 (Chicago, IL) Based on Different Thermal Zoning Methods

Table 19 provides a tabulated comparison of the total monthly thermal loads for the 1-Zone, 5-zone, and 9-Zone models. Both Figure 67 and Table 19 clearly show the 1-zone model is the most consumptive of the three models.

Table 19: Comparison of Annual Thermal Loads for Case 3 (Chicago, IL)

	1-Zone Model (kBtu)	5-Zone Model (kBtu)	9-Zone Model (kBtu)	1-Zone vs. 5 Zone (kBtu)	1-Zone vs. 9-Zone (kBtu)
Jan	21,321	13,820	13,854	-7,502(-35%)	-7,467(-35%)
Feb	19,529	11,952	11,899	-7,576(-39%)	-7,630(-39%)
Mar	18,764	10,446	10,446	-8,319(-44%)	-8,319(-44%)
Apr	14,714	7,357	7,107	-7,357(-50%)	-7,608(-52%)
May	9,767	4,269	3,856	-5,499(-56%)	-5,911(-61%)
Jun	4,429	1,709	1,706	-2,720(-61%)	-2,722(-61%)
Jul	1,413	1,707	2,039	295(21%)	626(44%)
Aug	1,207	1,362	1,592	155(13%)	385(32%)
Sep	2,280	1,716	1,735	-563(-25%)	-545(-24%)
Oct	7,014	4,734	4,683	-2,281(-33%)	-2,331(-33%)
Nov	11,834	8,003	8,022	-3,831(-32%)	-3,812(-32%)
Dec	18,582	12,694	12,793	-5,888(-32%)	-5,790(-31%)
Total	**130,855**	**82,327**	**79,732**	**-51,088(-39%)**	**-51,123(-39%)**

The model specification for Case 7 (i.e., an L-shape model) was summarized in Table 15 in Section 5.1.1.3. This case also does not have any exterior windows, and is located in Chicago, IL. Figure 68 shows the thermal zoning layouts of the different zoning models (i.e., a single-zone thermal zoning model, a seven-zone core-perimeter thermal zoning model, a twelve-zone grid/cluster thermal zoning model) for Case 7.

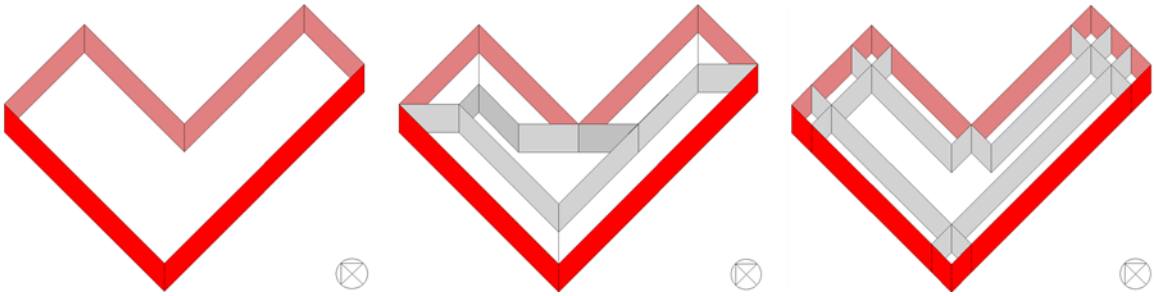

(1) 1-Zone Model (2) 7-Zone Model (3) 12-Zone Model

Figure 68: Different Zoning Models for Case 7 (Chicago, IL)

Figure 69 shows the total monthly thermal loads (i.e., heating + cooling) for the 1-Zone, 7-Zone, and 12-Zone thermal zoning models for Case 7 (Chicago, IL), which is the L-shape model with opaque walls. In addition, Figure 70 shows the total annual thermal loads (i.e., heating + cooling) for Case 7. In a similar fashion as Case 3 (Chicago, IL), the results show that the total monthly thermal loads of the 1-Zone model were generally higher than the other thermal zoning models. In a similar fashion as the rectangular model during the peak cooling period (i.e., July and August), the 1-Zone model produced the lowest thermal loads over the other thermal zoning models. In addition, the total monthly thermal load of the 7-Zone model were mostly higher than the 12-Zone model, which used the grid/cluster thermal zoning method. However, the simulated annual thermal loads of the 7-zone model were less than the 1-zone model.

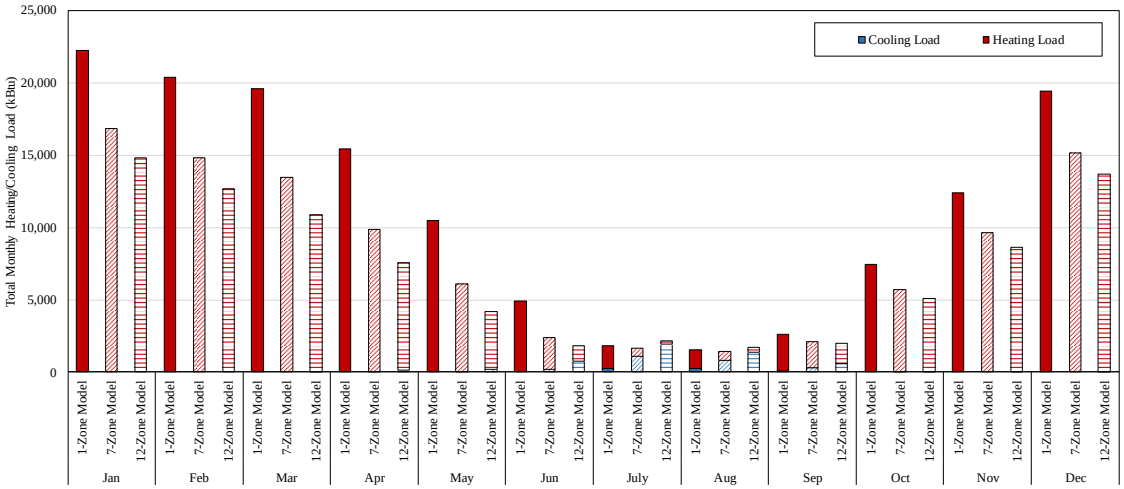

Figure 69: Total Monthly Heating/Cooling Loads for Case 7 (Chicago, IL) Based on Different Thermal Zoning Methods

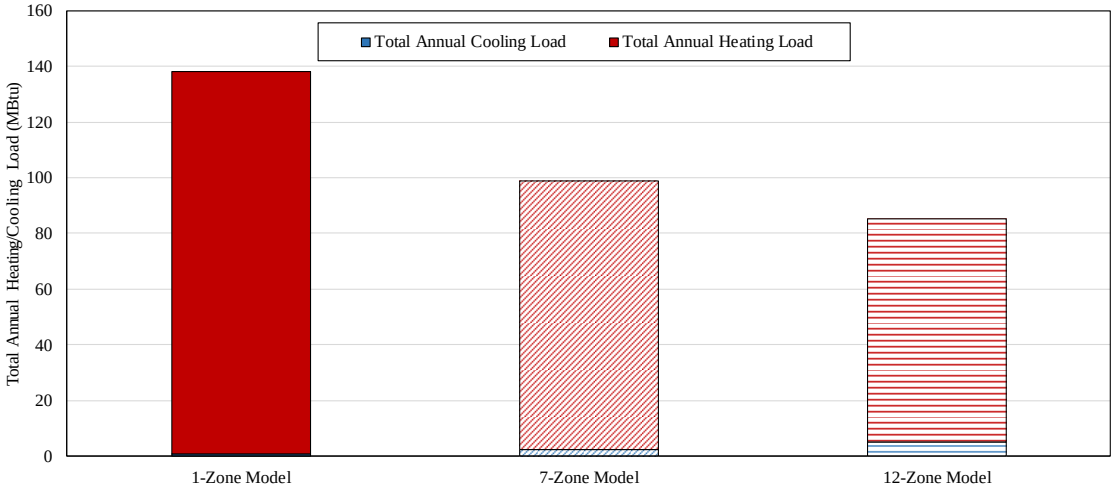

Figure 70: Total Annual Heating/Cooling Loads for Case 7 (Chicago, IL) Based on Different Thermal Zoning Methods

Table 20 provides a tabulated comparison of the monthly total thermal loads for the 1-Zone, 7-zone, and 12-Zone models. Both Figure 70 and Table 20 clearly show the 1-zone model is the most consumptive of the three models.

Table 20: Comparison of Annual Thermal Loads for Case 7 (Chicago, IL)

	1-Zone Model (kBtu)	7-Zone Model (kBtu)	12-Zone Model (kBtu)	1-Zone vs. 7 Zone (kBtu)	1-Zone vs. 12-Zone (kBtu)
Jan	22,255	16,820	14,802	-5,435(-24%)	-7,453(-33%)
Feb	20,364	14,834	12,675	-5,530(-27%)	-7,688(-38%)
Mar	19,589	13,443	13,443	-6,147(-31%)	-6,147(-31%)
Apr	15,413	9,847	7,555	-5,566(-36%)	-7,858(-51%)
May	10,491	6,090	4,204	-4,401(-42%)	-6,287(-60%)
Jun	4,912	2,365	1,833	2,547(-52%)	-3,078(-63%)
Jul	1,818	1,635	2,183	-183(-10%)	365(20%)
Aug	1,524	1,426	1,710	-98(-6%)	187(12%)
Sep	2,629	2,077	1,975	-552(-21%)	-655(-25%)
Oct	7,421	5,707	5,098	-1,715(-23%)	-2,323(-31%)
Nov	12,422	9,633	8,622	-2,789(-22%)	-3,800(-31%)
Dec	19,397	15,167	13,688	-4,230(-22%)	-5,709(-29%)
Total	**138,235**	**99,042**	**87,789**	**-39,193(-28%)**	**-50,446(-36%)**

5.1.2.3. Case 2 (Rectangle-Shape Model, w/ Windows, Houston, TX) vs. Case 6 (L-Shape Model, w/ Windows, Houston, TX)

The model specification of Case 2 (i.e., a rectangle-shape model) was summarized in Table 14 in Section 5.1.1.2. This case has an exterior window band with a WWR of 50%, located in Houston, TX. Figure 71 shows the thermal zoning layouts of the different zoning models (i.e., a single-zone thermal zoning model, a five-zone core-

perimeter thermal zoning model, ten-zone grid/cluster thermal zoning models for cooling and heating season) for Case 2.

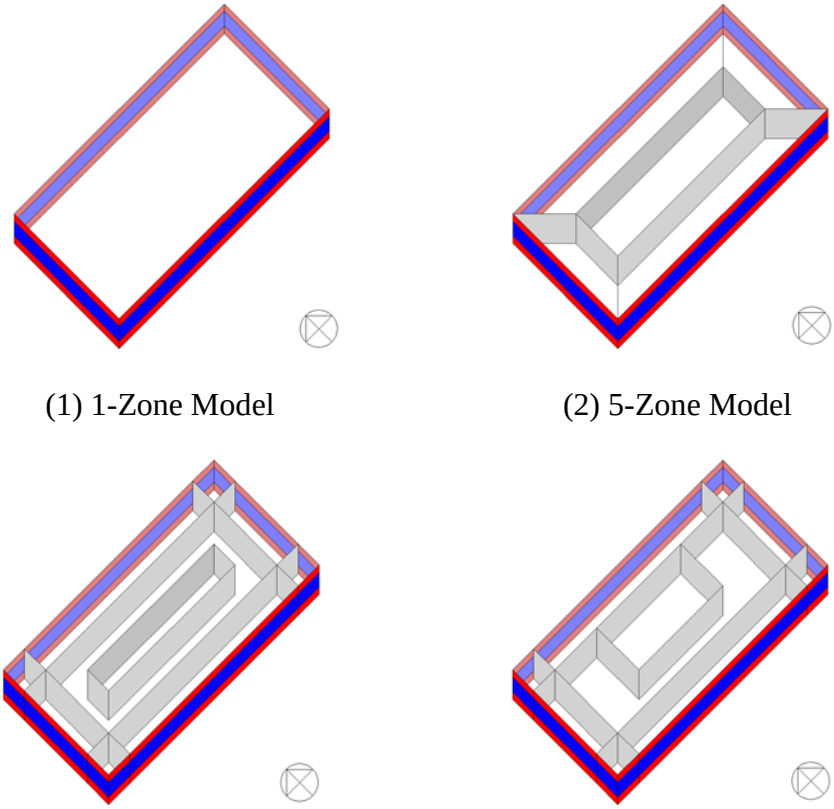

(1) 1-Zone Model (2) 5-Zone Model

(3) 10-Zone Model (for Summer) (4) 10-Zone Model (for Winter)

Figure 71: Different Zoning Models for Case 2 (Houston, TX)

Figure 72 shows the monthly total thermal loads (i.e., heating + cooling) for the 1-Zone, 5-Zone, and two 10-Zone thermal zoning models for Case 2 (Houston, TX) which is the rectangle-shape model with exterior windows. In addition, Figure 73 shows the total annual thermal loads (i.e., heating + cooling) for Case 2. The results show that the monthly total thermal loads of the 1-Zone model were mostly higher than other thermal zoning models during the cooling season. In addition, the monthly total thermal

loads of the 5-Zone and two 10-Zone models were very similar each other throughout the year. However, the simulated annual thermal loads of the 5-Zone and two 10-Zone models were less than the 1-zone model.

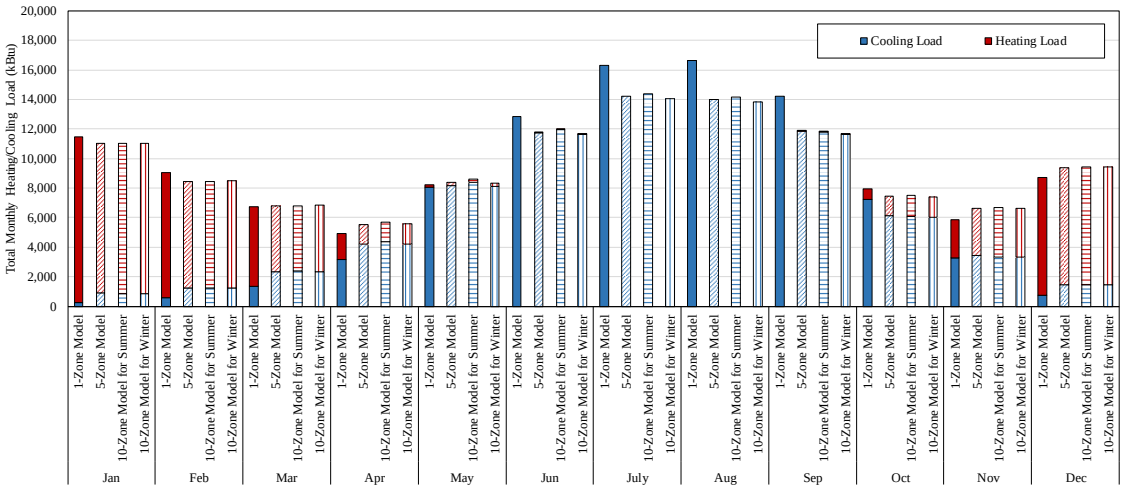

Figure 72: Total Monthly Heating/Cooling Loads for Case 2 (Houston, TX) Based on Different Thermal Zoning Methods

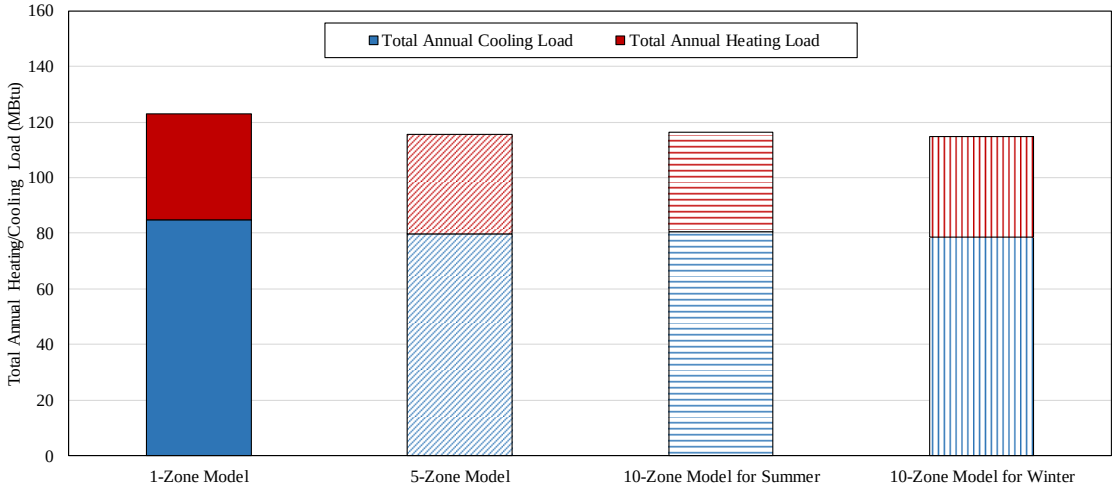

Figure 73: Total Annual Heating/Cooling Loads for Case 2 (Houston, TX) Based on Different Thermal Zoning Methods

Table 21 provides a tabulated comparison of the monthly total thermal loads for the 1-Zone, 5-zone, and two 10-Zone models. Both Figure 73 and Table 21 clearly show the 1-zone model is the most consumptive.

Table 21: Comparison of Annual Thermal Loads for Case 2 (Houston, TX)

	1-Zone Model (kBtu)	**5-Zone Model (kBtu)**	**10-Zone Model for Summer (kBtu)**	**10-Zone Model for Winter (kBtu)**	**1-Zone vs. 5 Zone (kBtu)**	**1-Zone vs. 10-Zone for Summer (kBtu)**	**1-Zone vs. 10-Zone for Winter (kBtu)**
Jan	11,457	11,002	11,007	11,003	-455 (-4%)	-450 (-4%)	-454 (-4%)
Feb	9,023	8,432	8,437	8,477	-591 (-7%)	-586 (-6%)	-546 (-6%)
Mar	6,726	6,782	6,793	6,839	56 (1%)	67 (1%)	113 (2%)
Apr	4,925	5,552	5,689	5,606	627 (13%)	764 (16%)	681 (14%)
May	8,211	8,377	8,596	8,330	166 (2%)	385 (5%)	119 (1%)
Jun	12,826	11,771	11,971	11,665	-1,055 (-8%)	-856 (-7%)	-1,161 (-9%)
Jul	16,310	14,228	14,383	14,063	-2,082 (-13%)	-1,927 (-12%)	-2,246 (-14%)
Aug	16,661	13,996	14,184	13,860	-2,665 (-16%)	-2,477 (-15%)	-2,801 (-17%)
Sep	14,195	11,887	11,804	11,633	-2,309 (-16%)	-2,391 (-17%)	-2,563 (-18%)
Oct	7,968	7,451	7,485	7,408	-518 (-6%)	-483 (-6%)	-560 (-7%)
Nov	5,856	6,635	6,669	6,655	779 (13%)	813 (14%)	798 (14%)
Dec	8,715	9,377	9,460	9,441	662 (8%)	745 (9%)	726 (8%)
Total	**122,874**	**115,489**	**116,478**	**114,981**	**-7,385 (-6%)**	**-6,396 (-5%)**	**-7,893 (-6%)**

The model specification of Case 6 (i.e., an L-shape model) was summarized in Table 16 in Section 5.1.1.4. This case also has an exterior window band with a WWR of 50%, located in Houston, TX. Figure 74 shows the thermal zoning layouts of the different zoning models (i.e., a single-zone thermal zoning model, a core-perimeter thermal zoning model, two grid/cluster thermal zoning models) for Case 6. For Case 6, the core-perimeter method gave a simulation model, which has 7 thermal zones. Also, the grid-cluster thermal zoning method gave two simulation models: one for summer (i.e., 12-Zone Model) and the other for winter (i.e., 14-Zone Model).

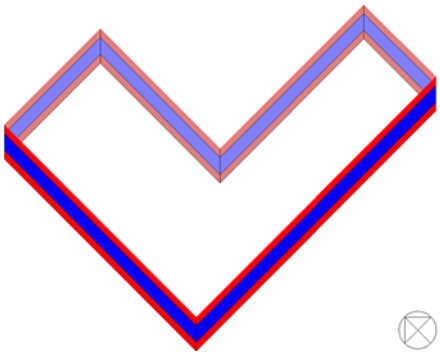

(1) 1-Zone Model

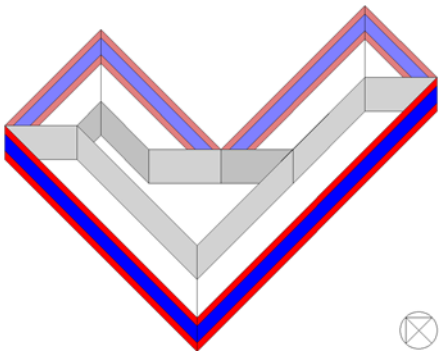

(2) 7-Zone Model

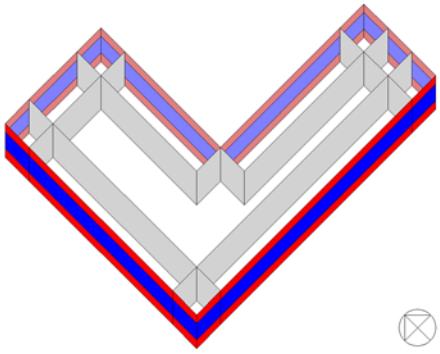

(3) 12-Zone Model for Summer

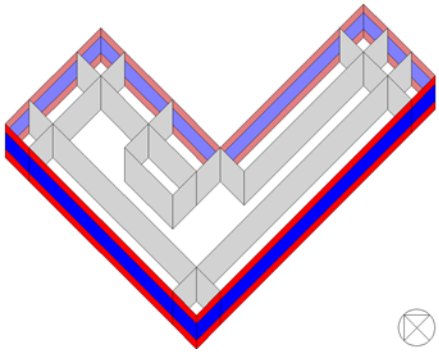

(4) 14-Zone Model for Winter

Figure 74: Different Zoning Models for Case 6 (Houston, TX)

Figure 75 shows the total monthly thermal loads (i.e., heating + cooling) for the 1-Zone, 7-Zone, 12-Zone, and 14-Zone thermal zoning models for Case 6 (Houston, TX), which is the L-shape model with exterior windows. In addition, Figure 76 shows the total annual thermal loads (i.e., heating + cooling) for Case 6. The results show that the total monthly thermal loads of the 1-Zone model were mostly higher than the other thermal zoning models during the cooling season. In addition, the total monthly thermal loads of the 12-Zone and two 14-Zone models were very similar each other throughout the year. However, the simulated annual thermal loads of the 7-Zone and two 10-Zone models were less than the 1-zone model.

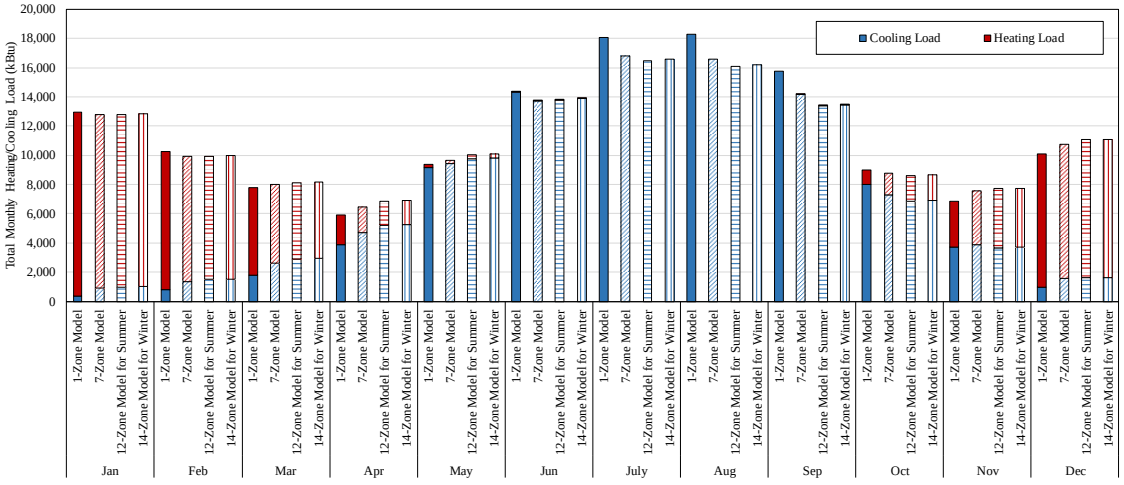

Figure 75: Total Monthly Heating/Cooling Loads for Case 6 (Houston, TX) Based on Different Thermal Zoning Methods

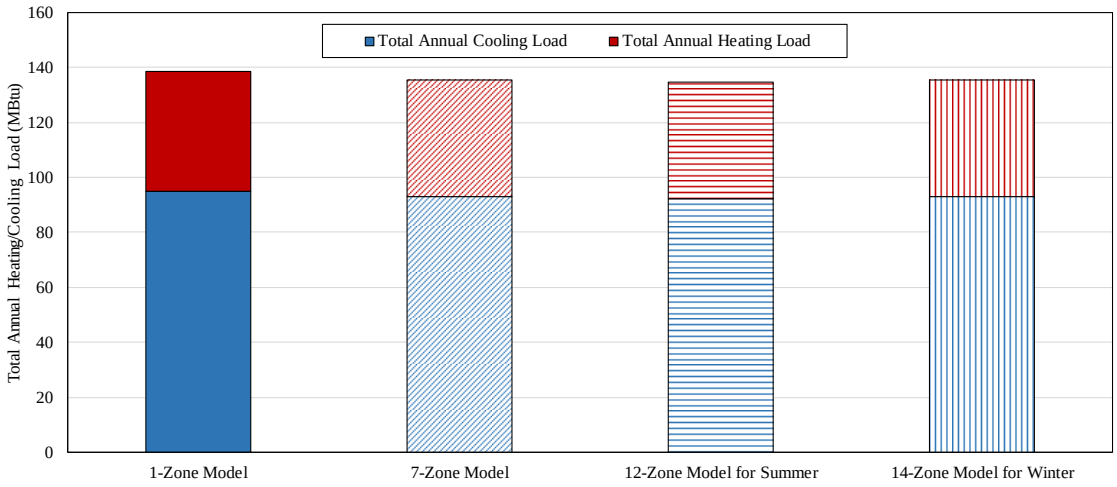

Figure 76: Total Annual Heating/Cooling Loads for Case 6 (Houston, TX) Based on Different Thermal Zoning Methods

Table 22: Comparison of Annual Thermal Loads for Case 6 (Houston, TX)

	1-Zone Model (kBtu)	**7-Zone Model (kBtu)**	**12-Zone Model (kBtu)**	**14-Zone Model (kBtu)**	**1-Zone vs. 7 Zone (kBtu)**	**1-Zone vs. 12-Zone (kBtu)**	**1-Zone vs. 14-Zone (kBtu)**
Jan	12,968	12,806	12,795	12,836	-161 (-1%)	-173 (-1%)	-132 (-1%)
Feb	10,283	9,932	9,932	9,966	-351 (-3%)	-351 (-3%)	-317 (-3%)
Mar	7,806	8,010	8,110	8,144	205 (3%)	304 (4%)	338 (4%)
Apr	5,894	6,450	6,830	6,882	556 (9%)	936 (16%)	987 (17%)
May	9,373	9,678	10,022	10,104	305 (3%)	649 (7%)	730 (8%)
Jun	14,309	13,754	13,784	13,881	-555 (-4%)	-525 (-4%)	-428 (-3%)
Jul	18,092	16,784	16,471	16,578	-1,308 (-7%)	-1,621 (-9%)	-1,514 (-8%)
Aug	18,280	16,583	16,104	16,205	-1,697 (-9%)	-2,176 (-12%)	-2,075 (-11%)
Sep	15,783	14,176	13,452	13,525	-1,606 (-10%)	-2,331 (-15%)	-2,258 (-14%)
Oct	9,020	8,770	8,621	8,678	-250 (-3%)	-399 (-4%)	-342 (-4%)
Nov	6,868	7,589	7,714	7,753	720 (10%)	845 (12%)	885 (13%)
Dec	10,072	10,774	11,062	11,106	701 (7%)	990 (10%)	1,033 (10%)
Total	**138,747**	**135,306**	**134,897**	**135,655**	**-3,442 (-2%)**	**-3,851 (-3%)**	**-3,092 (-2%)**

5.1.2.4. Case 4 (Rectangle-Shape Model, w/ Windows, Chicago, IL) vs. Case 8 (L-Shape Model, w/ Windows, Chicago, IL)

The model specification of Case 4 (i.e., a rectangle-shape model) was summarized in Table 14 in Section 5.1.1.2. This case has an exterior window band with a WWR of 50%, located in Chicago, IL. Figure 77 shows the thermal zoning layouts of the different zoning models (i.e., a single-zone thermal zoning model, a core-perimeter thermal zoning model, two Grid/Cluster thermal zoning models) for Case 4. For Case 4, the core-perimeter method gave a simulation model, which has five thermal zones. Also, the grid-cluster thermal zoning method gave two simulation models: one for summer (i.e., 10-Zone Model) and the other for winter (i.e., 11-Zone Model).

Figure 78 shows the total monthly thermal loads (i.e., heating + cooling) for the 1-Zone, 5-Zone, 10-Zone, and 11-Zone thermal zoning models for Case 4 (Chicago, IL), which is the rectangle-shape model with exterior windows. In addition, Figure 79 shows the total annual thermal loads (i.e., heating + cooling) for Case 4. The results show that the total monthly thermal loads of the 1-Zone model were mostly higher than other thermal zoning models during the heating season. In addition, the total monthly thermal loads of the 5-Zone, 10-Zone, 11-Zone models were very similar each other throughout the year. However, the simulated annual thermal loads of the 5-Zone and two 10-Zone models were less than the 1-zone model.

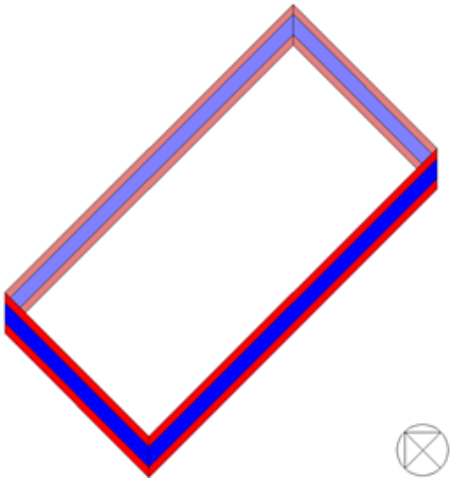

(1) 1-Zone Model

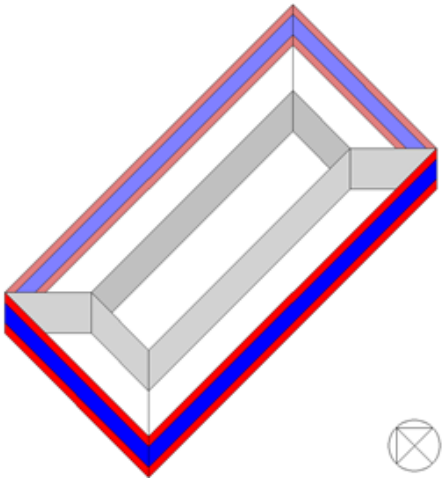

(2) 5-Zone Model

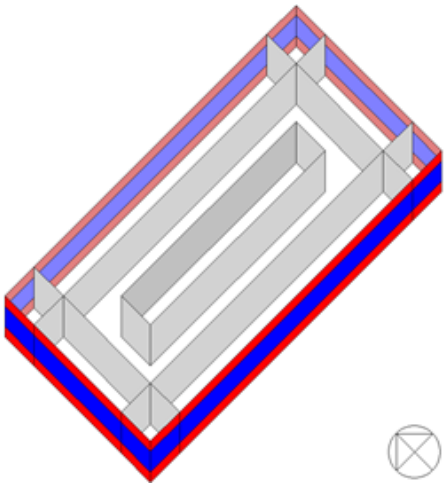

(3) 10-Zone Model for Summer

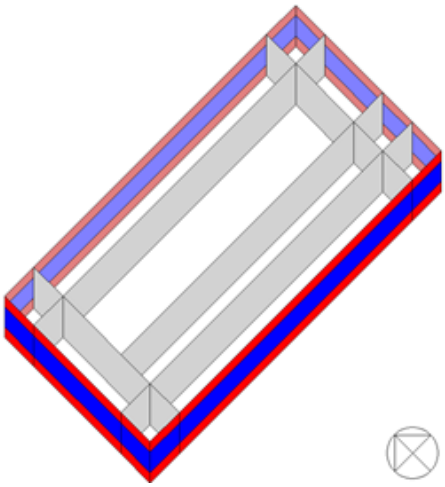

(4) 11-Zone Model for Winter

Figure 77: Different Zoning Models for Case 4 (Chicago, IL)

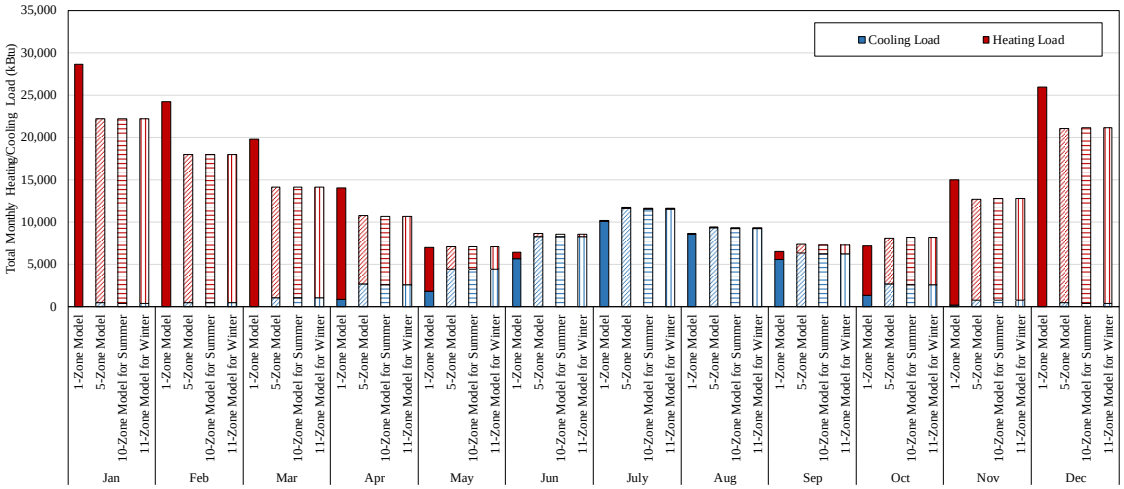

Figure 78: Total Monthly Heating/Cooling Loads for Case 4 (Chicago, IL) Based on Different Thermal Zoning Methods

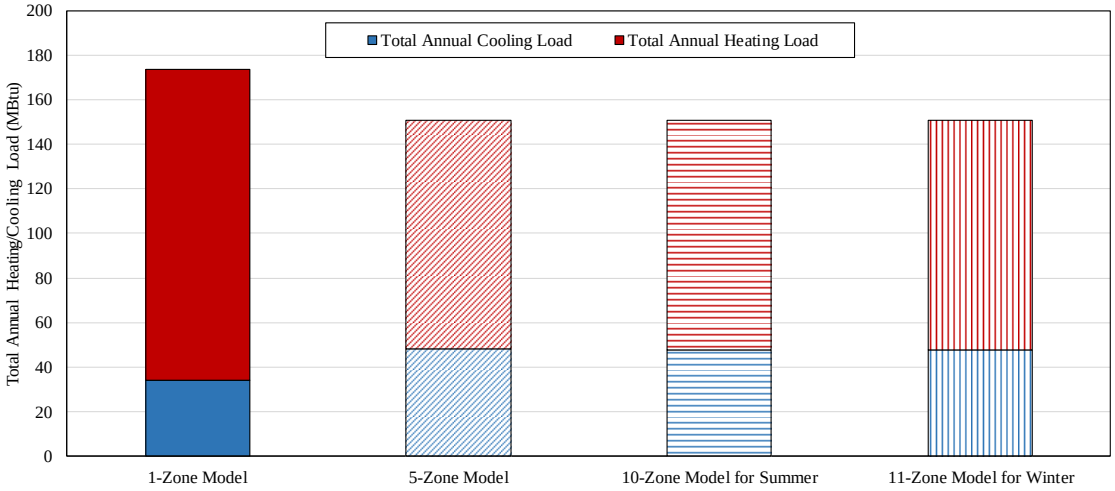

Figure 79: Total Annual Heating/Cooling Loads for Case 4 (Chicago, IL) Based on Different Thermal Zoning Methods

Table 23 provides a tabulated comparison of the total monthly thermal loads for the 1-Zone, 5-zone, 10-Zone, and 11-Zone models. Both Figure 79 and Table 23 clearly show the 1-zone model is the most consumptive.

Table 23: Comparison of Annual Thermal Loads for Case 4 (Chicago, IL)

	1-Zone Model (kBtu)	5-Zone Model (kBtu)	10-Zone Model (kBtu)	11-Zone Model (kBtu)	1-Zone vs. 5 Zone (kBtu)	1-Zone vs. 10-Zone (kBtu)	1-Zone vs. 11-Zone (kBtu)
Jan	28,628	22,208	22,229	22,229	-6,420 (-22%)	-6,399 (-22%)	-6,399 (-22%)
Feb	24,212	17,908	17,921	17,921	-6,304 (-26%)	-6,291 (-26%)	-6,291 (-26%)
Mar	19,825	14,063	14,071	14,071	-5,762 (-29%)	-5,754 (-29%)	-5,754 (-29%)
Apr	14,022	10,728	10,649	10,649	-3,294 (-23%)	-3,373 (-24%)	-3,373 (-24%)
May	7,031	7,053	7,087	7,087	22 (0%)	56 (1%)	56 (1%)
Jun	6,431	8,593	8,563	8,563	2,163 (34%)	2,132 (33%)	2,132 (33%)
Jul	10,168	11,652	11,557	11,557	1,484 (15%)	1,390 (14%)	1,390 (14%)
Aug	8,652	9,392	9,288	9,288	739 (9%)	635 (7%)	635 (7%)
Sep	6,548	7,348	7,295	7,295	799 (12%)	746 (11%)	746 (11%)
Oct	7,198	8,010	8,133	8,133	813 (11%)	936 (13%)	936 (13%)
Nov	15,015	12,671	12,752	12,752	-2,345 (-16%)	-2,263 (-15%)	-2,263 (-15%)
Dec	25,941	21,069	21,123	21,123	-4,873 (-19%)	-4,818 (-19%)	-4,818 (-19%)
Total	**173,672**	**150,695**	**150,669**	**150,669**	**-22,977 (-13%)**	**-23,003 (-13%)**	**-23,003 (-13%)**

The model specification of Case 8 (i.e., an L-shape model) was summarized in Table 16 in Section 5.1.1.4. This case also has an exterior window band with a WWR of 50%, located in Chicago, IL. Figure 80 shows the thermal zoning layouts of the different zoning models (i.e., a single-zone thermal zoning model, a core-perimeter thermal zoning model, two grid/cluster thermal zoning models) for Case 8. For Case 8, the core-perimeter method gave a simulation model, which has seven thermal zones. Also, the grid-cluster thermal zoning method gave two simulation models: one for summer and the other for winter. Both models have 14 thermal zones.

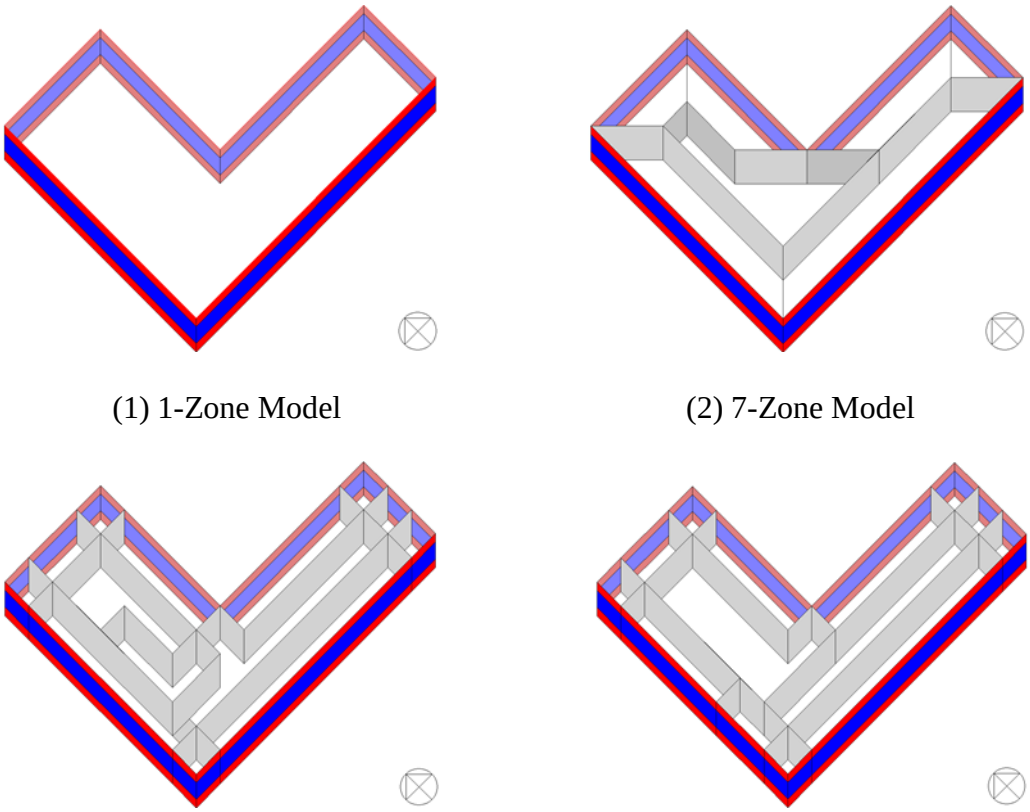

(1) 1-Zone Model (2) 7-Zone Model

(3) 14-Zone Model for Summer (4) 14-Zone Model for Winter

Figure 80: Different Zoning Models for Case 8 (Chicago, IL)

Figure 81 shows the total monthly thermal loads (i.e., heating + cooling) for the 1-Zone, 7-Zone, and two 14-Zone thermal zoning models for Case 8 (Chicago, IL), which is the L-shape model with exterior windows. In addition, Figure 82 shows the total annual thermal loads (i.e., heating + cooling) for Case 8. The results show that the total monthly thermal loads of the 1-Zone model were mostly higher than other thermal zoning models during the heating season. In addition, the total monthly thermal loads of the 7-Zone and two 14-Zone models were very similar each other throughout the year.

However, the simulated annual thermal loads of the 7-Zone and two 14-Zone models were less than the 1-zone model.

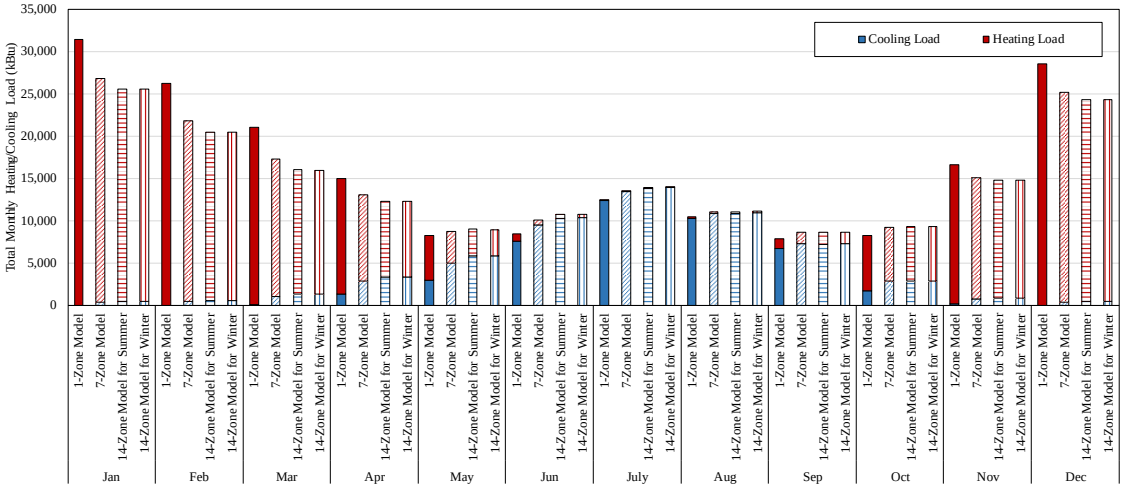

Figure 81: Total Monthly Heating/Cooling Loads for Case 8 (Chicago, IL) Based on Different Thermal Zoning Methods

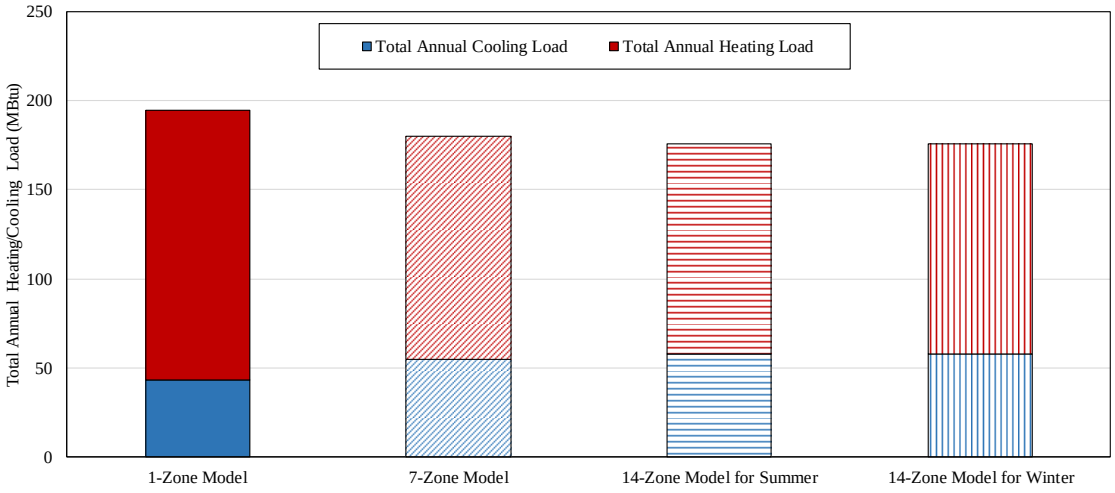

Figure 82: Total Annual Heating/Cooling Loads for Case 8 (Chicago, IL) Based on Different Thermal Zoning Methods

Table 24 provides a tabulated comparison of the monthly total thermal loads for the 1-Zone, 7-zone, and two 14-Zone models. Both Figure 82 and Table 24 clearly show the 1-zone model is the most consumptive.

Table 24: Comparison of Annual Thermal Loads for Case 8 (Chicago, IL)

	1-Zone Model (kBtu)	**7-Zone Model (kBtu)**	**14-Zone Model for Summer (kBtu)**	**14-Zone Model for Winter (kBtu)**	**1-Zone vs. 7 Zone (kBtu)**	**1-Zone vs. 14-Zone for Summer (kBtu)**	**1-Zone vs. 14-Zone for Winter (kBtu)**
Jan	31,377	26,792	25,545	25,570	-4,584 (-15%)	-5,831 (-19%)	-5,807 (-19%)
Feb	26,247	21,767	20,464	20,470	-4,480 (-17%)	-5,783 (-22%)	-5,777 (-22%)
Mar	21,020	17,308	16,007	15,979	-3,712 (-18%)	-5,013 (-24%)	-5,042 (-24%)
Apr	15,005	13,070	12,317	12,278	-1,935 (-13%)	-2,689 (-18%)	-2,728 (-18%)
May	8,268	8,667	8,966	8,898	399 (5%)	698 (8%)	630 (8%)
Jun	8,412	10,030	10,738	10,783	1,618 (19%)	2,327 (28%)	2,371 (28%)
Jul	12,450	13,527	13,889	13,987	1,077 (9%)	1,439 (12%)	1,538 (12%)
Aug	10,412	11,013	11,055	11,125	602 (6%)	643 (6%)	713 (7%)
Sep	7,890	8,586	8,601	8,603	695 (9%)	710 (9%)	713 (9%)
Oct	8,220	9,224	9,340	9,329	1,004 (12%)	1,119 (14%)	1,108 (13%)
Nov	16,580	15,084	14,747	14,757	-1,496 (-9%)	-1,833 (-11%)	-1,823 (-11%)
Dec	28,565	25,164	24,283	24,320	-3,401 (-12%)	-4,282 (-15%)	-4,244 (-15%)
Total	**194,446**	**180,232**	**175,951**	**176,10**	**-14,213 (-7%)**	**-18,495 (-10%)**	**-18,348 (-9%)**

5.1.3. Summary of Parametric Study of Thermal Zoning on Building Shape

In this section, the parametric study using two building shapes (i.e., rectangle-shape, L-shape) and three different thermal zoning methods (i.e., single zone, core-perimeter, grid/cluster thermal zoning method) was performed to investigate the impact of the building shape on building thermal zoning and heating/cooling loads.

The resultant thermal zoning layouts based on the grid/cluster thermal zoning method showed that the thermal zoning layouts were influenced primarily by the existence of exterior windows, and to a lesser extent by the building shape. The cases that do not have any exterior windows showed very similar thermal zoning layouts with the traditional core-perimeter thermal zoning layout, which means those cases have only one single interior space as a thermal zone. However, if the cases have exterior windows, the thermal zoning layout of the interior spaces have more than one thermal zone, regardless of building shape and climate condition.

Table 25 shows the summary of comparisons of annual total thermal loads reductions between the rectangle-shape and L-shape model. These results show how much thermal load reduction was achieved when the grid/cluster thermal zoning method was applied to each case compared to single-zone model. All the cases showed positive thermal load reduction with the thermal zoning layout, which used the grid/cluster thermal zoning method. In addition, comparing the building shapes, for the rectangle-shape models, about 3 to 6% more annual total thermal loads were reduced than the L-shape models. Figure 83 shows the comparison of the annual thermal load reduction between the rectangle-shape and L-shape model.

Table 25: Summary of Comparisons of Total Annual Loads Based on Thermal Zoning Methods

Case #	Building Shape	Single Zone Method (Btu)	Grid/Cluster Method (Btu)	Load Reduction (Btu)	Load Reduction (%)
Case 1 vs. Case 5	Rectangle-Shape	64,761,931	55,057,989	9,703,942	15%
	L-Shape	66,979,781	60,423,308	6,556,474	10%
Case 3 vs. Case 7	Rectangle-Shape	130,854,654	79,731,693	51,122,960	39%
	L-Shape	138,234,936	87,788,552	50,446,384	36%
Case 2 vs. Case 6	Rectangle-Shape	122,873,950	114,981,355	7,892,595	6%
	L-Shape	138,747,489	135,655,336	3,092,153	2%
Case 4 vs. Case 8	Rectangle-Shape	173,672,343	150,669,079	23,003,263	13%
	L-Shape	194,446,028	176,097,674	18,348,354	9%

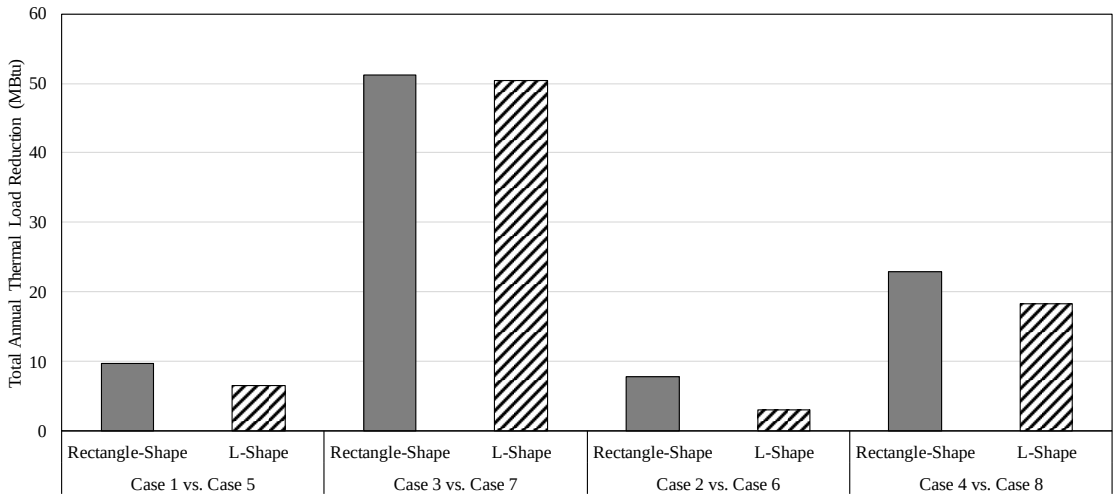

Figure 83: Annual Thermal Load Reductions from Different Building Shapes

5.2. Analysis of the Impact of Window-to-Wall Ratio on Thermal Zoning

In this section, the impact of changes to the window-to-wall ratio (WWR) of the building on thermal zoning in a simulation was investigated. For the analysis, eleven combinations of WWR and orientations were considered for two climate conditions (i.e., Houston, TX, Chicago, IL). In addition, for each WWR, three different thermal zoning simulation models were created using the single-zone thermal zoning method (i.e., 1-Zone model), the core-perimeter zoning method (i.e., 5-Zone model), and the grid/cluster thermal zoning method. The calculated annual/monthly heating/cooling loads for each case were then calculated, compared, and analyzed.

5.2.1. Impact of WWR on the Building Thermal Zoning

The geometric information of the façade modules that were used for the simulation models in this study are shown in Figure 38 in Section 4.3.2. All the simulation cases in this section used the simplified commercial base-case model, which was described in Table 9 in Section 4.2.2. Figure 84 to Figure 86 show the exterior views of the simulation models that were used in this study, including the exterior window with different WWR (i.e., 0%, 50%, 80%). In addition, Table 26 presents the information of the WWR in the four orientations (i.e., North, East, South, West) for all the simulation cases. Three different thermal zoning methods (i.e., the single-zone thermal zoning method, the traditional core-perimeter thermal zoning method, and the grid/cluster thermal zoning method) were applied to each simulation case to investigate

the differences in the annual and monthly heating/cooling loads between the models with three thermal zoning methods.

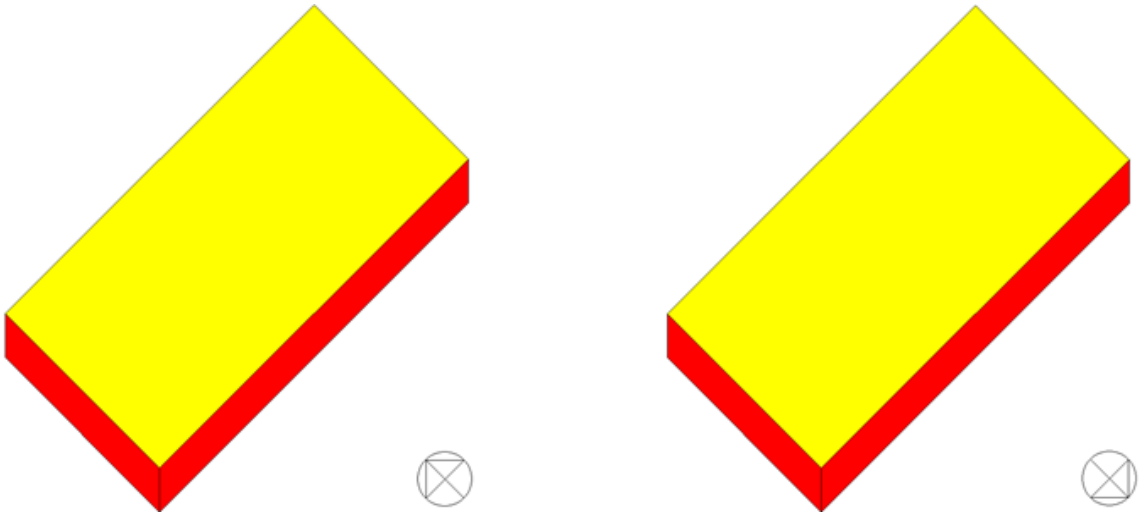

(a) Southwest View (b) Northeast View

Figure 84: View of a Simplified Base-case Model with WWR of 0%

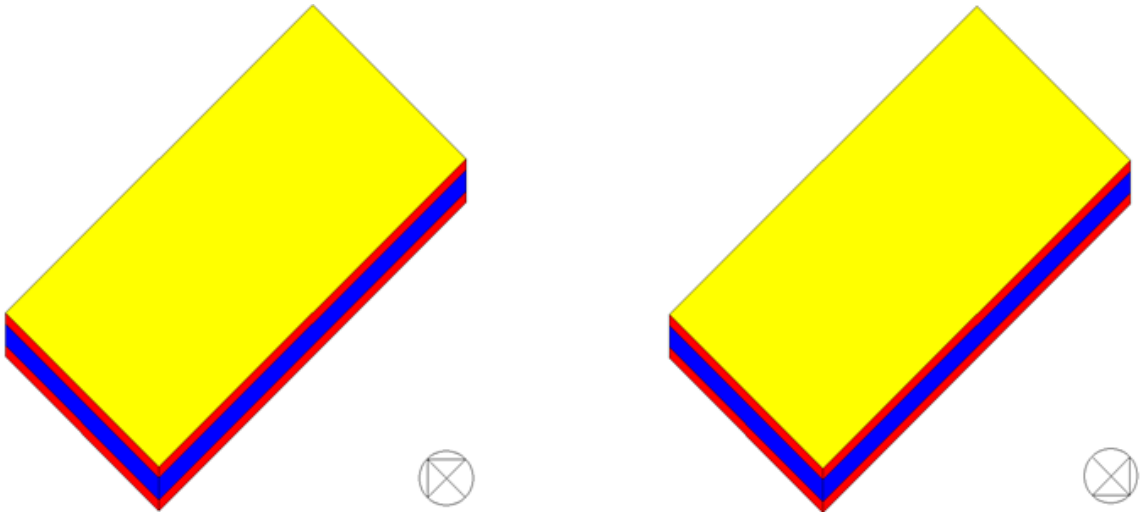

(a) Southwest View (b) Northeast View

Figure 85: View of a Simplified Base-case Model with WWR of 50%

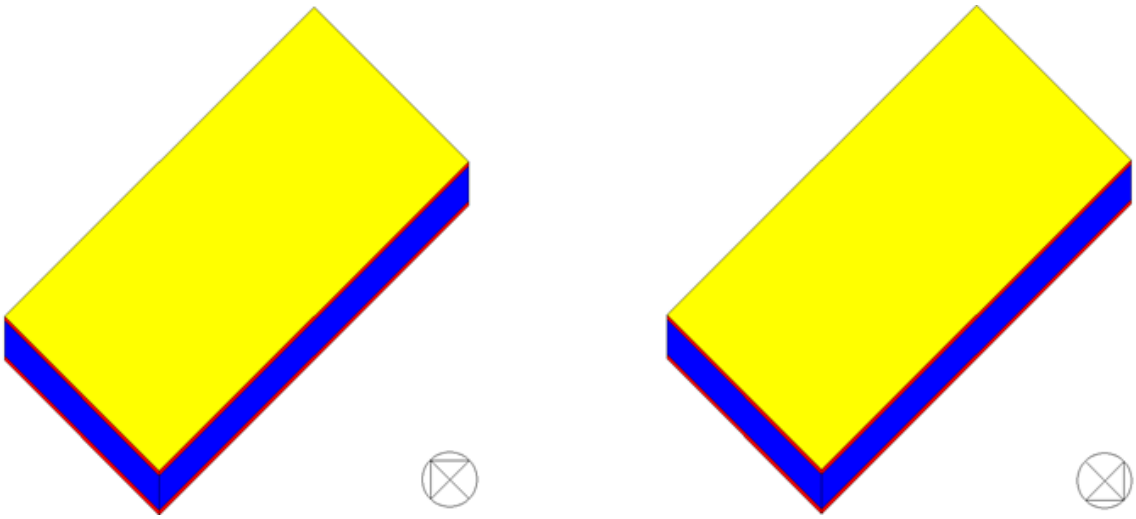

(a) Southwest View (b) Northeast View

Figure 86: View of a Simplified Base-case Model with WWR of 80%

Table 26: WWR in the Four Orientations for the Simulation Cases

Case #	Location	East	West	North	South
1	Houston	0 %	0 %	0 %	0 %
2		50 %	50 %	50 %	50 %
9		80 %	80 %	80 %	80 %
3	Chicago	0 %	0 %	0 %	0 %
4		50 %	50 %	50 %	50 %
14		80 %	80 %	80 %	80 %

Table 27 presents the resultant thermal zoning layouts using the grid/cluster thermal zoning method for the Case 1 (WWR 0%), Case 2 (WWR 50%), and Case 9 (WWR 80%) simulation models in Houston, TX. The results show that the grid/cluster thermal zoning method yielded a similar result to the traditional core/perimeter thermal zoning method for the Case 1, when the simulation model had no exterior windows. In Case 1, the layout has a single interior space and four different perimeter spaces along with each orientation. In addition, in Case 1 the four grid spaces located at each corner of the model became four different thermal zones. For Case 2, different thermal zoning layouts resulted for the heating and cooling seasons. For the cooling season, the interior thermal zone (i.e., Zone 23, Zone 24, Zone 25, Zone 26, Zone 27, Zone 28) was created in the center of the interior space. Therefore, the Case 2 model has two different thermal zones in the interior space. For the heating season, the model also has two different thermal zones in the interior space. However, the location and size of the thermal zone is different than the cooling season. In the Case 2 model, for the heating season these interior thermal zones are located in the center of the interior space (i.e., Zone 24, Zone 25, Zone 26, Zone 27, Zone 34, Zone 35, Zone 36, Zone 37), which covers the north side of the interior space as well. For the Case 9, the grid/cluster method gave exactly the same thermal zoning layout as the Case 2 for the cooling season. However, for the heating season, it also has two thermal zones in the interior space. In addition, the area is different with the thermal zoning layout of the Case 2 for the heating season. Using the grid/cluster thermal zoning method, four more grid spaces (i.e., Zone 23, Zone 28, Zone 33, Zone 38) were merged into the core thermal zone.

Table 27: Results of Thermal Zoning for Case 1, Case 2, Case 9 (Houston, TX)

	WWR	Cooling Season	Heating Season
Case 1	0 %	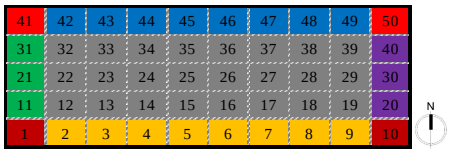	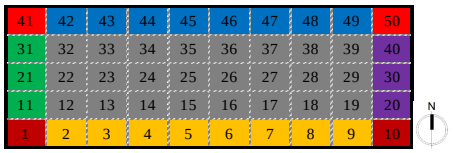
Case 2	50 %	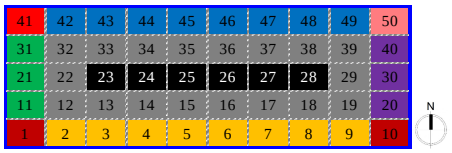	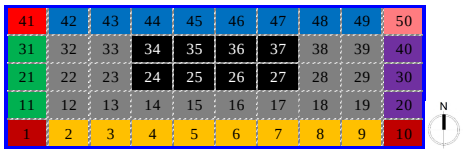
Case 9	80 %	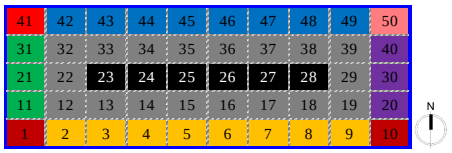	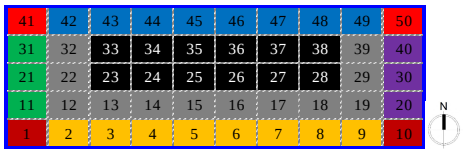

Table 28 presents the resultant thermal zoning layouts using the grid/cluster thermal zoning method for the Case 3 (WWR 0%), Case 4 (WWR 50%), and Case 14 (WWR 80%). The results show that the grid/cluster thermal zoning method yielded a similar result with one that follows the traditional core/perimeter thermal zoning method for the Case 3 (Chicago, IL), which is the same results given from the Case 1 (Houston, TX). For the Case 4 (Chicago, IL), it also yielded the same result from the Case 2 (Houston, TX) for the cooling season. However, for the heating season, there was some variation in thermal zoning layout in both interior and exterior spaces as compared to Case 2 and Case 9. In Case 4 and Case 14, the interior space was divided horizontally by two separate thermal zones. For the exterior spaces, the space in the east orientation was

divided into two thermal zones: one includes Zone 20, the other includes Zone 30 and Zone 31 (east side). On the other hand, the spaces facing North, South, and West were maintained as a single thermal zone. Interestingly, the resultant thermal zoning layouts of the Case 14 (Chicago, IL) show the same results with one that given from the Case 4 (Chicago, IL).

Table 28: Results of Thermal Zoning for Case 3, Case 4, Case 14 (Chicago, IL)

	WWR	Cooling Season	Heating Season
Case 3	**0 %**	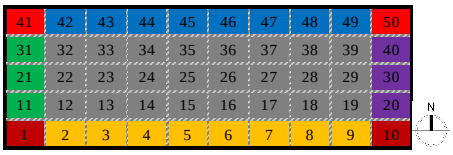	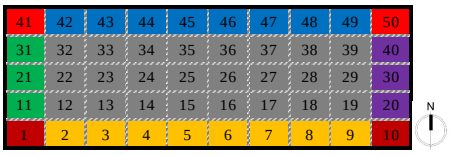
Case 4	**50 %**	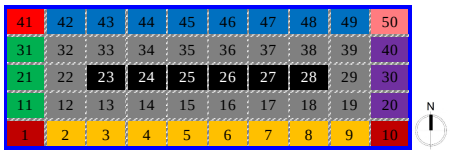	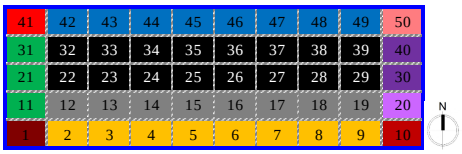
Case 14	**80 %**	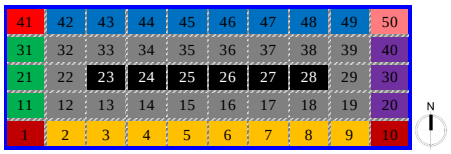	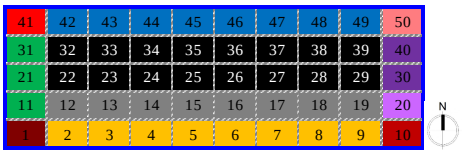

Figure 87 shows the thermal zoning layouts from the different zoning models (i.e., a single-zone thermal zoning model, a core-perimeter thermal zoning model, and two grid/cluster thermal zoning models) for Case 9 (Houston, TX). The model specification of Case 9 (i.e., a rectangle-shape model) was summarized in Table 9 in

Section 4.2.2. In this case only the WWR value was changed from 50% to 80%. The Case 9 simulation models have a band of exterior windows with a WWR of 80%, located in Houston, TX. For Case 9, the core-perimeter method yielded a simulation model with 5 thermal zones. Finally, it should be noted that the grid-cluster thermal zoning method gave two simulation models: one for summer and the other for the winter. Both models have 10 thermal zones.

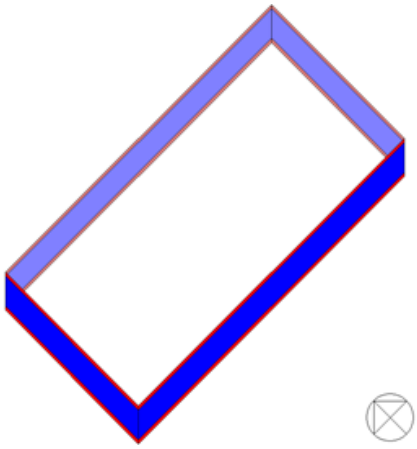

(1) 1-Zone Model

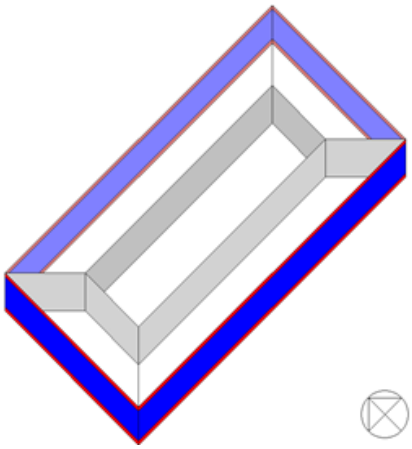

(2) 5-Zone Model

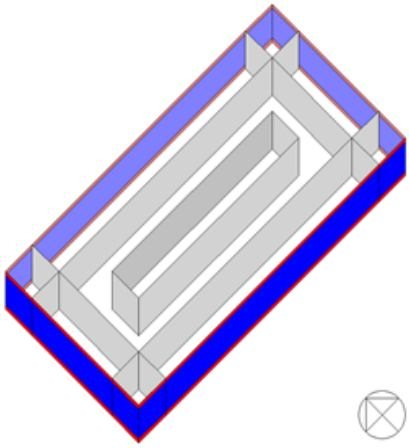

(3) 10-Zone Model (for Summer)

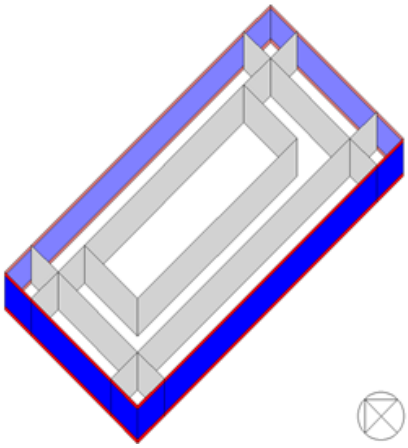

(4) 10-Zone Model (for Winter)

Figure 87: Different Zoning Models for Case 9 (Houston, TX)

Figure 88 shows the total monthly heating/cooling loads for the 1-Zone, 5-Zone, and two 10-Zone thermal zoning models for Case 9 (Houston, TX). The results show that the total monthly thermal loads of the 1-Zone model are mostly similar with the thermal zoning models in the heating season, while the cooling loads are higher than the other thermal zoning models in the cooling season. In addition, the total monthly thermal loads of the 5-Zone and two 10-Zone models are very similar throughout the year.

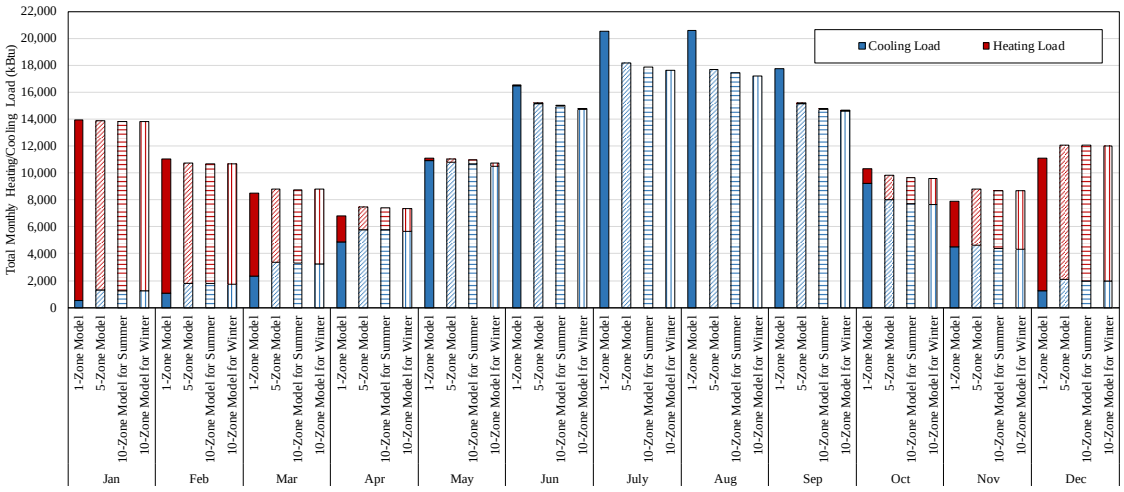

Figure 88: Total Monthly Heating/Cooling Loads for Case 9 (Houston, TX) Based on Different Zoning Methods

Figure 89 shows the total annual heating/cooling loads for the 1-Zone, 5-Zone, two 10-Zone thermal zoning models for Case 9 (Houston, TX). The results show that the 10-Zone thermal zoning models for the winter day for Case 9 gave the most energy efficient thermal zoning layout among the four thermal zoning strategies. In addition, this model yielded a 7% thermal load reduction compared to the 1-Zone thermal zoning model.

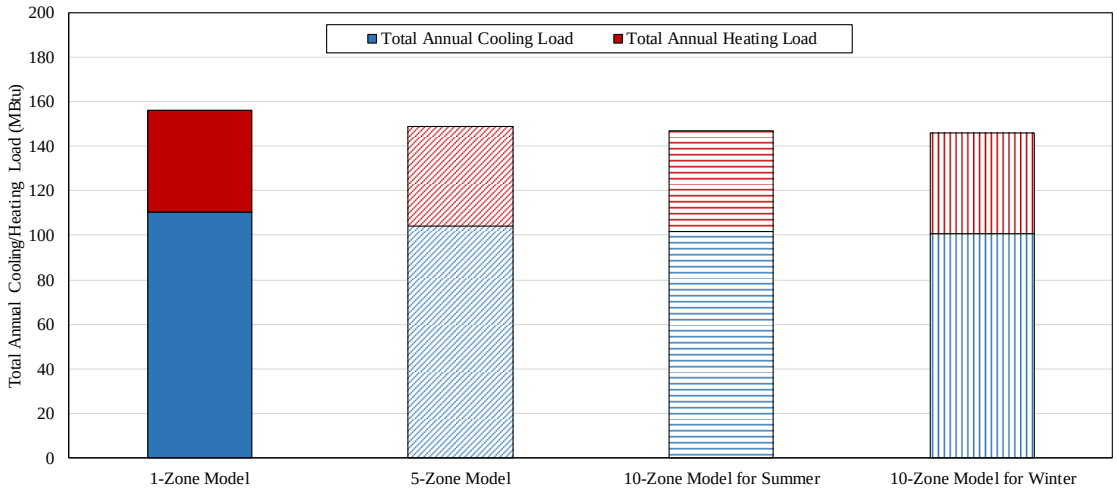

Figure 89: Total Annual Heating/Cooling Loads for Case 9 (Houston, TX) Based on Different Thermal Zoning Methods

Table 29 shows the total monthly thermal loads for Case 9 (Houston, TX) with the amount of the monthly thermal load reduction. As shown in the table, the 10-Zone model for the winter has a thermal load reduction compared to 1-Zone model, except March, April, November, and December. The grid/cluster thermal zoning method gave the highest load reduction of 18 % in September, with a load increase of 10 % in November. The total annual thermal load reduction of 7% indicates that the 10-Zone thermal zoning for winter model has an improved energy efficiency than 1-Zone thermal zoning model for the specific conditions of Case 9.

Figure 90 shows the thermal zoning layouts from the different zoning models (i.e., a single-zone thermal zoning model, a core-perimeter thermal zoning model, and two grid/cluster thermal zoning models) for Case 14 (Chicago). The model specification of Case 14 was summarized in Table 9 in Section 4.2.2. In this case only the WWR value was changed from 50% to 80%. The results showed the Case 14 models have a

band of exterior windows with a WWR of 80%, located in Chicago, IL. For Case 14, the core-perimeter method yielded a simulation model, that had 5 thermal zones. Finally, it should be noted that the grid-cluster thermal zoning method gave two simulation models: one for the summer day (i.e., 10-Zone Model) and the other for the winter day (i.e., 11-Zone Model).

Table 29: Comparison of Annual Thermal Load for Case 9 (Houston, TX)

	1-Zone Model (kBtu)	**5-Zone Model (kBtu)**	**10-Zone Model for Summer (kBtu)**	**10-Zone Model for Winter (kBtu)**	**1-Zone vs. 5 Zone (kBtu)**	**1-Zone vs. 10-Zone for Summer (kBtu)**	**1-Zone vs. 10-Zone for Winter (kBtu)**
Jan	13,933	13,907	13,814	13,811	-25 (0%)	-119 (-1%)	-121 (-1%)
Feb	11,025	10,720	10,661	10,691	-305 (-3%)	-364 (-3%)	-334 (-3%)
Mar	8,509	8,820	8,751	8,786	311 (4%)	242 (3%)	277 (3%)
Apr	6,814	7,455	7,443	7,380	641 (9%)	628 (9%)	566 (8%)
May	11,129	11,036	10,967	10,767	-93 (-1%)	-161 (-1%)	-361 (-3%)
Jun	16,506	15,144	14,978	14,749	-1,362 (-8%)	-1,528 (-9%)	-1,757 (-11%)
Jul	20,565	18,152	17,888	17,649	-2,412 (-12%)	-2,676 (-13%)	-2,916 (-14%)
Aug	20,622	17,669	17,463	17,220	-2,952 (-14%)	-3,158 (-15%)	-3,401 (-16%)
Sep	17,768	15,212	14,780	14,651	-2,556 (-14%)	-2,988 (-17%)	-3,117 (-18%)
Oct	10,304	15,212	9,640	9,582	-498 (-5%)	-664 (-6%)	-722 (-7%)
Nov	7,888	8,775	8,677	8,666	887 (11%)	789 (10%)	779 (10%)
Dec	11,111	12,056	12,047	12,033	945 (9%)	935 (8%)	922 (8%)
Total	**156,172**	**148,752**	**147,110**	**145,987**	**-7,420 (-5%)**	**-9,063 (-6%)**	**-10,185 (-7%)**

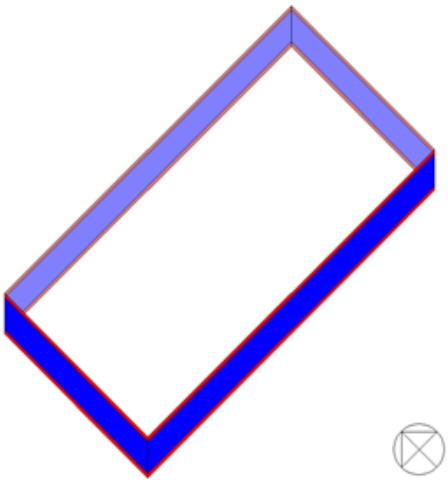

(1) 1-Zone Model

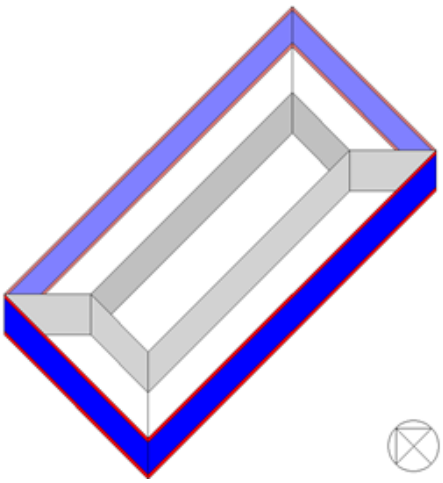

(2) 5-Zone Model

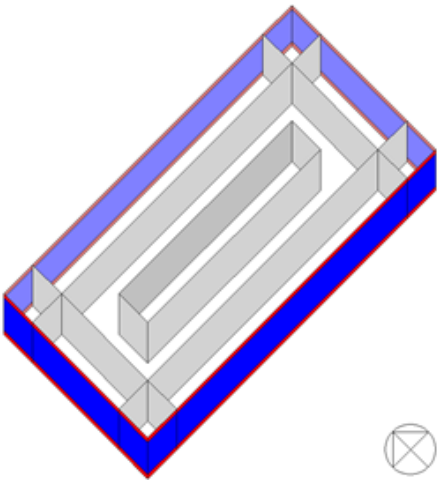

(3) 10-Zone Model (for Summer)

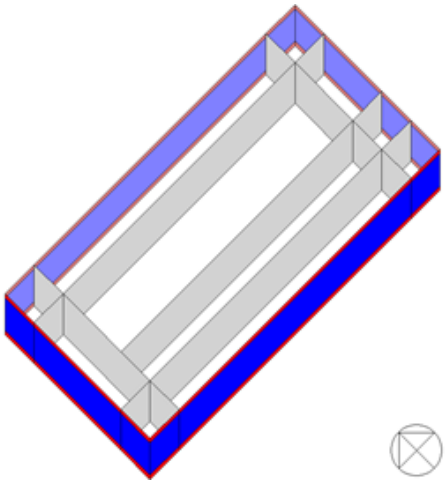

(4) 11-Zone Model (for Winter)

Figure 90: Different Zoning Models for Case 14 (Chicago, IL)

Figure 91 shows the total monthly heating/cooling loads for the 1-Zone, 5-Zone, 10-Zone, and 11-Zone thermal zoning models for Case 14 (Chicago, IL). The results show that the total monthly thermal loads of the 1-Zone model are mostly higher than the other thermal zoning models in the winter season, while the cooling loads are lower than the other thermal zoning models in the cooling season. In addition, the monthly

total thermal loads of the 5-Zone 10-Zone, 11-Zone models are very similar throughout the year.

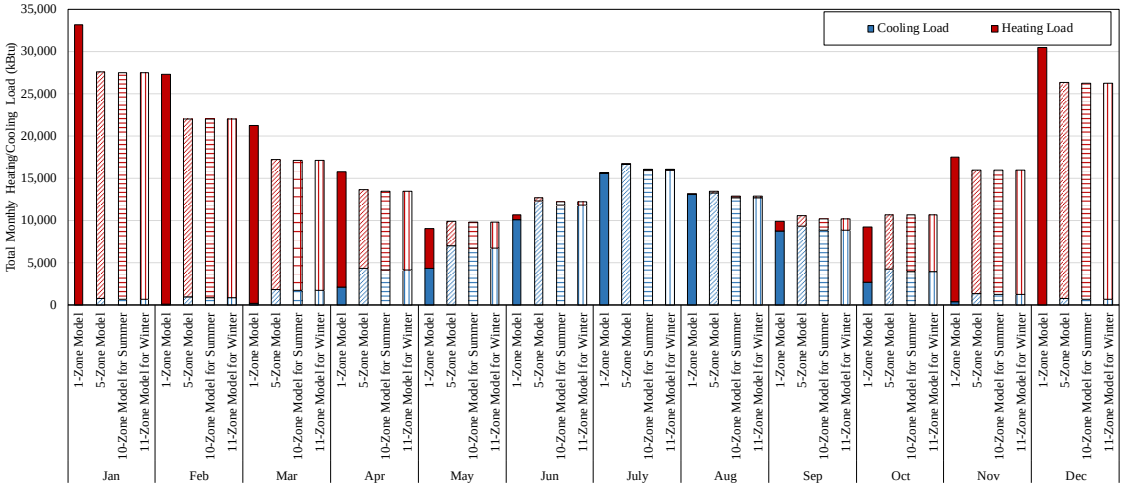

Figure 91: Total Monthly Heating/Cooling Loads for Case 14 (Chicago, IL) Based on Different Zoning Methods

Figure 92 shows the total annual heating/cooling loads for the 1-Zone, 5-Zone, 10-Zone, and 11-Zone thermal zoning models for Case 14 (Chicago, IL). The results show that the 10-Zone and 11-Zone thermal zoning models (i.e., the grid/cluster thermal zoning method) for Case 14 yielded the most energy efficient thermal zoning layout among the four thermal zoning strategies. In addition, these models showed a 9% thermal load reduction compared to the 1-Zone thermal zoning model.

Table 30 shows the total monthly thermal loads for Case 14 (Chicago, IL) with the amount of the monthly thermal load reduction. As shown in the table, the 11-Zone model for the winter day has a thermal load reduction compared to the 1-Zone model, except May, June, July, September, and October. The grid/cluster thermal zoning

method gave the highest load reduction of 20% in February, with a load increase of 16 % in October. The annual total thermal load reduction of 9 % indicates that the 10-Zone and 11-Zone thermal zoning for winter model has an improved energy efficiency than 1-Zone thermal zoning model for the specific conditions of Case 14.

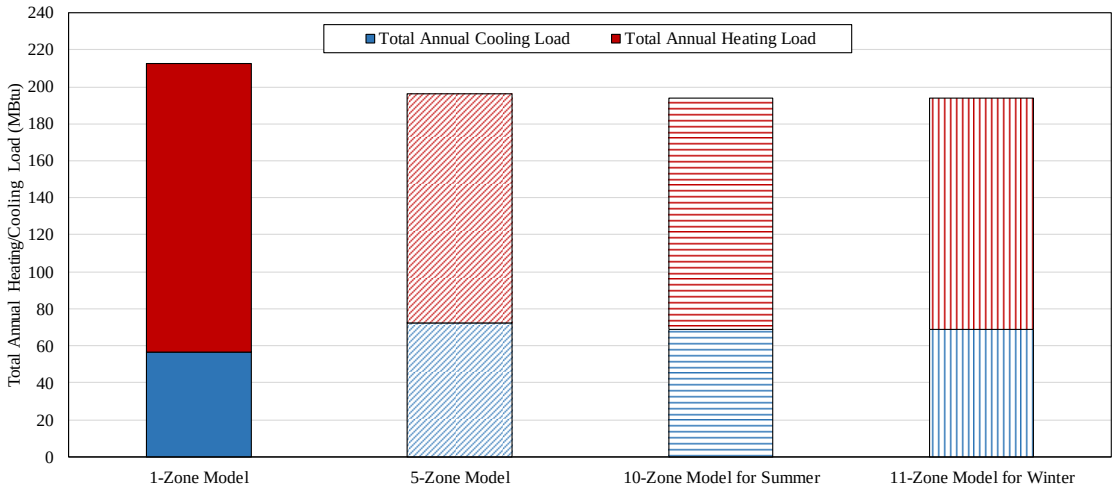

Figure 92: Total Annual Heating/Cooling Load for Case 14 (Chicago, IL) Based on Different Thermal Zoning Methods

Figure 93 shows the comparison of the calculated total annual heating/cooling loads between different WWR (i.e., 0%, 50%, 80%) models (i.e., Case 1, Case 2, Case 9) for the different thermal zoning strategies using the single zone, core-perimeter, and grid/cluster thermal zoning method. In general, the cooling loads are larger than the heating loads for each model, since the location of the simulation model was set to the hot and humid climate (i.e., Houston, TX). When the WWR is changed from 0% to 50% and from 50% to 80%, the total annual heating/cooling loads were increased about 90% to 124% and 26% to 29%, respectively compared to the model with WWR 0%. In

addition, for all the WWR cases, it was observed that the core-perimeter zoning and the grid/cluster zoning layouts provided total heating/cooling load reduction of 5% to 20%, compared to the single zone model. However, as WWR was increased, the amount of the load reduction was decreased.

Table 30: Comparison of Annual Thermal Load for Case 14 (Chicago, IL)

	1-Zone Model (kBtu)	**5-Zone Model (kBtu)**	**10-Zone Model for Summer (kBtu)**	**11-Zone Model for Winter (kBtu)**	**1-Zone vs. 5 Zone (kBtu)**	**1-Zone vs. 10-Zone for Summer (kBtu)**	**1-Zone vs. 11-Zone for Winter (kBtu)**
Jan	33,151	27,596	27,478	27,478	-5,555 (-17%)	-5,673 (-17%)	-5,673 (-17%)
Feb	27,298	22,022	21,952	21,951	-5,276 (-19%)	-5,346 (-20%)	-5,347 (-20%)
Mar	21,263	17,141	17,132	17,132	-4,122 (-19%)	-4,131 (-19%)	-4,131 (-19%)
Apr	15,703	13,641	13,478	13,478	-2,062 (-13%)	-2,225 (-14%)	-2,225 (-14%)
May	8,978	9,897	9,781	9,781	919 (10%)	802 (9%)	802 (9%)
Jun	10,616	12,633	12,193	12,193	2,017 (19%)	1,577 (15%)	1,577 (15%)
Jul	15,614	16,613	15,996	15,996	999 (6%)	382 (2%)	382 (2%)
Aug	13,076	13,412	12,860	12,860	336 (3%)	-216 (-2%)	-216 (-2%)
Sep	9,834	10,501	10,146	10,146	667 (7%)	311 (3%)	311 (3%)
Oct	9,183	10,595	10,618	10,618	1,411 (15%)	1,434 (16%)	1,434 (16%)
Nov	17,469	15,911	15,930	15,930	-1,558 (-9%)	-1,539 (-9%)	-1,539 (-9%)
Dec	30,456	26,328	26,242	26,242	4,128 (-14%)	4,214 (-14%)	4,214 (-14%)
Total	**212,642**	**196,290**	**193,805**	**193,805**	**-16,352 (-8%)**	**-18,837 (-9%)**	**-18,837 (-9%)**

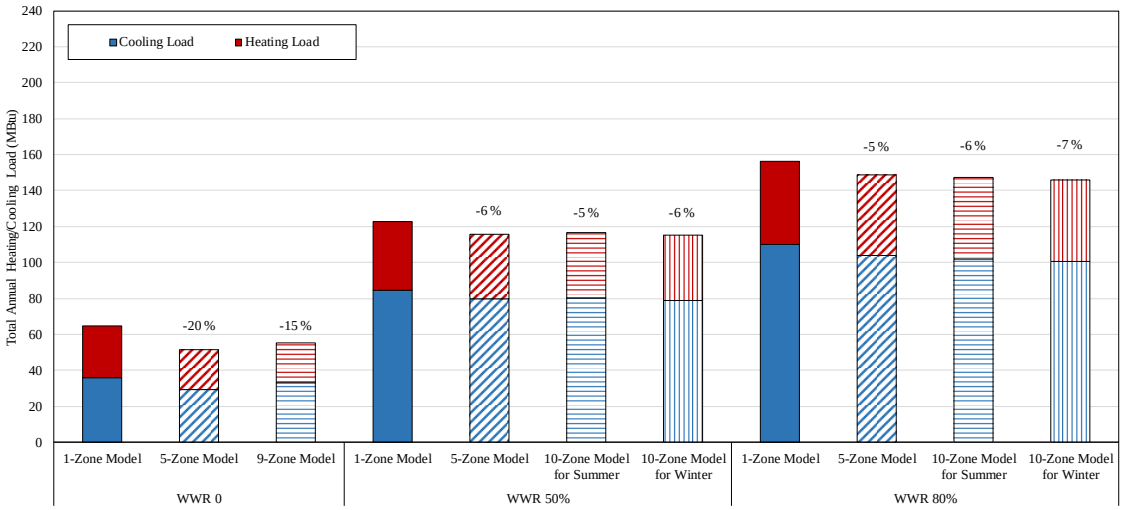

Figure 93: Comparison of the Total Annual Heating/Cooling Load between Different WWR Models for Houston

Figure 94 shows the comparison of the calculated total annual heating/cooling loads between different WWR (i.e., 0%, 50%, 80%) models (i.e., Case 3, Case 4, Case 14) for the different thermal zoning strategies using the single zone, core-perimeter, and grid/cluster thermal zoning method. In general, the heating loads are larger than the cooling loads for each model, since the location was set to the cold and humid climate (i.e., Chicago, IL). When the WWRs were changed from 0% to 50% and from 50% to 80%, the annual total heating/cooling loads were increased 33% to 89% and 22% to 30%, respectively compared to the model with WWR 0%. In addition, for all the WWR cases, it was observed that the core-perimeter zoning and the grid/cluster zoning layouts provided total heating/cooling load reduction of 5% to 39%, compared to the single zone model. However, as WWR was increased, the amount of the load reduction was decreased.

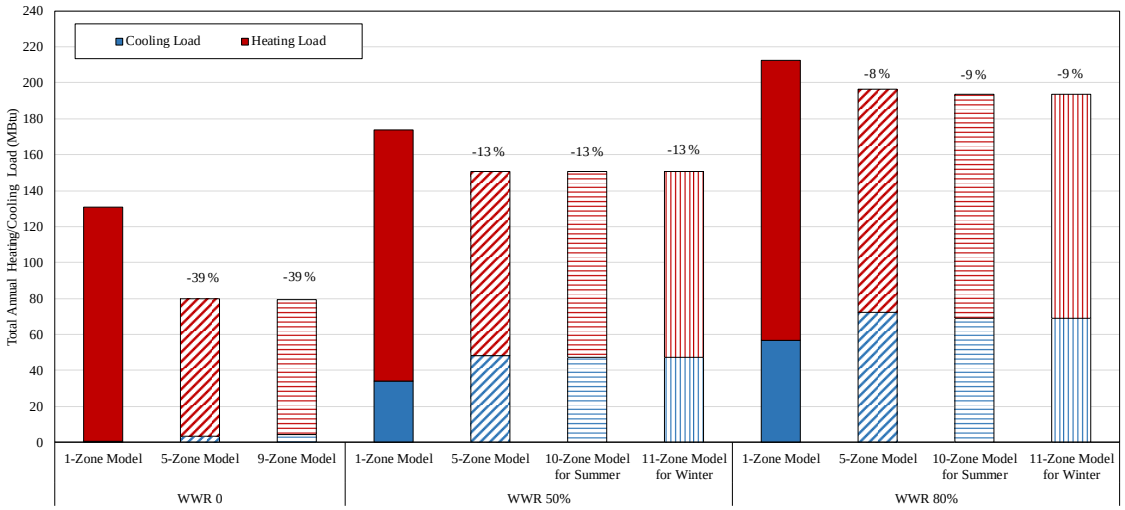

Figure 94: Comparison of the Total Annual Heating/Cooling Loads between Different WWR Models for Chicago

5.2.2. Impact of Window Orientation/Position on the Building Thermal Zoning

In this section, to investigate the impacts of the orientation/position changes of the window on the building thermal zoning and its heating/cooling load, simulation cases were created as shown in Table 31. In the cases, the WWR of the simulation models were set to 50% for all the cases, while the orientations of the windows were varied for each case. All the input parameters and other conditions were identical, except the shape of the model (i.e., model geometry). Using the same model geometry, the thermal zoning layouts given by the grid/cluster thermal zoning method for two climate conditions (i.e., Houston, TX, Chicago, IL) were compared. In addition, a single-zone thermal zoning model, the traditional core-perimeter thermal zoning model, and the grid/cluster thermal zoning model were created for each case and compared in regards to the heating/cooling

loads. The calculated annual/monthly heating/cooling loads for each case were investigated.

Table 31: WWR in the Four Orientations for the Simulation Cases

Case #	Location	East	West	North	South
10	Houston	50 %	0 %	0 %	0 %
11		0 %	50 %	0 %	0 %
12		0 %	0 %	50 %	0 %
13		0 %	0 %	0 %	50 %
19		50 %	50 %	0 %	0 %
20*		50 %	50 %	0 %	0 %
21		0 %	0 %	50 %	50 %
22*		0 %	0 %	50 %	50 %
15	Chicago	50 %	0 %	0 %	0 %
16		0 %	50 %	0 %	0 %
17		0 %	0 %	50 %	0 %
18		0 %	0 %	0 %	50 %
23		50 %	50 %	0 %	0 %
24*		50 %	50 %	0 %	0 %
25		0 %	0 %	50 %	50 %
26*		0 %	0 %	50 %	50 %

*: The windows in this case were installed on a half of the exterior walls.

5.2.2.1.Case 10 (Houston, TX) vs. Case 15 (Chicago, IL)

Figure 95 shows the 3D images of building geometry for the Case 10 and Case 15 models. The simulation models for these cases have a window band only on the exterior wall facing east. All the other exterior walls facing North, South and West were windowless. Using the same geometry for all models, for this analysis the Houston TMY3 weather file was used for the Case 10 model, while the Chicago TMY3 weather file was used for the Case 15 model. The grid/cluster thermal zoning method was applied to these two case models, and the variations of the thermal zoning layouts were compared. In the analysis, the simulated annual/monthly, heating/cooling loads for the single zone, the core-perimeter, the grid/cluster zoning models for the cases were compared and analyzed.

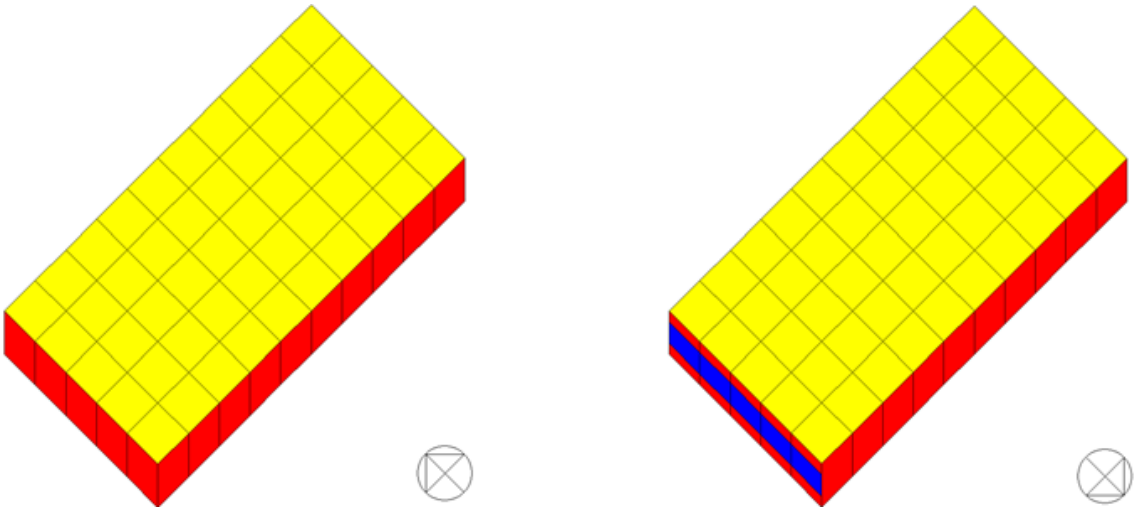

(a) Southwest View (b) Northeast View

Figure 95: View of Case 10 and Case 15 Models in the Simulation

Table 32 presents the common features of the Case 10 and Case 15 models along with the thermal zoning layouts of the Case 10 and Case 15 models for cooling and heating season. For all the cases, it should be noted that both cases have the windows only on the exterior wall facing east. Therefore, direct solar radiation penetrates into the space only from the east-side of the building in the morning. The results show that there is a similarity in the thermal zoning layouts between the Case 10 and Case 15 models. For the perimeter spaces, the grid/cluster thermal zoning method gave similar results with one that follows the traditional core-perimeter thermal zoning method. The layouts consist of four different perimeter spaces along with each orientation. In addition, the four unit spaces located at each corner of the model became four different thermal zones. For the interior space, the grid/cluster thermal zoning method divided the building into two different thermal zones. Interestingly, one of the interior thermal zones was created near the window location (i.e., east-side) for both cases. However, the thermal zoning layout for Case 10 (Houston, TX) for the heating season has only one single interior thermal zone.

The model specification of Case 10 was summarized in Table 9 in Section 4.2.2. This case has a band of exterior window only on the east-facing exterior wall with WWR of 50%, and located in Houston, TX. Figure 96 shows the thermal zoning layouts of the different zoning models (i.e., a single-zone thermal zoning model, a core-perimeter thermal zoning model, two grid/cluster thermal zoning models) for the Case 10. For Case 10, the core-perimeter method gave a simulation model, which has 5 thermal

zones. Also, the grid-cluster thermal zoning method gave two simulation models: one for summer (i.e., 12-Zone Model) and the other for winter (i.e., 14-Zone Model).

Table 32: Results of Thermal Zoning for the Case 10 (Houston) and Case 15 (Chicago)

	Case 10 (Houston)	**Case 15 (Chicago)**
Summary of Parameters	• Location: Houston, TX • Floor type: Slab-on-grade • WWR: 50 %, East Only • Floor area: 5,000 ft^2 • Number of thermal zone: 50	• Location: Chicago, IL • Floor type: Slab-on-grade • WWR: 50 %, East Only • Floor area: 5,000 ft^2 • Number of thermal zone: 50
Cooling Season	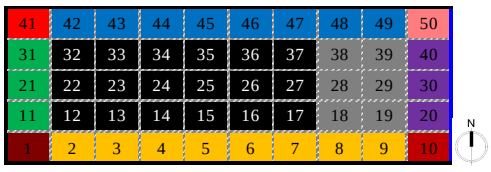	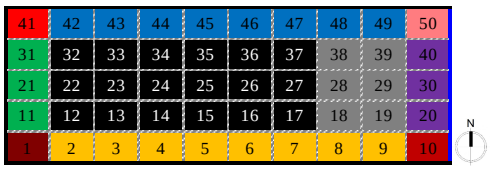
Heating Season	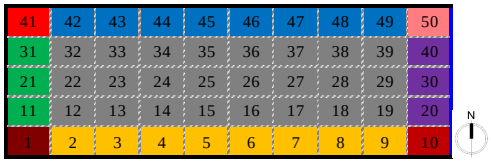	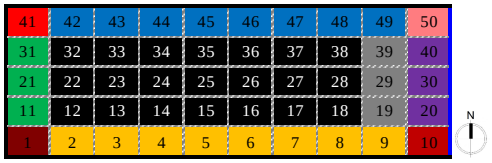

Figure 97 shows the total monthly heating/cooling loads for the 1-Zone, 5-Zone, 10-Zone, and 9-Zone thermal zoning models for Case 10 (Houston, TX). The results show that the total monthly heating/cooling loads of the 1-Zone model (i.e., the single-zone method) are mostly higher than the other thermal zoning models. In addition, the total monthly thermal loads of the 5-Zone (i.e., the core-perimeter method), 10-Zone

(i.e., the grid/cluster method for cooling season), 9-Zone models (i.e., the grid/cluster method for heating season) are very similar each other throughout the year.

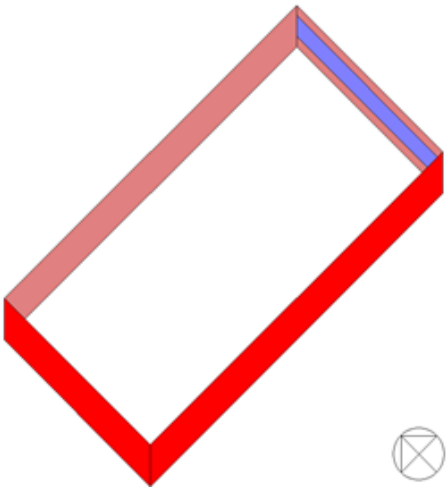

(1) 1-Zone Model

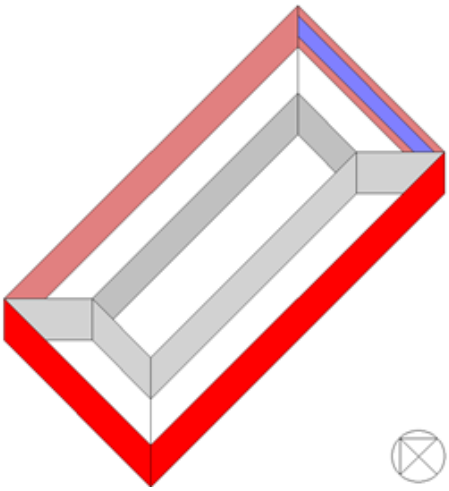

(2) 5-Zone Model

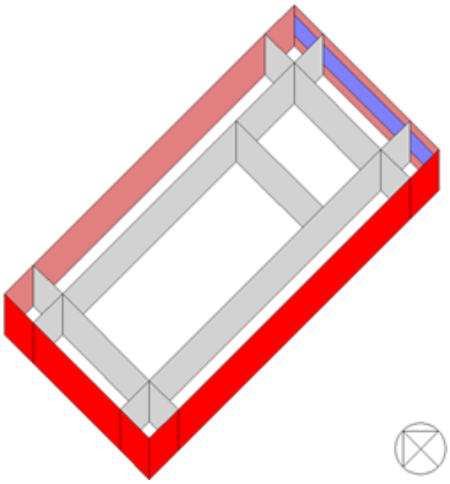

(3) 10-Zone Model (for Summer)

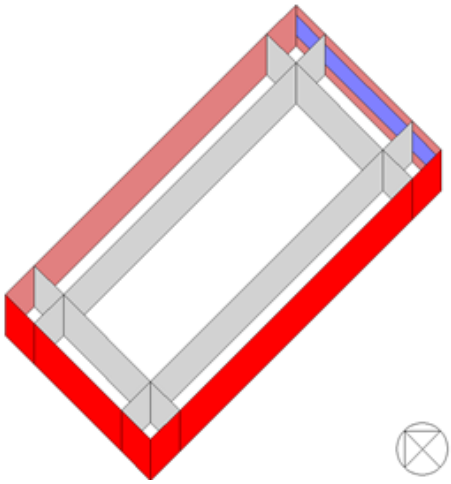

(4) 9-Zone Model (for Winter)

Figure 96: Different Zoning Models for Case 10 (Houston, TX)

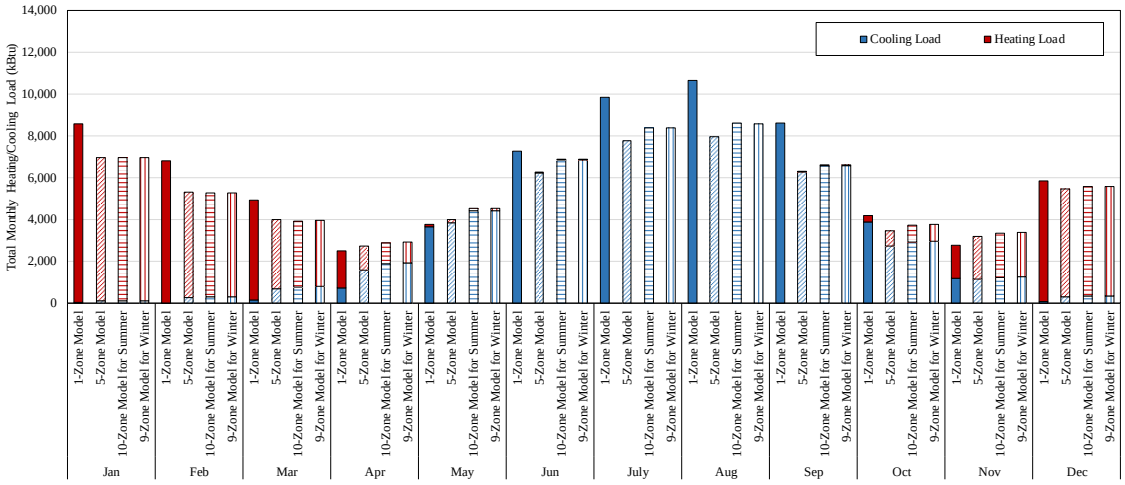

Figure 97: Total Monthly Heating/Cooling Loads for Case 10 (Houston, TX) Based on Different Zoning Methods

Table 33 shows the results of total monthly thermal loads for Case 10 (Houston, TX) with the amount of the monthly thermal load reduction. As shown in the table, the 9-Zone model for the heating season has a thermal load reduction compared to the 1-Zone model, except April, May, and November. The grid/cluster thermal zoning method yielded the highest load reduction of 23% in February, while the lowest load reduction of -21% in November. The total annual thermal load reduction of 12 % indicates that the 9-Zone thermal zoning model for the heating season has an improved energy efficiency than the 1-Zone thermal zoning model for the specific conditions of Case 10.

Figure 98 shows the total annual heating/cooling loads for the 1-Zone, 5-Zone, 10-Zone, and 9-Zone thermal zoning models for Case 10 (Houston, TX). The results show that the 5-Zone thermal zoning model for Case 10 yielded the most energy efficient thermal zoning layout among four thermal zoning strategies. In addition, this

model also showed about 16% thermal load reduction compared to the 1-Zone thermal zoning model.

Table 33: Comparison of Annual Thermal Loads for Case 10 (Houston, TX)

	1-Zone Model (kBtu)	5-Zone Model (kBtu)	10-Zone Model for Summer (kBtu)	9-Zone Model for Winter (kBtu)	1-Zone vs. 5 Zone (kBtu)	1-Zone vs. 10-Zone for Summer (kBtu)	1-Zone vs. 9-Zone for Winter (kBtu)
Jan	8,566	6,953	6,965	6,943	-1,613 (-19%)	-1,601 (-19%)	-1,623 (-19%)
Feb	6,811	5,290	5,243	5,241	-1,521 (-22%)	-1,568 (-23%)	-1,570 (-23%)
Mar	4,917	3,977	3,905	3,933	-940 (-19%)	-1,013 (-21%)	-984 (-20%)
Apr	2,467	2,708	2,874	2,919	241 (10%)	407 (16%)	451 (18%)
May	3,764	3,995	4,518	4,533	230 (6%)	754 (20%)	769 (20%)
Jun	7,271	6,234	6,843	6,839	-1,037 (-14%)	-428 (-6%)	-431 (-6%)
Jul	9,834	7,759	8,382	8,367	-2,076 (-21%)	-1,452 (-15%)	-1,468 (-15%)
Aug	10,650	7,959	8,590	8,571	-2,691 (-25%)	-2,060 (-19%)	-2,079 (-20%)
Sep	8,586	6,263	6,581	6,567	-2,323 (-27%)	-2,005 (-23%)	-2,019 (-24%)
Oct	4,173	3,464	3,713	3,765	-708 (-17%)	-461 (-11%)	-408 (-10%)
Nov	2,764	3,194	3,323	3,357	430 (16%)	559 (20%)	593 (21%)
Dec	5,845	5,464	5,556	5,557	-381 (-7%)	-288 (-5%)	-288 (-5%)
Total	**75,649**	**63,259**	**66,491**	**66,592**	**-12,391 (-16%)**	**-9,158 (-12%)**	**-9,058 (-12%)**

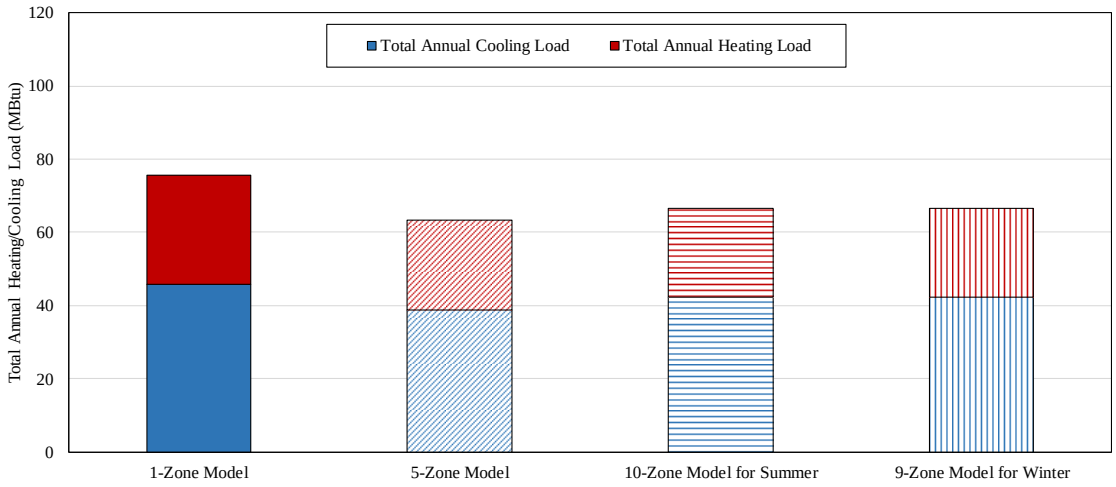

Figure 98: Total Annual Heating/Cooling Loads for Case 10 (Houston, TX) Based on Different Thermal Zoning Methods

The model specification of the Case 15 was summarized in Table 9 in Section 4.2.2. This case has a band of exterior window only on the east-facing exterior wall with WWR of 50%, and is located in Chicago, IL. Figure 99 shows the thermal zoning layouts of the different zoning models (i.e., a single-zone thermal zoning model, a core-perimeter thermal zoning model, two grid/cluster thermal zoning models) for the Case 15. For the Case 15, the core-perimeter method gave a simulation model, which has 5 thermal zones. Also, the grid-cluster thermal zoning method gave two simulation models: one for summer (i.e., 10-Zone Model) and the other for winter (i.e., 10-Zone Model).

Figure 100 shows the total monthly heating/cooling loads for the 1-Zone, 5-Zone, and two 10-Zone thermal zoning models for Case 15 (Chicago, IL). The results show that the total monthly heating/cooling loads of the 1-Zone model (i.e., the single-zone method) are mostly higher than other thermal zoning models, except the cooling season

(i.e., June, July, August, and September). In addition, the total monthly thermal loads of the 5-Zone (i.e., the core-perimeter method) and two 10-Zone (i.e., the grid/cluster method for cooling season) models (i.e., the grid/cluster method for heating/cooling season) are very similar each other throughout the year.

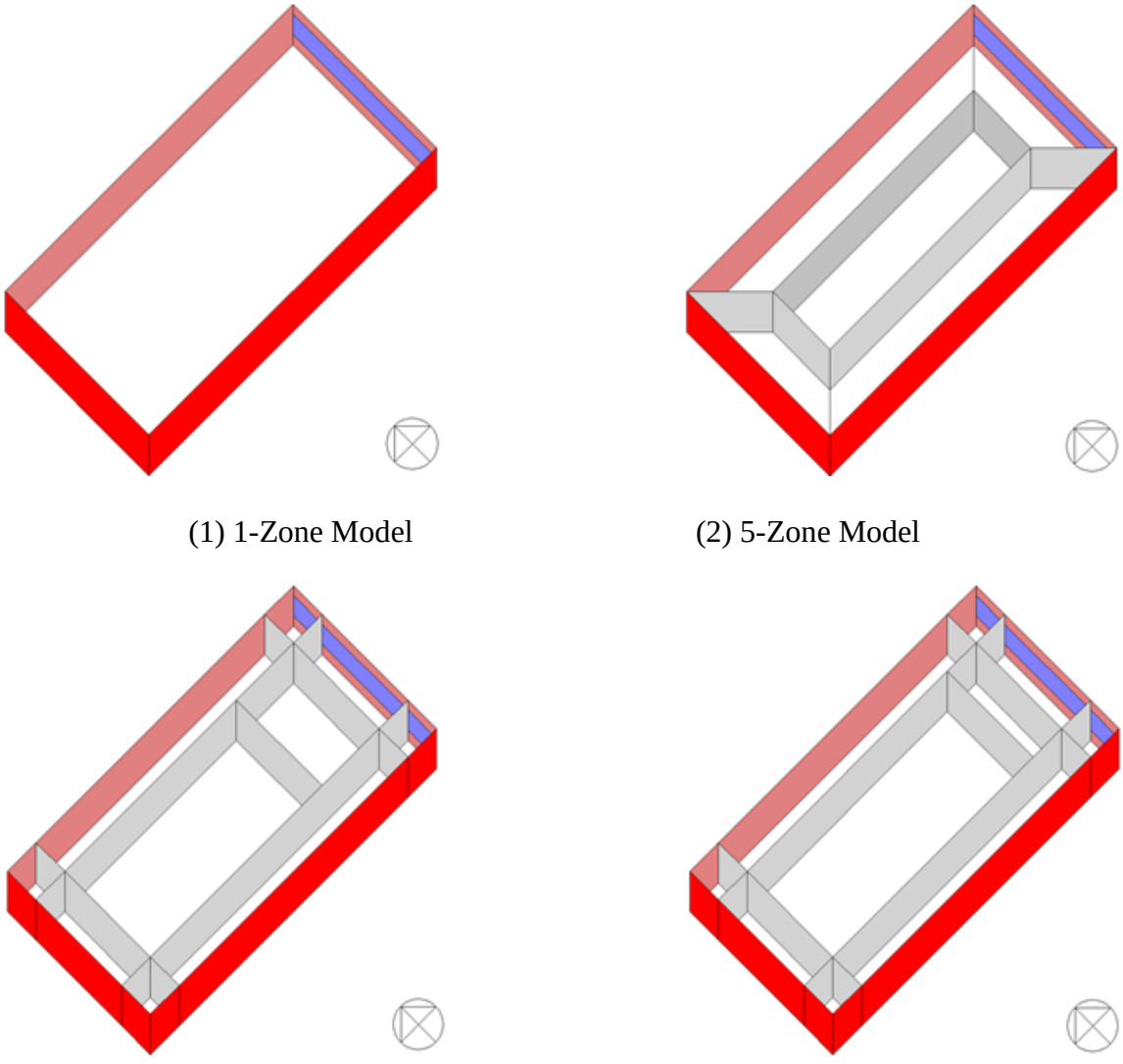

(1) 1-Zone Model (2) 5-Zone Model

(3) 10-Zone Model (for Summer) (4) 10-Zone Model (for Winter)

Figure 99: Different Zoning Models for Case 15 (Chicago, IL)

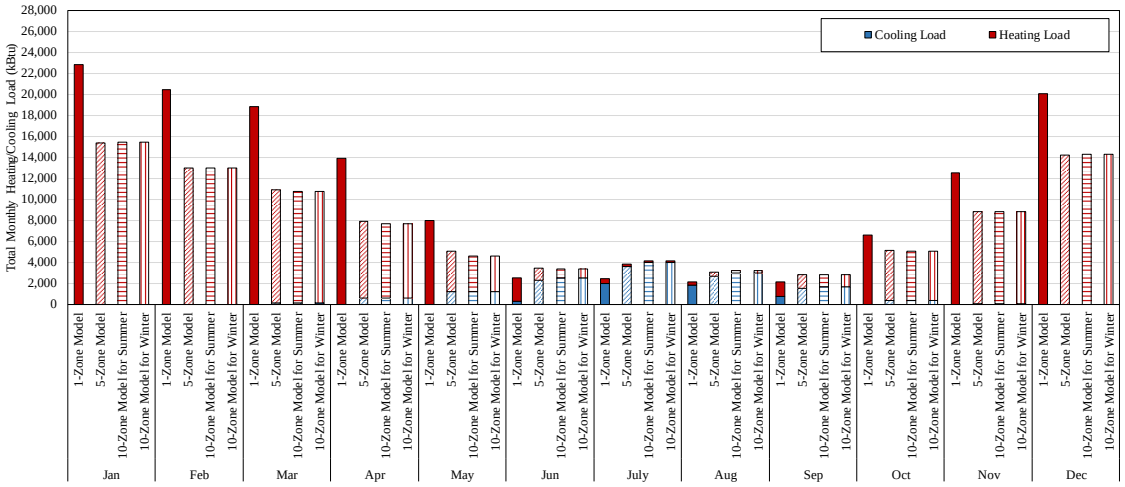

Figure 100: Total Monthly Heating/Cooling Loads for Case 15 (Chicago, IL) Based on Different Zoning Methods

Table 34 shows the results of total monthly thermal loads for Case 15 (Chicago, IL) with the amount of the monthly thermal load reduction. As shown in the table, the 10-Zone model for the heating season has a thermal load reduction compared to 1-Zone model, except June, July, August, and September. The grid/cluster thermal zoning method yielded the highest load reduction of 45% in April, while the lowest load reduction of -70% in July. The total annual thermal load reduction of 30 % indicates that the 10-Zone thermal zoning model for the heating season has an improved energy efficiency than the 1-Zone thermal zoning model for the specific conditions of Case 15.

Figure 101 shows the total annual heating/cooling loads for the 1-Zone, 5-Zone, and two 10-Zone thermal zoning models for Case 15 (Chicago, IL). The results show that the 10-Zone thermal zoning models for Case 15 yielded the most energy efficient thermal zoning layout among four thermal zoning strategies. In addition, this model also

showed about 30% thermal load reduction compared to the 1-Zone thermal zoning model.

Table 34: Comparison of Annual Thermal Loads for Case 15 (Chicago, IL)

	1-Zone Model (kBtu)	5-Zone Model (kBtu)	10-Zone Model for Summer (kBtu)	10-Zone Model for Winter (kBtu)	1-Zone vs. 5 Zone (kBtu)	1-Zone vs. 10-Zone for Summer (kBtu)	1-Zone vs. 10-Zone for Winter (kBtu)
Jan	22,803	15,337	15,404	15,404	-7,466 (-33%)	-7,399 (-32%)	-7,399 (-32%)
Feb	20,455	12,961	12,950	12,950	-7,495 (-37%)	-7,506 (-37%)	-7,506 (-37%)
Mar	18,833	10,914	10,731	10,731	-7,919 (-42%)	-8,102 (-43%)	-8,102 (-43%)
Apr	13,937	7,920	7,629	7,629	-6,017 (-43%)	-6,308 (-45%)	-6,308 (-45%)
May	7,983	5,077	4,611	4,611	-2,906 (-36%)	-3,372 (-42%)	-3,372 (-42%)
Jun	2,517	3,422	3,345	3,345	905 (36%)	828 (33%)	828 (33%)
Jul	2,408	3,800	4,088	4,088	1,391 (58%)	1,680 (70%)	1,680 (70%)
Aug	2,111	3,041	3,229	3,229	930 (44%)	1,118 (53%)	1,118 (53%)
Sep	2,101	2,793	2,782	2,782	692 (33%)	681 (32%)	681 (32%)
Oct	6,589	5,130	5,071	5,071	-1,458 (-22%)	-1,518 (-23%)	-1,518 (-23%)
Nov	12,488	8,786	8,810	8,810	-3,702 (-30%)	-3,677 (-29%)	-3,677 (-29%)
Dec	20,041	14,172	14,299	14,299	-5,869 (-29%)	-5,742 (-29%)	-5,742 (-29%)
Total	**132,266**	**93,353**	**92,950**	**92,950**	**-38,913 (-29%)**	**-39,316 (-30%)**	**-39,316 (-30%)**

Figure 101: Total Annual Heating/Cooling Loads for Case 15 (Chicago, IL) Based on Different Thermal Zoning Methods

5.2.2.2.Case 11 (Houston, TX) vs. Case 16 (Chicago, IL)

Figure 102 shows the 3D images of building geometry for Case 11 and Case 16 models. The simulation models for these cases have a window band only on the exterior wall facing west. All the other exterior walls facing North, East, and South were windowless. Using the same geometry for all models, for this analysis the Houston TMY3 weather file was used for the Case 11 model, while the Chicago TMY3 weather file was used for the Case 16 model. The grid/cluster thermal zoning method was applied to these two case models, and the variations of the thermal zoning layouts were compared. In the analysis, the simulated annual/monthly, heating/cooling loads for the single zone, the core-perimeter, the grid/cluster zoning models for the cases were compared and analyzed.

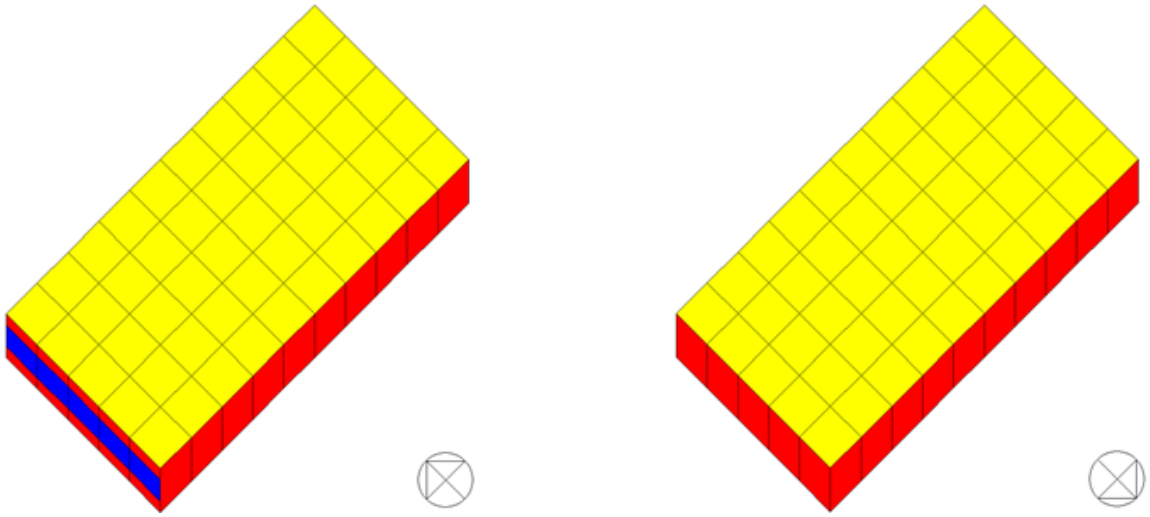

(a) Southwest View (b) Northeast View

Figure 102: View of Case 11 and Case 16 Models in the Simulation

Table 35 presents the common features of the Case 11 and Case 16 models along with the thermal zoning layouts of the Case 11 and Case 16 models for cooling and heating season. For all the cases, it should be noted that both cases have the windows only on the exterior wall facing west. Therefore, direct solar radiation penetrates into the space only from the west-side of the building in the evening. The resultant thermal zoning layouts show that there is no difference between the Case 11 and Case 16 models, regardless of heating/cooling season. The grid/cluster thermal zoning method gave the same results with one that follows the traditional core-perimeter thermal zoning method. The layout has a single interior space and four different perimeter spaces along with each orientation. In addition, four unit spaces located at each corner of the model become four different thermal zones.

Table 35: Results of Thermal Zoning for the Case 11 (Houston) and Case 16 (Chicago)

	Case 11 (Houston)	**Case 16 (Chicago)**
Summary of Parameters	• Location: Houston, TX • Floor type: Slab-on-grade • WWR: 50 %, West only • Floor area: 5,000 ft^2 • Number of thermal zone: 50	• Location: Chicago, IL • Floor type: Slab-on-grade • WWR: 50 %, West only • Floor area: 5,000 ft^2 • Number of thermal zone: 50
Cooling Season	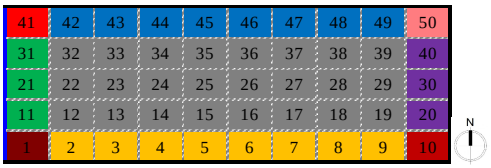	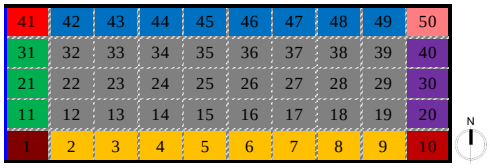
Heating Season	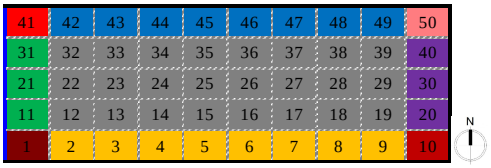	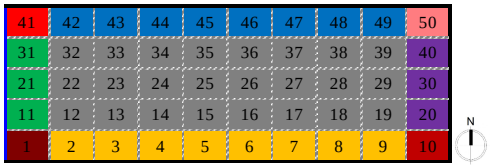

The model specification of Case 11 was summarized in Table 9 in Section 4.2.2. This case has a band of exterior window only on the west-facing exterior wall with WWR of 50%, and is located in Houston, TX. Figure 103 shows the thermal zoning layouts of the different zoning models (i.e., a single-zone thermal zoning model, a core-perimeter thermal zoning model, a grid/cluster thermal zoning model) for Case 11. For Case 11, the core-perimeter method gave a simulation model, which has 5 thermal zones. Also, the grid-cluster thermal zoning method gave a simulation model, which has 9 thermal zones.

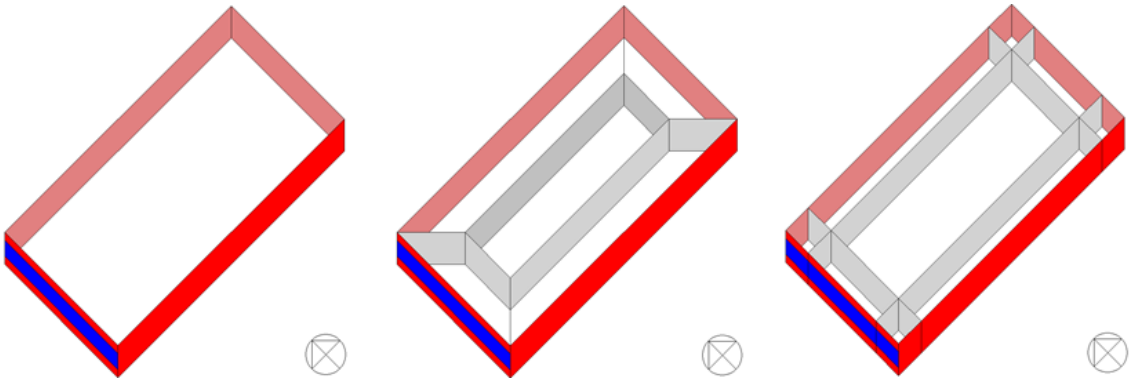

(1) 1-Zone Model (2) 5-Zone Model (3) 9-Zone Model

Figure 103: Different Zoning Models for Case 11 (Houston, TX)

Figure 104 shows the total monthly heating/cooling loads for the 1-Zone, 5-Zone, 9-Zone thermal zoning models for Case 11. The results show that the total monthly heating/cooling loads of the 1-Zone model (i.e., the single-zone method) are mostly higher than the other thermal zoning models, except May and November. In addition, the total monthly thermal loads of the 5-Zone (i.e., the core-perimeter method) are mostly little lower than the 9-Zone models (i.e., the grid/cluster method for heating/cooling season).

Figure 105 shows the total annual heating/cooling loads for the 1-Zone, 5-Zone, and 9-Zone thermal zoning models for Case 11 (Houston, TX). The results show that the 5-Zone thermal zoning model for Case 11 yielded the most energy efficient thermal zoning layout among four thermal zoning strategies. In addition, this model also showed about 20% thermal load reduction compared to the 1-Zone thermal zoning model.

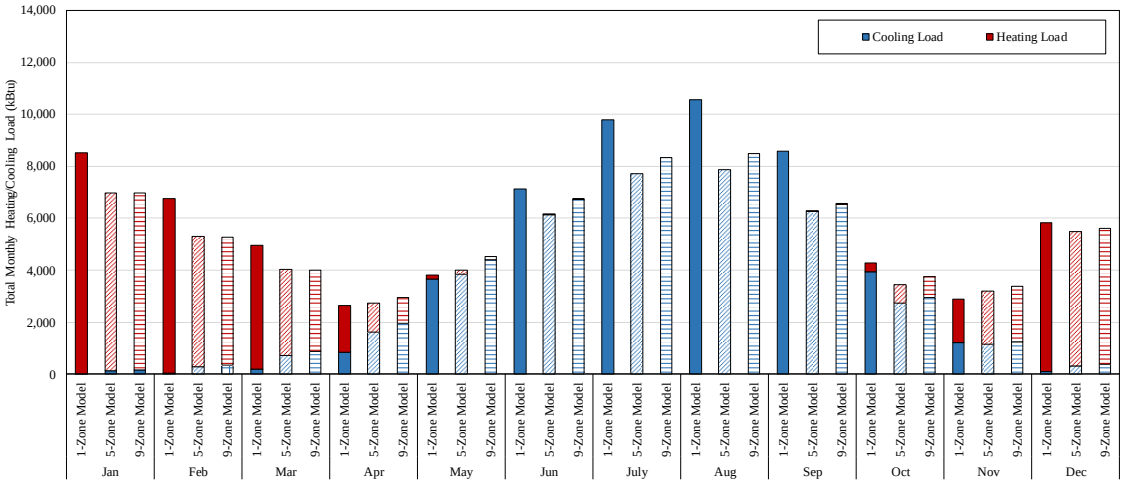

Figure 104: Total Monthly Heating/Cooling Loads for Case 11 (Houston, TX) Based on Different Thermal Zoning Methods

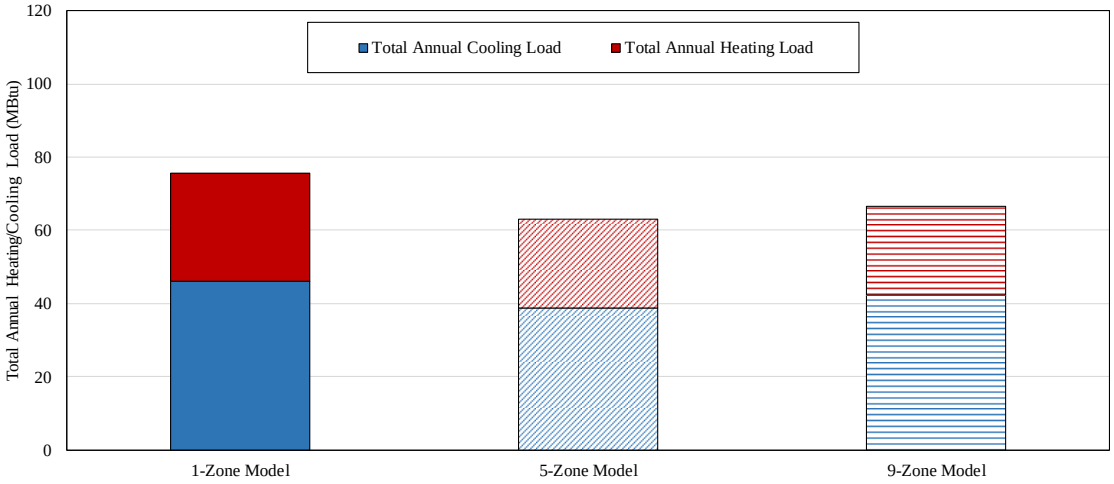

Figure 105: Total Annual Heating/Cooling Loads for Case 11 (Houston, TX) Based on Different Thermal Zoning Methods

Table 36 shows the results of total monthly thermal loads for Case 11 (Houston, TX) with the amount of the monthly thermal load reduction. As shown in the table, the 9-Zone model has a thermal load reduction compared to 1-Zone model, except May and November. The grid/cluster thermal zoning method the highest load reduction of 32% in

March, while the lowest load reduction of -36% in May. The annual total thermal load reduction of 15% indicates that the 9-Zone thermal zoning model for heating season has an improved energy efficiency than 1-Zone thermal zoning model for the specific conditions of Case 11.

Table 36: Comparison of Annual Thermal Loads for Case 11 (Houston, TX)

	1-Zone Model (kBtu)	**5-Zone Model (kBtu)**	**9-Zone Model (kBtu)**	**1-Zone vs. 5 Zone (kBtu)**	**1-Zone vs. 9-Zone (kBtu)**
Jan	8,525	6,972	6,972	-1,553 (-18%)	-1,553 (-18%)
Feb	6,762	5,302	5,260	-1,461 (-22%)	-1,502 (-22%)
Mar	4,970	4,025	4,025	-945 (-19%)	-944 (-19%)
Apr	2,650	2,748	2,961	98 (4%)	311 (12%)
May	3,815	3,992	4,530	177 (5%)	715 (19%)
Jun	7,142	6,129	6,736	-1,012 (-14%)	-405 (-6%)
Jul	9,785	7,722	8,329	-2,063 (-21%)	-1,456 (-15%)
Aug	10,552	7,882	8,496	-2,671 (-25%)	-2,056 (-19%)
Sep	8,574	6,252	6,555	-2,322 (-27%)	-2,019 (-24%)
Oct	4,273	3,462	3,768	-811 (-19%)	-505 (-12%)
Nov	2,881	3,200	3,372	318 (11%)	490 (17%)
Dec	5,829	5,503	5,607	-326 (-6%)	-222 (-4%)
Total	**75,759**	**63,188**	**66,612**	**-12,570 (-17%)**	**-9,146 (-12%)**

The model specification of Case 16 was summarized in Table 9 in Section 4.2.2. This case has a band of exterior window only on the west-facing exterior wall with WWR of 50%, and is located in Chicago, IL. Figure 106 shows the thermal zoning

layouts of the different zoning models (i.e., a single-zone thermal zoning model, a core-perimeter thermal zoning model, a grid/cluster thermal zoning model) for Case 16. For Case 16, the core-perimeter method gave a simulation model, which has 5 thermal zones. Also, in a similar fashion as previous case, the grid-cluster thermal zoning method gave a simulation model, which has 9 thermal zones.

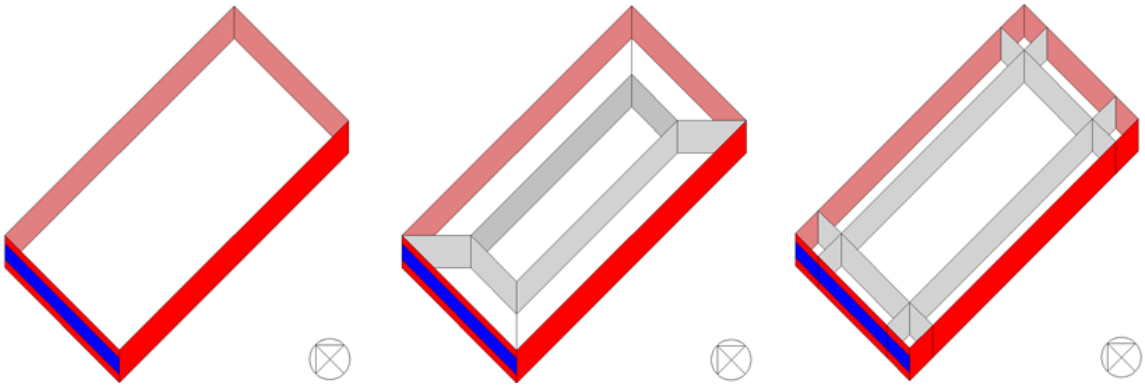

(1) 1-Zone Model (2) 5-Zone Model (3) 9-Zone Model

Figure 106: Different Zoning Models for Case 16 (Chicago, IL)

Figure 107 shows the total monthly heating/cooling loads for the 1-Zone, 5-Zone, 9-Zone thermal zoning models for Case 16 (Chicago, IL). The results show that the total monthly heating/cooling loads of the 1-Zone model (i.e., the single-zone method) are mostly higher than the other thermal zoning models, except May and November. In addition, the total monthly thermal loads of the 5-Zone model (i.e., the core-perimeter method) are mostly little lower than the 9-Zone models (i.e., the grid/cluster method).

Figure 108 shows the total annual heating/cooling loads for the 1-Zone, 5-Zone, and 9-Zone thermal zoning models for Case 16 (Chicago, IL). The results show that the

5-Zone thermal zoning model for Case 16 yielded the most energy efficient thermal zoning layout among four thermal zoning strategies. In addition, this model also showed about 12% thermal load reduction compared to the 1-Zone thermal zoning model.

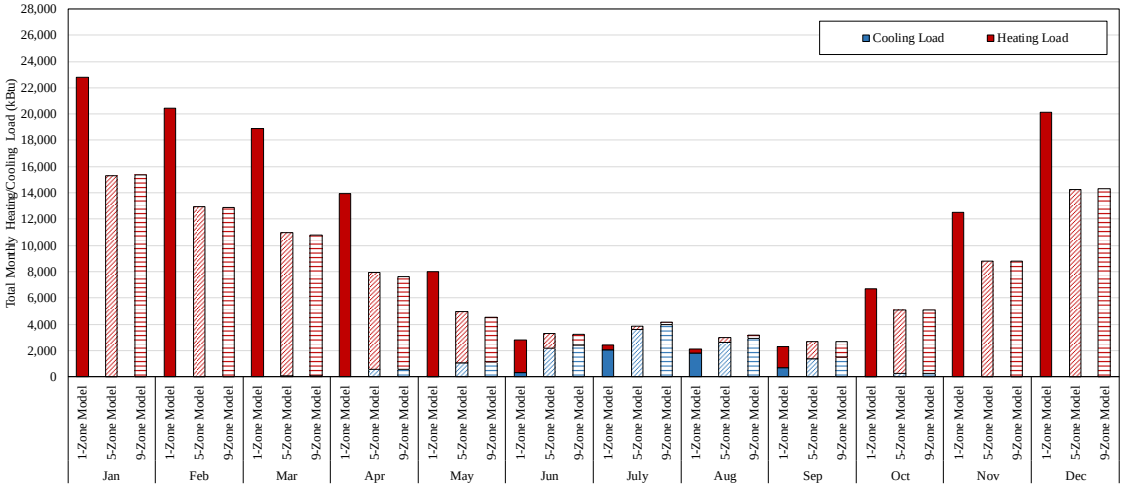

Figure 107: Total Monthly Heating/Cooling Loads for Case 16 (Chicago, IL) Based on Different Zoning Methods

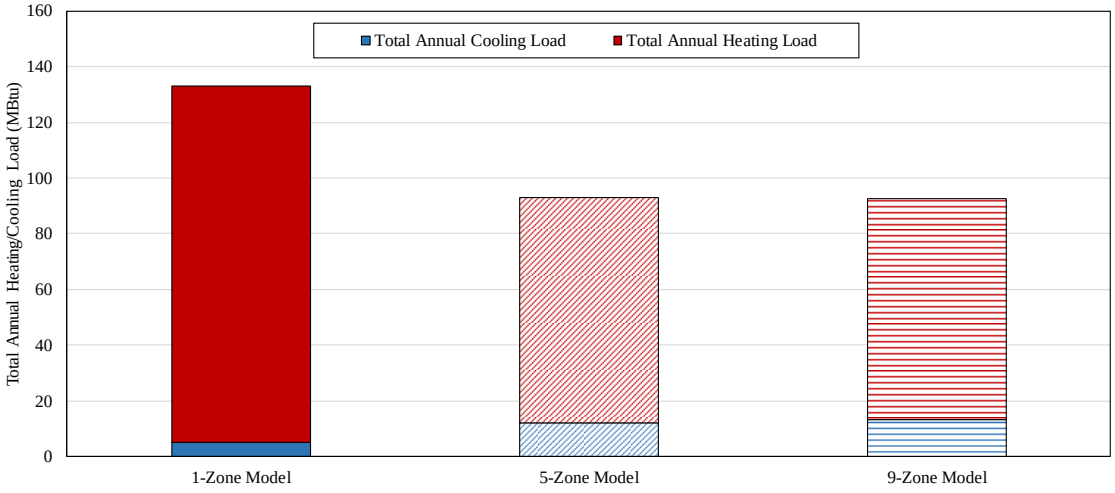

Figure 108: Total Annual Heating/Cooling Loads for Case 16 (Chicago, IL) Based on Different Thermal Zoning Methods

Table 37 shows the results of monthly total thermal loads for the 1-Zone model and 9-Zone model with the amount of the monthly thermal load reduction. As shown in the table, the 9-Zone model has a thermal load reduction compared to the 1-Zone model, except May, June, and November. The grid/cluster thermal zoning method gave the highest load reduction of 26% in February, while the lowest load reduction of -52% in May. The total annual thermal load reduction of 10% indicates that the 9-Zone thermal zoning model for the heating season has an improved energy efficiency than the 1-Zone thermal zoning model for Case 16 (Chicago, IL).

Table 37: Comparison of Annual Thermal Loads for Case 16 (Chicago, IL)

	1-Zone Model (kBtu)	**5-Zone Model (kBtu)**	**9-Zone Model (kBtu)**	**1-Zone vs. 5 Zone (kBtu)**	**1-Zone vs. 9-Zone (kBtu)**
Jan	22,803	15,338	15,360	-7,465 (-33%)	-7,443 (-33%)
Feb	20,442	12,977	12,911	-7,465 (-37%)	-7,530 (-37%)
Mar	18,908	10,989	10,989	-7,919 (-42%)	-7,919 (-42%)
Apr	13,954	7,941	7,646	-6,013 (-43%)	-6,308 (-45%)
May	8,037	4,975	4,534	-3,061 (-38%)	-3,503 (-44%)
Jun	2,834	3,278	3,234	444 (16%)	400 (14%)
Jul	2,463	3,849	4,149	1,386 (56%)	1,685 (68%)
Aug	2,157	2,994	3,197	837 (39%)	1,040 (48%)
Sep	2,288	2,665	2,680	377 (16%)	392 (17%)
Oct	6,709	5,128	5,088	-1,582 (-24%)	-1,621 (-24%)
Nov	12,513	8,809	8,825	-3,704 (-30%)	-3,688 (-29%)
Dec	20,105	14,229	14,318	-5,875 (-29%)	-5,787 (-29%)
Total	**133,212**	**93,172**	**92,931**	**-40,041 (-30%)**	**-40,282 (-30%)**

5.2.2.3.Case 12 (Houston, TX) vs. Case 17 (Chicago, IL)

Figure 109 shows the 3D images of building geometry for the Case 12 and Case 17 models. The simulation models for these cases have a window band only on the exterior wall facing north. All the other exterior walls facing East, South and West were windowless. Using the same geometry for all models, for this analysis, the Houston TMY3 weather file was used for the Case 12 model, while the Chicago TMY3 weather file was used for the Case 17 model. The grid/cluster thermal zoning method was applied to these two case models, and the variations of the thermal zoning layouts were compared. In addition, the simulated annual/monthly, heating/cooling loads for the single zone, the core-perimeter, and the grid/cluster zoning models for the cases were compared and analyzed.

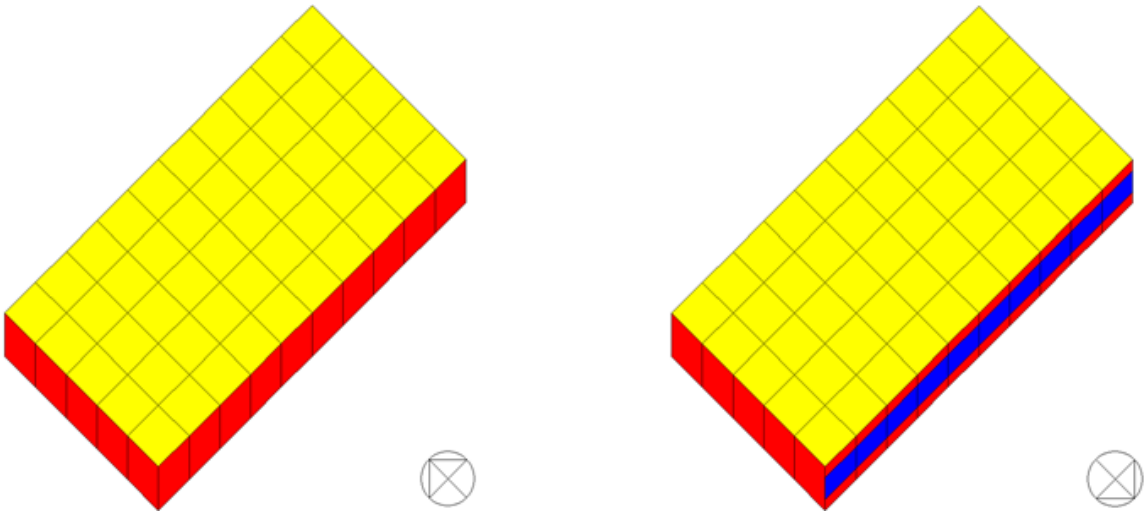

(a) Southwest View (b) Northeast View

Figure 109: View of Case 12 and Case 17 Models in the Simulation

Table 38 presents the common features of the Case 12 and Case 17 models along with the thermal zoning layouts of the Case 12 and Case 17 models for cooling and heating season. For all the cases, it should be noted that both cases have the windows only on the exterior wall facing north. Therefore, direct solar radiation penetrates into the space only from the north-side of the building. The resultant thermal zoning layouts show that there is no difference between the Case 12 and Case 17 model, regardless of heating/cooling season. The grid/cluster thermal zoning method gave the same results with one that follows the traditional core/perimeter thermal zoning method. The layout has a single interior space and four different perimeter spaces along with each orientation. In addition, four unit spaces located at each corner of the model become four different thermal zones.

Table 38: Results of Thermal Zoning for the Case 12 (Houston) and Case 17 (Chicago)

	Case 12 (Houston)	**Case 17 (Chicago)**
Summary of Parameters	• Location: Houston, TX • Floor type: Slab-on-grade • WWR: 50 %, North only • Floor area: 5,000 ft^2 • Number of thermal zone: 50	• Location: Chicago, IL • Floor type: Slab-on-grade • WWR: 50 %, North only • Floor area: 5,000 ft^2 • Number of thermal zone: 50
Cooling Season	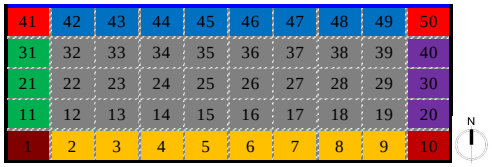	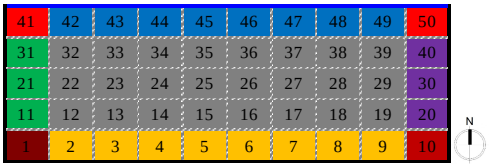
Heating Season	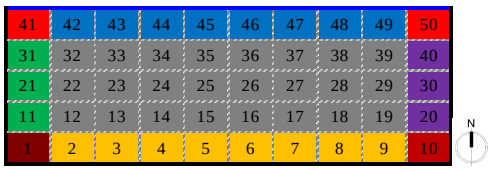	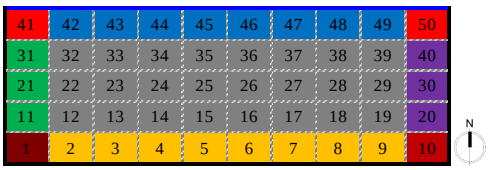

The model specification of Case 12 was summarized in Table 9 in Section 4.2.2. This case has a band of exterior window only on the north-facing exterior wall with WWR of 50%, and is located in Houston, TX. Figure 110 shows the thermal zoning layouts of the different zoning models (i.e., a single-zone thermal zoning model, a core-perimeter thermal zoning model, a grid/cluster thermal zoning model) for Case 12. For Case 12, the core-perimeter method gave a simulation model, which has 5 thermal zones. Also, the grid-cluster thermal zoning method gave a simulation model, which has 9 thermal zones.

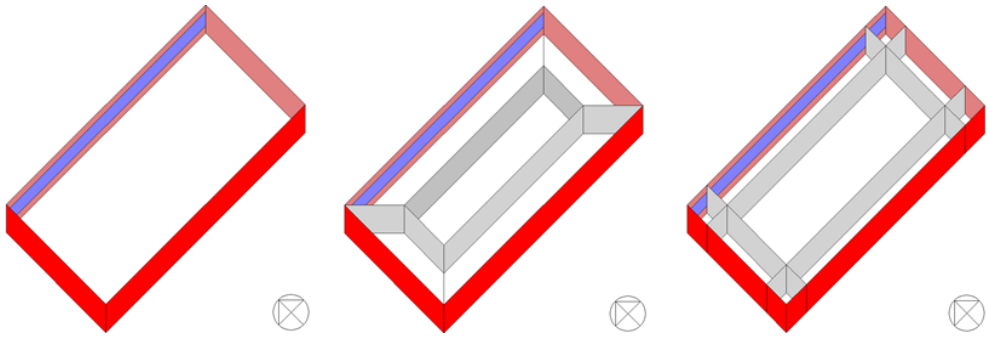

(1) 1-Zone Model (2) 5-Zone Model (3) 9-Zone Model

Figure 110: Different Zoning Models for Case 12 (Houston, TX)

Figure 111 shows the total monthly heating/cooling loads for the 1-Zone, 5-Zone, 9-Zone thermal zoning models for Case 12 (Houston, TX). The results show that the total monthly heating/cooling loads of the 1-Zone model (i.e., the single-zone method) are mostly higher than the other thermal zoning models, except May and November. In addition, the total monthly thermal loads of the 5-Zone model (i.e., the core-perimeter method) are mostly little lower than 9-Zone models (i.e., the grid/cluster method).

Figure 112 shows the total annual heating/cooling loads for the 1-Zone, 5-Zone, and 9-Zone thermal zoning models for Case 12 (Houston, TX). The results show that the 5-Zone thermal zoning model for Case 12 gave the most energy efficient thermal zoning layout among four thermal zoning strategies. In addition, this model also showed about 20% thermal load reduction compared to 1-Zone thermal zoning model.

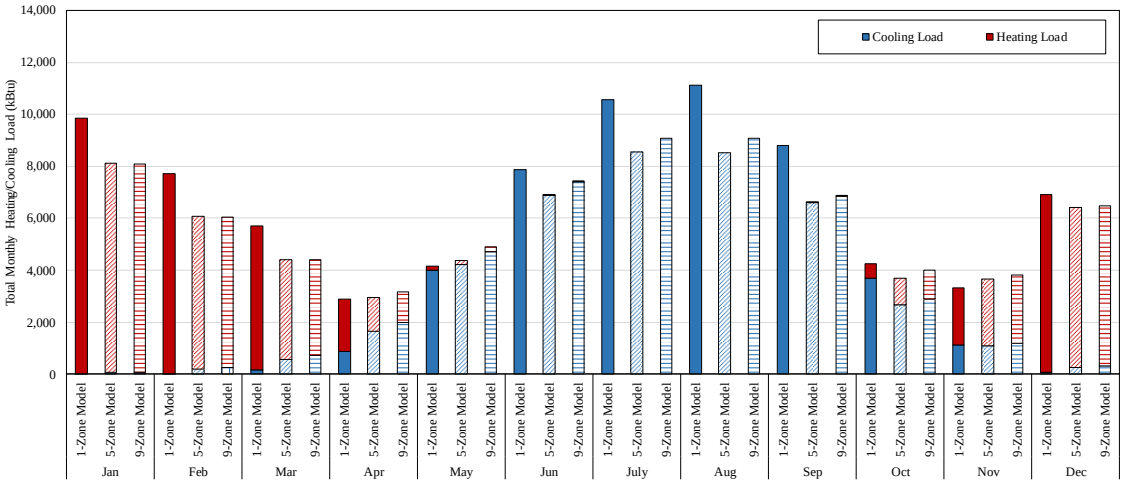

Figure 111: Total Monthly Heating/Cooling Loads for Case 12 (Houston, TX) Based on Different Zoning Methods

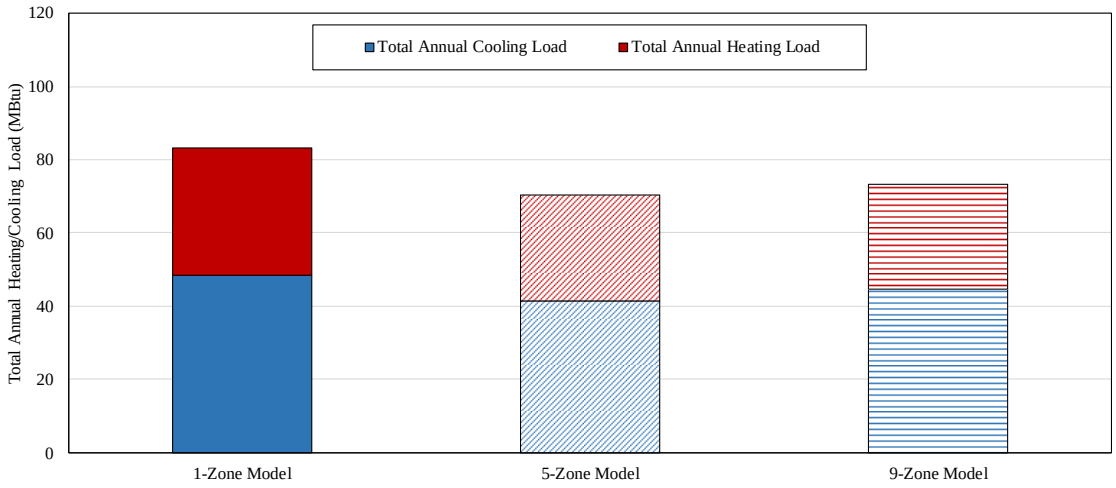

Figure 112: Total Annual Heating/Cooling Loads for Case 12 (Houston, TX) Based on Different Thermal Zoning Methods

Table 39 shows the results of total monthly thermal loads for the 1-Zone model and 9-Zone model with the amount of the monthly thermal load reduction. As shown in the table, the 9-Zone model has a thermal load reduction compared to the 1-Zone model, except May and November. The grid/cluster thermal zoning method gave the highest load reduction of 32% in March, while the lowest load reduction of -36% in May. The total annual thermal load reduction of 15% indicates that the 9-Zone thermal zoning model for the heating season has an improved energy efficiency than the 1-Zone thermal zoning model for the specific conditions of Case 12 (Houston, TX).

Table 39: Comparison of Annual Thermal Loads for Case 12 (Houston, TX)

	1-Zone Model (kBtu)	**5-Zone Model (kBtu)**	**9-Zone Model (kBtu)**	**1-Zone vs. 5 Zone (kBtu)**	**1-Zone vs. 9-Zone (kBtu)**
Jan	9,860	8,107	8,072	-1,753 (-18%)	-1,788 (-18%)
Feb	7,728	6,079	6,032	-1,649 (-21%)	-1,696 (-22%)
Mar	5,693	4,417	4,417	-1,276 (-22%)	-1,276 (-22%)
Apr	2,894	2,938	3,171	44 (2%)	277 (10%)
May	4,165	4,390	4,887	226 (5%)	722 (17%)
Jun	7,869	6,881	7,416	-988 (-13%)	-453 (-6%)
Jul	10,559	8,541	9,070	-2,018 (-19%)	-1,489 (-14%)
Aug	11,123	8,526	9,072	-2,597 (-23%)	-2,051 (-18%)
Sep	8,806	6,603	6,866	-2,202 (-25%)	-1,940 (-22%)
Oct	4,244	3,702	3,990	-542 (-13%)	-254 (-6%)
Nov	3,321	3,660	3,828	339 (10%)	506 (15%)
Dec	6,917	6,409	6,494	-509 (-7%)	-424 (-6%)
Total	**83,179**	**70,253**	**73,314**	**-12,926 (-16%)**	**-9,865 (-12%)**

The model specification of Case 17 was summarized in Table 9 in Section 4.2.2. This case has a band of exterior window only on the north-facing exterior wall with WWR of 50%, and is located in Chicago, IL. Figure 113 shows the thermal zoning layouts of the different zoning models (i.e., a single-zone thermal zoning model, a core-perimeter thermal zoning model, a grid/cluster thermal zoning model) for Case 17. For Case 17, the core-perimeter thermal zoning method gave a simulation model, which has 5 thermal zones. Also, in a similar fashion as previous case, the grid-cluster thermal zoning method yielded a simulation model, which has 9 thermal zones.

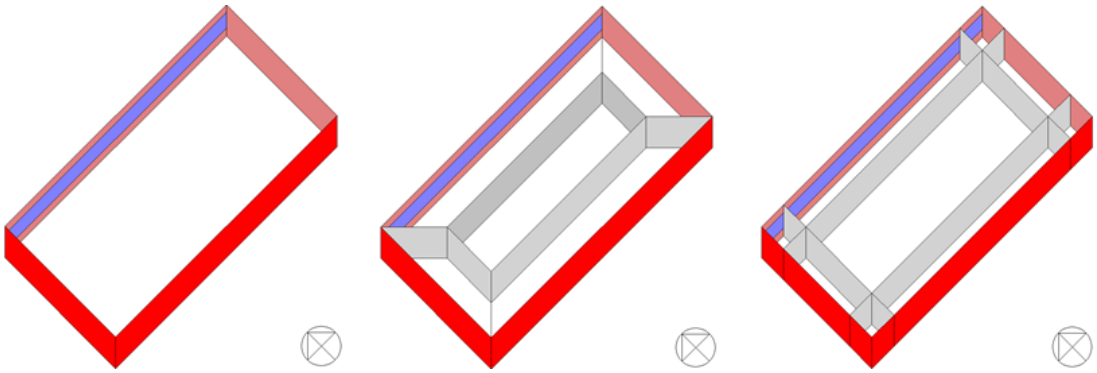

(1) 1-Zone Model (2) 5-Zone Model (3) 9-Zone Model

Figure 113: Different Zoning Models for Case 17 (Chicago, IL)

Figure 114 shows the total monthly heating/cooling loads for the 1-Zone, 5-Zone, 9-Zone thermal zoning models for Case 17 (Chicago, IL). The results show that the total monthly heating/cooling loads of the 1-Zone model (i.e., the single-zone method) are mostly higher than the other thermal zoning models, except May and November. In

addition, the total monthly thermal loads of the 5-Zone (i.e., the core-perimeter method) are mostly little lower than the 9-Zone models (i.e., the grid/cluster method).

Figure 115 shows the total annual heating/cooling loads for the 1-Zone, 5-Zone, and 9-Zone thermal zoning models for Case 17 (Chicago, IL). The results show that the 5-Zone thermal zoning model for Case 17 gave the most energy efficient thermal zoning layout among four thermal zoning strategies. In addition, this model also showed about 12% thermal load reduction compared to 1-Zone thermal zoning model.

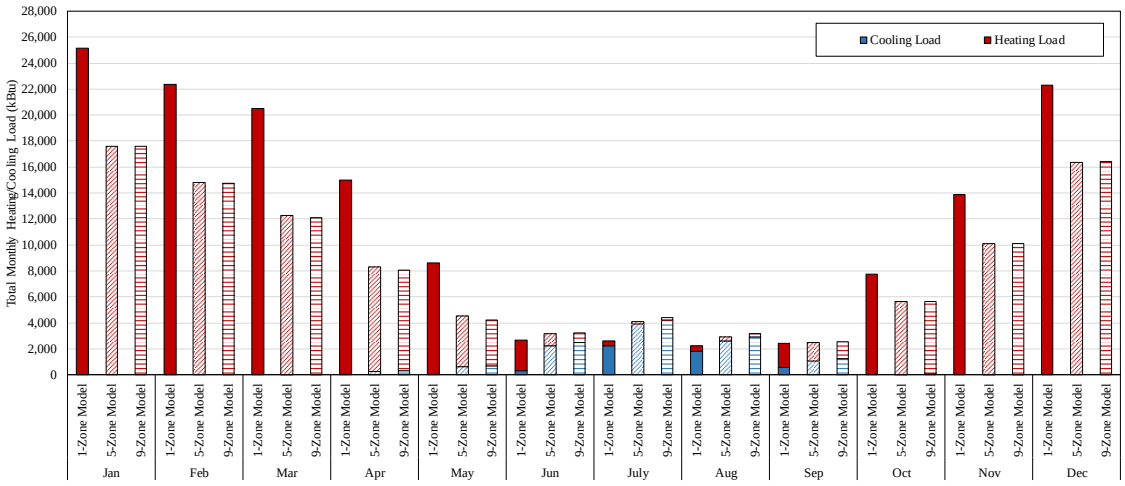

Figure 114: Total Monthly Heating/Cooling Loads for Case 17 (Chicago, IL) Based on Different Zoning Methods

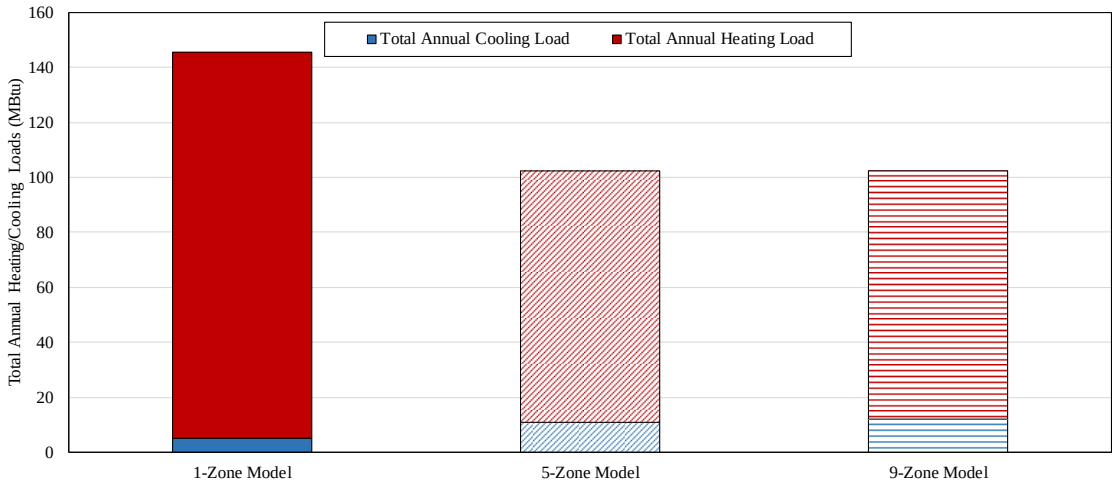

Figure 115: Total Annual Heating/Cooling Load for Case 17 (Chicago, IL) Based on Different Thermal Zoning Methods

Table 40 shows the results of monthly total thermal loads for 1-Zone model and 9-Zone model with the amount of the monthly thermal load reduction. As shown in the table, the 9-Zone model has a thermal load reduction compared to 1-Zone model, except May and November. The grid/cluster thermal zoning method gave the highest load reduction of 26% in February, while the lowest load reduction of -52% in May. The annual total thermal load reduction of 10% indicates that the 9-Zone thermal zoning model for heating season has an improved energy efficiency than 1-Zone thermal zoning model for the specific conditions of Case 17.

Table 40: Comparison of Annual Thermal Load for Case 17 (Chicago, IL)

	1-Zone Model (kBtu)	5-Zone Model (kBtu)	9-Zone Model (kBtu)	1-Zone vs. 5 Zone (kBtu)	1-Zone vs. 9-Zone (kBtu)
Jan	25,136	17,621	17,593	-7,516 (-30%)	-7,544 (-30%)
Feb	22,379	14,839	14,742	-7,541 (-34%)	-7,638 (-34%)
Mar	20,490	12,293	12,293	-8,197 (-40%)	-8,197 (-40%)
Apr	15,021	8,312	8,074	-6,708 (-45%)	-6,947 (-46%)
May	8,605	4,525	4,237	-4,081 (-47%)	-4,369 (-51%)
Jun	2,705	3,211	3,271	506 (19%)	565 (21%)
Jul	2,646	4,104	4,391	1,458 (55%)	1,745 (66%)
Aug	2,241	2,958	3,194	717 (32%)	952 (42%)
Sep	2,432	2,473	2,565	41 (2%)	133 (5%)
Oct	7,789	5,668	5,641	-2,120 (-27%)	-2,147 (-28%)
Nov	13,894	10,092	10,090	-3,802 (-27%)	-3,804 (-27%)
Dec	22,311	16,386	16,426	-5,925 (-27%)	-5,885 (-26%)
Total	**145,651**	**102,482**	**102,516**	**-43,169(-30%)**	**-43,135(-30%)**

5.2.2.4.Case 13 (Houston, TX) vs. Case 18 (Chicago, IL)

Figure 116 shows the 3D images of building geometry for Case 13 and Case 18 models. The simulation models for these cases have a window band only on the exterior wall facing south. All the other exterior walls facing North, East and West were windowless. Using the same geometry for all models, for this analysis the Houston TMY3 weather file was used for the Case 13 model, while the Chicago TMY3 weather file was used for the Case 18 model. The grid/cluster thermal zoning method was applied to these two case models, and the variations of the thermal zoning layouts were compared. In the analysis, the simulated annual/monthly, heating/cooling loads for the single zone, the core-perimeter, the grid/cluster zoning models for the cases were compared and analyzed.

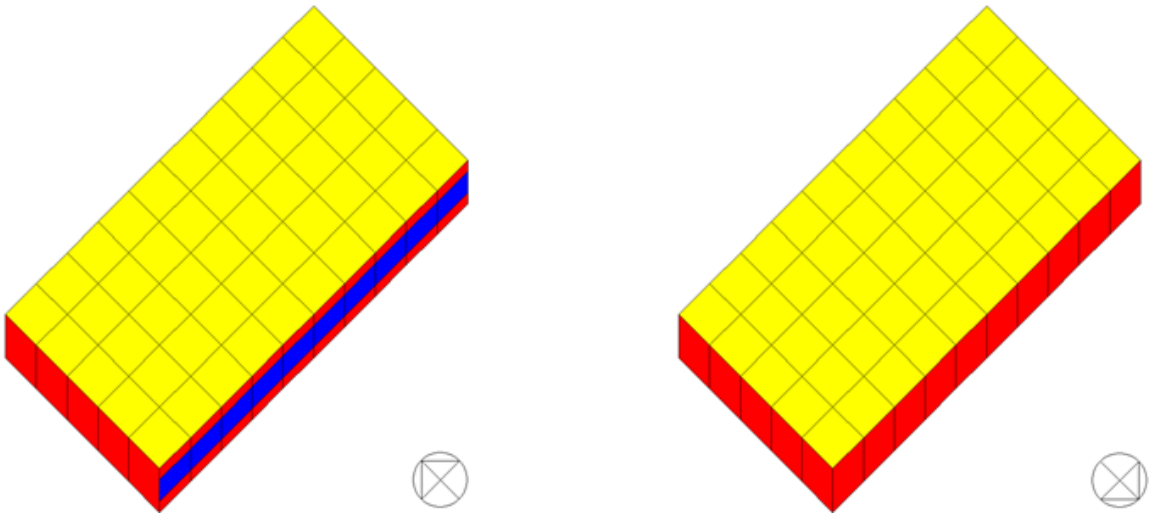

(a) Southwest View (b) Northeast View

Figure 116: View of Case 13 and Case 18 Models in the Simulation

Table 41 presents the common features of the Case 13 and Case 18 models along with the thermal zoning layouts of the Case 13 and Case 18 models for cooling and heating season. For all the cases, it should be noted that both cases have the windows only on the exterior wall facing south. Therefore, direct solar radiation penetrates into the space only from the south-side of the building. The results show that there is a similarity in the thermal zoning layouts between the Case 13 and Case 18 models. For the perimeter spaces, the grid/cluster thermal zoning method gave similar results with one that follows the traditional core/perimeter thermal zoning method for the cooling season layouts. The layouts consist of four different perimeter spaces along with each orientation. In addition, four unit spaces located at each corner of the model become four different thermal zones. In addition, it was found that for the cooling season layouts, two thermal zones were created for the perimeter spaces facing east and west. One of two thermal zones was created near the window location (i.e., south-side). For the interior space, the grid/cluster thermal zoning method divided the building into two different thermal zones. Interestingly, one of the interior thermal zones was also created near the window location (i.e., south-side) for both cases. However, the thermal zoning layout for Case 18 for the cooling season has only one single interior thermal zone.

The model specification of Case 13 was summarized in Table 9 in Section 4.2.2. This case has a band of exterior window only on the south-facing exterior wall with WWR of 50%, and is located in Houston, TX. Figure 117 shows the thermal zoning layouts of the different zoning models (i.e., a single-zone thermal zoning model, a core-perimeter thermal zoning model, two grid/cluster thermal zoning models) for Case 13.

For Case 13, the core-perimeter thermal zoning method yielded 5 thermal zones. In addition, the grid-cluster thermal zoning method yielded two simulation models: one for summer (i.e., 10-Zone Model) and the other for winter (i.e., 11-Zone Model).

Table 41: Results of Thermal Zoning for the Case 13 (Houston) and Case 18 (Chicago)

	Case 13 (Houston)	**Case 18 (Chicago)**
Summary of Parameters	• Location: Houston, TX • Floor type: Slab-on-grade • WWR: 50 %, South only • Floor area: 5,000 ft^2 • Number of thermal zone: 50	• Location: Chicago, IL • Floor type: Slab-on-grade • WWR: 50 %, South only • Floor area: 5,000 ft^2 • Number of thermal zone: 50
Cooling Season	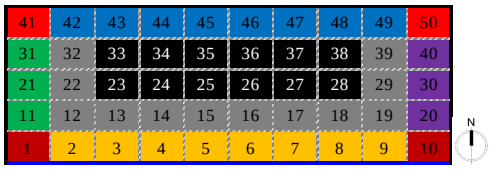	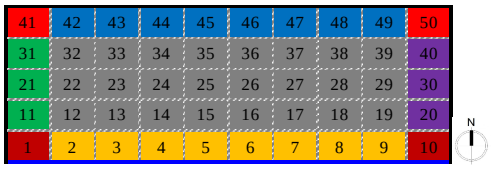
Heating Season	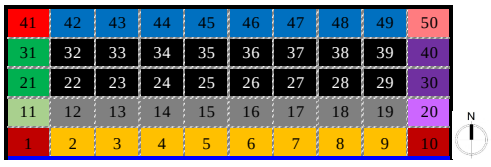	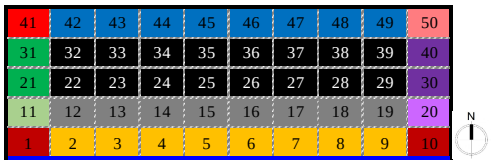

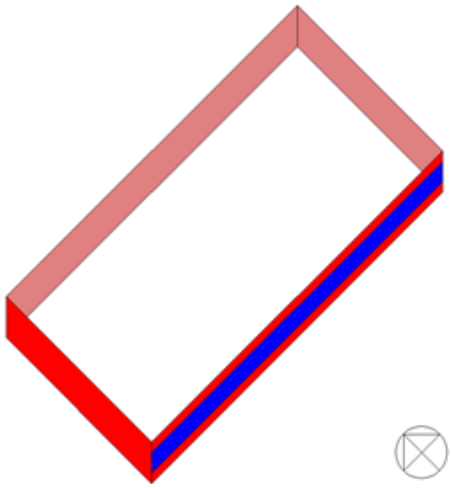

(1) 1-Zone Model

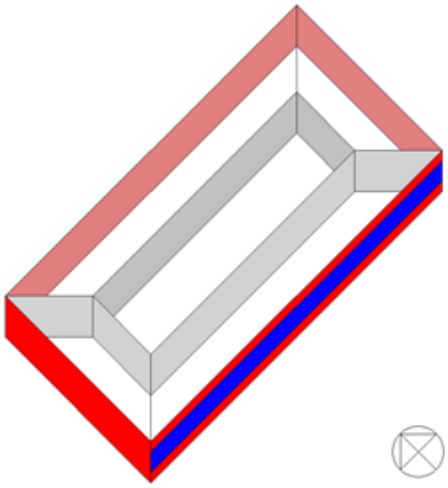

(2) 5-Zone Model

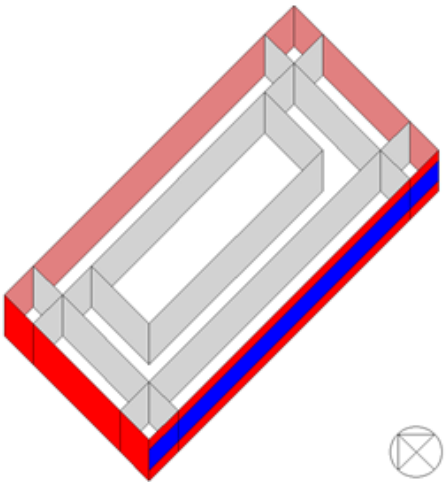

(3) 10-Zone Model (for Summer)

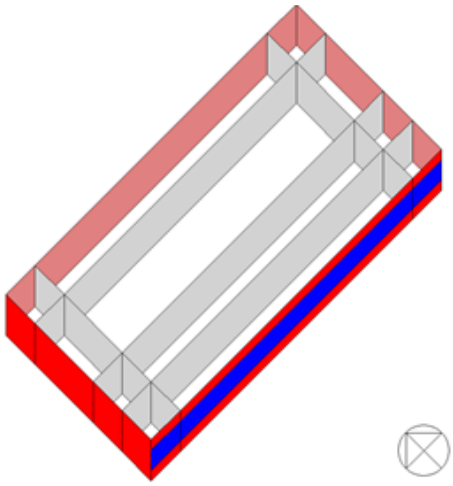

(4) 12-Zone Model (for Winter)

Figure 117: Different Zoning Models for Case 13 (Houston, TX)

Figure 118 shows the total monthly heating/cooling loads for the 1-Zone, 5-Zone, 10-Zone, 12-Zone thermal zoning models for Case 13 (Houston, TX). The results show that the total monthly heating/cooling loads of the 1-Zone model (i.e., the single-zone method) are mostly higher than other thermal zoning models, except April, May,

November, and December. In addition, the total monthly thermal loads of the 5-Zone (i.e., the core-perimeter method), 10-Zone (i.e., the grid/cluster method for cooling season), 12-Zone models (i.e., the grid/cluster method for heating season) are very similar each other throughout the year.

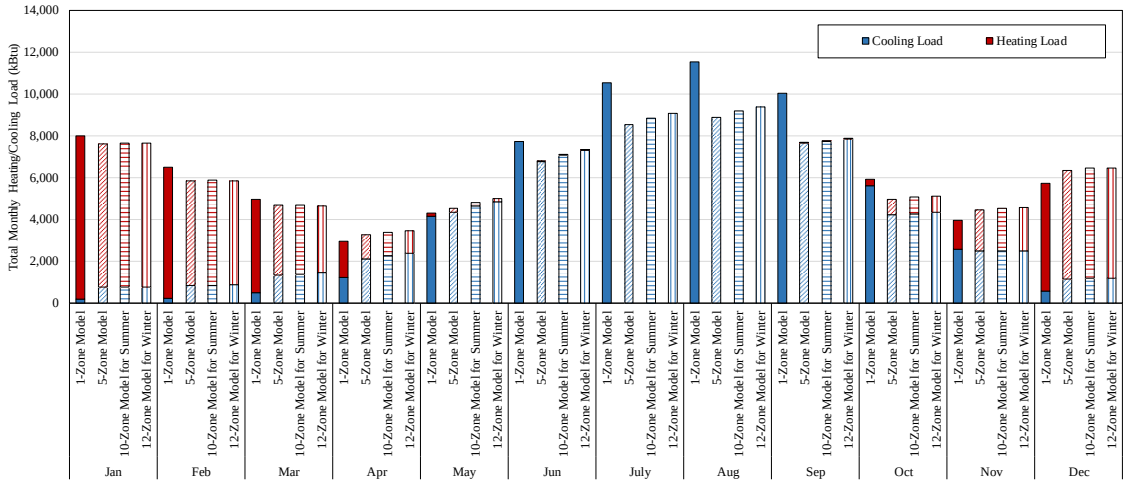

Figure 118: Total Monthly Heating/Cooling Loads for Case 13 (Houston, TX) Based on Different Zoning Methods

Figure 119 shows the total annual heating/cooling loads for the 1-Zone, 5-Zone, 10-Zone, and 12-Zone thermal zoning models for Case 13 (Houston, TX). The results show that the 5-Zone thermal zoning models for Case 13 gave the most energy efficient thermal zoning layout among four thermal zoning strategies. In addition, this model also showed about 11% thermal load reduction compared to the 1-Zone thermal zoning model.

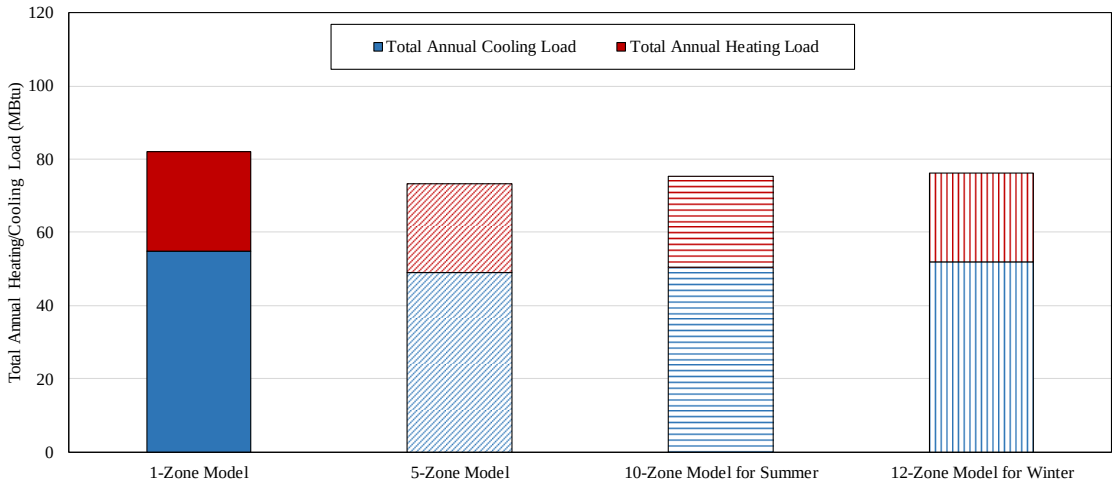

Figure 119: Total Annual Heating/Cooling Loads for Case 13 (Houston, TX) Based on Different Thermal Zoning Methods

Table 42 shows the results of total monthly thermal loads for Case 13 (Houston, TX) with the amount of the monthly thermal load reduction. As shown in the table, the 12-Zone model for the heating season has a thermal load reduction compared to the 1-Zone model, except April, May, November, and December. The grid/cluster thermal zoning method gave the highest load reduction of 22% in September, while the lowest load reduction of -17% in April. The annual total thermal load reduction of 7% indicates that the 12-Zone thermal zoning model for heating season has an improved energy efficiency than 1-Zone thermal zoning model for the specific conditions of Case 13.

Table 42: Comparison of Annual Thermal Loads for Case 13 (Houston, TX)

	1-Zone Model (kBtu)	5-Zone Model (kBtu)	10-Zone Model for Summer (kBtu)	12-Zone Model for Winter (kBtu)	1-Zone vs. 5 Zone (kBtu)	1-Zone vs. 10-Zone for Summer (kBtu)	1-Zone vs. 12-Zone for Winter (kBtu)
Jan	7,992	7,589	7,644	7,626	-366 (-5%)	-348 (-4%)	-366 (-5%)
Feb	6,492	5,845	5,870	5,825	-667 (-10%)	-622 (-10%)	-667 (-10%)
Mar	4,944	4,680	4,684	4,644	-299 (-6%)	-260 (-5%)	-299 (-6%)
Apr	2,932	3,257	3,368	3,444	512 (17%)	436 (15%)	512 (17%)
May	4,302	4,510	4,786	5,002	700 (16%)	484 (11%)	700 (16%)
Jun	7,734	6,771	7,087	7,316	-418 (-5%)	-647 (-8%)	-418 (-5%)
Jul	10,542	8,531	8,839	9,064	-1,478 (-14%)	-1,703 (-16%)	-1,478 (-14%)
Aug	11,519	8,863	9,169	9,389	-2,130 (-18%)	-2,350 (-20%)	-2,130 (-18%)
Sep	10,026	7,631	7,724	7,830	-2,196 (-22%)	-2,302 (-23%)	-2,196 (-22%)
Oct	5,892	4,935	5,059	5,121	-771 (-13%)	-834 (-14%)	-771 (-13%)
Nov	3,947	4,456	4,543	4,566	619 (16%)	596 (15%)	619 (16%)
Dec	5,708	6,335	6,448	6,460	753 (13%)	740 (13%)	752 (13%)
Total	**82,029**	**73,404**	**75,220**	**76,286**	**-5,743 (-7%)**	**-6,810 (-8%)**	**-5,743 (-7%)**

The model specification of Case 18 was summarized in Table 9 in Section 4.2.2. This case has a band of exterior window only on the south-facing exterior wall with WWR of 50%, and is located in Chicago, IL. Figure 120 shows the thermal zoning layouts of the different zoning models (i.e., a single-zone thermal zoning model, a core-perimeter thermal zoning model, two grid/cluster thermal zoning models) for Case 18. For Case 18, the core-perimeter method yielded 5 thermal zones. Also, in a similar fashion as previous case, the grid-cluster thermal zoning method gave two simulation models: one for the summer (i.e., 9-Zone Model) and the other for the winter (i.e., 12-Zone Model).

Figure 121 shows the total monthly heating/cooling loads for the 1-Zone, 5-Zone, 9-Zone, and 12-Zone thermal zoning models for Case 18 (Chicago, IL). The results show that the total monthly heating/cooling loads of the 1-Zone model (i.e., the single-zone method) are mostly higher than the other thermal zoning models, except June, July, August, September, and October. In addition, the total monthly thermal loads of the 5-Zone (i.e., the core-perimeter method), 9-Zone (i.e., the grid/cluster method for cooling season), 12-Zone models (i.e., the grid/cluster method for heating season) are very similar each other throughout the year.

Figure 122 shows the total annual heating/cooling loads for the 1-Zone, 5-Zone, 9-Zone, and 12-Zone thermal zoning models for Case 18 (Chicago, IL). The results show that the 12-Zone thermal zoning models for Case 18 gave the most energy efficient thermal zoning layout among four thermal zoning strategies. In addition, this model also showed about 22% thermal load reduction compared to 1-Zone thermal zoning model.

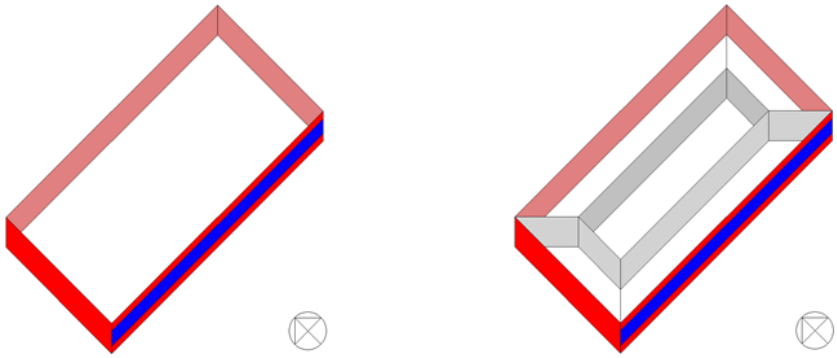

(1) 1-Zone Model (2) 5-Zone Model

(3) 9-Zone Model (for Summer) (4) 12-Zone Model (for Winter)

Figure 120: Different Zoning Models for Case 18 (Chicago, IL)

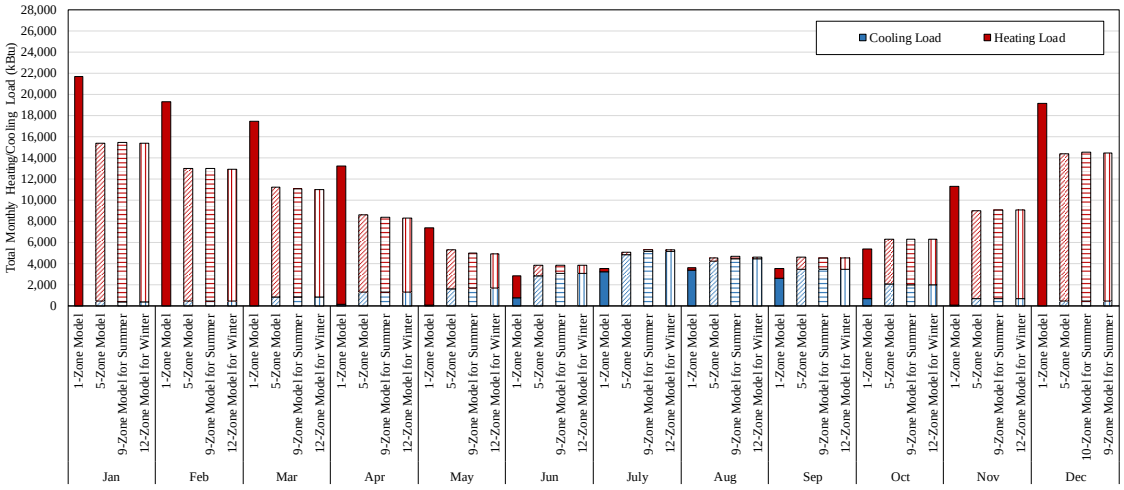

Figure 121: Total Monthly Heating/Cooling Loads for Case 18 (Chicago, IL) Based on Different Zoning Methods

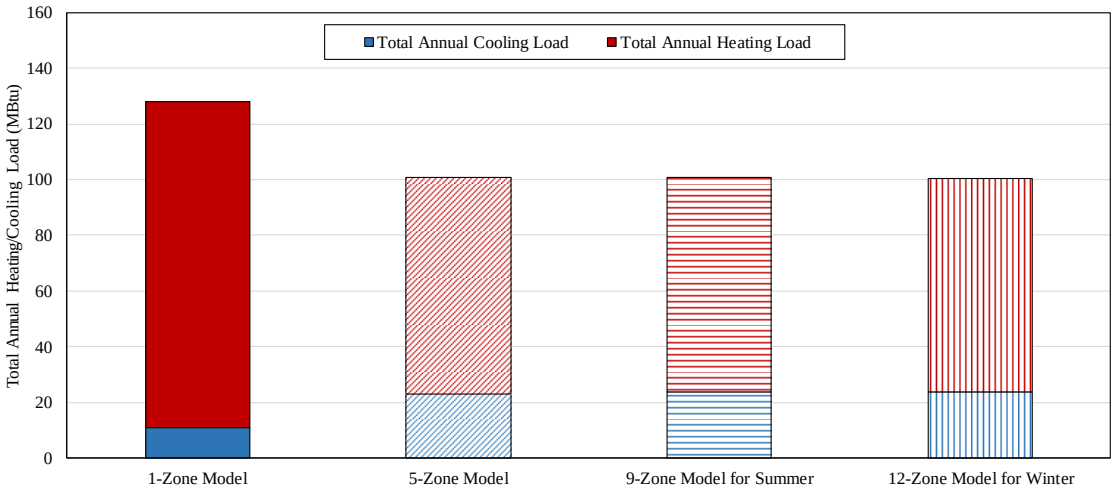

Figure 122: Total Annual Heating/Cooling Load for Case 18 (Chicago, IL) Based on Different Thermal Zoning Methods

Table 43 shows the results of total monthly thermal loads for Case 18 (Chicago, IL) with the amount of the monthly thermal load reduction. As shown in the table, the 12-Zone model for the heating season has a thermal load reduction compared to the 1-Zone model, except June, July, August, September, and October. The grid/cluster thermal zoning method gave the highest load reduction of 37% in March and April, while the lowest load reduction of -50% in July. The total annual thermal load reduction of 22% indicates that the 12-Zone thermal zoning model for the heating season has an improved energy efficiency than the 1-Zone thermal zoning model for the specific conditions of Case 18.

Table 43: Comparison of Annual Thermal Loads for Case 18 (Chicago, IL)

	1-Zone Model (kBtu)	5-Zone Model (kBtu)	9-Zone Model for Summer (kBtu)	12-Zone Model for Winter (kBtu)	1-Zone vs. 5 Zone (kBtu)	1-Zone vs. 9-Zone for Summer (kBtu)	1-Zone vs. 12-Zone for Winter (kBtu)
Jan	21,704	15,371	15,447	15,388	-6,333 (-29%)	-6,256 (-29%)	-6,316 (-29%)
Feb	19,275	12,988	12,979	12,924	-6,287 (-33%)	-6,296 (-33%)	-6,351 (-33%)
Mar	17,424	11,204	11,074	11,007	-6,220 (-36%)	-6,350 (-36%)	-6,417 (-37%)
Apr	13,231	8,626	8,392	8,317	-4,605 (-35%)	-4,839 (-37%)	-4,913 (-37%)
May	7,395	5,281	4,995	4,931	-2,114 (-29%)	-2,400 (-32%)	-2,464 (-33%)
Jun	2,806	3,809	3,833	3,794	1,003 (36%)	1,027 (37%)	988 (35%)
Jul	3,520	5,020	5,264	5,270	1,501 (43%)	1,745 (50%)	1,750 (50%)
Aug	3,599	4,485	4,628	4,619	886 (25%)	1,029 (29%)	1,020 (28%)
Sep	3,543	4,565	4,536	4,511	1,021 (29%)	992 (28%)	967 (27%)
Oct	5,372	6,285	6,291	6,269	913 (17%)	919 (17%)	897 (17%)
Nov	11,254	8,992	9,060	9,020	-2,261 (-20%)	-2,194 (-19%)	-2,234 (-20%)
Dec	19,123	14,363	14,500	14,458	-4,760 (-25%)	-4,622 (-24%)	-4,665 (-24%)
Total	**128,245**	**100,989**	**101,000**	**100,508**	**-27,256 (-21%)**	**-27,245 (-21%)**	**-27,736 (-22%)**

5.2.2.5.Case 19 (Houston, TX) vs. Case 23 (Chicago, IL)

Figure 123 shows the 3D images of building geometry for Case 19 and Case 23 models. The simulation models for these cases have window bands on the exterior walls facing East and West. All the other exterior walls facing North and South were windowless. Using the same geometry for all models, for this analysis the Houston TMY3 weather file was used for the Case 19 model, while the Chicago TMY3 weather file was used for the Case 23 model. The grid/cluster thermal zoning method was applied to these two case models, and the variations of the thermal zoning layouts were compared. In the analysis, the simulated annual/monthly, heating/cooling loads for the single zone, the core-perimeter, the grid/cluster zoning models for the cases were compared and analyzed.

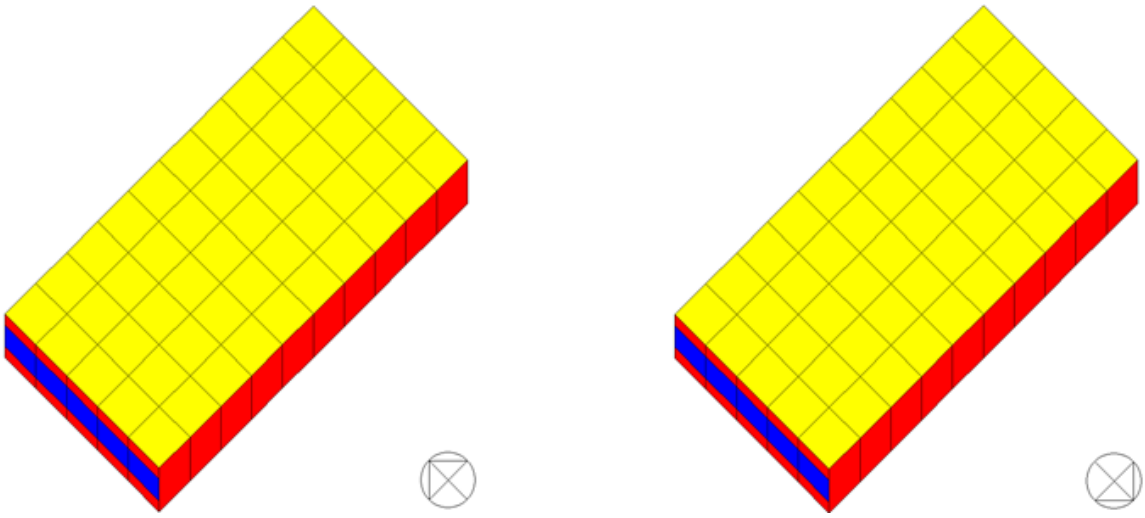

(a) Southwest View (b) Northeast View

Figure 123: View of Case 19 and Case 23 Models in the Simulation

Table 44 presents the common features of the Case 19 and Case 23 models along with the thermal zoning layouts of the Case 19 and Case 23 models for cooling and heating season. For all the cases, it should be noted that both cases have the windows on the exterior wall facing east and west. Therefore, direct solar radiation penetrates into the space only from the east and west side of the building in the morning and evening, respectively. The results show that there is a similarity in the thermal zoning layouts between the Case 19 and Case 23 models. For the interior space, the grid/cluster thermal zoning method divided the building vertically into three different thermal zones. Interestingly, two of the interior thermal zones was created near the window location (i.e., east-, west-side) for both cases. However, the thermal zoning layout for Case 19 for the heating season has only a single interior thermal zone. For the perimeter spaces, the grid/cluster thermal zoning method gave similar results for Case 19 with one that follows the traditional core-perimeter thermal zoning method. The layouts consist of four different perimeter spaces along with each orientation. In addition, four unit spaces located at each corner of the model become four different thermal zones. However, for Case 23, the perimeter spaces facing north and south, where the windows were not located, also were divided into three different thermal zones.

The model specification of Case 19 was summarized in Table 9 in Section 4.2.2. This case has a band of exterior window on the east-facing and west-facing exterior walls with WWR of 50%, and is located in Houston, TX. Figure 124 shows the thermal zoning layouts of the different zoning models (i.e., a single-zone thermal zoning model, a core-perimeter thermal zoning model, two grid/cluster thermal zoning models) for

Case 19. For Case 19, the core-perimeter thermal zoning method yielded 5 thermal zones. Also, the grid-cluster thermal zoning method gave two simulation models: one for summer (i.e., 11-Zone Model) and the other for winter (i.e., 9-Zone Model).

Table 44: Results of Thermal Zoning for the Case 19 (Houston) and Case 23 (Chicago)

	Case 19 (Houston)	**Case 23 (Chicago)**
Summary of Parameters	• Location: Houston, TX • Floor type: Slab-on-grade • WWR: 50 %, East-West only • Floor area: 5,000 ft^2 • Number of thermal zone: 50	• Location: Chicago, IL • Floor type: Slab-on-grade • WWR: 50 %, East-West only • Floor area: 5,000 ft^2 • Number of thermal zone: 50
Cooling Season	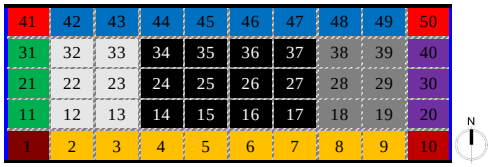	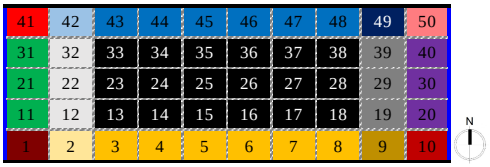
Heating Season	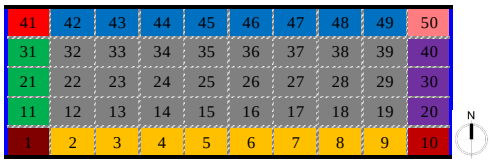	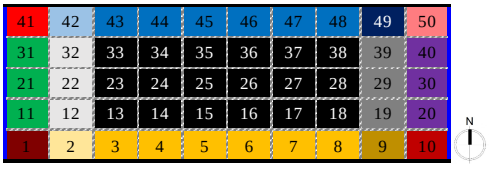

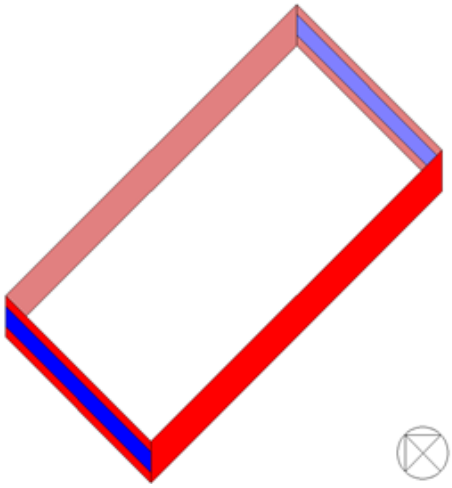

(1) 1-Zone Model

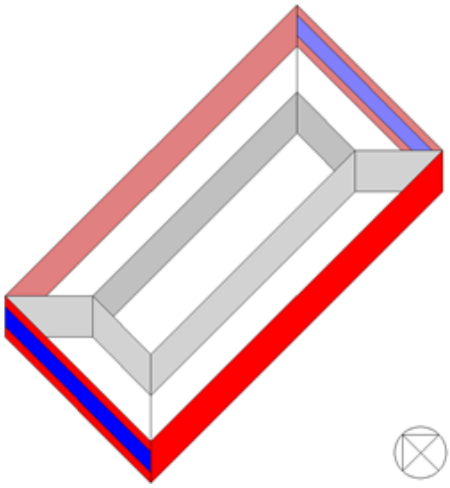

(2) 5-Zone Model

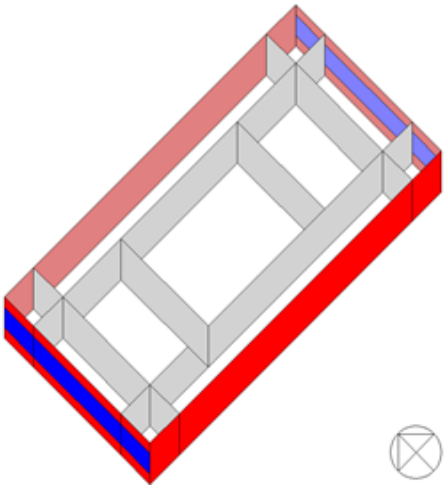

(3) 11-Zone Model (for Summer)

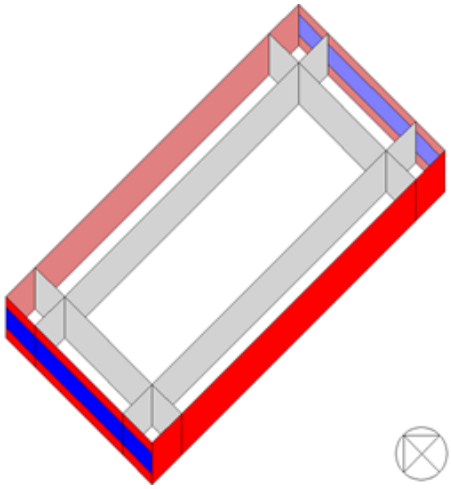

(4) 9-Zone Model (for Winter)

Figure 124: Different Zoning Models for Case 19 (Houston, TX)

Figure 125 shows the total monthly heating/cooling loads for the 1-Zone, 5-Zone, 11-Zone, and 9-Zone thermal zoning models for Case 19 (Houston, TX). The results show that the total monthly heating/cooling loads of the 1-Zone model (i.e., the single-

zone method) are mostly higher than the other thermal zoning models, except April, May, and November. In addition, the total monthly thermal loads of the 5-Zone (i.e., the core-perimeter method), 11-Zone (i.e., the grid/cluster method for the cooling season), 9-Zone models (i.e., the grid/cluster method for the heating season) are very similar each other throughout the year.

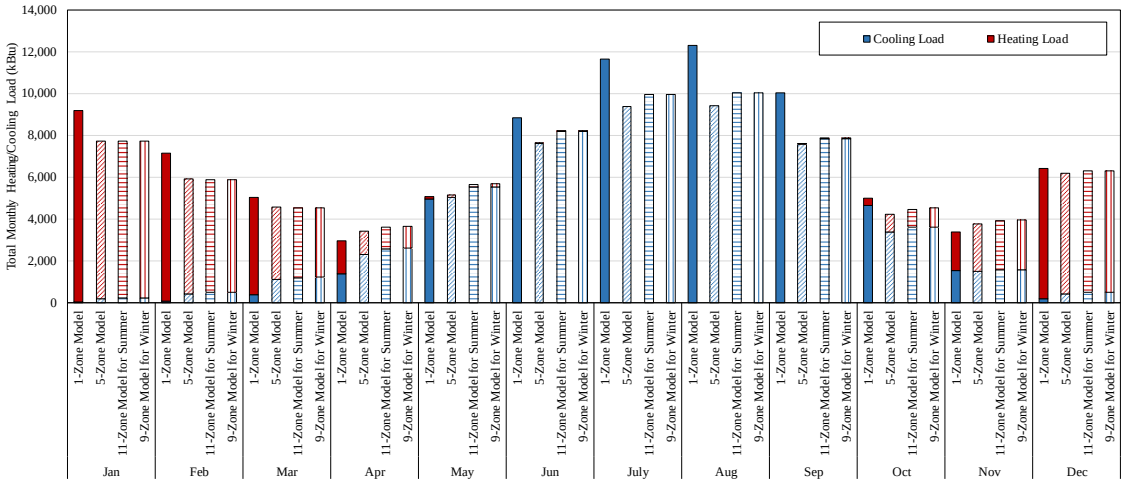

Figure 125: Total Monthly Heating/Cooling Loads for Case 19 (Houston, TX) Based on Different Zoning Methods

Figure 126 shows the total annual heating/cooling loads for the 1-Zone, 5-Zone, 11-Zone, and 9-Zone thermal zoning models for Case 19 (Houston, TX). The results show that the 5-Zone thermal zoning models for Case 19 gave the most energy efficient thermal zoning layout among four thermal zoning strategies. In addition, this model also showed about 14% thermal load reduction compared to the 1-Zone thermal zoning model.

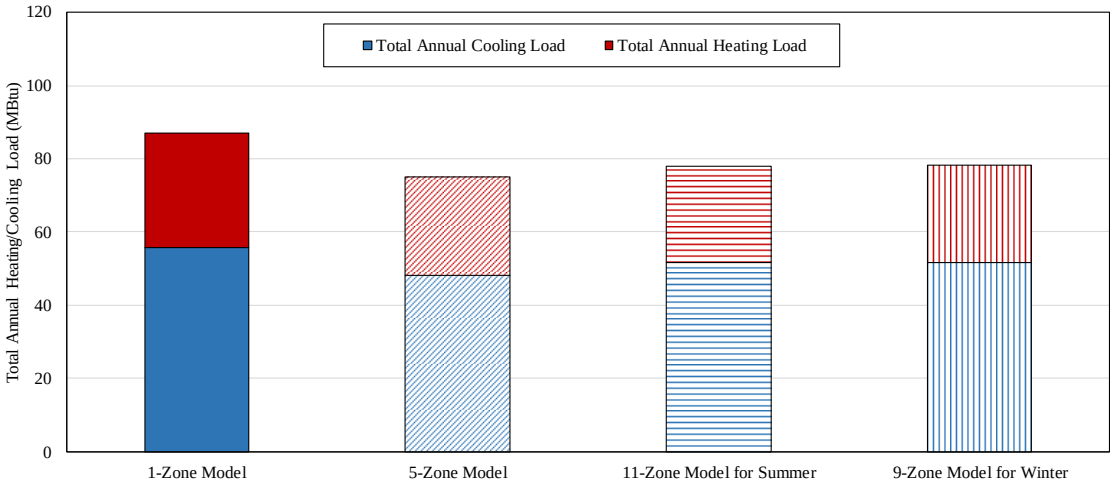

Figure 126: Total Annual Heating/Cooling Loads for Case 19 (Houston, TX) Based on Different Thermal Zoning Methods

Table 45 shows the results of total monthly thermal loads for Case 19 (Houston, TX) with the amount of the monthly thermal load reduction. As shown in the table, the 9-Zone model for the heating season has a thermal load reduction compared to the 1-Zone model, except April, May, and November. The grid/cluster thermal zoning method gave the highest load reduction of 22% in September, while the lowest load reduction of -23% in April. The annual total thermal load reduction of 10% indicates that the 9-Zone thermal zoning model for heating season has an improved energy efficiency than the 1-Zone thermal zoning model for the specific conditions of Case 19.

Table 45: Comparison of Annual Thermal Load for Case 19 (Houston, TX)

	1-Zone Model (kBtu)	5-Zone Model (kBtu)	11-Zone Model for Summer (kBtu)	9-Zone Model for Winter (kBtu)	1-Zone vs. 5 Zone (kBtu)	1-Zone vs. 11-Zone for Summer (kBtu)	1-Zone vs. 9-Zone for Winter (kBtu)
Jan	9,180	7,719	7,739	7,717	-1,461 (-16%)	-1,441 (-16%)	-366 (-5%)
Feb	7,131	5,897	5,864	5,862	-1,234 (-17%)	-1,266 (-18%)	-667 (-10%)
Mar	5,041	4,563	4,506	4,535	-477 (-9%)	-534 (-11%)	-299 (-6%)
Apr	2,963	3,423	3,591	3,636	460 (16%)	628 (21%)	512 (17%)
May	5,072	5,150	5,654	5,669	78 (2%)	582 (11%)	700 (16%)
Jun	8,821	7,615	8,197	8,194	-1,205 (-14%)	-623 (-7%)	-418 (-5%)
Jul	11,637	9,372	9,963	9,947	-2,265 (-19%)	-1,674 (-14%)	-1,478 (-14%)
Aug	12,284	9,429	10,029	10,010	-2,855 (-23%)	-2,255 (-18%)	-2,130 (-18%)
Sep	10,039	7,561	7,852	7,838	-2,478 (-25%)	-2,187 (-22%)	-2,196 (-22%)
Oct	5,002	4,222	4,467	4,520	-780 (-16%)	-535 (-11%)	-771 (-13%)
Nov	3,359	3,769	3,906	3,940	409 (12%)	546 (16%)	619 (16%)
Dec	6,429	6,189	6,292	6,293	-240 (-4%)	-137 (-2%)	752 (13%)
Total	**86,957**	**74,909**	**78,061**	**78,161**	**-12,048 (-14%)**	**-8,896 (-10%)**	**-5,743 (-7%)**

The model specification of Case 23 was summarized in Table 9 in Section 4.2.2. This case has a band of exterior window on the east-facing and west-facing exterior walls with WWR of 50%, and is located in Chicago, IL. Figure 127 shows the thermal zoning layouts of the different zoning models (i.e., a single-zone thermal zoning model,

a core-perimeter thermal zoning model, a grid/cluster thermal zoning model) for Case 23. For Case 23, the core-perimeter method yielded 5 thermal zones. In addition, the grid-cluster thermal zoning method gave 15 thermal zones.

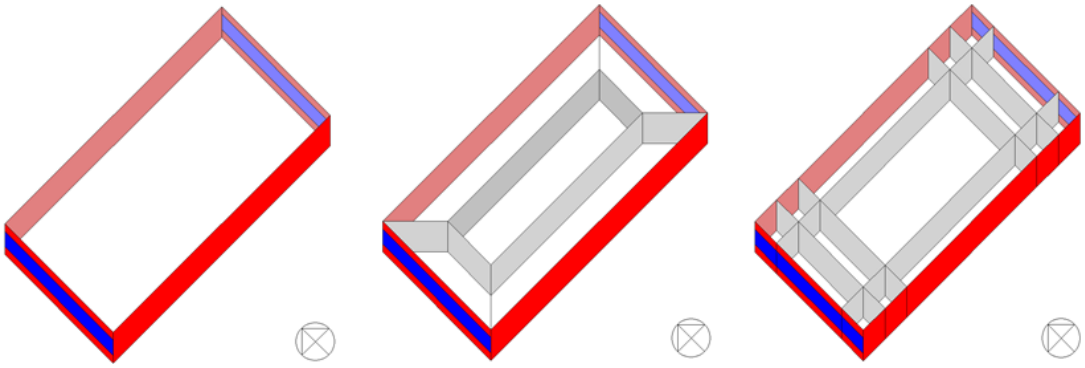

(1) 1-Zone Model (2) 5-Zone Model (3) 15-Zone Model

Figure 127: Different Zoning Models for Case 23 (Chicago, IL)

Figure 128 shows the total monthly heating/cooling loads for the 1-Zone, 5-Zone, and 15-Zone thermal zoning models for Case 23 (Chicago, IL). The results show that the total monthly heating/cooling loads of the 1-Zone model (i.e., the single-zone method) are mostly higher than the other thermal zoning models, except the cooling season (i.e., June, July, August, and September). In addition, the total monthly thermal loads of the 5-Zone (i.e., the core-perimeter method), 15-Zone (i.e., the grid/cluster method), are very similar each other throughout the year.

Figure 129 shows the total annual heating/cooling loads for the 1-Zone, 5-Zone, and 15-Zone thermal zoning models for Case 23 (Chicago, IL). The results show that the 15-Zone thermal zoning model for Case 23 gave the most energy efficient thermal

zoning layout among four thermal zoning strategies. In addition, this model also showed about 24% thermal load reduction compared to the 1-Zone thermal zoning model.

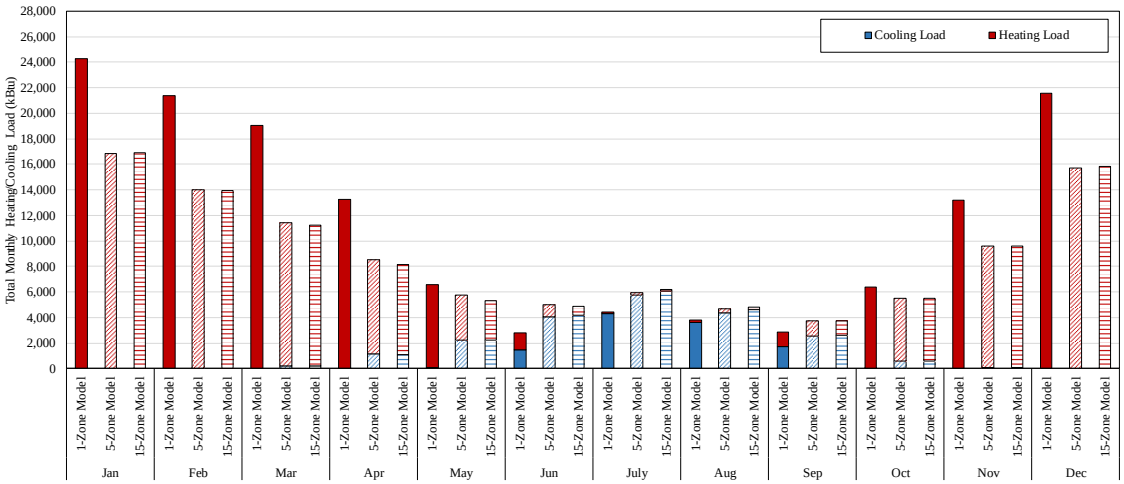

Figure 128: Total Monthly Heating/Cooling Loads for Case 23 (Chicago, IL) Based on Different Zoning Methods

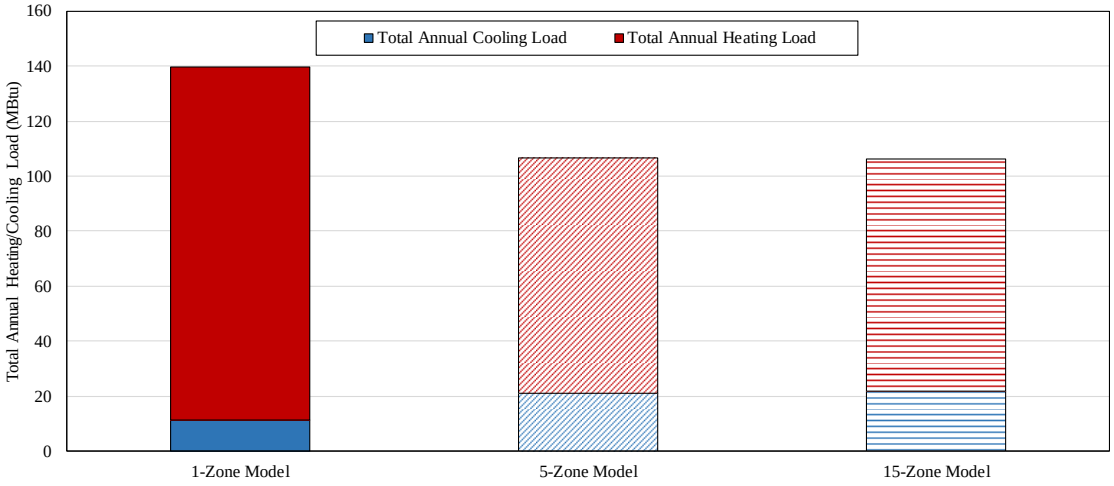

Figure 129: Total Annual Heating/Cooling Loads for Case 23 (Chicago, IL) Based on Different Thermal Zoning Methods

Table 46 shows the results of total monthly thermal loads for Case 23 (Chicago, IL) with the amount of the monthly thermal load reduction. As shown in the table, the 15-Zone model has a thermal load reduction compared to the 1-Zone model, except June, July, August, and September. The grid/cluster thermal zoning method gave the highest load reduction of 41% in March, while the lowest load reduction of -72% in June. The total annual thermal load reduction of 24% indicates that the 15-Zone thermal zoning model for the heating season has an improved energy efficiency than 1-Zone thermal zoning model for the specific conditions of Case 23.

Table 46: Comparison of Annual Thermal Load for Case 23 (Chicago, IL)

	1-Zone Model (kBtu)	**5-Zone Model (kBtu)**	**15-Zone Model (kBtu)**	**1-Zone vs. 5 Zone (kBtu)**	**1-Zone vs. 15-Zone (kBtu)**
Jan	24,288	16,856	16,911	-7,432 (-31%)	-7,378 (-30%)
Feb	21,384	13,986	13,963	-7,398 (-35%)	-7,422 (-35%)
Mar	19,017	11,457	11,256	-7,559 (-40%)	-7,761 (-41%)
Apr	13,274	8,504	8,170	-4,770 (-36%)	-5,104 (-38%)
May	6,559	5,784	5,290	-775 (-12%)	-1,269 (-19%)
Jun	2,826	4,991	4,873	2,165 (77%)	2,047 (72%)
Jul	4,467	5,942	6,197	1,475 (33%)	1,730 (39%)
Aug	3,799	4,673	4,832	873 (23%)	1,033 (27%)
Sep	2,881	3,742	3,727	861 (30%)	845 (29%)
Oct	6,369	5,524	5,476	-845 (-13%)	-892 (-14%)
Nov	13,180	9,592	9,614	-3,588 (-27%)	-3,567 (-27%)
Dec	21,563	15,708	15,824	-5,855 (-27%)	-5,739 (-27%)
Total	**139,607**	**106,758**	**106,132**	**-32,849 (-24%)**	**-33,476 (-24%)**

5.2.2.6.Case 20 (Houston, TX) vs. Case 24 (Chicago, IL)

Figure 130 shows the 3D images of building geometry for Case 20 and Case 24 models. The simulation models for these cases have a window band on the exterior walls facing East and West. In addition, it should be noted that the windows mounted for these cases have a width of 20 ft and are located on the east-side of each wall. All the other exterior walls facing North and South were windowless. Using the same geometry for all models, for this analysis the Houston TMY3 weather file was used for the Case 20 model, while the Chicago TMY3 weather file was used for the Case 24 model. The grid/cluster thermal zoning method was applied to these two case models, and the variations of the thermal zoning layouts were compared. In the analysis, the simulated annual/monthly, heating/cooling loads for the single zone, the core-perimeter, the grid/cluster zoning models for the cases were compared and analyzed.

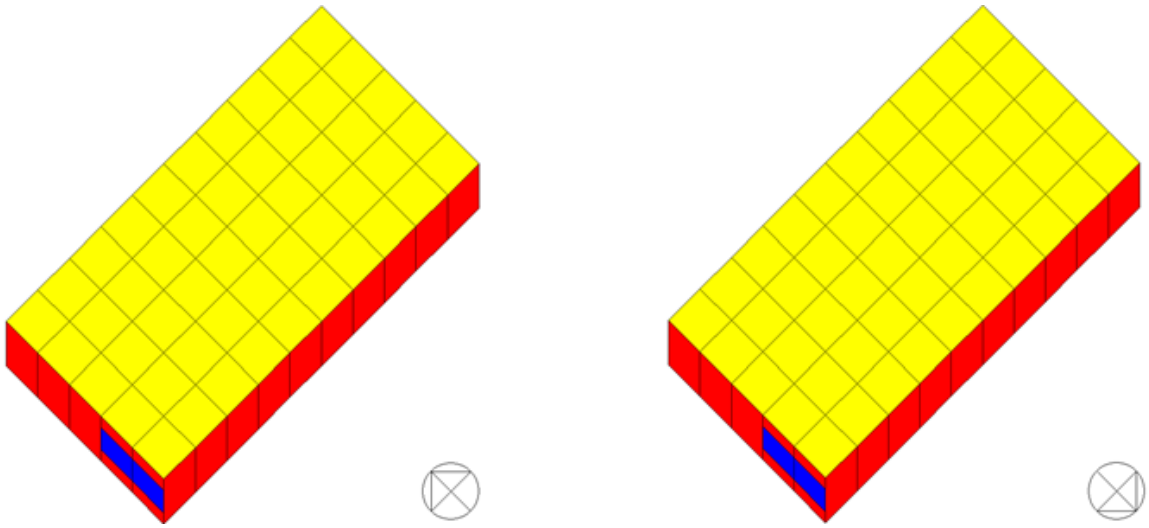

(a) Southwest View (b) Northeast View

Figure 130: View of Case 20 and Case 24 Models in the Simulation

Table 47 presents the common features of the Case 20 and Case 24 models along with the thermal zoning layouts of the Case 20 and Case 24 models for the cooling and heating season. The results show that there is a similarity in the thermal zoning layouts between the Case 20 and Case 24 models. For the interior spaces, the grid/cluster thermal zoning method gave the same results with one that follows the traditional core-perimeter thermal zoning method. The both models were given a single thermal zone for the interior spaces. For the perimeter spaces, the grid/cluster thermal zoning method divided the building into two different thermal zones for east and west side zones, where the windows were located (i.e., east-, west-side). However, the spaces facing north and south were given a single thermal zone for both cases.

Table 47: Results of Thermal Zoning for the Case 20 (Houston) and Case 24 (Chicago)

	Case 20 (Houston)	**Case 24 (Chicago)**
Summary of Parameters	• Location: Houston, TX • Floor type: Slab-on-grade • WWR: 50 %, East-West Offset • Floor area: 5,000 ft^2 • Number of thermal zone: 50	• Location: Chicago, IL • Floor type: Slab-on-grade • WWR: 50 %, East-West Offset • Floor area: 5,000 ft^2 • Number of thermal zone: 50
Cooling Season	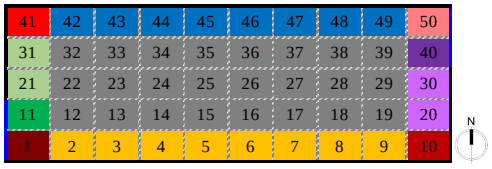	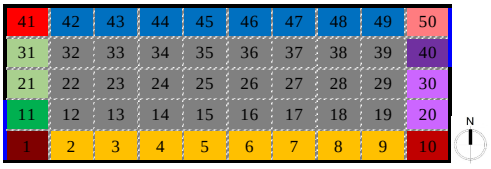
Heating Season	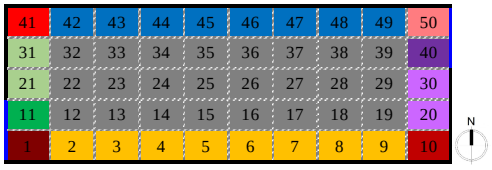	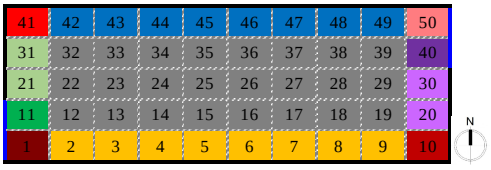

The model specification of Case 20 was summarized in Table 9 in Section 4.2.2. This case has two exterior windows, which has width of 20 ft, at the right corner of the east- and west-facing exterior walls with WWR of 50%, and is located in Houston, TX. Figure 131 shows the thermal zoning layouts of the different zoning models (i.e., a single-zone thermal zoning model, a core-perimeter thermal zoning model, a grid/cluster thermal zoning model) for Case 20. For Case 20, the core-perimeter method yielded 5 thermal zones. In addition, the grid-cluster thermal zoning method gave 11 thermal zones.

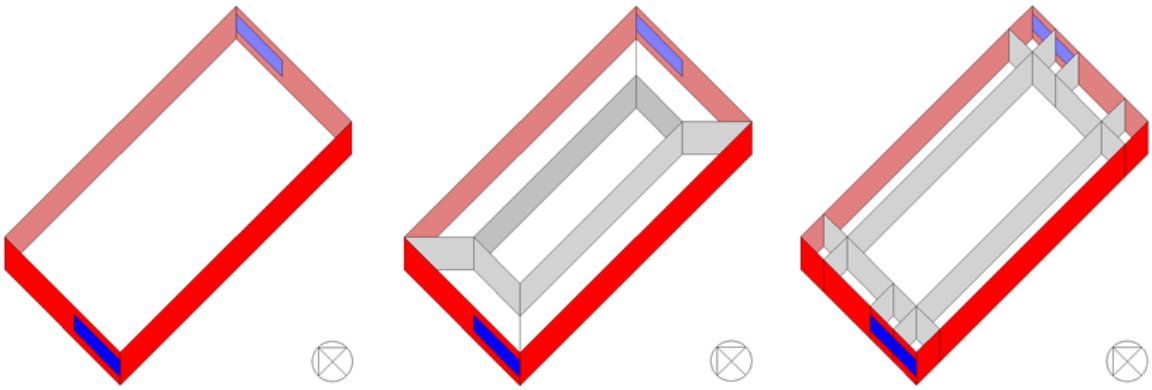

(1) 1-Zone Model (2) 5-Zone Model (3) 11-Zone Model

Figure 131: Different Zoning Models for Case 20 (Houston, TX)

Figure 132 shows the total monthly heating/cooling loads for the 1-Zone, 5-Zone, and 11-Zone thermal zoning models for Case 20 (Houston, TX). The results show that the total monthly heating/cooling loads of the 1-Zone model (i.e., the single-zone method) are mostly higher than the other thermal zoning models, except May and November. In addition, the total monthly thermal loads of the 5-Zone (i.e., the core-

perimeter method) are mostly little lower than the 9-Zone models (i.e., the grid/cluster method for heating/cooling season).

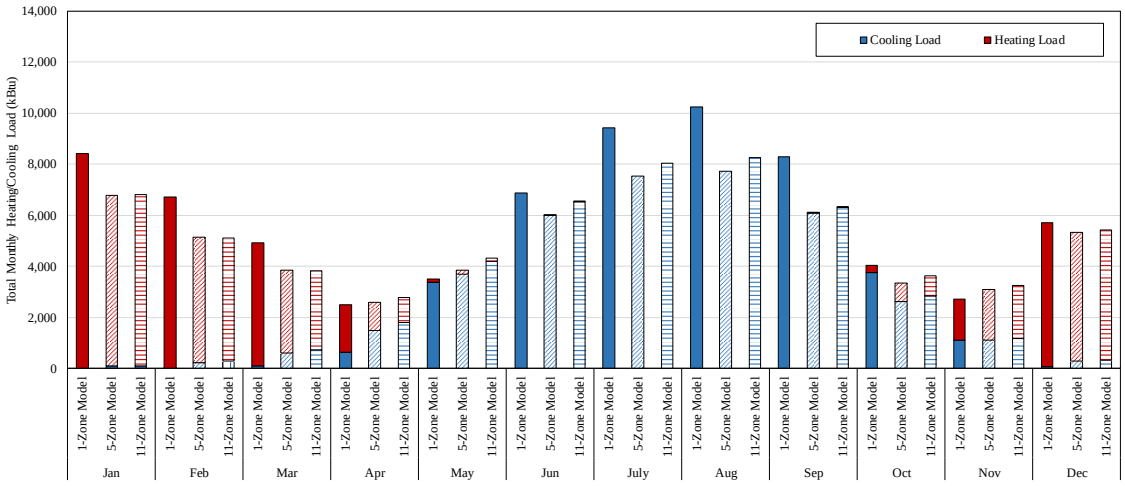

Figure 132: Total Monthly Heating/Cooling Loads for Case 20 (Houston, TX) Based on Different Zoning Methods

Figure 133 shows the total annual heating/cooling loads for the 1-Zone, 5-Zone, and 11-Zone thermal zoning models for Case 20 (Houston, TX). The results show that the 5-Zone thermal zoning model for Case 20 gave the most energy efficient thermal zoning layout among four thermal zoning strategies. In addition, this model also showed about 20% thermal load reduction compared to the 1-Zone thermal zoning model.

Table 48 shows the results of monthly total thermal loads for 1-Zone model and 11-Zone model with the amount of the monthly thermal load reduction. As shown in the table, the 11-Zone model has a thermal load reduction compared to 1-Zone model, except May and November. The grid/cluster thermal zoning method gave the highest load reduction of 32% in March, while the lowest load reduction of -36% in May. The

annual total thermal load reduction of 15% indicates that the 11-Zone thermal zoning model for heating season has an improved energy efficiency than 1-Zone thermal zoning model for the specific conditions of Case 20.

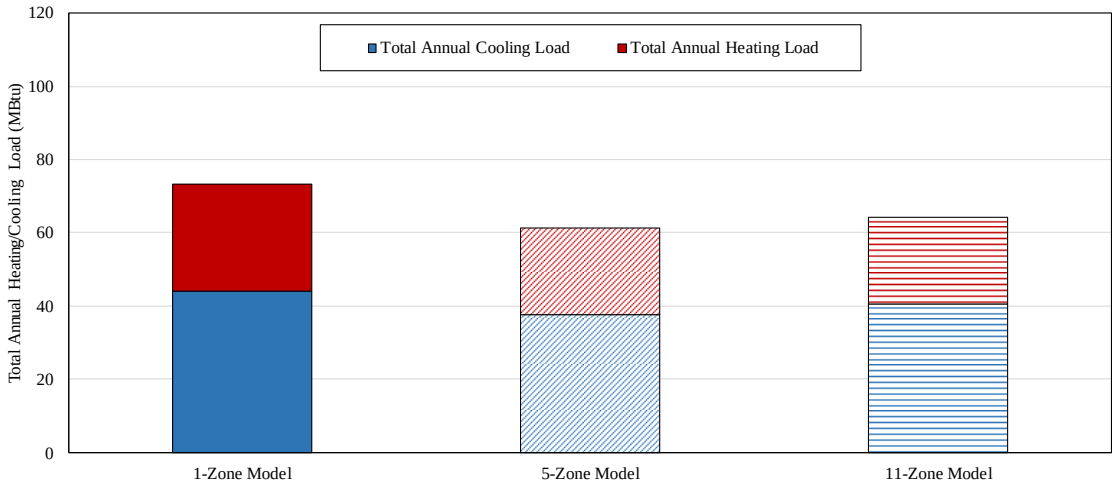

Figure 133: Total Annual Heating/Cooling Loads for Case 20 (Houston, TX) Based on Different Thermal Zoning Methods

Table 48: Comparison of Annual Thermal Loads for Case 20 (Houston, TX)

	1-Zone Model (kBtu)	**5-Zone Model (kBtu)**	**11-Zone Model (kBtu)**	**1-Zone vs. 5 Zone (kBtu)**	**1-Zone vs. 11-Zone (kBtu)**
Jan	8,420	6,785	6,802	-1,635 (-19%)	-1,618 (-19%)
Feb	6,719	5,151	5,125	-1,567 (-23%)	-1,594 (-24%)
Mar	4,932	3,840	3,840	-1,091 (-22%)	-1,091 (-22%)
Apr	2,492	2,585	2,797	93 (4%)	305 (12%)
May	3,523	3,847	4,317	324 (9%)	794 (23%)
Jun	6,876	6,006	6,522	-869 (-13%)	-353 (-5%)
Jul	9,436	7,537	8,044	-1,898 (-20%)	-1,391 (-15%)
Aug	10,257	7,731	8,253	-2,525 (-25%)	-2,004 (-20%)
Sep	8,282	6,099	6,319	-2,183 (-26%)	-1,963 (-24%)
Oct	4,058	3,354	3,630	-704 (-17%)	-428 (-11%)
Nov	2,711	3,088	3,253	378 (14%)	542 (20%)
Dec	5,719	5,327	5,439	-392 (-7%)	-280 (-5%)
Total	**73,423**	**61,352**	**64,341**	**-12,071 (-16%)**	**-9,082 (-12%)**

The model specification of Case 24 was summarized in Table 9 in Section 4.2.2. This case has two exterior windows, which has width of 20 ft, at the right corner of the east- and west-facing exterior walls with WWR of 50%, and is located in Chicago, IL. Figure 134 shows the thermal zoning layouts of the different zoning models (i.e., a single-zone thermal zoning model, a core-perimeter thermal zoning model, a grid/cluster thermal zoning model) for Case 24. For Case 24, the core-perimeter thermal zoning method yielded 5 thermal zones. In addition, the grid-cluster thermal zoning method gave 11 thermal zones.

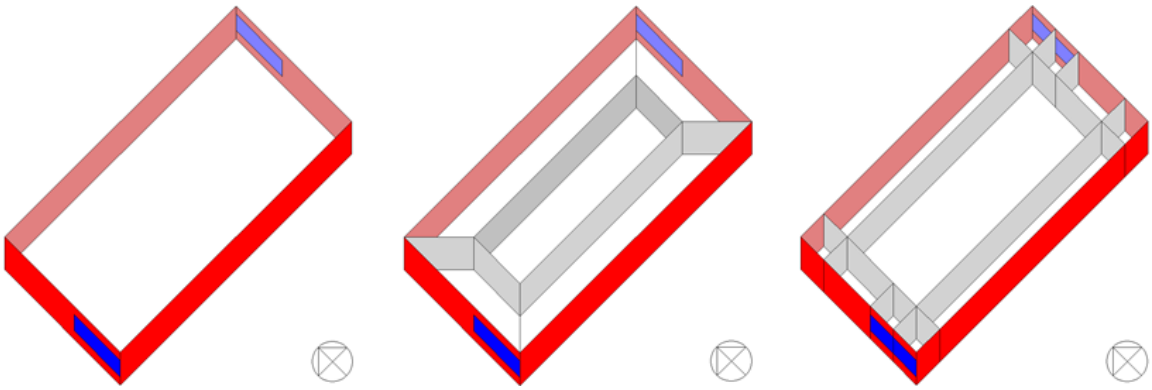

(1) 1-Zone Model (2) 5-Zone Model (3) 11-Zone Model

Figure 134: Different Zoning Models for Case 24 (Chicago, IL)

Figure 135 shows the total monthly heating/cooling loads for the 1-Zone, 5-Zone, 11-Zone thermal zoning models for Case 24 (Chicago, IL). The results show that the total monthly heating/cooling loads of the 1-Zone model (i.e., the single-zone method) are mostly higher than the other thermal zoning models, except May and November. In

addition, the total monthly thermal loads of the 5-Zone (i.e., the core-perimeter method) are mostly little lower than the 11-Zone models (i.e., the grid/cluster method).

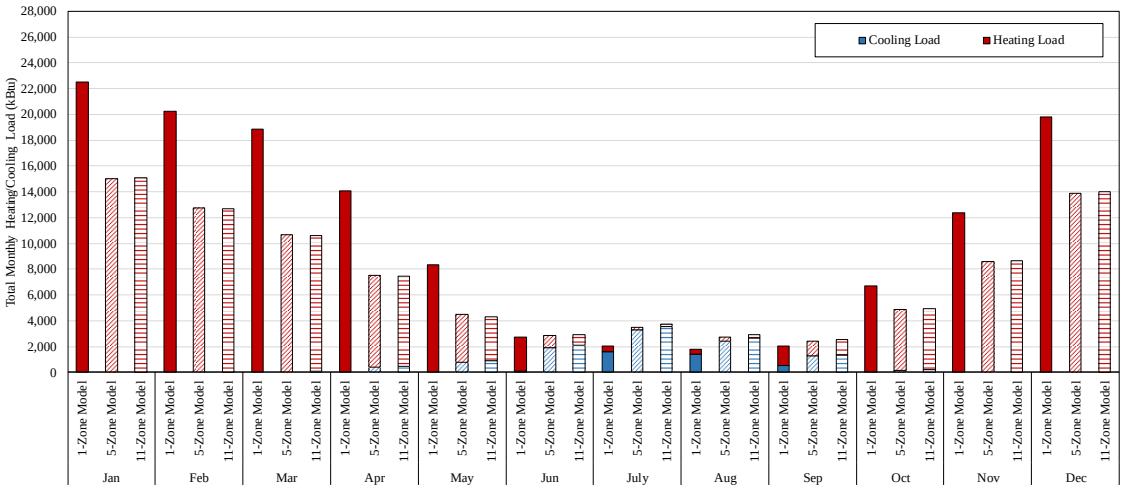

Figure 135: Total Monthly Heating/Cooling Loads for Case 24 (Chicago, IL) Based on Different Zoning Methods

Figure 136 shows the total annual heating/cooling loads for the 1-Zone, 5-Zone, and 11-Zone thermal zoning models for Case 24 (Chicago, IL). The results show that the 5-Zone thermal zoning model for Case 24 gave the most energy efficient thermal zoning layout among four thermal zoning strategies. In addition, this model also showed about 12% thermal load reduction compared to the 1-Zone thermal zoning model.

Table 49 shows the results of monthly total thermal loads for Case 24 (Chicago, IL) with the amount of the monthly thermal load reduction. As shown in the table, the 11-Zone model has a thermal load reduction compared to the 1-Zone model, except May, June, and November. The grid/cluster thermal zoning method gave the highest load reduction of 26% in February, while the lowest load reduction of -52% in May. The

annual total thermal load reduction of 10% indicates that the 11-Zone thermal zoning model for heating season has an improved energy efficiency than the 1-Zone thermal zoning model for the specific conditions of Case 24.

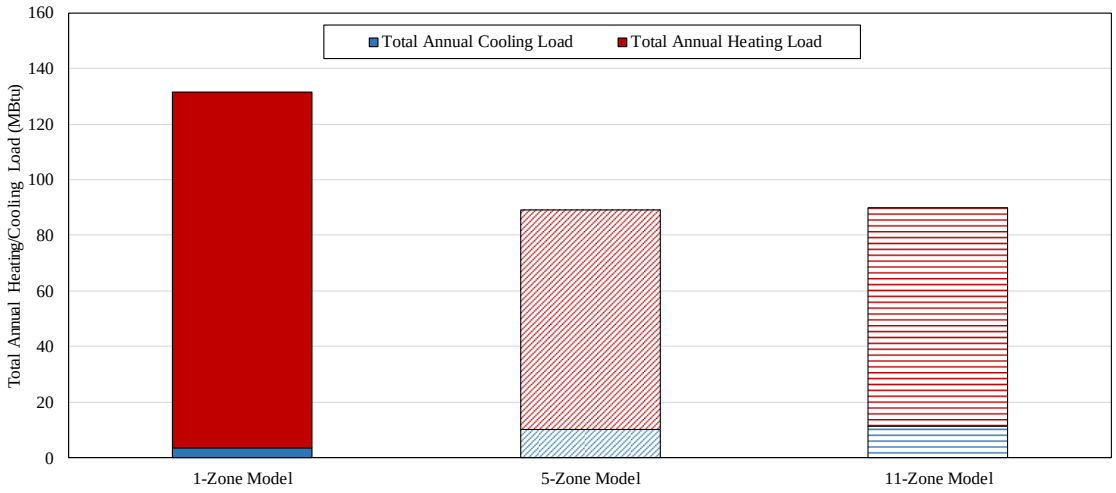

Figure 136: Total Annual Heating/Cooling Loads for Case 24 (Chicago, IL) Based on Different Thermal Zoning Methods

Table 49: Comparison of Annual Thermal Loads for Case 24 (Chicago, IL)

	1-Zone Model (kBtu)	**5-Zone Model (kBtu)**	**11-Zone Model (kBtu)**	**1-Zone vs. 5 Zone (kBtu)**	**1-Zone vs. 11-Zone (kBtu)**
Jan	22,507	15,034	15,051	-7,472 (-33%)	-7,456 (-33%)
Feb	20,263	12,734	12,694	-7,530 (-37%)	-7,569 (-37%)
Mar	18,846	10,661	10,661	-8,185 (-43%)	-8,185 (-43%)
Apr	14,094	7,518	7,434	-6,576 (-47%)	-6,660 (-47%)
May	8,351	4,484	4,327	-3,866 (-46%)	-4,024 (-48%)
Jun	2,767	2,888	2,947	122 (4%)	181 (7%)
Jul	2,063	3,486	3,715	1,423 (69%)	1,652 (80%)
Aug	1,795	2,729	2,903	935 (52%)	1,108 (62%)
Sep	2,053	2,452	2,531	399 (19%)	478 (23%)
Oct	6,716	4,848	4,959	-1,868 (-28%)	-1,757 (-26%)
Nov	12,366	8,593	8,641	-3,774 (-31%)	-3,725 (-30%)
Dec	19,775	13,905	13,984	-5,870 (-30%)	-5,791 (-29%)
Total	**131,595**	**89,332**	**89,847**	**-42,263 (-32%)**	**-41,747 (-32%)**

5.2.2.7.Case 21 (Houston, TX) vs. Case 25 (Chicago, IL)

Figure 137 shows the 3D images of building geometry for Case 21 and Case 25 models. The simulation models for these cases have a window band on the exterior walls facing North and South. All the other exterior walls facing East and West were windowless. Using the same geometry for all models, for this analysis the Houston TMY3 weather file was used for the Case 21 model, while the Chicago TMY3 weather file was used for the Case 25 model. The grid/cluster thermal zoning method was applied to these two case models, and the variations of the thermal zoning layouts were compared. In the analysis, the simulated annual/monthly, heating/cooling loads for the single zone, the core-perimeter, the grid/cluster zoning models for the cases were compared and analyzed.

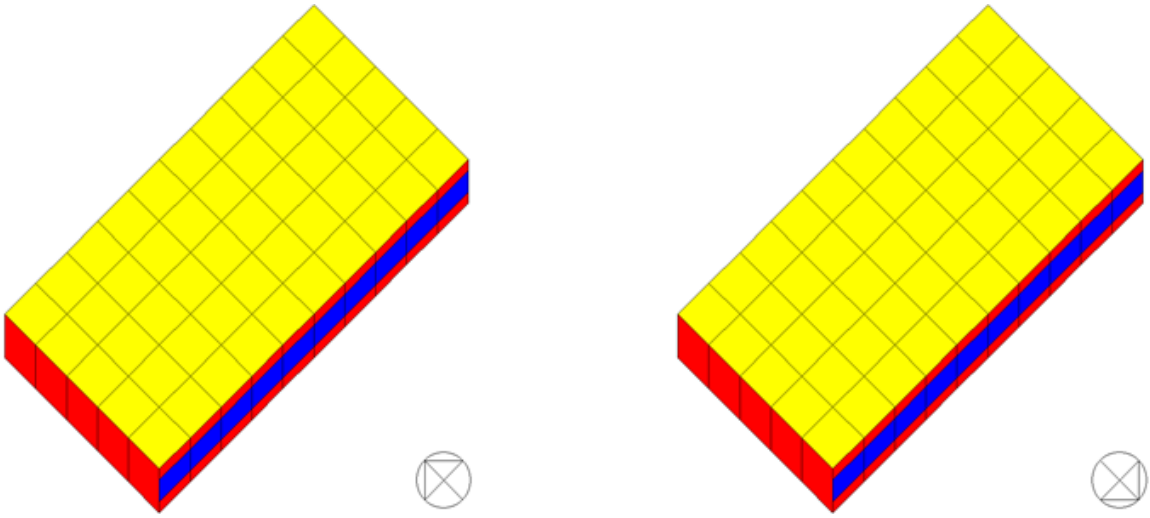

(a) Southwest View (b) Northeast View

Figure 137: View of Case 21 and Case 25 Models in the Simulation

Table 50 presents the common features of the Case 21 and Case 25 models along with the thermal zoning layouts of the Case 21 and Case 25 models for the cooling and heating season. For all the cases, it should be noted that both cases have the windows on the exterior wall facing north and south. Therefore, direct solar radiation penetrates into the space only from the north- and south-side of the building. The results show that the grid/cluster thermal zoning method gave the same results with one that follows the traditional core/perimeter thermal zoning method for most cases, except Case 25 for the cooling season. For Case 25 for the cooling season layout, it was found that two thermal zones were created for the perimeter spaces facing east and west. For the interior space, the grid/cluster thermal zoning method divided the building horizontally into two different thermal zones. One of the interior thermal zones was also created near the window location (i.e., south-side) for this case.

Table 50: Results of Thermal Zoning for the Case 21 (Houston) and Case 25 (Chicago)

	Case 21 (Houston)	**Case 25 (Chicago)**
Summary of Parameters	• Location: Houston, TX • Floor type: Slab-on-grade • WWR: 50 %, North-South only • Floor area: 5,000 ft^2 • Number of thermal zone: 50	• Location: Chicago, IL • Floor type: Slab-on-grade • WWR: 50 %, North-South only • Floor area: 5,000 ft^2 • Number of thermal zone: 50
Cooling Season	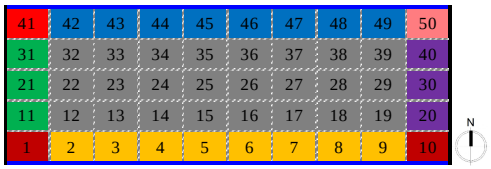	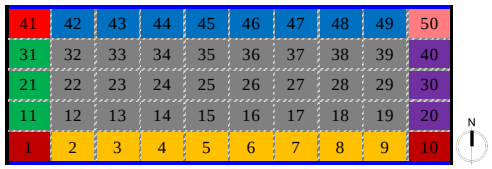
Heating Season	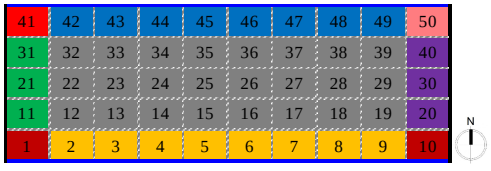	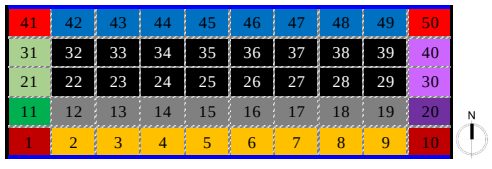

The model specification of Case 21 was summarized in Table 9 in Section 4.2.2. This case has a band of exterior window on the north-facing and south-facing exterior walls with WWR of 50%, and is located in Houston, TX. Figure 138 shows the thermal zoning layouts of the different zoning models (i.e., a single-zone thermal zoning model, a core-perimeter thermal zoning model, a grid/cluster thermal zoning model) for Case 21. For Case 21, the core-perimeter thermal zoning method yielded 5 thermal zones. In addition, the grid-cluster thermal zoning method gave 9 thermal zones.

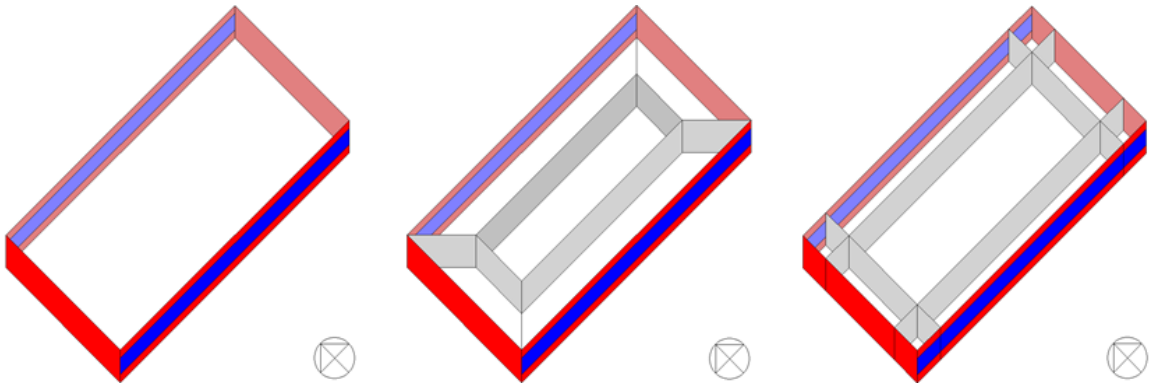

(1) 1-Zone Model (2) 5-Zone Model (3) 9-Zone Model

Figure 138: Different Zoning Models for Case 21 (Houston, TX)

Figure 139 shows the total monthly heating/cooling loads for the 1-Zone, 5-Zone, and 9-Zone thermal zoning models for Case 21 (Houston, TX). The results show that the total monthly heating/cooling loads of the 1-Zone model (i.e., the single-zone method) are mostly higher than the other thermal zoning models, except April, May, and November. In addition, the total monthly thermal loads of the 5-Zone model (i.e., the

core-perimeter method) are mostly little lower than the 9-Zone models (i.e., the grid/cluster method).

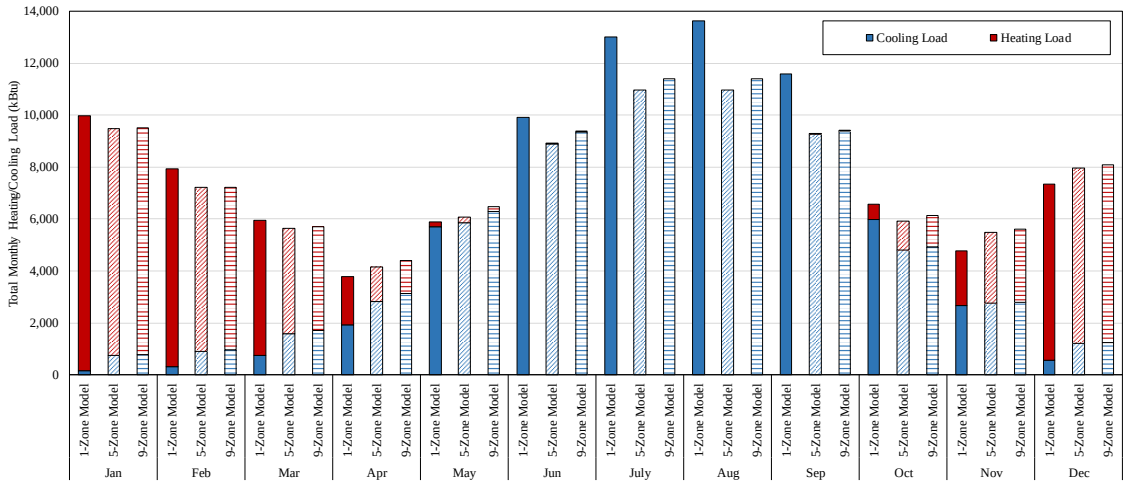

Figure 139: Total Monthly Heating/Cooling Loads for Case 21 (Houston, TX) Based on Different Zoning Methods

Figure 140 shows the total annual heating/cooling loads for the 1-Zone, 5-Zone, and 9-Zone thermal zoning models for Case 21 (Houston, TX). The results show that the 5-Zone thermal zoning model for Case 21 gave the most energy efficient thermal zoning layout among four thermal zoning strategies. In addition, this model also showed about 8% thermal load reduction compared to the 1-Zone thermal zoning model.

Table 51 shows the results of total monthly thermal loads for Case 21 (Houston, TX) with the amount of the monthly thermal load reduction. As shown in the table, the 9-Zone model has a thermal load reduction compared to the 1-Zone model, except April, May, November, and December. The grid/cluster thermal zoning method gave the highest load reduction of 19% in September, while the lowest load reduction of -18% in

November. The total annual thermal load reduction of 6% indicates that the 9-Zone thermal zoning model for the heating season has an improved energy efficiency than the 1-Zone thermal zoning model for the specific conditions of Case 21.

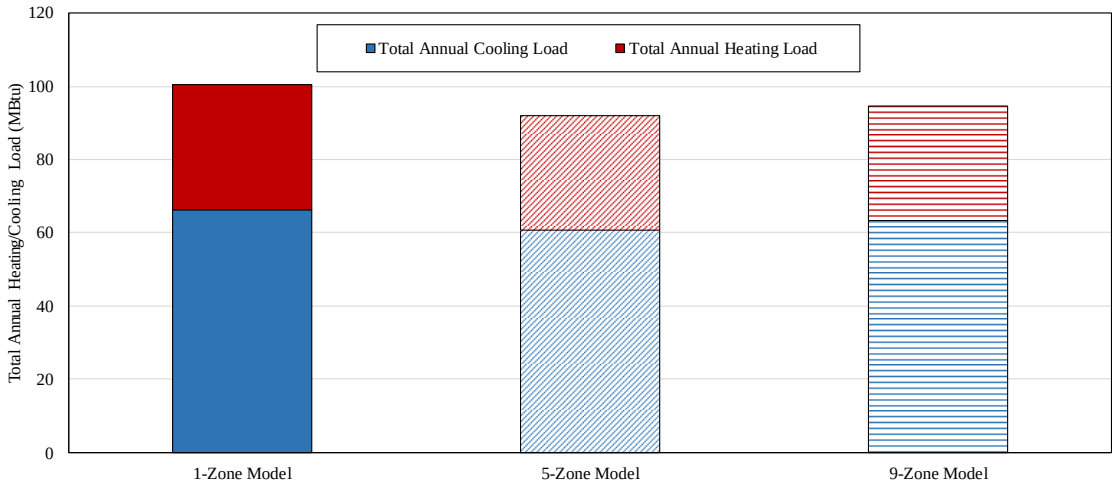

Figure 140: Total Annual Heating/Cooling Loads for Case 21 (Houston, TX) Based on Different Thermal Zoning Methods

Table 51: Comparison of Annual Thermal Loads for Case 21 (Houston, TX)

	1-Zone Model (kBtu)	**5-Zone Model (kBtu)**	**9-Zone Model (kBtu)**	**1-Zone vs. 5-Zone (kBtu)**	**1-Zone vs. 9-Zone (kBtu)**
Jan	9,983	9,490	9,499	-493 (-5%)	-484 (-5%)
Feb	7,932	7,230	7,230	-703 (-9%)	-702 (-9%)
Mar	5,942	5,658	5,694	-284 (-5%)	-248 (-4%)
Apr	3,781	4,162	4,402	381 (10%)	621 (16%)
May	5,884	6,063	6,494	179 (3%)	610 (10%)
Jun	9,919	8,904	9,347	-1,015 (-10%)	-572 (-6%)
Jul	13,014	10,964	11,383	-2,049 (-16%)	-1,630 (-13%)
Aug	13,625	10,978	11,408	-2,648 (-19%)	-2,217 (-16%)
Sep	11,597	9,280	9,421	-2,317 (-20%)	-2,176 (-19%)
Oct	6,566	5,933	6,145	-633 (-10%)	-420 (-6%)
Nov	4,784	5,492	5,627	707 (15%)	843 (18%)
Dec	7,335	7,966	8,086	631 (9%)	751 (10%)
Total	**100,362**	**92,119**	**94,737**	**-8,244 (-8%)**	**-5,626 (-6%)**

The model specification of Case 25 was summarized in Table 9 in Section 4.2.2. This case has a band of exterior window on the north- and south-facing exterior walls with WWR of 50%, and is located in Chicago, IL. Figure 141 shows the thermal zoning layouts of the different zoning models (i.e., a single-zone thermal zoning model, a core-perimeter thermal zoning model, two grid/cluster thermal zoning models) for Case 25. For Case 25, the core-perimeter thermal zoning method yielded 5 thermal zones. In addition, the grid-cluster thermal zoning method gave two simulation models: one for summer (i.e., 9-Zone Model) and the other for winter (i.e., 12-Zone Model).

Figure 142 shows the total monthly heating/cooling loads for the 1-Zone, 5-Zone, 9-Zone, and 11-Zone thermal zoning models for Case 25 (Chicago, IL). The results show that the total monthly heating/cooling loads of the 1-Zone model (i.e., the single-zone method) are mostly higher than the other thermal zoning models, except June, July, August, September, and October. In addition, the total monthly thermal loads of the 5-Zone (i.e., the core-perimeter method), 9-Zone (i.e., the grid/cluster method for cooling season), 11-Zone models (i.e., the grid/cluster method for heating season) are very similar each other throughout the year.

Figure 143 shows the total annual heating/cooling loads for the 1-Zone, 5-Zone, 9-Zone, and 12-Zone thermal zoning models for Case 25 (Chicago, IL). The results show that the 12-Zone thermal zoning model for Case 25 gave the most energy efficient thermal zoning layout among four thermal zoning strategies. In addition, this model also showed about 18% thermal load reduction compared to the 1-Zone thermal zoning model.

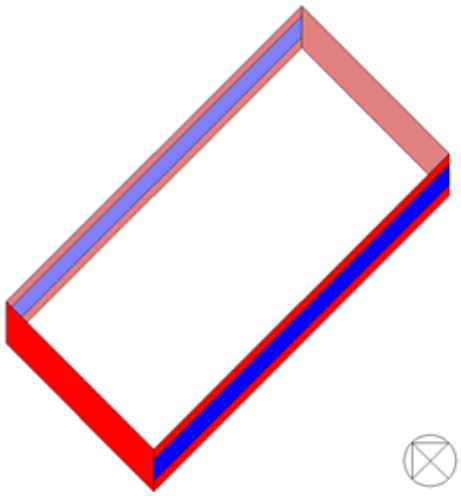

(1) 1-Zone Model

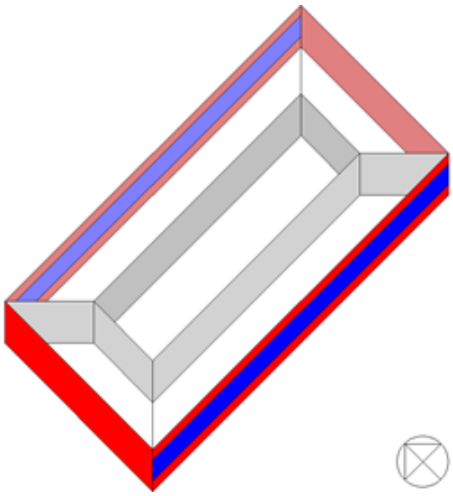

(2) 5-Zone Model

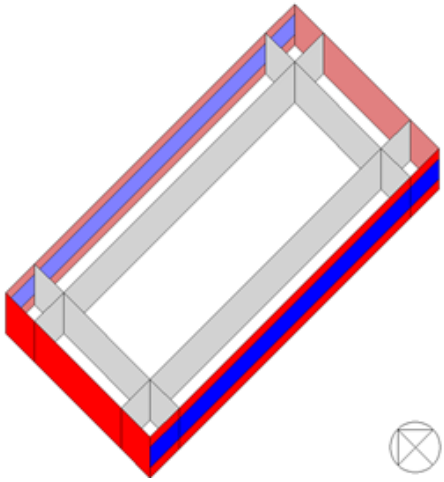

(3) 9-Zone Model (for Summer)

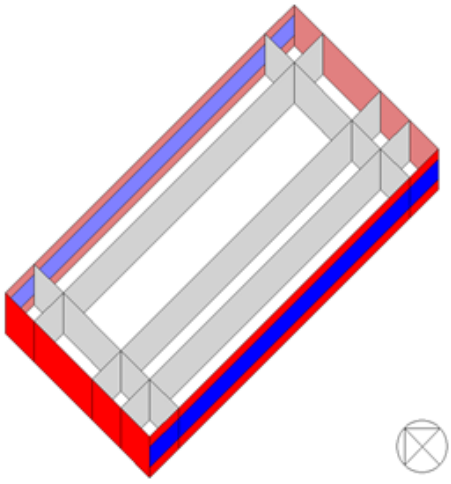

(4) 12-Zone Model (for Winter)

Figure 141: Different Zoning Models for Case 25 (Chicago, IL)

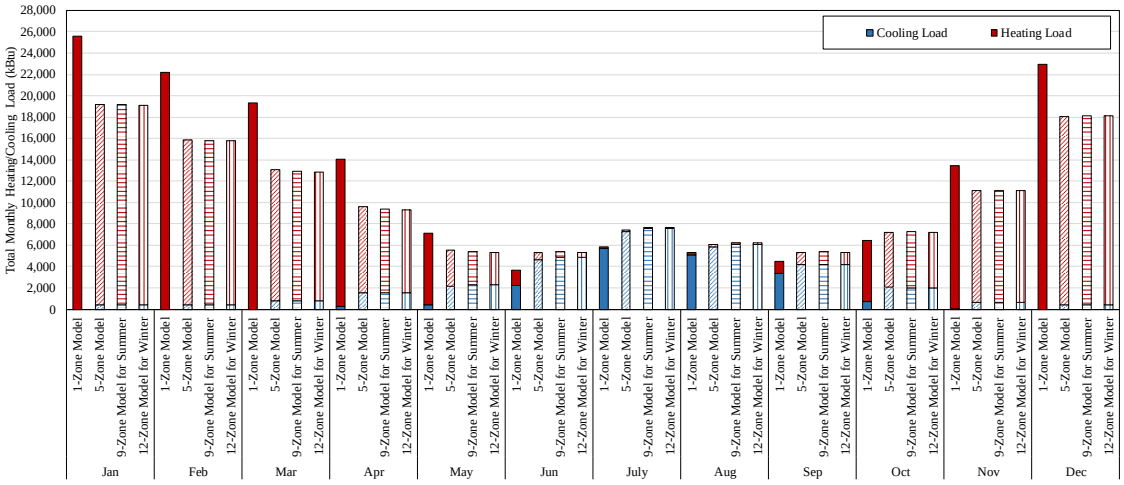

Figure 142: Total Monthly Heating/Cooling Loads for Case 25 (Chicago, IL) Based on Different Zoning Methods

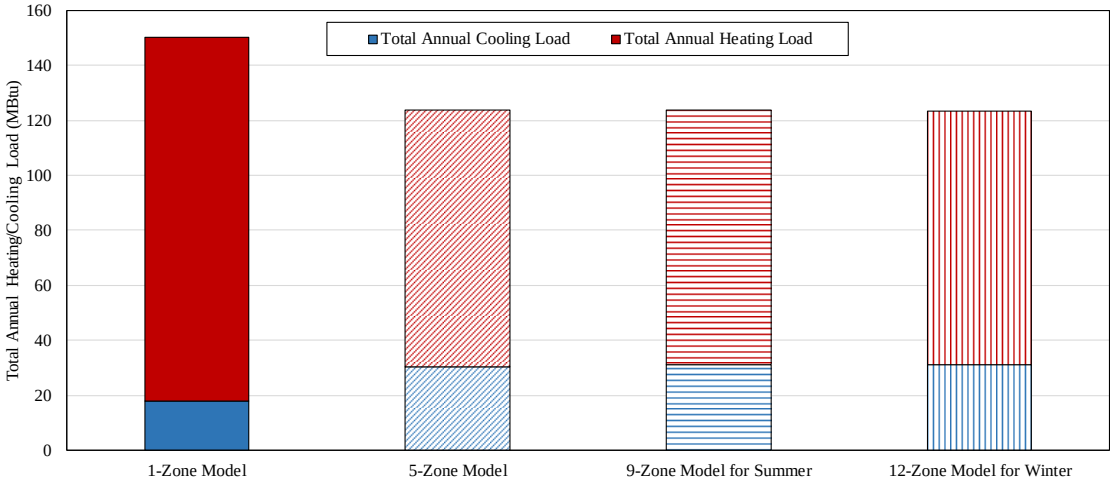

Figure 143: Total Annual Heating/Cooling Loads for Case 25 (Chicago, IL) Based on Different Thermal Zoning Methods

Table 52 shows the results of monthly total thermal loads for Case 25 (Chicago, IL) with the amount of the monthly thermal load reduction. As shown in the table, the 12-Zone model has a thermal load reduction compared to the 1-Zone model, except June, July, August, September, and October. The grid/cluster thermal zoning method

gave the highest load reduction of 34% in April, while the lowest load reduction of -46% in June. The total annual thermal load reduction of 18% indicates that the 12-Zone thermal zoning model for the heating season has an improved energy efficiency than the 1-Zone thermal zoning model for the specific conditions of Case 25.

Table 52: Comparison of Annual Thermal Loads for Case 25 (Chicago, IL)

	1-Zone Model (kBtu)	**5-Zone Model (kBtu)**	**9-Zone Model for Summer (kBtu)**	**12-Zone Model for Winter (kBtu)**	**1-Zone vs. 5 Zone (kBtu)**	**1-Zone vs. 9-Zone for Summer (kBtu)**	**1-Zone vs. 12-Zone for Winter (kBtu)**
Jan	25,592	19,172	19,187	19,130	-6,420 (-25%)	-6,405 (-25%)	-6,462 (-25%)
Feb	22,221	15,875	15,822	15,771	-6,346 (-29%)	-6,399 (-29%)	-6,450 (-29%)
Mar	19,298	13,051	12,907	12,844	-6,247 (-33%)	-6,391 (-33%)	-6,454 (-33%)
Apr	14,020	9,581	9,360	9,289	-4,439 (-32%)	-4,660 (-33%)	-4,731 (-34%)
May	7,150	5,537	5,377	5,311	-1,613 (-23%)	-1,773 (-25%)	-1,839 (-26%)
Jun	3,662	5,311	5,397	5,352	1,649 (45%)	1,735 (45%)	1,690 (46%)
Jul	5,881	7,417	7,615	7,614	1,537 (26%)	1,735 (30%)	1,733 (29%)
Aug	5,289	6,081	6,229	6,214	792 (15%)	939 (18%)	925 (17%)
Sep	4,488	5,321	5,366	5,339	833 (19%)	878 (20%)	851 (19%)
Oct	6,455	7,220	7,249	7,230	764 (12%)	794 (12%)	775 (12%)
Nov	13,423	11,081	11,128	11,090	-2,341 (-17%)	-2,295 (-17%)	-2,332 (-17%)
Dec	22,913	18,055	18,134	18,094	-4,858 (-21%)	-4,779 (-21%)	-4,819 (-21%)
Total	**150,392**	**123,704**	**123,770**	**123,277**	**-26,688 (-18%)**	**-26,622 (-18%)**	**-27,115 (-18%)**

5.2.2.8.Case 22 (Houston, TX) vs. Case 26 (Chicago, IL)

Figure 144 shows the 3D images of building geometry for Case 22 and Case 26 models. The simulation models for these cases have a window band on the exterior walls facing North and South. In addition, it should be noted that the windows mounted for these cases have a width of 50 ft and are located on the East side of each wall. All the other exterior walls facing east and West were windowless. Using the same geometry for all models, for this analysis the Houston TMY3 weather file was used for the Case 22 model, while the Chicago TMY3 weather file was used for the Case 26 model. The grid/cluster thermal zoning method was applied to these two case models, and the variations of the thermal zoning layouts were compared. In the analysis, the simulated annual/monthly, heating/cooling loads for the single zone, the core-perimeter, the grid/cluster zoning models for the cases were compared and analyzed.

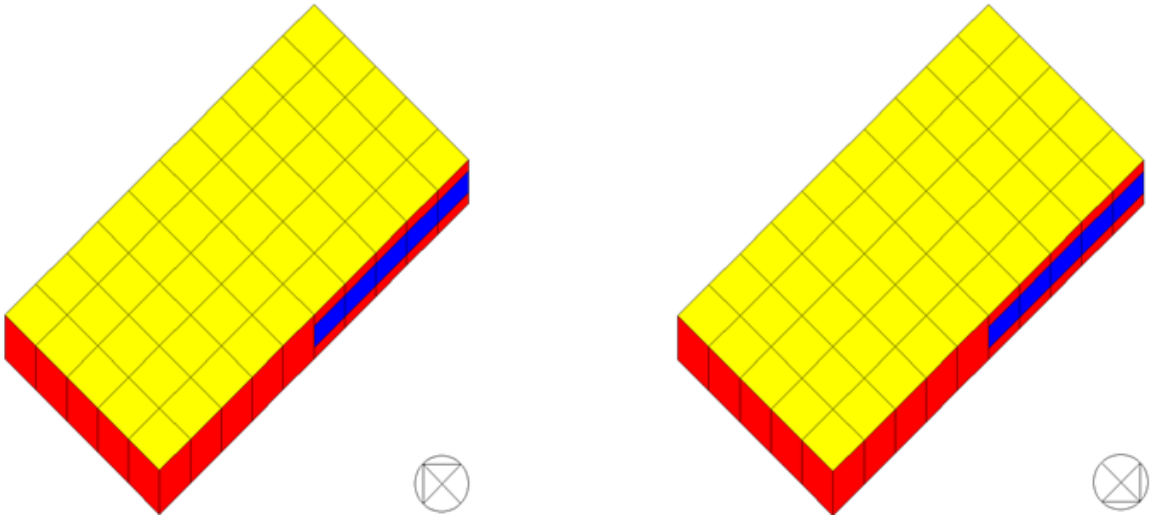

(a) Southwest View (b) Northeast View

Figure 144: View of Case 22 and Case 26 Models in the Simulation

Table 53 presents the common features of the Case 22 and Case 26 models along with the thermal zoning layouts of the Case 22 and Case 26 models for the cooling and heating season. The results show that there is a similarity in the thermal zoning layouts between the Case 22 and Case 26 models. For the cooling season models, the grid/cluster thermal zoning method gave the same results for the interior spaces with one that follows the traditional core-perimeter thermal zoning method. The both models were given one single thermal zone for the interior spaces. For the perimeter spaces, the grid/cluster thermal zoning method divided the building into two different thermal zones for the south-side zones, where the windows were located (i.e., south-side) for Case 26. However, the thermal zoning layout of the perimeter space for Case 22 was followed the traditional core-perimeter thermal zoning method, which consist of four different perimeter spaces along with each orientation. For the heating season models, the interior spaces were divided into two different thermal zones, respectively. One of the interior thermal zones was created near the window location (i.e., south-side) for both cases. For the perimeter spaces facing east and south were given two different thermal zones, respectively. The perimeter spaces facing other orientations (i.e., north, west) were given one single thermal zone in a similar fashion with the traditional core-perimeter thermal zoning layout.

The model specification of Case 22 was summarized in Table 9 in Section 4.2.2. This case has two exterior windows, which has width of 50 ft, at the right corner of the north- and south-facing exterior walls with WWR of 50%, and is located in Houston, TX. Figure 145 shows the thermal zoning layouts of the different zoning models (i.e., a

single-zone thermal zoning model, a core-perimeter thermal zoning model, a grid/cluster thermal zoning model) for Case 22. For Case 22, the core-perimeter thermal zoning method yielded 5 thermal zones. In addition, the grid-cluster thermal zoning method gave two simulation models: one for summer (i.e., 9-Zone Model) and the other for winter (i.e., 10-Zone Model).

Table 53: Results of Thermal Zoning for the Case 22 (Houston) and Case 26 (Chicago)

	Case 22 (Houston)	**Case 26 (Chicago)**
Summary of Parameters	• Location: Houston, TX • Floor type: Slab-on-grade • WWR: 50 %, North-South offset • Floor area: 5,000 ft^2 • Number of thermal zone: 50	• Location: Chicago, IL • Floor type: Slab-on-grade • WWR: 50 %, North-South offset • Floor area: 5,000 ft^2 • Number of thermal zone: 50
Cooling Season	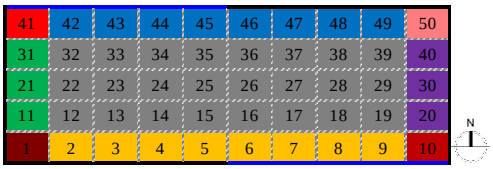	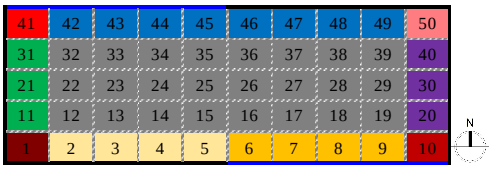
Heating Season	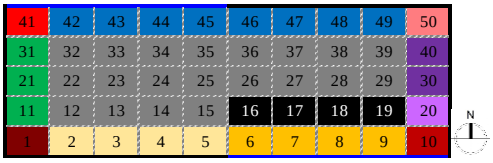	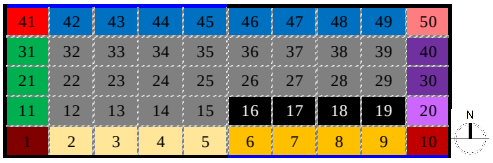

Figure 146 shows the total monthly heating/cooling loads for the 1-Zone, 5-Zone, 9-Zone, and 10-Zone thermal zoning models for Case 22 (Houston, TX). The results show that the total monthly heating/cooling loads of the 1-Zone model (i.e., the single-zone method) are mostly higher than other thermal zoning models, except April, May, November, and December. In addition, the total monthly thermal loads of the 5-Zone

(i.e., the core-perimeter method), 9-Zone (i.e., the grid/cluster method for cooling season), 10-Zone models (i.e., the grid/cluster method for heating season) are very similar each other throughout the year.

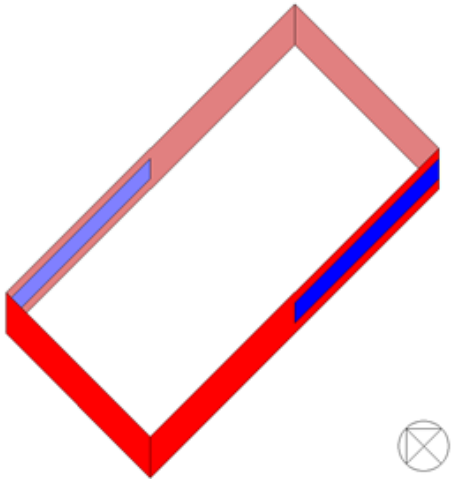

(1) 1-Zone Model

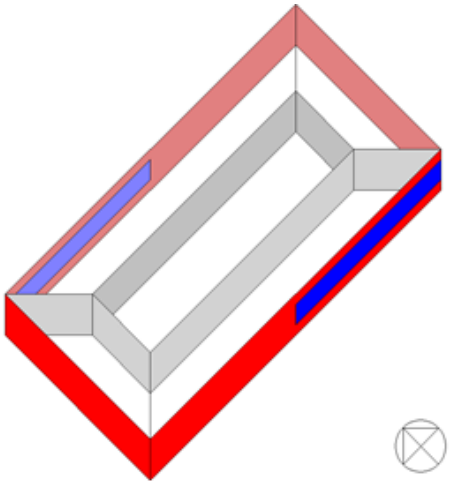

(2) 5-Zone Model

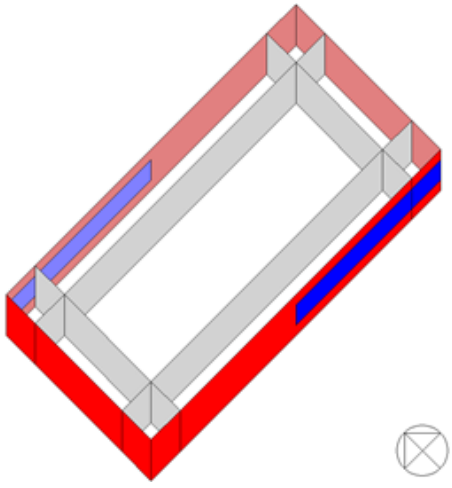

(3) 9-Zone Model (for Summer)

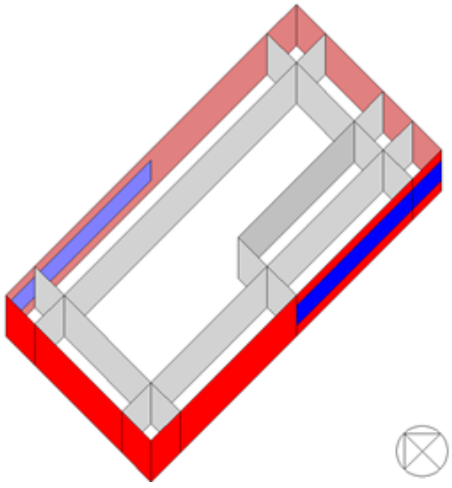

(4) 10-Zone Model (for Winter)

Figure 145: Different Zoning Models for Case 22 (Houston, TX)

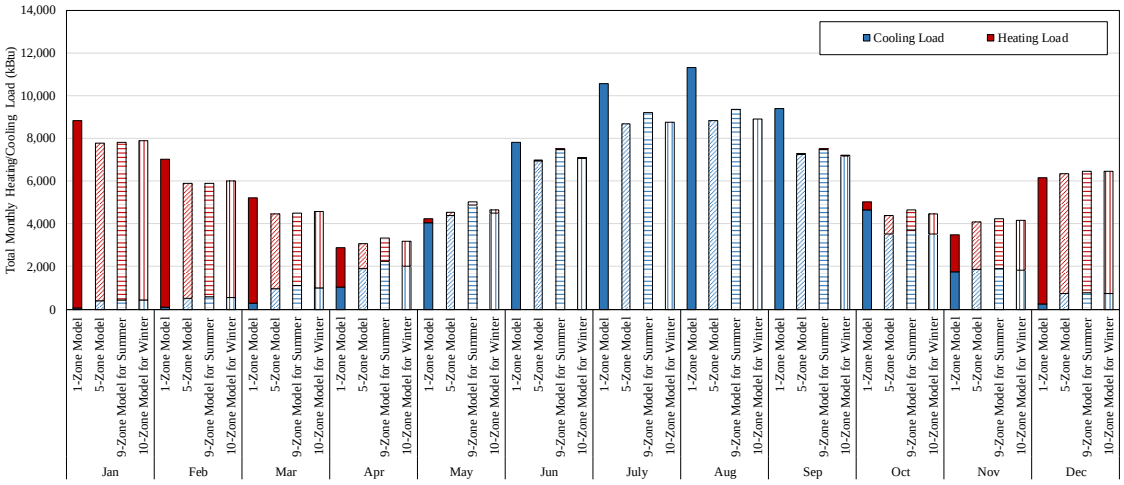

Figure 146: Total Monthly Heating/Cooling Loads for Case 22 (Houston, TX) Based on Different Zoning Methods

Table 54 shows the results of total monthly thermal loads for Case 22 (Houston, TX) with the amount of the monthly thermal load reduction. As shown in the table, the 10-Zone model has a thermal load reduction compared to the 1-Zone model, except April, May, November, and December. The grid/cluster thermal zoning method gave the highest load reduction of 24% in September, while the lowest load reduction of -19% in November. The total annual thermal load reduction of 11% indicates that the 10-Zone thermal zoning model for the heating season has an improved energy efficiency than the 1-Zone thermal zoning model for the specific conditions of Case 22.

Figure 147 shows the total annual heating/cooling loads for the 1-Zone, 5-Zone, 9-Zone, and 10-Zone thermal zoning models for Case 22 (Houston, TX). The results show that the 5-Zone thermal zoning model for Case 22 gave the most energy efficient thermal zoning layout among four thermal zoning strategies. In addition, this model also showed about 12% thermal load reduction compared to 1-Zone thermal zoning model.

Table 54: Comparison of Annual Thermal Loads for Case 22 (Houston, TX)

	1-Zone Model (kBtu)	5-Zone Model (kBtu)	9-Zone Model for Summer (kBtu)	10-Zone Model for Winter (kBtu)	1-Zone vs. 5 Zone (kBtu)	1-Zone vs. 9-Zone for Summer (kBtu)	1-Zone vs. 10-Zone for Winter (kBtu)
Jan	8,852	7,784	7,819	7,893	-1,068 (-12%)	-1,033 (-12%)	-959 (-11%)
Feb	7,030	5,892	5,898	6,000	-1,137 (-16%)	-1,131 (-16%)	-1,030 (-15%)
Mar	5,225	4,478	4,514	4,576	-746 (-14%)	-710 (-14%)	-648 (-12%)
Apr	2,896	3,075	3,333	3,189	178 (6%)	437 (15%)	293 (10%)
May	4,234	4,545	5,034	4,649	311 (7%)	800 (19%)	416 (10%)
Jun	7,802	6,958	7,483	7,059	-844 (-11%)	-319 (-4%)	-743 (-10%)
Jul	10,552	8,686	9,201	8,763	-1,865 (-18%)	-1,350 (-13%)	-1,788 (-17%)
Aug	11,322	8,834	9,358	8,915	-2,488 (-22%)	-1,963 (-17%)	-2,407 (-21%)
Sep	9,416	7,257	7,478	7,201	-2,159 (-23%)	-1,939 (-21%)	-2,215 (-24%)
Oct	5,038	4,400	4,653	4,451	-637 (-13%)	-384 (-8%)	-586 (-12%)
Nov	3,494	4,088	4,245	4,173	594 (17%)	750 (21%)	679 (19%)
Dec	6,160	6,351	6,479	6,480	191 (3%)	319 (5%)	320 (5%)
Total	**82,019**	**72,348**	**75,495**	**73,350**	**-191,128 (-12%)**	**-6,524 (-8%)**	**-8,669 (-11%)**

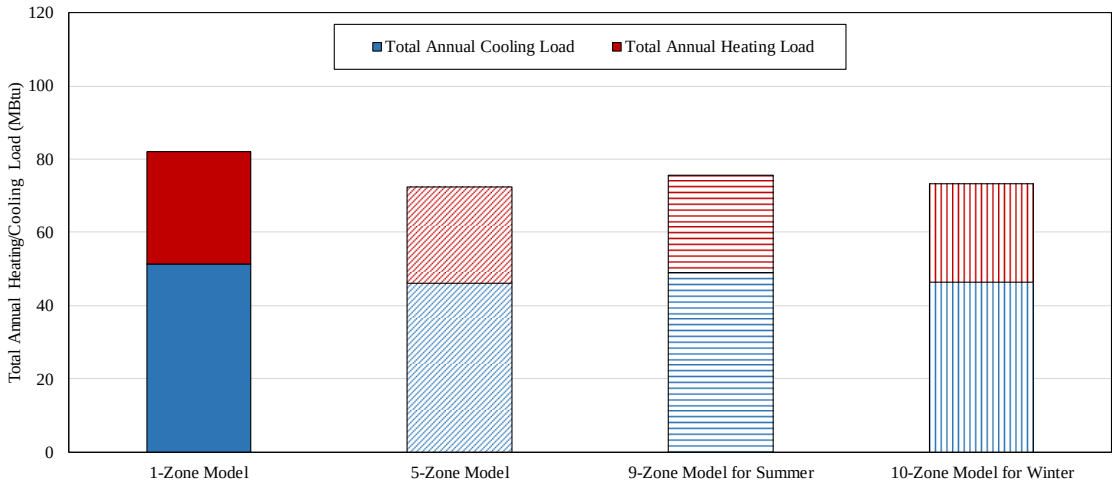

Figure 147: Total Annual Heating/Cooling Loads for Case 22 (Houston, TX) Based on Different Thermal Zoning Methods

The model specification of Case 26 was summarized in Table 9 in Section 4.2.2. This case has two exterior windows, which has width of 50 ft, at the right corner of the north- and south-facing exterior walls with WWR of 50%, and is located in Chicago, IL. Figure 148 shows the thermal zoning layouts of the different zoning models (i.e., a single-zone thermal zoning model, a core-perimeter thermal zoning model, a grid/cluster thermal zoning model) for Case 26. For Case 26, the core-perimeter method yielded 5 thermal zones. In addition, the grid-cluster thermal zoning method gave two simulation models: one for summer (i.e., 10-Zone Model) and the other for winter (i.e., 12-Zone Model).

Figure 149 shows the monthly total heating/cooling loads for 1-Zone, 5-Zone, 10-Zone, 12-Zone thermal zoning models for the Case 26. The results show that the monthly total heating/cooling loads of the 1-Zone model (i.e., the single-zone method) are mostly higher than other thermal zoning models, except June, July, August, and

September. In addition, the monthly total thermal loads of the 5-Zone (i.e., the core-perimeter method), 10-Zone (i.e., the grid/cluster method for cooling season), 12-Zone models (i.e., the grid/cluster method for heating season) are very similar each other throughout the year.

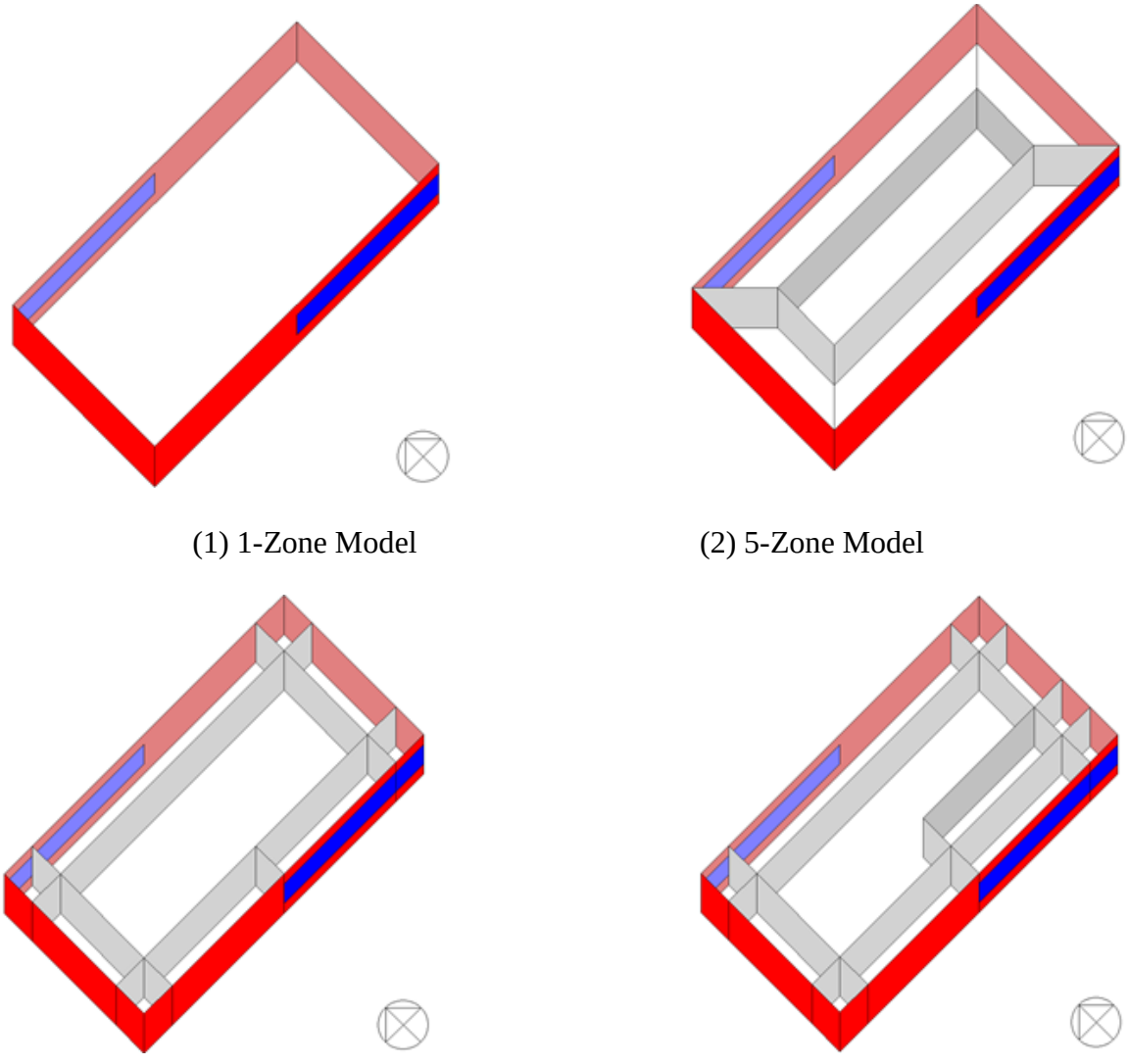

(1) 1-Zone Model (2) 5-Zone Model

(3) 10-Zone Model (for Summer) (4) 12-Zone Model (for Winter)

Figure 148: Different Zoning Models for Case 26 (Chicago, IL)

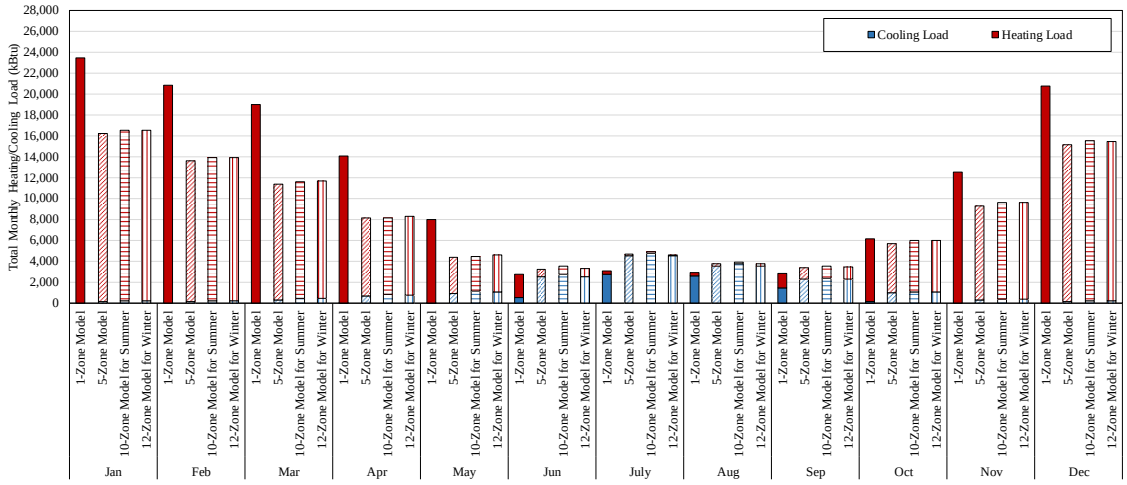

Figure 149: Total Monthly Heating/Cooling Load for Case 26 (Chicago, IL) Based on Different Zoning Methods

Table 55 shows the results of total monthly thermal loads for Case 26 (Chicago, IL) with the amount of the monthly thermal load reduction. As shown in the table, the 12-Zone model has a thermal load reduction compared to the 1-Zone model, except June, July, August, and September. The grid/cluster thermal zoning method gave the highest load reduction of 42% in May, while the lowest load reduction of -50% in July. The total annual thermal load reduction of 26% indicates that the 12-Zone thermal zoning model for the heating season has an improved energy efficiency than the 1-Zone thermal zoning model for the specific conditions of Case 26.

Figure 150 shows the total annual heating/cooling loads for the 1-Zone, 5-Zone, 10-Zone, and 12-Zone thermal zoning models for Case 26 (Chicago, IL). The results show that the 5-Zone thermal zoning model for Case 26 gave the most energy efficient thermal zoning layout among four thermal zoning strategies. In addition, this model also

showed about 27% thermal load reduction compared to the 1-Zone thermal zoning model.

Table 55: Comparison of Annual Thermal Loads for Case 26 (Chicago, IL)

	1-Zone Model (kBtu)	**5-Zone Model (kBtu)**	**10-Zone Model for Summer (kBtu)**	**12-Zone Model for Winter (kBtu)**	**1-Zone vs. 5 Zone (kBtu)**	**1-Zone vs. 10-Zone for Summer (kBtu)**	**1-Zone vs. 12-Zone for Winter (kBtu)**
Jan	23,421	16,224	16,549	16,528	-7,197 (-31%)	-6,871 (-29%)	-6,893 (-29%)
Feb	20,827	13,615	13,876	13,911	-7,212 (-35%)	-6,952 (-33%)	-6,917 (-33%)
Mar	18,958	11,363	11,575	11,694	-7,594 (-40%)	-7,382 (-39%)	-7,263 (-38%)
Apr	14,043	8,090	8,161	8,279	-5,953 (-42%)	-5,882 (-42%)	-5,763 (-41%)
May	7,945	4,322	4,422	4,583	-3,623 (-46%)	-3,523 (-44%)	-3,361 (-42%)
Jun	2,711	3,210	3,471	3,315	499 (18%)	760 (28%)	604 (22%)
Jul	3,074	4,632	4,875	4,612	1,558 (51%)	1,801 (59%)	1,538 (50%)
Aug	2,889	3,751	3,931	3,735	863 (30%)	1,042 (36%)	846 (29%)
Sep	2,799	3,385	3,496	3,464	586 (21%)	697 (25%)	665 (24%)
Oct	6,112	5,638	5,935	5,969	-474 (-8%)	-177 (-3%)	-143 (-2%)
Nov	12,516	9,286	9,579	9,563	-3,231 (-26%)	-2,938 (-23%)	-2,953 (-24%)
Dec	20,717	15,134	15,493	15,434	-5,583 (-27%)	-5,224 (-25%)	-5,283 (-26%)
Total	**136,011**	**98,650**	**101,362**	**101,088**	**-37,361 (-27%)**	**-34,649 (-25%)**	**-34,923 (-26%)**

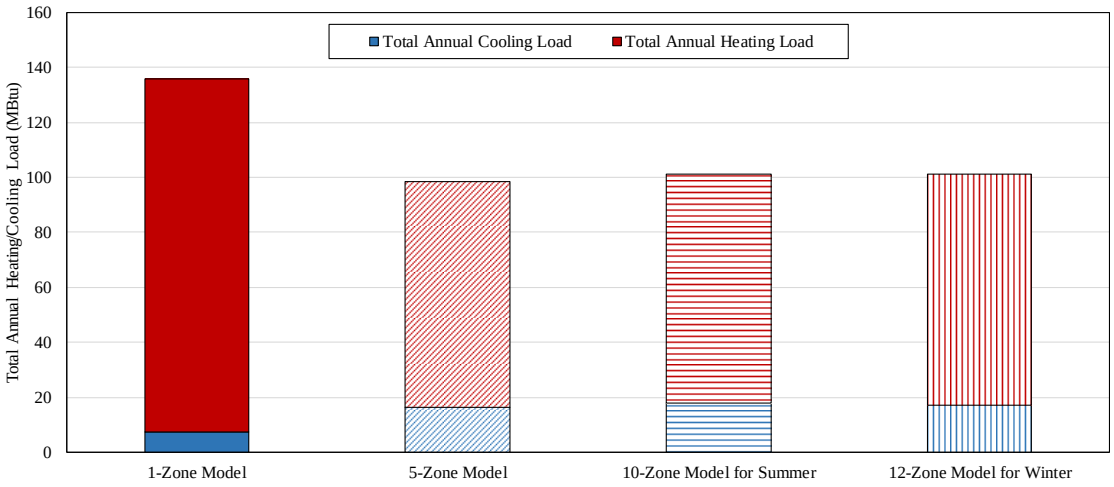

Figure 150: Total Annual Heating/Cooling Loads for Case 26 (Chicago, IL) Based on Different Thermal Zoning Methods

5.2.3. Summary of Parametric Study of Thermal Zoning on WWR

In this section, the parametric study using 11 combinations of WWR and orientations was performed for two climate conditions (i.e., Houston, TX and Chicago, IL) to investigate the impact of the building WWR and the orientations of the exterior windows on the building thermal zoning and the annual/monthly heating/cooling loads.

To investigate the impacts of the WWR on the building thermal zoning layouts, three different WWRs (i.e., 0%, 50%, 80%) were applied to the simulation models. The results showed that when the WWR were set to 0%, which means there is no windows in the model, the thermal zoning layouts were created as similar as the 5-Zone models (i.e., the traditional core-perimeter thermal zoning layouts). However, if the WWRs were increased to 50% or 80%, the interior thermal zone was separated into two different thermal zones. The shape and area of the interior thermal zones of the models with WWR of 50% and 80% were very similar each other, regardless of the climate

conditions. For the perimeter thermal zones, mostly the layouts consisted of four different perimeter thermal zones along with each orientation. However, for the thermal zoning layouts for heating season for the cold climate condition (i.e., Chicago, IL), the grid/cluster thermal zoning method gave some variations in the east-facing perimeter zones, which were given two different thermal zones.

To investigate the impacts of the orientation/position changes of the window on the building thermal zoning and its heating/cooling load, 8 different cases for two climate conditions (i.e., Houston, TX, Chicago, IL) were used for the parametric study.

The results showed that when the building has windows facing east or south, the thermal zoning layouts were created differently, compare to the 5-Zone models (i.e., the traditional core-perimeter thermal zoning method). The thermal zones for both the perimeter and interior spaces tended to be created along with the location of the windows. However, it was appeared that when the building has windows facing north and west, there was little impacts on the thermal zoning layouts. It resulted in similar thermal zoning layouts with the core-perimeter thermal zoning layouts.

Figure 151 shows the comparison of the simulated annual total heating/cooling loads between two climate conditions (i.e., Houston, TX and Chicago, IL) by the orientations of the windows. In general, the annual total and heating loads of the thermal zoning models for Chicago were higher than ones for Houston. In addition, for each climate condition, the models have the windows in north-south orientations had the highest annual total heating/cooling loads. On the contrary, the models have windows in north or west orientation had the lowest annual total heating/cooling loads.

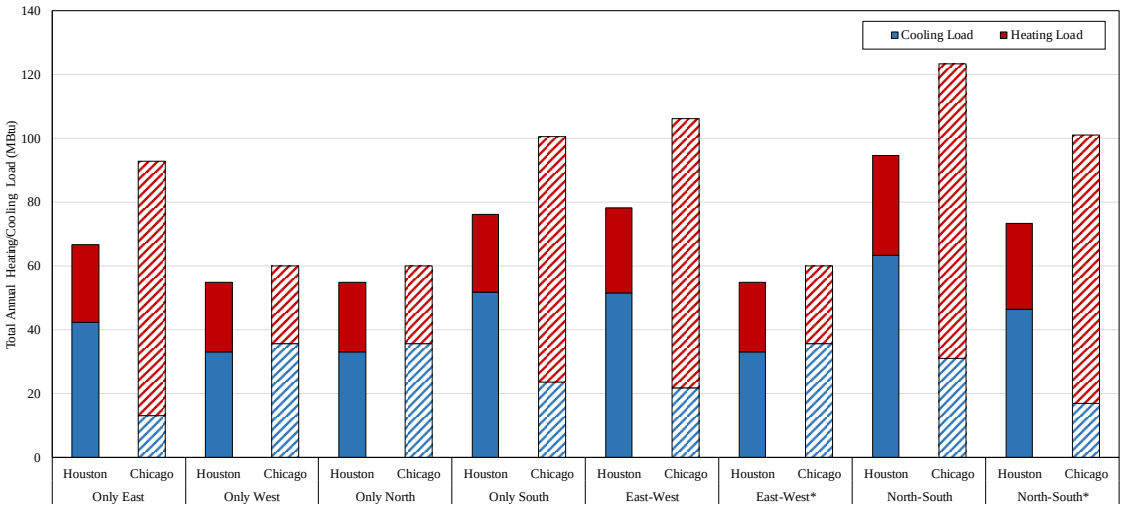

Figure 151: Comparison of Annual Heating/Cooling Loads between Two Climate Conditions by Orientations of Windows

Table 56 and Table 57 shows the comparisons of annual total thermal loads reductions between the single zone models and grid/cluster thermal zoning models by different orientations of the windows for Houston and Chicago, respectively. These results show how much thermal load reduction was achieved when the grid/cluster thermal zoning method was applied to each case compared to single-zone model. All the cases could have positive thermal load reduction with the thermal zoning layout, which used the grid/cluster thermal zoning method. In addition, comparing the orientations of the windows, for the rectangle-shape models, about 3 to 6% more annual total thermal loads were reduced than the L-shape models.

For Houston, the highest annual thermal loads reduction (15%) was shown in Case 11, where the window orientation was only east. In the contrary, the lowest annual thermal loads reduction (6%) was shown in Case 21, where the window orientation was north-south.

For Chicago, the highest annual thermal loads reduction (30%) was shown in Case 10, Case 12, and Case 20, where the window orientations were only west, only east, and east-west. In the contrary, the lowest annual thermal loads reduction (10%) were shown in Case 16, Case 17, and Case 24, where the window orientation were only west, only north, and east-west.

Table 56: Comparison of Annual Total Thermal Load for Houston, TX

Case #	Orientation of Window	Single Zone Method (Btu)	Grid/Cluster Method (Btu)	Load Reduction (Btu)	Load Reduction (%)
Case 10	Only East	75,649,356	66,591,678	9,057,679	12%
Case 11	Only West	64,761,931	55,057,989	9,703,942	15%
Case 12	Only North	64,761,931	55,057,989	9,703,942	15%
Case 13	Only South	82,029,324	76,286,362	5,742,962	7%
Case 19	East-West	86,956,940	78,161,312	8,795,629	10%
Case 20*	East-West	64,761,931	55,057,989	9,703,942	15%
Case 21	North-South	100,362,385	94,736,769	5,625,615	6%
Case 22*	North-South	82,019,134	73,349,948	8,669,187	11%

*: The windows of this case were installed on a half of the exterior walls.

Table 57: Comparison of Annual Total Thermal Load for Chicago, IL

Case #	Orientation of Window	Single Zone Method (Btu)	Grid/Cluster Method (Btu)	Load Reduction (Btu)	Load Reduction (%)
Case 15	Only East	132,265,883	92,949,711	39,316,172	30%
Case 16	Only West	66,979,781	60,423,308	6,556,474	10%
Case 17	Only North	66,979,781	60,423,308	6,556,474	10%
Case 18	Only South	128,244,779	100,508,440	27,736,339	22%
Case 23	East-West	139,607,331	106,131,715	33,475,616	24%
Case 24*	East-West	66,979,781	60,423,308	6,556,474	10%
Case 25	North-South	150,391,647	123,276,761	27,114,886	18%
Case 26*	North-South	136,010,771	101,087,722	34,923,049	26%

*: The windows of this case were installed on a half of the exterior walls.

5.3. Analysis of the Impact of Climate Condition on Thermal Zoning

In this section, how the climate conditions impact on the building thermal zoning in a simulation were examined. As mentioned earlier, two different climate conditions (i.e., Houston, TX and Chicago, IL) were chosen and corresponding weather files used for the simulation models that have the identical geometric information. The detail model specification is shown in Table 9 in Section 4.2.2. The thermal zoning layouts, which were created using the grid/cluster thermal zoning method, and those were compared under the two climate conditions. In addition, the simulated annual/monthly heating/cooling loads for each case were compared and examined.

Figure 152 shows the variation of monthly average outdoor dry-bulb temperature and global solar radiation of two cities. These climatic data was extracted from TMY3 weather data for two locations. The original format of the data was hourly based information, so it was converted to daily and monthly data. Two cities representing different climate zones defined by ASHRAE (Baechler et al. 2010) in the US: Houston (i.e., Zone 2A: hot and humid) and Chicago (i.e., Zone 5A: Cold and Humid).

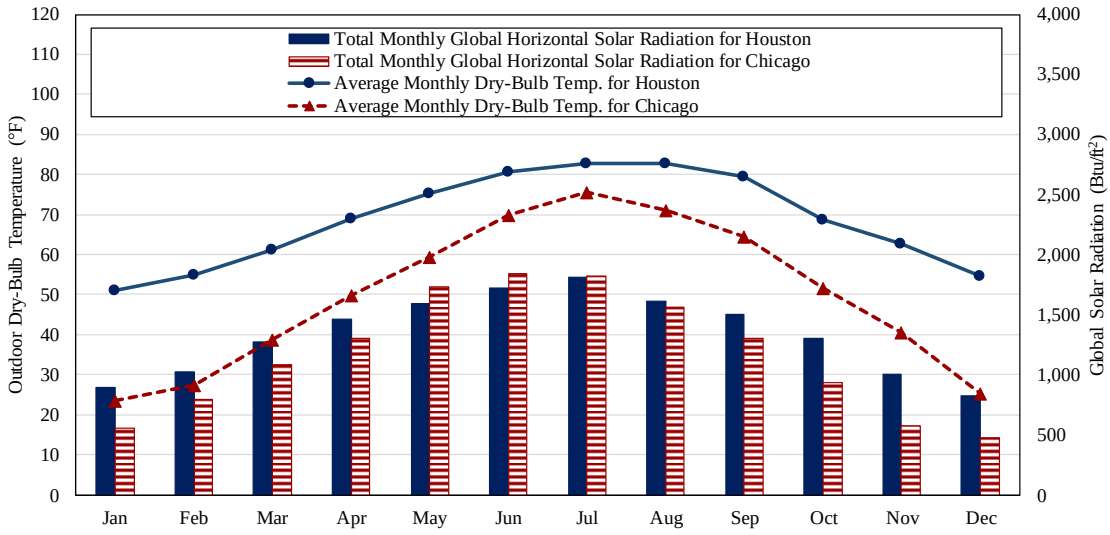

Figure 152: Monthly Average Outdoor Dry-Bulb Temperature and Global Solar Radiation for the Two Locations (i.e., Houston and Chicago)

5.3.1. Comparison of Thermal Zoning Layout for Varying Climate Conditions

In this section, the resultant thermal zoning layouts of 12 different simulation models with two different climate conditions (i.e., Hot and Humid, Cold and Humid) were examined and compared using the grid/cluster thermal zoning method. In

Subsection 5.3.1.1, the analysis of the rectangle- and L-shape simulation models with only opaque walls (i.e., no exterior windows) is presented. In Subsection 5.3.1.2, the analysis of the rectangle- and L-shape simulation models with a horizontal band of exterior windows with the WWR of 50%. In Subsection 5.3.1.3, the analysis of the rectangle-shape simulation models with varied orientations of the exterior windows for each case. In Subsection 5.3.1.4, the analysis of the rectangle-shape simulation models with the offset exterior windows for each case.

5.3.1.1. Thermal Zoning Layouts for Simulation Models with Only Opaque Walls

The images of the building geometry for the Case 1 and Case 3 models, which are the rectangle-shape models are shown in Figure 189. In the analysis, the Houston and Chicago TMY3 weather files were used for the simulation runs for the hot and cold climates, respectively. As mentioned earlier in Section 5.1.1.1, the Case 1 and Case 3 simulation models were simulated with only opaque walls (i.e., no exterior windows). The resultant thermal zoning layouts of the Case 1 and Case 3 simulation models for the cooling and heating season are also presented in Figure 190 and Figure 155 in The resultant thermal zoning layouts show that there was no difference between the Case 1 (Houston, TX) and Case 3 (Chicago, IL) models, regardless of the heating/cooling season.

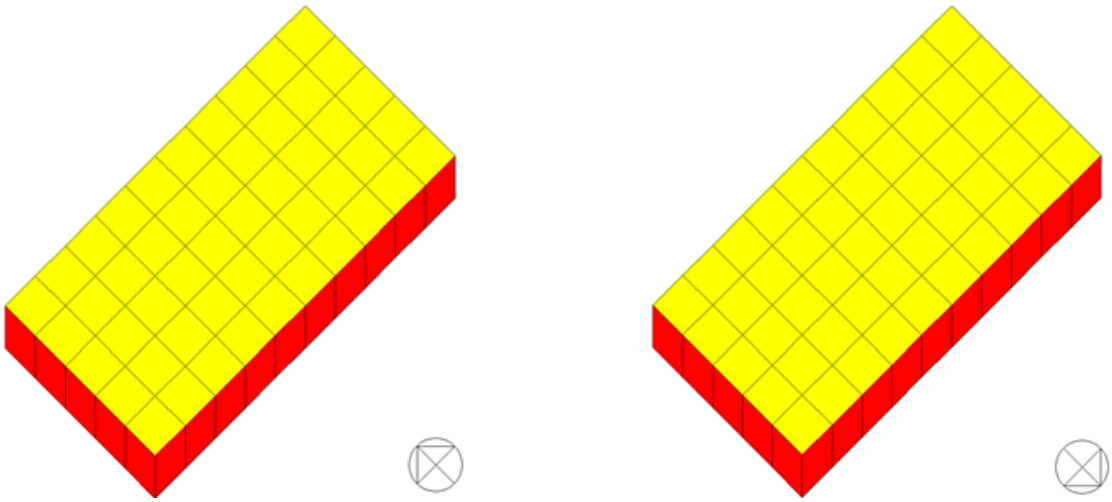

(a) Southwest View (b) Northeast View

Figure 153: View of Case 1 (Houston, TX) and Case 3 (Chicago, IL) Models in the Simulation (w/o windows)

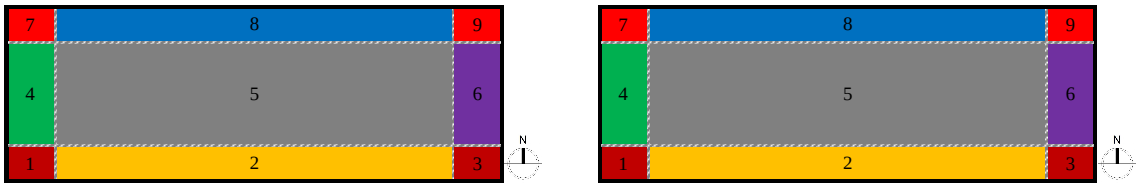

(a) For Cooling Season (b) For Heating Season

Figure 154: Resultant Thermal Zoning Layouts for Case 1 (Houston, TX)

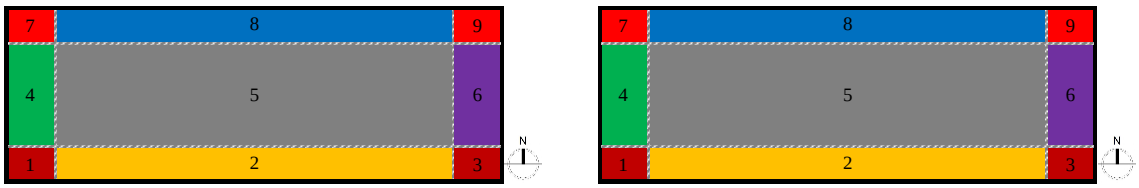

(a) For Cooling Season (b) For Heating Season

Figure 155: Resultant Thermal Zoning Layouts for Case 3 (Chicago, IL)

The images of the building geometry for the Case 5 and Case 7 models, which are the L-shape models are shown in Figure 192. In the analysis, the Houston and Chicago TMY3 weather files were used for the simulation runs for the hot and cold climates, respectively. As mentioned earlier in Section 5.1.1.3, the Case 5 and Case 7 simulation models were simulated with only opaque walls (i.e., no exterior windows). The resultant thermal zoning layouts of the Case 5 and Case 7 simulation models for the cooling and heating season are also presented in Figure 157 and Figure 158. The resultant thermal zoning layouts show that there was no difference between the Case 5 (Houston, TX) and Case 7 (Chicago, IL) models, regardless of the heating/cooling season.

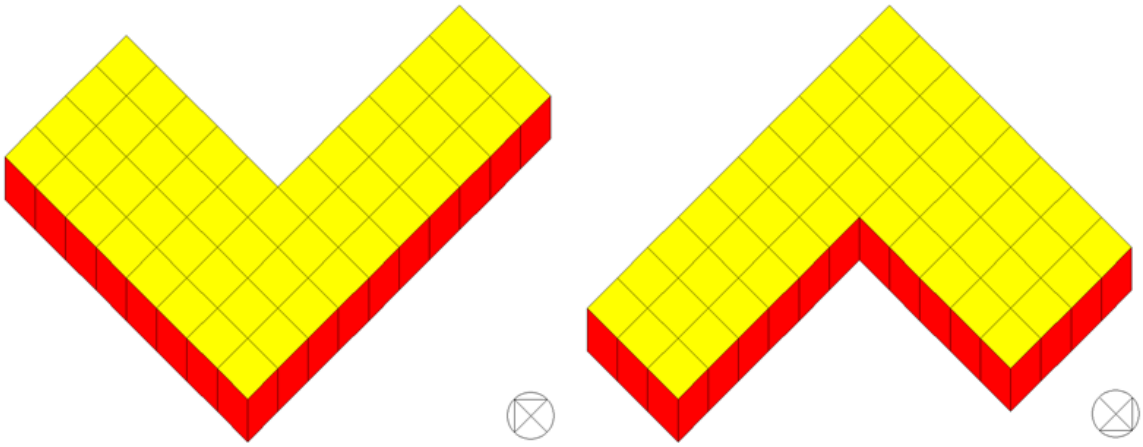

(a) Southwest View (b) Northeast View

Figure 156: View of Case 5 (Houston, TX) and Case 7 (Chicago, IL) Models in the Simulation

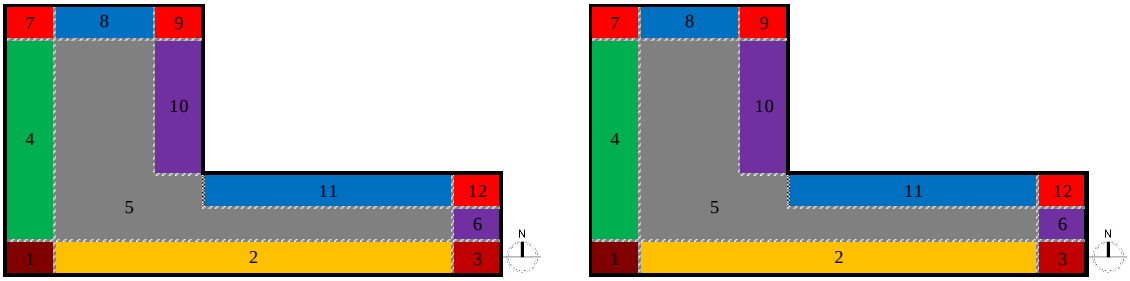

(a) For Cooling Season (b) For Heating Season

Figure 157: Resultant Thermal Zoning Layouts for Case 5 (Houston, TX)

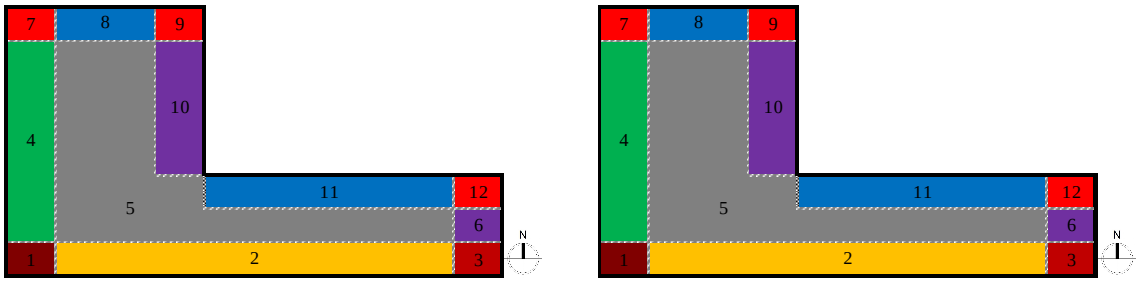

(a) For Cooling Season (b) For Heating Season

Figure 158: Resultant Thermal Zoning Layouts for Case 7 (Chicago, IL)

Table 58 shows the number of thermal zones created by the grid/cluster thermal zoning method for each simulation case with only opaque walls. For the rectangular-shape models, a total of 9 thermal zones were created for each case. For the L-Shape models, the grid/cluster thermal zoning method yielded a total of 12 thermal zones for both cases. There was no difference in number of thermal zones found between different climate conditions.

Table 58: Results of Thermal Zoning for Simulation Models with Opaque Walls

Climate	Case #	Building Shape	WWR	Number of Thermal Zones					
				East	West	North	South	Core	Total
Houston	1	Rectangle	0%	1	1	1	1	1	9
Chicago	3	Rectangle	0%	1	1	1	1	1	9
Houston	5	L-Shape	0%	2	1	2	1	1	12
Chicago	7	L-Shape	0%	2	1	2	1	1	12

5.3.1.2. Thermal Zoning Layouts for Simulation Models with Exterior Windows on All Orientations

The images of the building geometry for the Case 2 and Case 4 models, which are the rectangle-shape models are shown in Figure 195. In the analysis, the Houston and Chicago TMY3 weather files were used for the simulation runs for the hot and cold climates, respectively. As mentioned earlier in Section 5.1.1.2, the Case 2 and Case 4 simulation models have a horizontal band of exterior windows with the WWR of 50%. The resultant thermal zoning layouts of the Case 2 and Case 4 simulation models for the cooling and heating season are also presented in Figure 160 and Figure 161. The resultant thermal zoning layouts show that the interior space of both cases have two different thermal zones, and its shapes and pattern are very similar. However, it was found that the number of East-perimeter thermal zone is different based on the case.

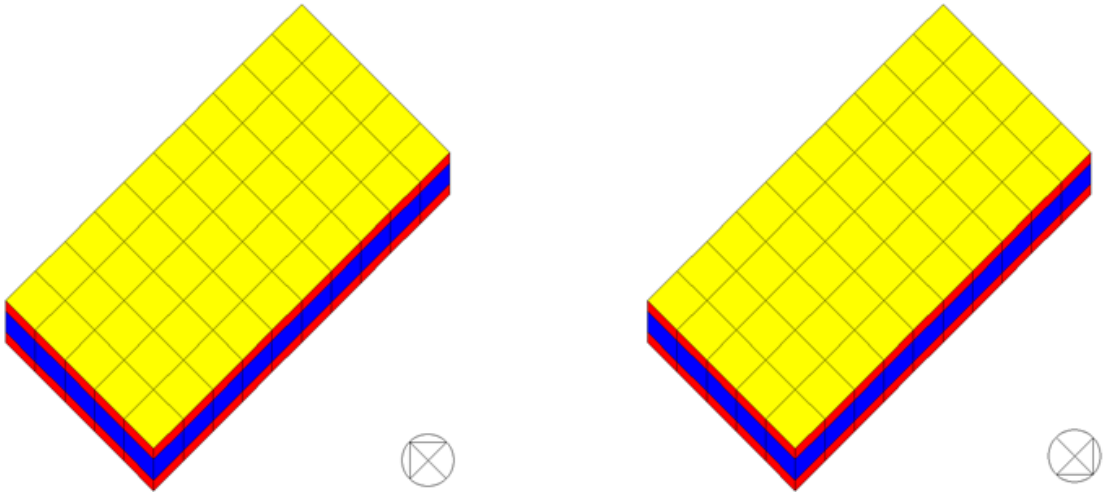

(a) Southwest View (b) Northeast View

Figure 159: View of Case 2 (Houston, TX) and Case 4 (Chicago, IL) Models in the Simulation

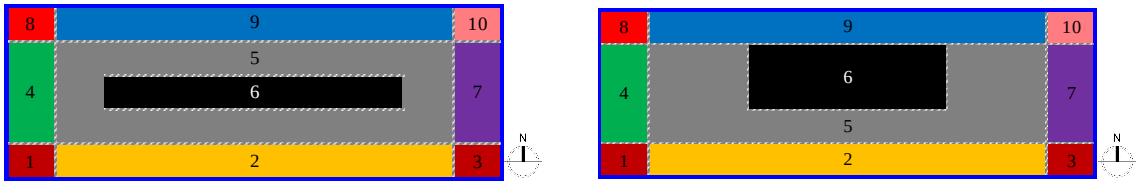

(a) For Cooling Season (b) For Heating Season

Figure 160: Resultant Thermal Zoning Layouts for Case 2 (Houston, TX)

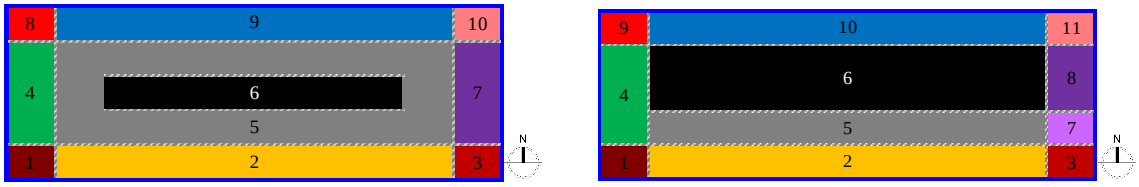

(a) For Cooling Season (b) For Heating Season

Figure 161: Resultant Thermal Zoning Layouts for Case 4 (Chicago, IL)

The images of the building geometry for the Case 6 and Case 8 models, which are the L-shape models are shown in Figure 162. In the analysis, the Houston and Chicago TMY3 weather files were used for the simulation runs for the hot and cold climates, respectively. As mentioned earlier in Section 5.1.1.4, the Case 6 and Case 8 simulation models have a horizontal band of exterior windows with the WWR of 50%. The resultant thermal zoning layouts of the Case 6 and Case 8 simulation models for the cooling and heating season are also presented in Figure 163 and Figure 164. The resultant thermal zoning layouts show that the interior space of Case 6 (Houston, TX) has one single thermal zone for summer and two thermal zones for winter thermal zoning layouts, while Case 8 (Chicago, IL) shows two interior thermal zones for both summer and winter. In addition, for heating season, the Case 6 and Case 8 have a different number of the East-perimeter thermal zones.

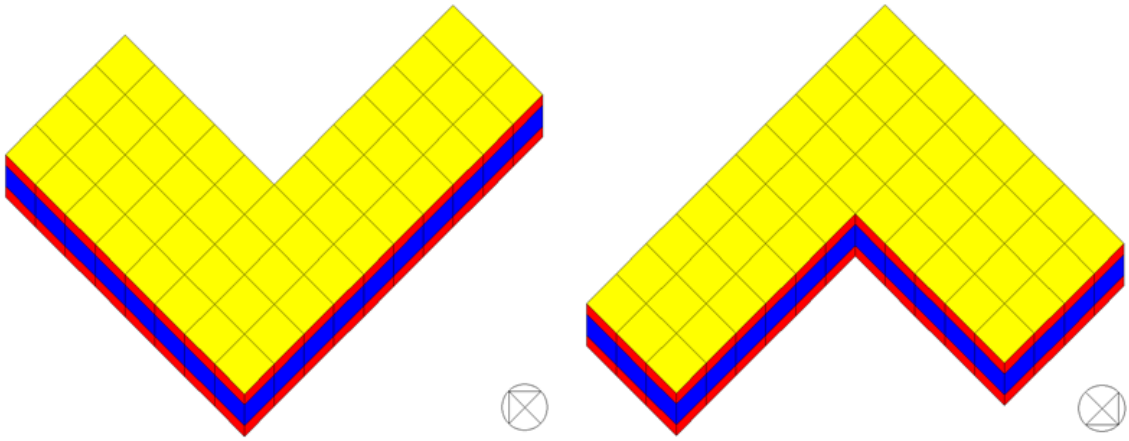

(a) Southwest View (b) Northeast View

Figure 162: View of Case 6 (Houston, TX) and Case 8 (Chicago, IL) Models in the Simulation

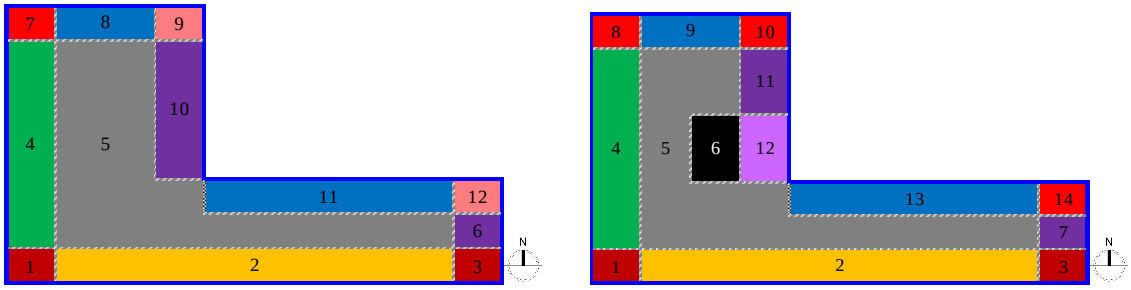

(a) For Cooling Season (b) For Heating Season

Figure 163: Resultant Thermal Zoning Layouts for Case 6 (Houston, TX)

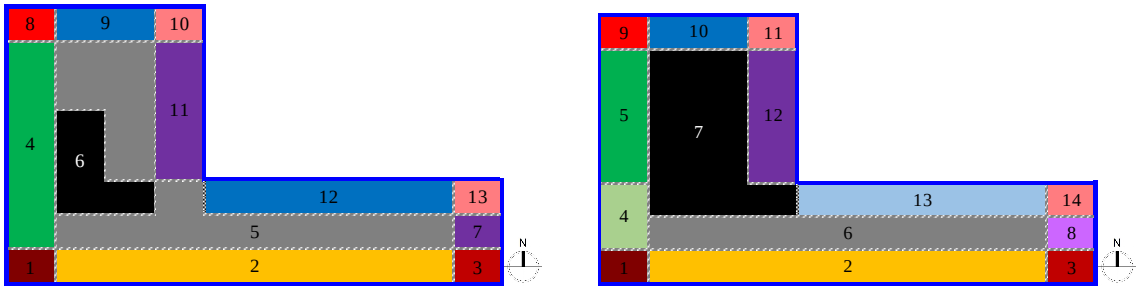

(a) For Cooling Season (b) For Heating Season

Figure 164: Resultant Thermal Zoning Layouts for Case 8 (Chicago, IL)

Table 59 shows the number of thermal zones created by the grid/cluster thermal zoning method for each simulation case with exterior windows on all orientations. For the rectangular-shape models, a total of 10 and 11 thermal zones were created for Houston and Chicago, respectively. For the L-Shape models, the grid/cluster thermal zoning method yielded a total of 14 and 12 thermal zones for Houston and Chicago, respectively. There was some differences in number and shape of thermal zones found between different climate conditions, when the models have exterior windows.

Table 59: Results of Thermal Zoning for Simulation Models with Exterior Windows on All Orientations (Houston, TX and Chicago, IL)

Climate	Case #	Building Shape	WWR	Number of Thermal Zones					
				East	West	North	South	Core	Total
Houston	2	Rectangle	50%	1	1	1	1	2	10
Chicago	4	Rectangle	50%	2	1	1	1	2	11
Houston	6	L-Shape	50%	3	1	2	1	2	14
Chicago	8	L-Shape	50%	2	1	2	1	1	12

5.3.1.3. Thermal Zoning Layouts for Simulation Models with Exterior Windows Only on Specific Orientations

The images of the building geometry for the Case 10 (Houston, TX) and Case 15 (Chicago, IL) models, which are the rectangle-shape models are shown in Figure 165. In the analysis, the Houston and Chicago TMY3 weather files were used for the simulation runs for the hot and cold climates, respectively. As mentioned earlier in Section 5.2.2.1, the Case 10 and Case 15 simulation models have a window band only on the exterior wall facing east with a 50% WWR. The resultant thermal zoning layouts of the Case 10 and Case 15 simulation models for the cooling and heating season are also presented in Figure 166 and Figure 167. The resultant thermal zoning layouts show that there was no difference between the Case 10 and Case 15 models, regardless of the heating/cooling season.

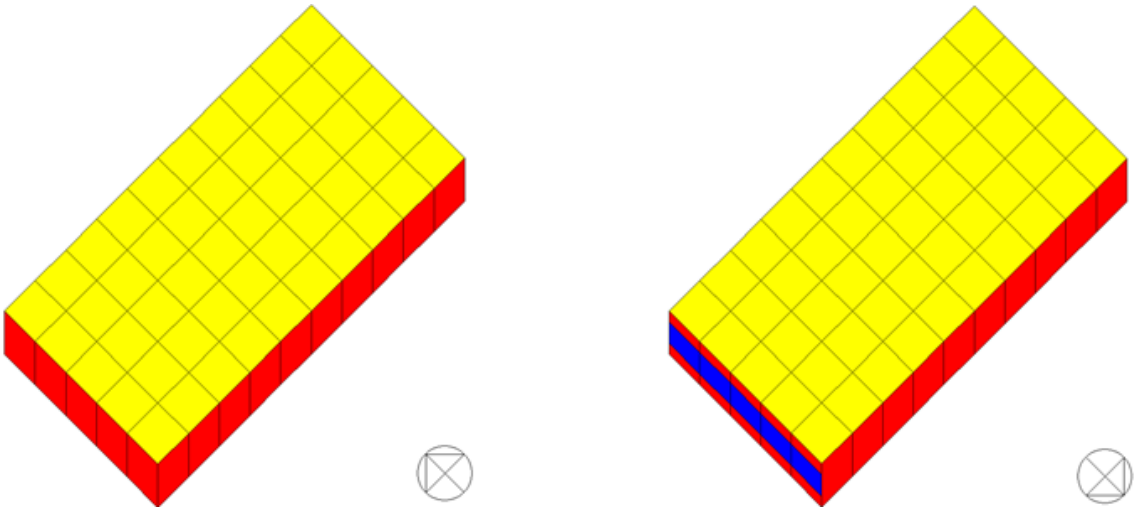

(a) Southwest View (b) Northeast View

Figure 165: View of Case 10 and Case 15 Models in the Simulation

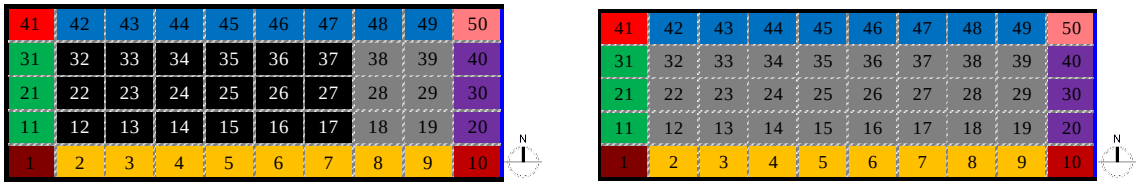

(a) For Cooling Season (b) For Heating Season

Figure 166: Resultant Thermal Zoning Layouts for Case 10 (Houston, TX)

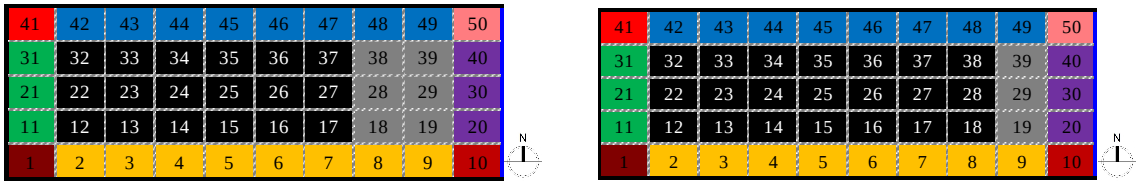

(a) For Cooling Season (b) For Heating Season

Figure 167: Resultant Thermal Zoning Layouts for Case 15 (Chicago, IL)

The images of the building geometry for the Case 11 (Houston, TX) and Case 16 (Chicago, IL) models, which are the rectangle-shape models are shown in Figure 168. In the analysis, the Houston and Chicago TMY3 weather files were used for the simulation runs for the hot and cold climates, respectively. As mentioned earlier in Section 5.2.2.2, the Case 11 and Case 16 simulation models have a window band only on the exterior wall facing west with a 50% WWR. The resultant thermal zoning layouts of the Case 11 and Case 16 simulation models for the cooling and heating season are also presented in Figure 169 and Figure 170. The resultant thermal zoning layouts show that there was no difference between the Case 11 and Case 16 models, regardless of the heating/cooling season.

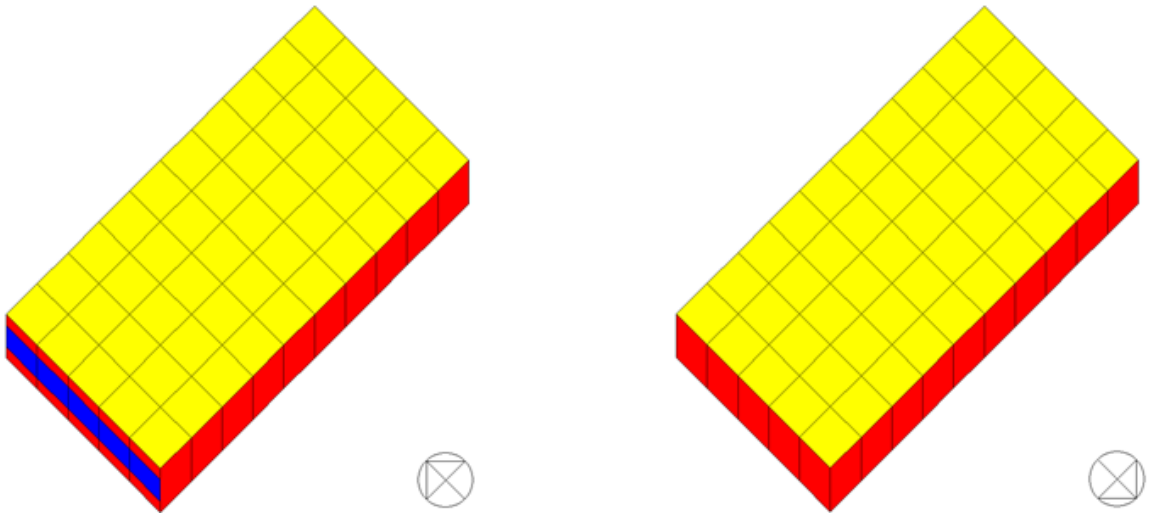

(a) Southwest View (b) Northeast View

Figure 168: View of Case 11 (Houston, TX) and Case 16 (Chicago, IL) Models in the Simulation

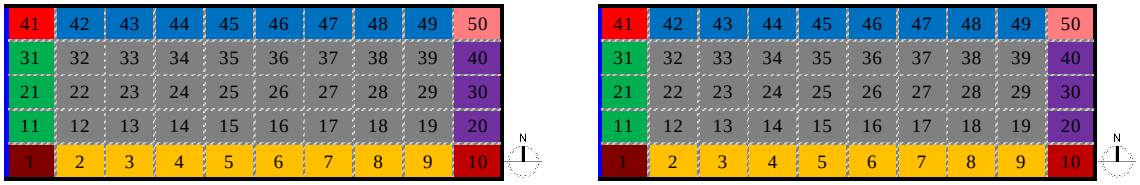

(a) For Cooling Season (b) For Heating Season

Figure 169: Resultant Thermal Zoning Layouts for Case 11 (Houston, TX)

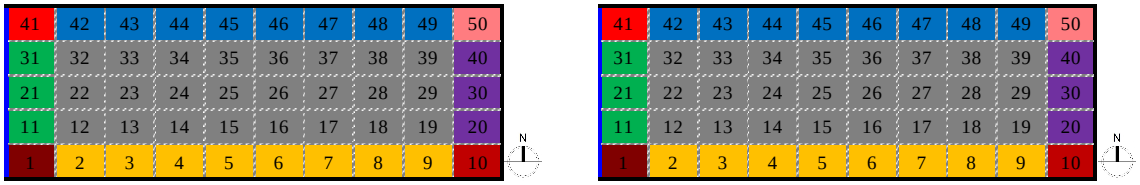

(a) For Cooling Season (b) For Heating Season

Figure 170: Resultant Thermal Zoning Layouts for Case 16 (Chicago, IL)

The images of the building geometry for the Case 12 (Houston, TX) and Case 17 (Chicago, IL) models, which are the rectangle-shape models are shown in Figure 171. In the analysis, the Houston and Chicago TMY3 weather files were used for the simulation runs for the hot and cold climates, respectively. As mentioned earlier in Section 5.2.2.3, the Case 12 and Case 17 simulation models have a window band only on the exterior wall facing north with a 50% WWR. The resultant thermal zoning layouts of the Case 12 and Case 17 simulation models for the cooling and heating season are also presented in Figure 172 and Figure 173. The resultant thermal zoning layouts show that there was no difference between the Case 12 and Case 17 models, regardless of the heating/cooling season.

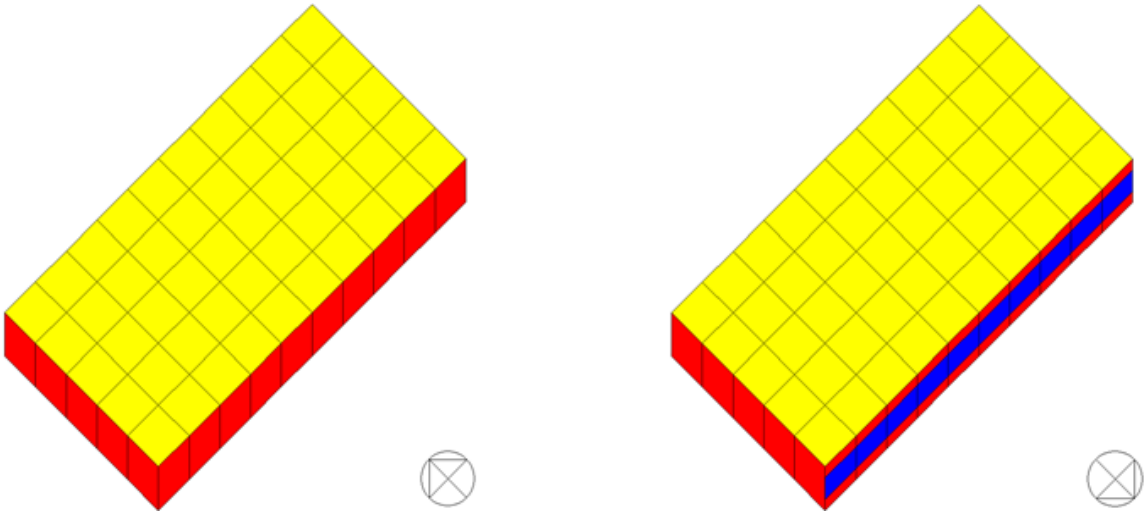

(a) Southwest View (b) Northeast View

Figure 171: View of Case 12 (Houston, TX) and Case 17 (Chicago, IL) Models in the Simulation

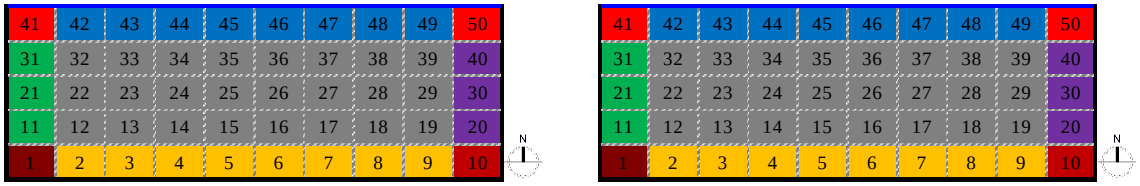

(a) For Cooling Season (b) For Heating Season

Figure 172: Resultant Thermal Zoning Layouts for Case 12 (Houston, TX)

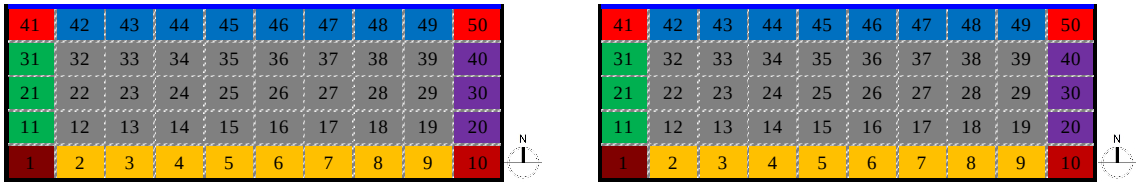

(a) For Cooling Season (b) For Heating Season

Figure 173: Resultant Thermal Zoning Layouts for Case 17 (Chicago, IL)

The images of the building geometry for the Case 13 (Houston, TX) and Case 18 (Chicago, IL) models, which are the rectangle-shape models are shown in Figure 174. In the analysis, the Houston and Chicago TMY3 weather files were used for the simulation runs for the hot and cold climates, respectively. As mentioned earlier in Section 5.2.2.4, the Case 13 and Case 18 simulation models have a window band only on the exterior wall facing south with a 50% WWR. The resultant thermal zoning layouts of the Case 13 and Case 18 simulation models for the cooling and heating season are also presented in Figure 175 and Figure 176. The resultant thermal zoning layouts show that there was no difference between the Case 13 and Case 18 models, regardless of the heating/cooling season.

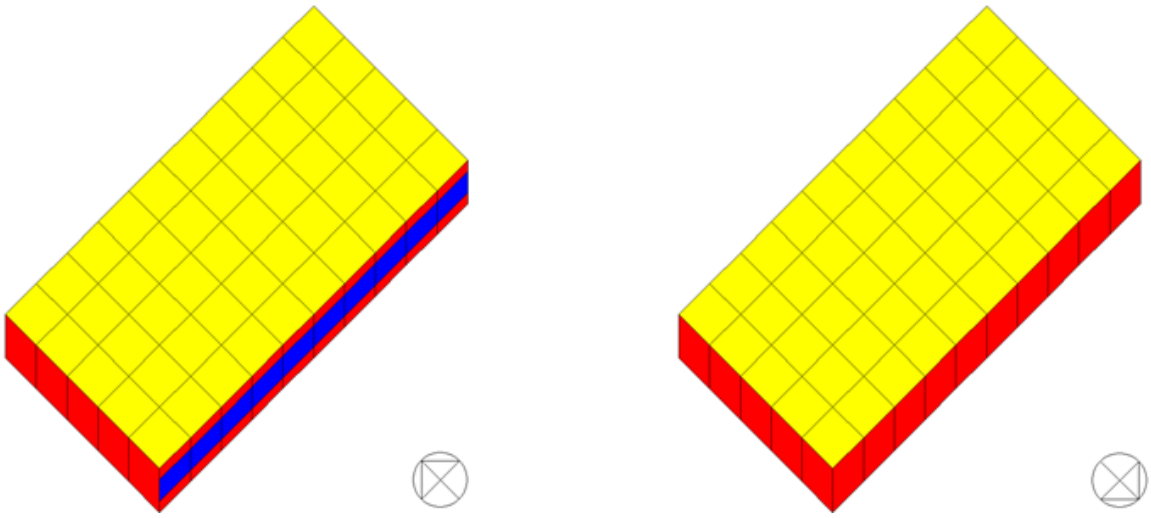

(a) Southwest View (b) Northeast View

Figure 174: View of Case 13 (Houston, TX) and Case 18 (Chicago, IL) Models in the Simulation

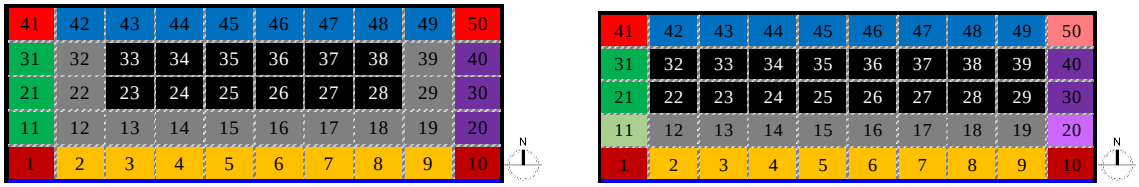

(a) For Cooling Season (b) For Heating Season

Figure 175: Resultant Thermal Zoning Layouts for Case 13 (Houston, TX)

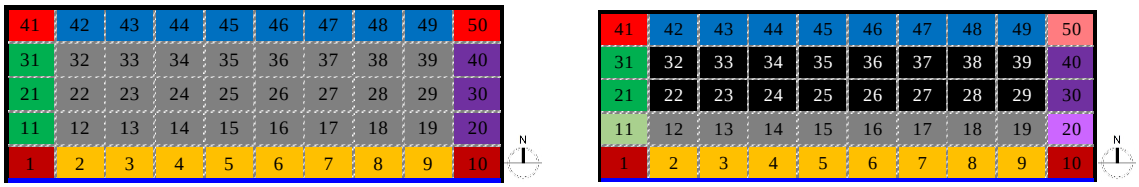

(a) For Cooling Season (b) For Heating Season

Figure 176: Resultant Thermal Zoning Layouts for Case 18 (Chicago, IL)

Table 60 shows the number of thermal zones created by the grid/cluster thermal zoning method for each simulation case with exterior windows on all orientations. For the cases have the windows only on the exterior wall facing east, a total of 10 thermal zones were created for both case. For the cases have the windows only on the exterior wall facing west, a total of 9 thermal zones were created for both case. For the cases have the windows only on the exterior wall facing north, a total of 9 thermal zones were created for both case. For the cases have the windows only on the exterior wall facing south, a total of 12 thermal zones were created for both case. There was no difference in number of thermal zones found between different climate conditions.

Table 60: Results of Thermal Zoning for Simulation Models with Exterior Windows Only on Specific Orientations (Houston, TX and Chicago, IL)

Climate	Case #	Building Shape	Orientation of the Window	Number of Thermal Zones					
				East	West	North	South	Core	Total
Houston	10	Rectangle	Only East	1	1	1	1	2	10
Chicago	15	Rectangle	Only East	1	1	1	1	2	10
Houston	11	Rectangle	Only West	1	1	1	1	1	9
Chicago	16	Rectangle	Only West	1	1	1	1	1	9
Houston	12	Rectangle	Only North	1	1	1	1	1	9
Chicago	17	Rectangle	Only North	1	1	1	1	1	9
Houston	13	Rectangle	Only South	2	2	1	1	2	12
Chicago	18	Rectangle	Only South	2	2	1	1	2	12

5.3.1.4. Thermal Zoning Layouts for Simulation Models with Offset Exterior Windows

The images of the building geometry for the Case 19 (Houston, TX) and Case 23 (Chicago, IL) models, which are the rectangle-shape models are shown in Figure 177. In the analysis, the Houston and Chicago TMY3 weather files were used for the simulation runs for the hot and cold climates, respectively. As mentioned earlier in Section 5.2.2.5, the Case 19 and Case 23 simulation models have window bands on the exterior walls facing East and West with a 50% WWR. The resultant thermal zoning layouts of the Case 19 and Case 23 simulation models for the cooling and heating season are also

presented in Figure 178 and Figure 179. The resultant thermal zoning layouts show that there is a similarity in the thermal zoning layouts between the Case 19 and Case 23 models. For the interior space, the grid/cluster thermal zoning method divided the building vertically into three different thermal zones.

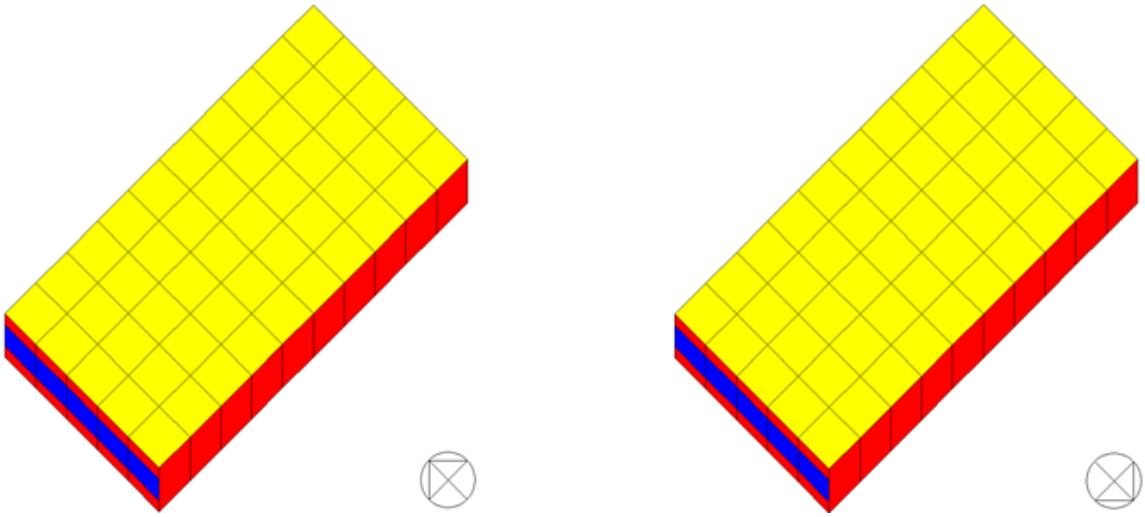

(a) Southwest View (b) Northeast View

Figure 177: View of Case 19 (Houston, TX) and Case 23 (Chicago, IL) Models in the Simulation

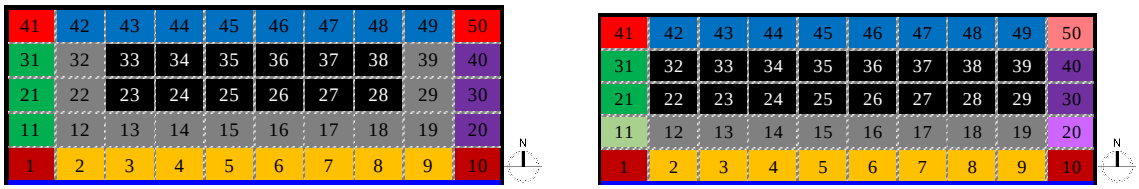

(a) For Cooling Season (b) For Heating Season

Figure 178: Resultant Thermal Zoning Layouts for Case 13 (Houston, TX)

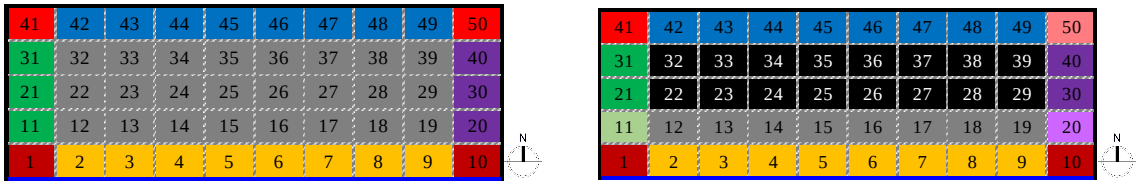

(a) For Cooling Season (b) For Heating Season

Figure 179: Resultant Thermal Zoning Layouts for Case 18 (Chicago, IL)

The images of the building geometry for the Case 20 (Houston, TX) and Case 24 (Chicago, IL) models, which are the rectangle-shape models are shown in Figure 180. In the analysis, the Houston and Chicago TMY3 weather files were used for the simulation runs for the hot and cold climates, respectively. As mentioned earlier in Section 5.2.2.6, the Case 20 and Case 24 simulation models have a window band only on the exterior wall facing East and West with a 50% WWR. For these cases, the size of the window is a width of 20 ft and are located on the east-side of each wall. The resultant thermal zoning layouts of the Case 20 and Case 24 simulation models for the cooling and heating season are also presented in Figure 181 and Figure 182. The resultant thermal zoning layouts show that there was no difference between the Case 20 and Case 24 models, regardless of the heating/cooling season.

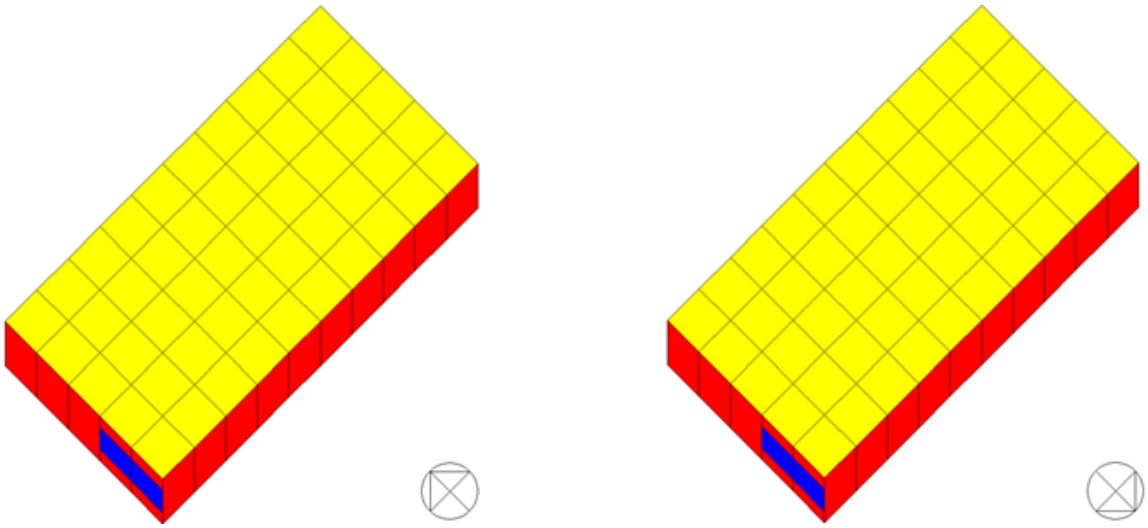

(a) Southwest View (b) Northeast View

Figure 180: View of Case 20 (Houston, TX) and Case 24 (Chicago, IL) Models in the Simulation

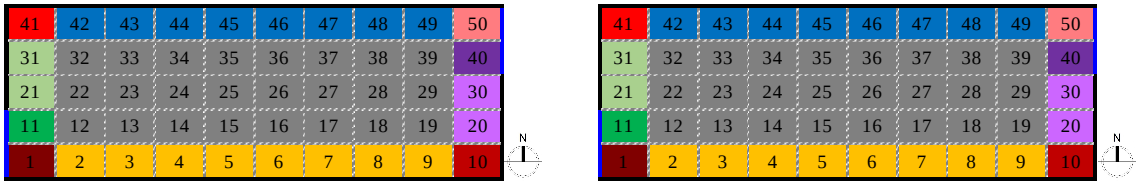

(a) For Cooling Season (b) For Heating Season

Figure 181: Resultant Thermal Zoning Layouts for Case 20 (Houston, TX)

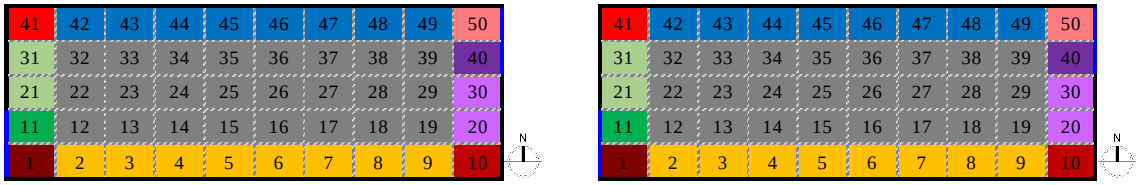

(a) For Cooling Season (b) For Heating Season

Figure 182: Resultant Thermal Zoning Layouts for Case 24 (Chicago, IL)

The images of the building geometry for the Case 21 (Houston, TX) and Case 25 (Chicago, IL) models, which are the rectangle-shape models are shown in Figure 183. In the analysis, the Houston and Chicago TMY3 weather files were used for the simulation runs for the hot and cold climates, respectively. As mentioned earlier in Section 5.2.2.7, the Case 21 and Case 25 simulation models have window bands on the exterior walls facing North and South with a 50% WWR. The resultant thermal zoning layouts of the Case 21 and Case 25 simulation models for the cooling and heating season are also presented in Figure 184 and Figure 185. The resultant thermal zoning layouts show that there was no difference between the Case 21 and Case 25 models, regardless of the heating/cooling season.

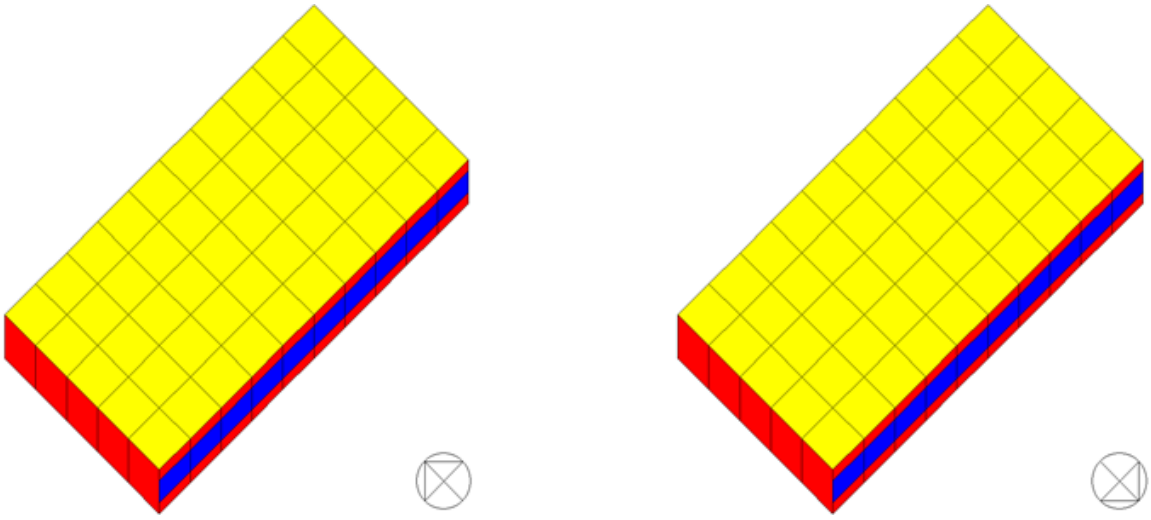

(a) Southwest View (b) Northeast View

Figure 183: View of Case 21 (Houston, TX) and Case 25 (Chicago, IL) Models in the Simulation

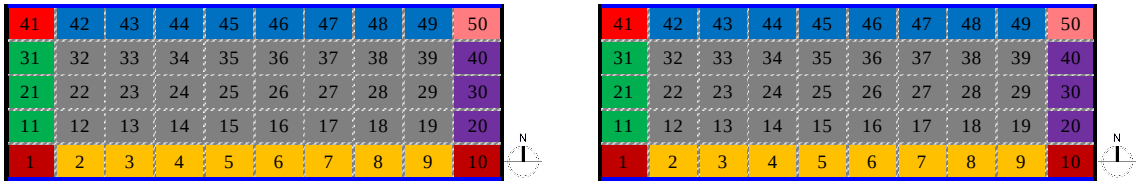

(a) For Cooling Season (b) For Heating Season

Figure 184: Resultant Thermal Zoning Layouts for Case 21 (Houston, TX)

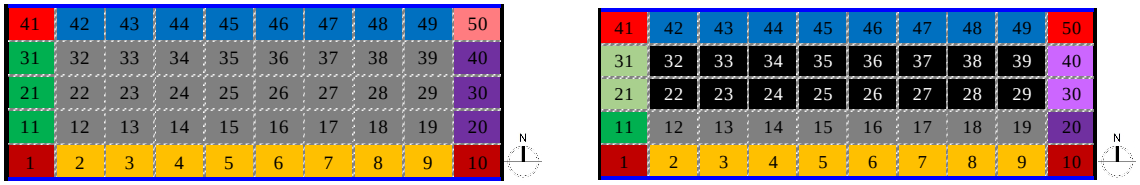

(a) For Cooling Season (b) For Heating Season

Figure 185: Resultant Thermal Zoning Layouts for Case 25 (Chicago, IL)

The images of the building geometry for the Case 22 (Houston, TX) and Case 26 (Chicago, IL) models, which are the rectangle-shape models are shown in Figure 186. In the analysis, the Houston and Chicago TMY3 weather files were used for the simulation runs for the hot and cold climates, respectively. As mentioned earlier in Section 5.2.2.8, the Case 22 and Case 26 simulation models have a window band only on the exterior wall facing North and South with a 50% WWR. For these cases, the size of the window is a width of 20 ft and are located on the east-side of each wall. The resultant thermal zoning layouts of the Case 22 and Case 26 simulation models for the cooling and heating season are also presented in Figure 187 and Figure 188. The resultant thermal zoning layouts show that there was no difference between the Case 22 and Case 26 models, regardless of the heating/cooling season.

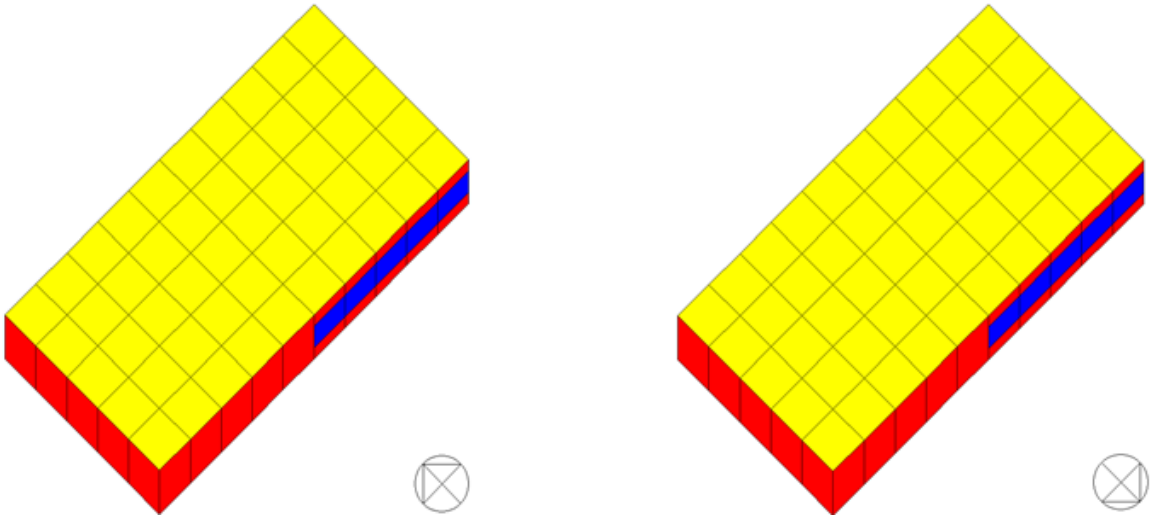

(a) Southwest View (b) Northeast View

Figure 186: View of Case 22 (Houston, TX) and Case 26 (Chicago, IL) Models in the Simulation

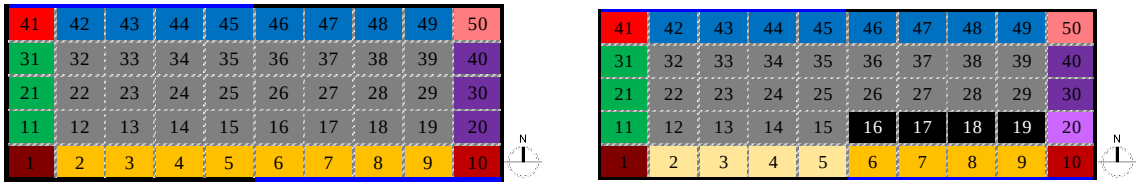

(a) For Cooling Season (b) For Heating Season

Figure 187: Resultant Thermal Zoning Layouts for Case 22 (Houston, TX)

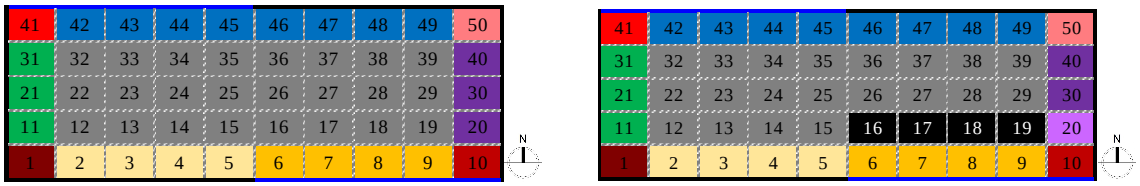

(a) For Cooling Season (b) For Heating Season

Figure 188: Resultant Thermal Zoning Layouts for Case 26 (Chicago, IL)

Table 61 shows the number of thermal zones created by the grid/cluster thermal zoning method for each simulation case w/ and w/o offset exterior windows. For the cases have the windows only on the exterior wall facing east and west, a total of 11 thermal zones were created for Houston, while a total of 15 thermal zones were developed for Chicago. For the cases have the offset windows on the exterior wall facing east and west, a total of 11 thermal zones were created for both case. For the cases have the windows only on the exterior wall facing south and north, a total of 9 thermal zones were created for Houston, while a total of 12 thermal zones were developed for Chicago. For the cases have the offset windows on the exterior wall facing south and north, a total of 12 thermal zones were created for both case.

Table 61: Results of Thermal Zoning for Simulation Models with Offset Exterior Windows (Houston, TX and Chicago, IL)

Climate	Case #	Building Shape	Orientation of the Window	Number of Thermal Zones					
				East	West	North	South	Core	Total
Houston	19	Rectangle	East-West	1	1	1	1	3	11
Chicago	23	Rectangle	East-West	1	1	3	3	3	15
Houston	20*	Rectangle	East-West	2	2	1	1	1	11
Chicago	24*	Rectangle	East-West	2	2	1	1	1	11
Houston	21	Rectangle	South-North	1	1	1	1	1	9
Chicago	25	Rectangle	South-North	2	2	1	1	2	12
Houston	22*	Rectangle	South-North	2	1	1	2	2	12
Chicago	26*	Rectangle	South-North	2	1	1	2	2	12

* The windows in this case were installed on a half of the exterior walls.

5.3.2. Comparison of Heating/Cooling Loads Between Different Climate Conditions

In this section, to investigate the impacts of the climate condition on the building thermal zoning and its heating/cooling loads, simulation cases were created as shown in Table 12 in Section 4.3.3. Using the same model geometry, the thermal zoning layouts given by the grid/cluster thermal zoning method for two climate conditions (i.e., Houston, TX, Chicago, IL) were compared. In addition, a single-zone thermal zoning model and the grid/cluster thermal zoning model were created for each case and compared in regards to the heating/cooling loads. The calculated annual/monthly heating/cooling loads for each case were investigated.

5.3.2.1. Comparison of Cooling/Heating Loads for Simulation Models with Only Opaque Walls

Figure 189 shows the comparison of the total annual heating/cooling loads for the 1-Zone and Grid/Cluster thermal zoning models for Case 1 (Houston, TX) and Case 3 (Chicago, IL), which are the rectangle-shape models with only opaque walls (i.e., no exterior windows). For the hot and humid climate, the total annual heating and cooling loads were reduced using the grid/cluster thermal zoning method by -8% and -24%, respectively. For the cold and humid climate, the total annual cooling load was increased by 699% and the total annual heating load was reduced by -42%. The results show that the total annual load reduction of the simulation models for Houston and Chicago are -15% and -39%, respectively.

Figure 190 shows the comparison of the total annual heating/cooling loads for the 1-Zone and Grid/Cluster thermal zoning models for Case 5 (Houston, TX) and Case 7 (Chicago, IL), which are the L-shape models with only opaque walls (i.e., no exterior windows). For the hot and humid climate, the total annual heating load was increased using the grid/cluster thermal zoning method by 1%, while the total annual cooling load was reduced by -23%. For the cold and humid climate, the total annual cooling load was increased by 760% and the total annual heating load was reduced by -42%. The results show that the total annual load reduction of the simulation models for Houston and Chicago are -10% and -38%, respectively.

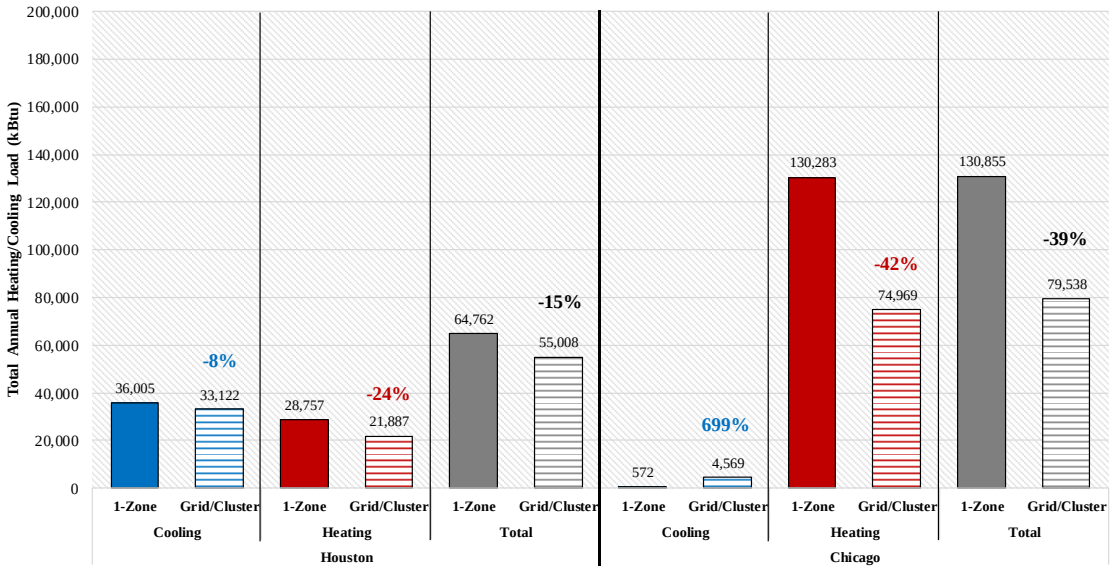

Figure 189: Total Annual Heating/Cooling Loads for Rectangle-Shape Models with Only Opaque Walls for Houston and Chicago

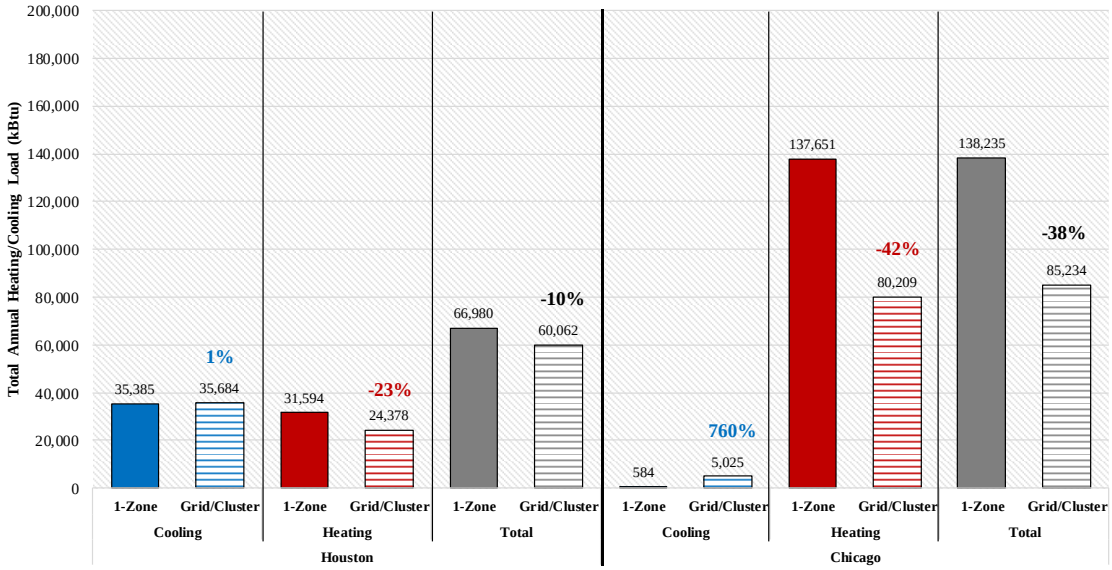

Figure 190: Total Annual Heating/Cooling Loads for L-Shape Models with Only Opaque Walls for Houston and Chicago

5.3.2.2. Comparison of Cooling/Heating Loads for Simulation Models with Only Opaque Walls

Figure 191 shows the comparison of the total annual heating/cooling loads for the 1-Zone and Grid/Cluster thermal zoning models for Case 2 (Houston, TX) and Case 4 (Chicago, IL), which are rectangle-shape models with a horizontal band of exterior windows with the WWR of 50%. For the hot and humid climate, the total annual heating and cooling loads were reduced using the grid/cluster thermal zoning method by -7% and -5%, respectively. For the cold and humid climate, the total annual cooling load was increased by 40% and the total annual heating load was reduced by -26%. The results show that the total annual load reduction of the simulation models for Houston and Chicago are -6% and -13%, respectively.

Figure 192 shows the comparison of the total annual heating/cooling loads for the 1-Zone and Grid/Cluster thermal zoning models for Case 6 (Houston, TX) and Case 8 (Chicago, IL), which are L-shape models with a horizontal band of exterior windows with the WWR of 50%. For the hot and humid climate, the total annual heating and cooling loads were reduced using the grid/cluster thermal zoning method by -3% and -2%, respectively. For the cold and humid climate, the total annual cooling load was increased by 34% and the total annual heating load was reduced by -22%. The results show that the total annual load reduction of the simulation models for Houston and Chicago are -3% and -10%, respectively.

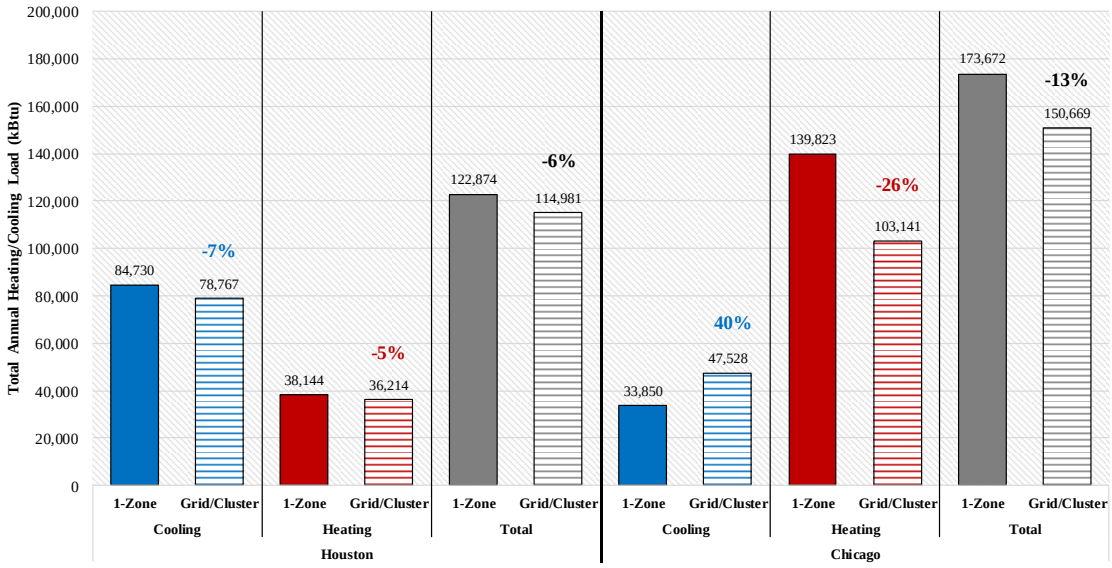

Figure 191: Total Annual Heating/Cooling Loads for Rectangle-Shape Models with Exterior Windows (WWR 50%) for Houston and Chicago

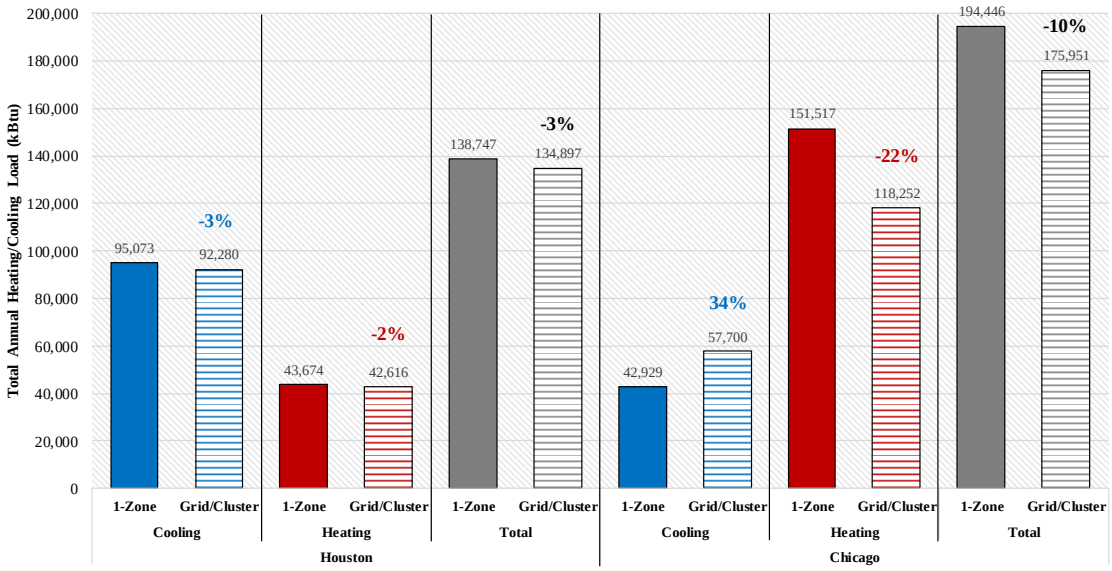

Figure 192: Total Annual Heating/Cooling Loads for L-Shape Models with Exterior Windows (WWR 50%) for Houston and Chicago

5.3.2.3. Comparison of Cooling/Heating Loads for Simulation Models with Exterior Windows Only on Specific Orientations

Figure 193 shows the comparison of the total annual heating/cooling loads for the 1-Zone and Grid/Cluster thermal zoning models for Case 10 (Houston, TX) and Case 15 (Chicago, IL), which are rectangle-shape models with a window band only on the exterior wall facing East with a 50% WWR. For the hot and humid climate, the total annual heating and cooling loads were reduced using the grid/cluster thermal zoning method by -8% and -18%, respectively. For the cold and humid climate, the total annual cooling load was increased by 179% and the total annual heating load was reduced by -37%. The results show that the total annual load reduction of the simulation models for Houston and Chicago are -12% and -30%, respectively.

Figure 194 shows the comparison of the total annual heating/cooling loads for the 1-Zone and Grid/Cluster thermal zoning models for Case 11 (Houston, TX) and Case 16 (Chicago, IL), which are rectangle-shape models with a window band only on the exterior wall facing West with a 50% WWR. For the hot and humid climate, the total annual heating and cooling loads were reduced using the grid/cluster thermal zoning method by -8% and -19%, respectively. For the cold and humid climate, the total annual cooling load was increased by 164% and the total annual heating load was reduced by -38%. The results show that the total annual load reduction of the simulation models for Houston and Chicago are -12% and -30%, respectively.

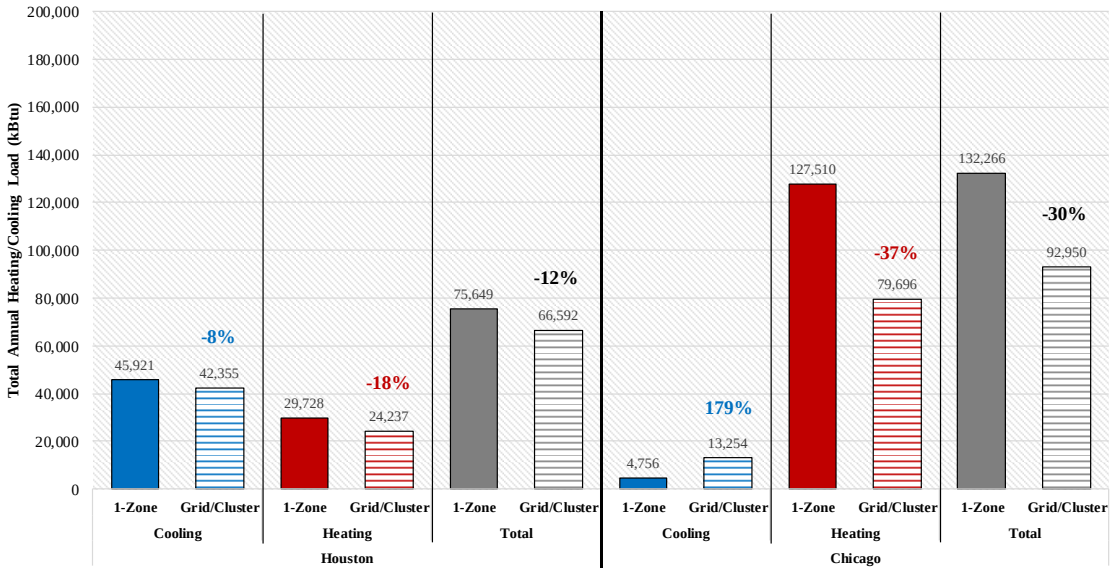

Figure 193: Total Annual Heating/Cooling Loads for Rectangle-Shape Models with Exterior Windows (WWR 50%) Only on East for Houston and Chicago

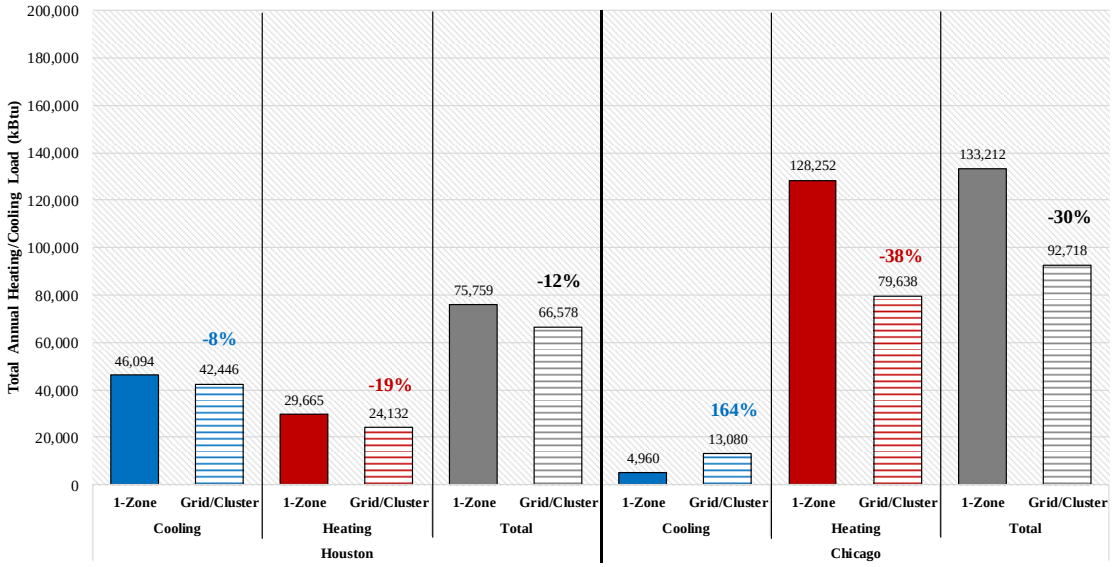

Figure 194: Total Annual Heating/Cooling Loads for Rectangle-Shape Models with Exterior Windows (WWR 50%) Only on West for Houston and Chicago

Figure 195 shows the comparison of the total annual heating/cooling loads for the 1-Zone and Grid/Cluster thermal zoning models for Case 12 (Houston, TX) and Case 17 (Chicago, IL), which are rectangle-shape models with a window band only on the exterior wall facing North with a 50% WWR. For the hot and humid climate, the total annual heating and cooling loads were reduced using the grid/cluster thermal zoning method by -8% and -18%, respectively. For the cold and humid climate, the total annual cooling load was increased by 142% and the total annual heating load was reduced by -36%. The results show that the total annual load reduction of the simulation models for Houston and Chicago are -12% and -30%, respectively.

Figure 196 shows the comparison of the total annual heating/cooling loads for the 1-Zone and Grid/Cluster thermal zoning models for Case 13 (Houston, TX) and Case 18 (Chicago, IL), which are rectangle-shape models with a window band only on the

exterior wall facing South with a 50% WWR. For the hot and humid climate, the total annual heating and cooling loads were reduced using the grid/cluster thermal zoning method by -8% and -10%, respectively. For the cold and humid climate, the total annual cooling load was increased by 120% and the total annual heating load was reduced by -35%. The results show that the total annual load reduction of the simulation models for Houston and Chicago are -8% and -22%, respectively.

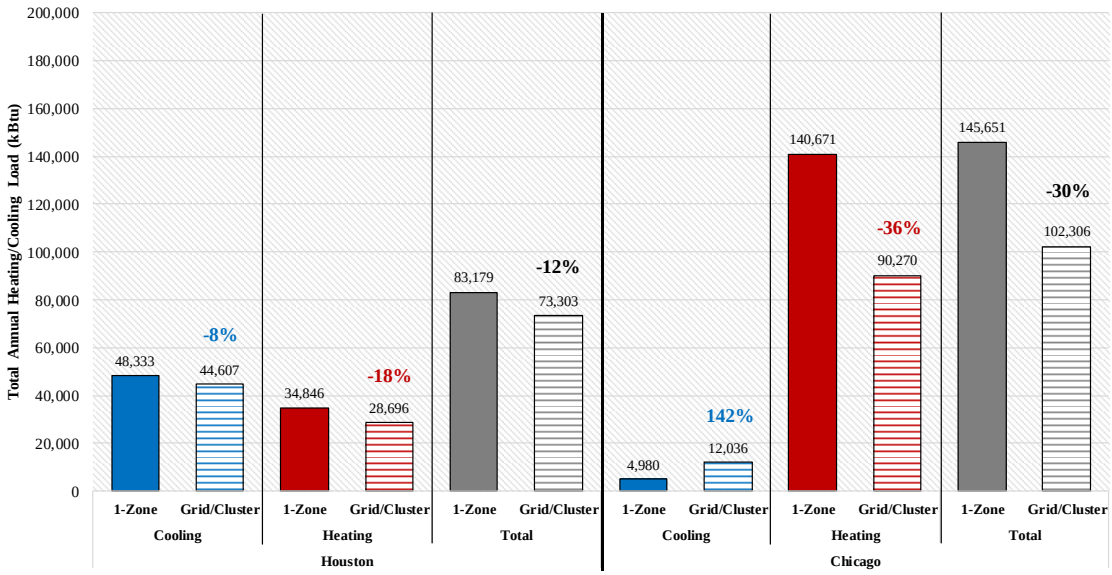

Figure 195: Total Annual Heating/Cooling Loads for Rectangle-Shape Models with Exterior Windows (WWR 50%) Only on North for Houston and Chicago

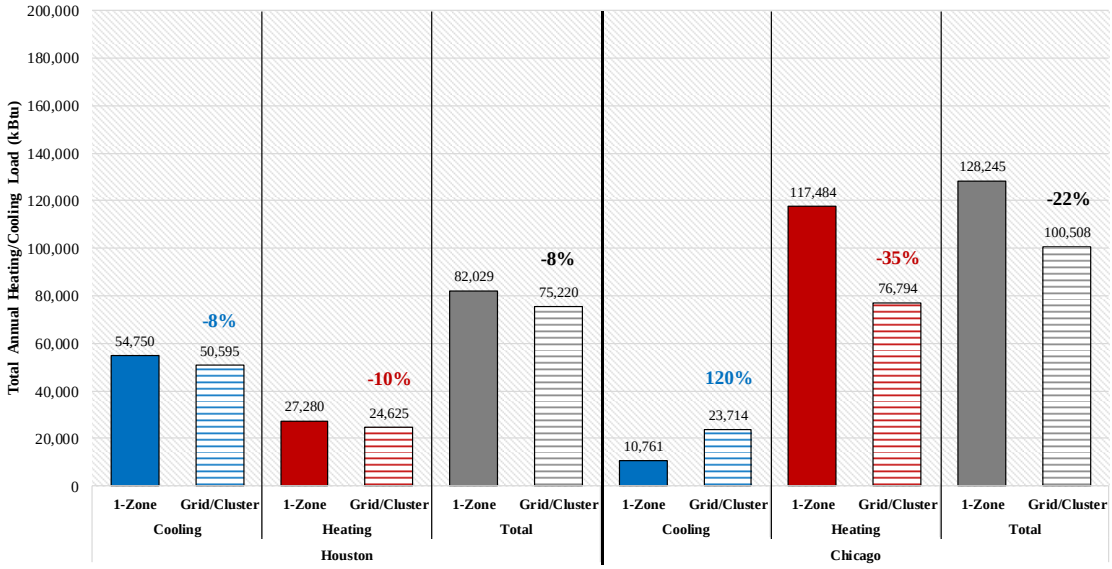

Figure 196: Total Annual Heating/Cooling Loads for Rectangle-Shape Models with Exterior Windows (WWR 50%) Only on South for Houston and Chicago

5.3.2.4. Comparison of Cooling/Heating Loads for Simulation Models with Offset Exterior Windows

Figure 197 shows the comparison of the total annual heating/cooling loads for the 1-Zone and Grid/Cluster thermal zoning models for Case 19 (Houston, TX) and Case 23 (Chicago, IL), which are rectangle-shape models with window bands on the exterior walls facing East and West with a 50% WWR. For the hot and humid climate, the total annual heating and cooling loads were reduced using the grid/cluster thermal zoning method by -8% and -15%, respectively. For the cold and humid climate, the total annual cooling load was increased by 92% and the total annual heating load was reduced by -34%. The results show that the total annual load reduction of the simulation models for Houston and Chicago are -10% and -24%, respectively.

Figure 198 shows the comparison of the total annual heating/cooling loads for the 1-Zone and Grid/Cluster thermal zoning models for Case 20 (Houston, TX) and Case 24 (Chicago, IL), which are rectangle-shape models with a window band only on the exterior wall facing East and West with a 50% WWR. For these cases, the size of the window is a width of 20 ft and are located on the east-side of each wall. For the hot and humid climate, the total annual heating and cooling loads were reduced using the grid/cluster thermal zoning method by -8% and -20%, respectively. For the cold and humid climate, the total annual cooling load was increased by 213% and the total annual heating load was reduced by -39%. The results show that the total annual load reduction of the simulation models for Houston and Chicago are -12% and -32%, respectively.

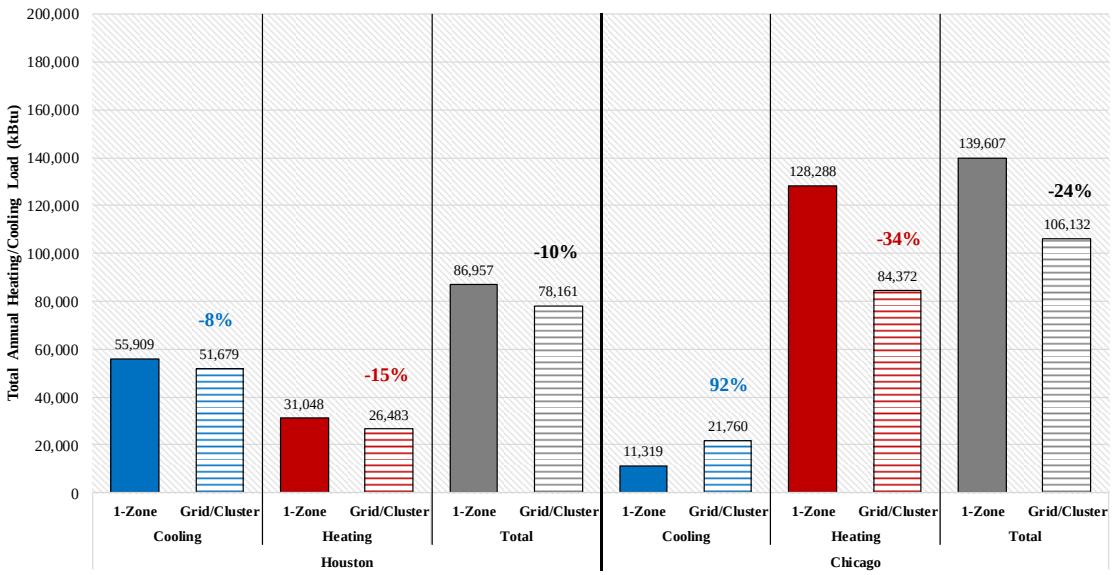

Figure 197: Total Annual Heating/Cooling Loads for Rectangle-Shape Models with Exterior Windows (WWR 50%) on East and West for Houston and Chicago

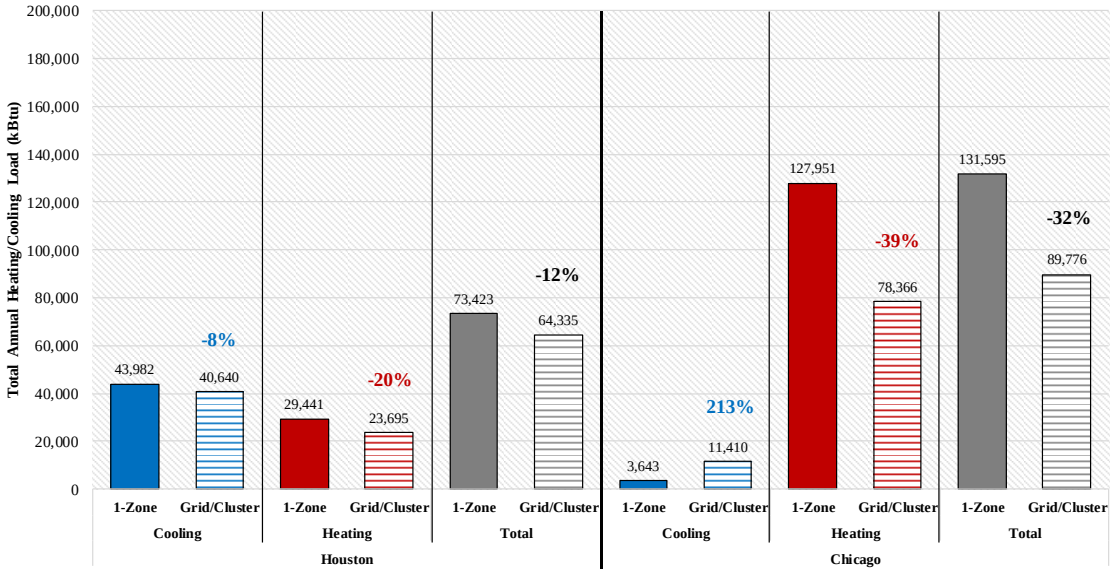

Figure 198: Total Annual Heating/Cooling Loads for Rectangle-Shape Models with Offset Exterior Windows (WWR 50%) on East and West for Houston and Chicago

Figure 199 shows the comparison of the total annual heating/cooling loads for the 1-Zone and Grid/Cluster thermal zoning models for Case 21 (Houston, TX) and Case 25 (Chicago, IL), which are rectangle-shape models with window bands on the exterior walls facing South and North with a 50% WWR. For the hot and humid climate, the total annual heating and cooling loads were reduced using the grid/cluster thermal zoning method by -4% and -8%, respectively. For the cold and humid climate, the total annual cooling load was increased by 75% and the total annual heating load was reduced by -30%. The results show that the total annual load reduction of the simulation models for Houston and Chicago are -6% and -18%, respectively.

Figure 200 shows the comparison of the total annual heating/cooling loads for the 1-Zone and Grid/Cluster thermal zoning models for Case 22 (Houston, TX) and Case 26 (Chicago, IL), which are rectangle-shape models with a window band only on the

exterior wall facing South and North with a 50% WWR. For these cases, the size of the window is a width of 20 ft and are located on the east-side of each wall. For the hot and humid climate, the total annual heating and cooling loads were reduced using the grid/cluster thermal zoning method by -9% and -13%, respectively. For the cold and humid climate, the total annual cooling load was increased by 129% and the total annual heating load was reduced by -35%. The results show that the total annual load reduction of the simulation models for Houston and Chicago are -11% and -26%, respectively.

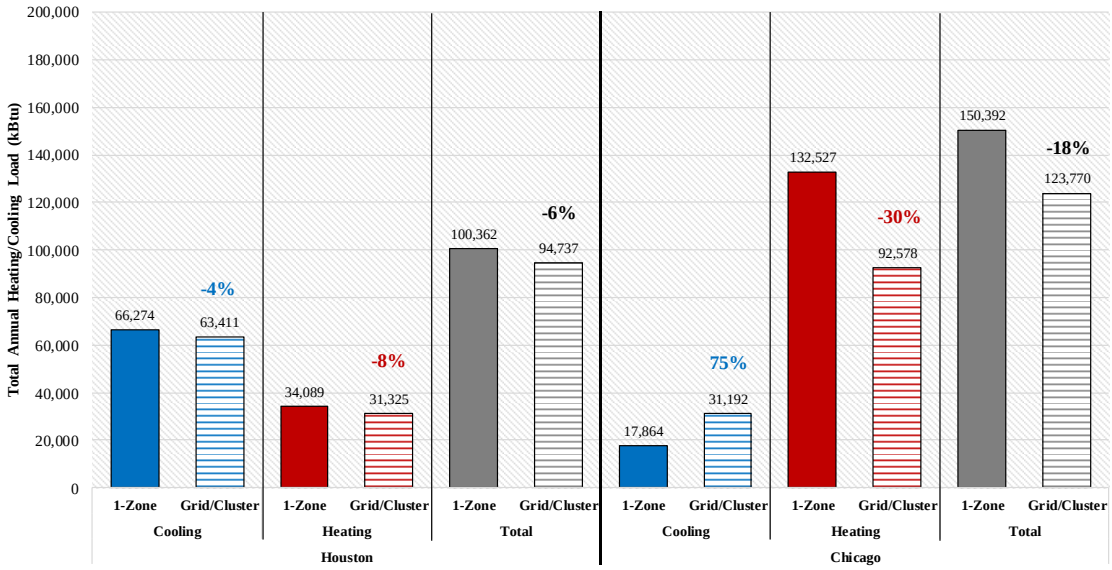

Figure 199: Total Annual Heating/Cooling Loads for Rectangle-Shape Models with Exterior Windows (WWR 50%) on South and North for Houston and Chicago

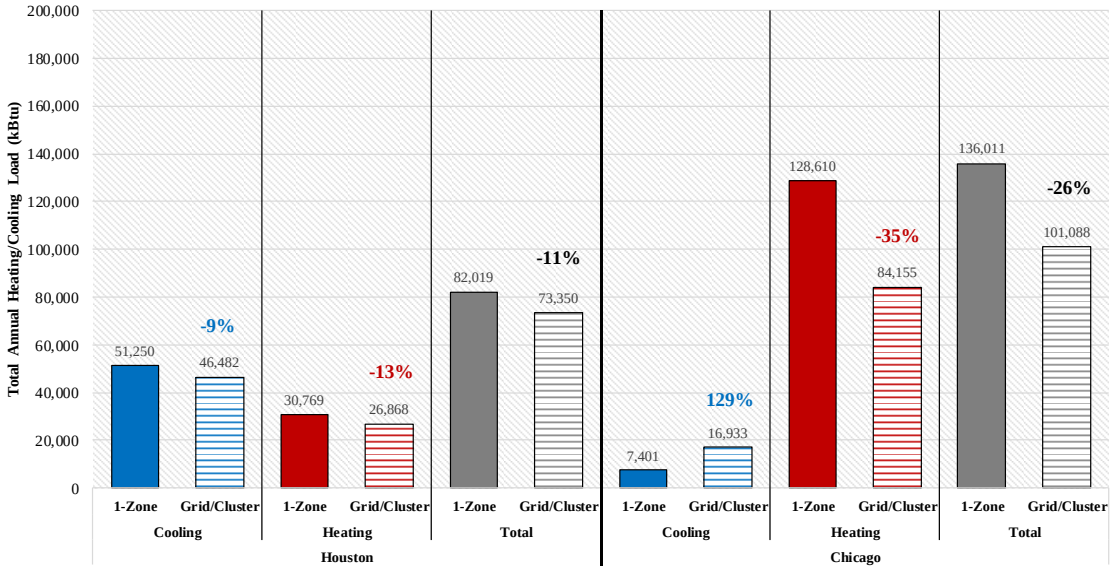

Figure 200: Total Annual Heating/Cooling Loads for Rectangle-Shape Models with Offset Exterior Windows (WWR 50%) on South and North for Houston and Chicago

5.3.3. Summary of Parametric Study of Thermal Zoning on Climate Condition

In this section, the resultant thermal zoning layouts of 12 different simulation models with two different climate conditions (i.e., Hot and Humid, Cold and Humid) were examined and compared using the grid/cluster thermal zoning method to investigate the impact of the climate conditions on the building thermal zoning in a simulation. In addition, the simulated total annual heating/cooling loads for each case were compared and examined.

The resultant thermal zoning layouts based on the grid/cluster thermal zoning method showed that the thermal zoning layouts tend to less influenced by the climate condition. The cases that do not have any exterior windows resulted in the same thermal zoning layouts for two different climate conditions. In addition, the cases that have

exterior windows with diverse orientations also create very similar thermal zoning layouts for two different climate conditions.

Table 62 shows the comparisons of total annual heating/cooling loads reductions between the single zone models and grid/cluster thermal zoning models for Houston and Chicago. These results show how much thermal load reduction was achieved when the grid/cluster thermal zoning method was applied to each case compared to single-zone model. For all the cases, total annual thermal loads reductions for Chicago are larger than the ones that for Houston. In addition, regardless of the climate condition, it was found that the heating load reductions were mostly larger than the cooling load when the grid/cluster thermal zoning method was applied to group the spaces.

Table 62: Total Annual Heating/Cooling Loads Reduction using Grid/Cluster Thermal Zoning Method for Different Climate Conditions

Case #	Climate	Heating/Cooling Load Reduction		
		Heating	Cooling	Total
1	Houston	-6,870,314 (-24%)	-2,883,137 (-8%)	-9,753,451 (-15%)
3	Chicago	-55,313,882 (-42%)	3,997,417 (699%)	-51,316,466 (-39%)
5	Houston	-7,216,185 (-23%)	298,530 (1%)	-6,917,655 (-10%)
7	Chicago	-57,442,040 (-42%)	4,440,924 (760%)	-53,001,116 (-38%)
2	Houston	-1,930,074 (-5%)	-5,962,521 (-7%)	-7,892,595 (-6%)
4	Chicago	-36,681,628 (-26%)	13,678,390 (40%)	-23,003,238 (-13%)
6	Houston	-1,057,982 (-2%)	-2,792,707 (-3%)	-3,850,689 (-3%)
8	Chicago	-33,264,902 (-22%)	14,770,175 (34%)	-18,494,726 (-10%)
9	Houston	-579,527 (-1%)	-9,605,390 (-9%)	-10,184,918 (-7%)
14	Chicago	-30,972,892 (-20%)	12,135,588 (21%)	-18,837,304 (-9%)
10	Houston	-5,491,261 (-18%)	-3,566,417 (-8%)	-9,057,679 (-12%)
15	Chicago	-47,813,788 (-37%)	8,497,616 (179%)	-39,316,172 (-30%)
11	Houston	-5,532,239 (-19%)	-3,648,275 (-8%)	-9,180,514 (-12%)
16	Chicago	-48,613,745 (-38%)	8,119,513 (164%)	-40,494,233 (-30%)
12	Houston	-6,150,378 (-18%)	-3,726,075 (-8%)	-9,876,453 (-12%)
17	Chicago	-50,401,066 (-36%)	7,056,376 (142%)	-43,344,690 (-30%)
13	Houston	-2,654,873 (-10%)	-4,154,663 (-8%0	-6,809,536 (-18%)
18	Chicago	-40,689,953 (-35%)	12,953,613 (120%)	-27,736,339 (-22%)
19	Houston	-4,565,476 (-15%)	-4,230,153 (-8%)	-8,795,629 (-10%)
23	Chicago	-43,916,337 (-34%)	10,440,721 (92%)	-33,475,616 (-24%)
20	Houston	-5,745,904 (-20%)	-3,342,371 (-8%)	-9,088,276 (-12%)
24	Chicago	-49,584,993 (-39%)	7,766,139 (213%)	-41,818,854 (-32%)
21	Houston	-2,763,513 (-8%)	-2,862,102 (-4%)	-5,625,615 (-6%)
25	Chicago	-39,949,321 (-30%)	13,327,476 (75%)	-26,621,845 (-18%)
22	Houston	-3,901,154 (-13%)	-4,768,033 (-9%)	-8,669,187 (-11%)
26	Chicago	-44,454,967 (-35%)	9,531,919 (129%)	-34,923,049 (-26%)

CHAPTER VI

SUMMARY AND FUTURE WORK

This chapter presents a summary of this study. In addition, the future work based on the limitations of the study is discussed.

6.1. Summary of the Methodology

This study has provided a new thermal zoning method (i.e., Grid/Cluster thermal zoning method) to automatically divide a commercial building into HVAC thermal zones for a building energy simulation. The existing thermal zoning methods that can be used in this work were investigated and reviewed from the previous studies. The only previous method (Georgescu et al. 2012) that presented results that could be compared had additional parameters in those results, which go beyond the scope of this work. For example, the function of the use of the space, internal loads, and HVAC systems were the additional parameters included in the previous methods. Since this study only covers the envelope loads, it was not clear how to separate the envelope loads from all the total loads. In addition, to identify building features (i.e., building shape, window-to-wall ratio, window orientation, climate condition) that are most likely to have the greatest impact on the thermal zoning approach, a parametric analysis was developed that uses a simplified commercial base-case model with varying simulation scenarios. For the parametric study, a simplified commercial base-case model was developed and used to demonstrate the developed new thermal zoning method.

To provide an accurate building energy simulation results and comfortable indoor conditions, the developed method for thermal zoning of commercial buildings for the whole-building energy simulation uses the step-by-step procedure below:

1) **Step 1** (Define grid unit) - The size of a grid unit should be defined by the user based on the usage of the space and its function. In addition, if an air distribution system is used, the throw of the air diffuser should be considered also specifying the size of a grid unit. In this study, the size of a grid unit set at 10 ft X 10 ft, or 100 ft^2, which is based on a typical size of an individual office space and the coverage of a typical diffuser.

2) **Step 2** (Application of the grid unit to building floor plan) - A grid unit that was defined in the previous step is applied to the building floor plan in this step. In this study, a rectangular- and a L-shape floor plan were used as examples.

3) **Step 3** (Whole-building energy simulation model) - Based on the information regarding the thermal zoning layout and building physical characteristics, a whole-building energy simulation model can be created using the zones created by the Grid/Cluster (G/C) thermal zoning method.

4) **Step 4** (Hourly heating/cooling loads for each grid unit) - The hourly heating/cooling loads are calculated for each grid unit.

5) **Step 5** (Annual heating/cooling loads for each grid unit) - The annual heating/cooling loads for each grid unit are calculated based on the hourly heating/cooling loads to identify the spaces that have similar thermal loads.

6) **Step 6** (Defining thermal zones based on annual thermal load data) - Based on the annual heating/cooling loads for each grid space, the grid spaces that have the same total annual thermal loads are identified.

7) **Step 7** (Calibration of the combined thermal zones) - The indoor temperature profiles of the grouped thermal zones are analyzed to verify the grid-based thermal zoning strategy. To accomplish this, 24-hour simulated indoor temperature profiles of the combined thermal zones for peak days (i.e., hot/cold clear days) are analyzed and compared using the linear correlation coefficient.

6.2. Summary of the Results

This section provides a summary of results from the parametric study using the proposed new thermal zoning method, which includes: 1) an analysis of the impact of building shape on thermal zoning; 2) analysis of the impact of window-to-wall ratio on thermal zoning; and 3) analysis of the impact of climate conditions on thermal zoning.

6.2.1. Summary of Parametric Study of Thermal Zoning on Building Shape

The parametric study using two building shapes (i.e., rectangular-shape, L-shape) and three different thermal zoning methods (i.e., single zone, core-perimeter, grid/cluster thermal zoning method) was performed to investigate the impact of the building shape on building thermal zoning and heating/cooling loads.

The resultant thermal zoning layouts based on the grid/cluster (G/C) thermal zoning method showed:

(1) The thermal zoning layouts were influenced primarily by the existence of exterior windows, and to a lesser extent by the building shape;

(2) The cases that do not have any exterior windows showed very similar thermal zoning layouts with the traditional core-perimeter thermal zoning layout, which means those cases have only one single interior space as a thermal zone.

(3) If the cases have exterior window(s), the thermal zoning layout of the interior spaces may have one or more than one thermal zone, regardless of building shape and climate condition.

In addition, the results showed how much thermal load reduction was achieved when the G/C thermal zoning method was applied to each case compared to single-zone model as follow:

(4) All the cases showed thermal load reductions with the thermal zoning layout, which used the G/C thermal zoning method.

(5) When comparing the building shapes, rectangular-shape models has 3 to 6% more annual total thermal loads than the L-shape models.

6.2.2. Summary of Parametric Study of Thermal Zoning on WWR

A parametric study using 11 combinations of WWR and orientations was performed for two climate conditions (i.e., Houston and Chicago) to investigate the impact of the building WWR and the orientations of the exterior windows on the building thermal zoning and the annual/monthly heating/cooling loads.

To investigate the impacts of the WWR on the building thermal zoning layouts, three different WWRs (i.e., 0%, 50%, 80%) were applied to the simulation models. The results showed:

(1) When the WWR were set to 0%, which means there are no windows in the model, the thermal zoning layouts that were created are similar to the 5-Zone models (i.e., the traditional core-perimeter thermal zoning layouts).

(2) If the WWRs were increased to 50% or 80%, the interior thermal zone became separated into two different thermal zones.

(3) The shape and area of the interior thermal zones of the models with WWR of 50% and 80% were very similar each other, regardless of the climate conditions.

(4) For the perimeter thermal zones, most of the layouts consisted of four different perimeter thermal zones along with each orientation.

(5) For the thermal zoning layouts for heating season for the cold climate condition (i.e., Chicago), the G/C thermal zoning method yielded variations in the east-facing perimeter zones, which were different than the west-facing thermal zones.

To investigate the impacts of the orientation/position changes of the window on the building thermal zoning and its heating/cooling load, eight different cases for two climate conditions (i.e., Houston, TX, Chicago, IL) were used for the parametric study. The results showed:

(6) When the building has windows facing east or south, the G/C thermal zoning layouts were created differently than the 5-Zone models (i.e., the traditional core-perimeter thermal zoning method).

(7) In the G/C thermal zoning method thermal zones for both the perimeter and interior spaces were sensitive to the location of the windows, with the exception of when the building has windows facing north and west, there was little impact on the thermal zoning layouts. In these case, the G/C thermal zoning method resulted in similar thermal zoning layouts with the core-perimeter thermal zoning layouts.

(8) In general, the annual total and heating loads of the thermal zoning models for Chicago were higher than loads for Houston, as expected.

(9) For each climate condition, the models with the windows in north-south orientations had the highest annual total heating/cooling loads versus models with east-west windows.

(10) The models with windows only in north or west orientation had the lowest annual total heating/cooling loads.

(11) The annual thermal load reduction using the G/C thermal zoning method was about 3 to 6% versus the loads from a core-perimeter for a rectangular-shape building.

(12) For Houston, the highest annual thermal loads reduction (15%) was shown in Case 11, where the window orientation was for east-facing windows only.

The lowest annual thermal loads reduction (6%) was shown in Case 21, where the window orientation was north-south.

(13) For Chicago, the highest annual thermal loads reduction (30%) was shown in Case 10, Case 12, and Case 20, where the window orientations were west, east, and east-west only. In contrast, the lowest annual thermal loads reduction (10%) were shown in Case 16, Case 17, and Case 24, where the window orientations were west, north, and east-west only.

6.2.3. Summary of Parametric Study of Thermal Zoning for Varying Climate Conditions

The resultant thermal zoning layouts of 12 different simulation models with two different climate conditions (i.e., Hot and Humid, Cold and Humid) were examined and compared using the Grid/Cluster (G/C) thermal zoning method to investigate the impact of the climate conditions on the building thermal zoning in a simulation. In addition, the simulated total annual heating/cooling energy use for each case were compared and examined.

The resultant thermal zoning layouts based on the G/C thermal zoning method showed:

(1) The thermal zoning layouts tended to be less influenced by the climate conditions.

(2) The cases that do not have any exterior windows resulted in the same thermal zoning layouts as the core-perimeter thermal zoning for two different climate conditions.

(3) The cases that have asymmetric exterior windows also create very similar thermal zoning layouts for two different climate conditions.

The results showed how much thermal load reduction was achieved when the G/C thermal zoning method was applied to each case compared to a single-zone model as follow:

(4) For all the cases, total annual thermal energy use reductions for Chicago are larger than the ones that for Houston.

(5) Regardless of the climate condition, it was found that the heating energy use reductions were larger than the cooling energy use reductions, when the G/C thermal zoning method was applied.

6.3. Recommendations for Future Research

This study proposed and tested a new procedure for the automated thermal zoning of a building using building energy performance software. The new thermal zoning method proposed in this study was limited to the following:

- Single-story office building, slab-on-grade;
- Small size building (less than 5,000 ft^2);
- No attic space or plenum was used in the simulation model;
- No significant internal loads were used in the simulation model;

- Uniform interior temperatures in each grid unit;
- The size of a unit space was defined as 10 ft × 10 ft over the given space.
- The indoor temperature profiles were calculated only for a peak cooling and heating days under clear sky conditions;
- Interior walls were assumed to be "air wall" between the thermal zones;
- No HVAC system was used in the simulation (i.e., System "sum");
- This study was performed using the DOE-2.1e building energy simulation program.

The recommendations for future research include:

- Application of the new G/C thermal zoning method to the other types of commercial buildings such as schools, hotels, and industrial buildings;
- Application of the new G/C thermal zoning method to multi-story buildings to investigate the effect of heat transfer between floors;
- Analyzing the impact of the ground-coupling on the thermal zoning;
- Analyzing the impact of an attic space/plenum of the simulation model used for thermal zoning;
- Analyzing the impact of the significant internal loads in the simulation model on the G/C thermal zoning method;
- Investigation of the impact of non-uniform indoor temperature profiles in a space using CFD simulation;
- Investigation of the impact of varying the size of the grid unit on thermal zoning;

- Investigation of the impact of multi-zoning on thermal zoning;
- Investigation of the impact of ventilation on thermal zoning;
- Analyzing the new G/C thermal zoning method using the calculated indoor temperature profiles for the intermediate seasons (i.e., Spring and Fall);
- Analyzing the impact of more realistic interior walls between the thermal zones on the thermal zoning method;
- Analyzing the impact of the various HVAC systems on the thermal zoning.
- Validating the G/C thermal zoning method with experimental measurement from selected buildings.
- Confirming all the analysis results from this study with EnergyPlus with multi-zone nodal airflow.
- Research on the potential dynamic reallocation of thermostat/HVAC system paring based on winter and summer conditions using the G/C thermal zoning method.
- Application of the new G/C thermal zoning method in BIM to BEM simulation.
- Analyzing the actual thermal comfort in a building where the G/C thermal zoning method has been applied.
- Analyzing the thermal comfort of corner zones compared to the adjacent corner zones.

REFERENCES

ASHRAE. 2013. ASHRAE/IESNA Standard 90.1-2013, *Energy Standard for Buildings except Low-Rise Residential Buildings.* Atlanta, GA: ASHRAE.

Autodesk. 2013. *Vasari*, San Fransisco, CA: Autodesk Inc.

Bachman, L.R. 2003. *Integrated buildings : the systems basis of architecture*: John Wiley & Sons, Inc.

Baechler, M., J. Williamson, T. Gilbride, P. Cole, M. Hefty, and P. Love. 2010. *Guide to Determining Climate Regions by County* PNNL-17211, Richland, WA: Pacific Northwest National Laboratory.

Bazjanac, V. 2005. Model based cost and energy performance estimation during schematic design. *Proceedings of the 22nd Conference on Information Technology in Construction, Dresden, Germany*, 677-688.

Bleil De Souza, C., and S. Alsaadani. 2012. Thermal zoning in speculative office buildings: discussing the connections between space layout and inside temperature control. *Proceedings of the 1st Building Simulation and Optimization Conference, Loughborough, UK*, 417-424.

Bordass, B., A. Leaman, and P. Ruyssevelt. 2001. Assessing building performance in use 5: conclusions and implications. *Building Research and Information* 29(2):144-157.

Bovay, H.E. 1981. *Handbook of mechanical and electrical systems for buildings*: McGraw-Hill, Inc.

Catalina, T., J. Virgone, and V. Iordache. 2011. Study on the impact of the building form on the energy consumption. *Proceedings of the Proceedings of building simulation*.

CIBSE. 1998. Applications Manual AM11: Building Energy and Environmental Modelling, London, UK: The Chartered Institution of Building Services Engineers.

Clayton, M., J. Haberl, and W. Yan. 2012. *Development of a reference building information model (BIM) for Thermal Model Compliance Testing.* Atlanta, GA: Texas A&M University.

Coakley, D., P. Raftery, and M. Keane. 2014. A review of methods to match building energy simulation models to measured data. *Renewable and Sustainable Energy Reviews* 37:123-141.

COMNET. 2010. Commercial Buildings Energy Modeling Guidelines and Procedures, Commercial Energy Services Network.

Crawley, D., J.W. Hand, M. Kummert, and B.T. Griffith. 2008. Contrasting the capabilities of building energy performance simulation programs. *Building and Environment* 43(4):661-673.

Crawley, D., L.K. Lawrie, F.C. Winkelmann, W.F. Buhl, Y.J. Huang, C.O. Pedersen, R.K. Strand, R.J. Liesen, D.E. Fisher, M.J. Witte, and J. Glazer. 2001. EnergyPlus: creating a new-generation building energy simulation program. *Energy and Buildings* 33:319-331.

Davies, M.G. 2004. *Building Heat Transfer*, Hoboken, NJ: Wiley.

Deru, M., B. Liu, M. Yazdanian, J. Huang, and D. Crawley. 2011. *U.S. Department of Energy commercial reference building models of the national building stock.* Golden, CO: National Renewable Energy Laboratory.

DOE. 2012. *2011 Buildings Energy Data Book*, Washington, DC: United States Department of Energy.

DOE. 2015. EnergyPlus Example File Generator Help. Washington, DC: United States Department of Energy. Retrieved June 12, 2015, from http://apps1.eere.energy.gov/buildings/energyplus/file_generator_help.cfm

Dogan, T. 2015. Procedures for automated building energy model production for urban and early design. Massachusetts Institute of Technology.

Dogan, T., C. Reinhart, and P. Michalatos. 2014. Automated Multi-zone Building Energy Model Generation for Schematic Design and Urban Massing Studies. *Proceedings of the 2014 IBPSA eSim conference, Ottawa, Canada*.

Dogan, T., C. Reinhart, and P. Michalatos. 2015. Autozoner: an algorithm for automatic thermal zoning of buildings with unknown interior space definitions. *Journal of Building Performance Simulation*:1-14.

Eskin, N., and H. Türkmen. 2008. Analysis of annual heating and cooling energy requirements for office buildings in different climates in Turkey. *Energy & Buildings* 40:763-773.

Felkel, P., and S. Obdrzalek. 1998. Straight skeleton implementation. *Proceedings of the Proceedings of spring conference on computer graphics, Budmerice, Slovakia*, 210-218.

Gaasch, W., J. Travis, F. Zhao, M. Kaplan, and C. Muth. 2014. A Comparison of Methods for Early-Stage Retrofit Analyses. *2014 ACEEE Summer Study on Energy Efficiency in Buildings, Pacific Grove, CA*.

Gay, C.M., and C.D.V. Fawcett. 1935. *Mechanical and electrical equipment for buildings,* 1st ed.: John Wiley & Sons, Inc.

Georgescu, M. 2014. Analysis of systems in buildings using spectral Koopman operator methods. Doctoral Dissertation, Department of Mechanical Engineering, University of California, Santa Barbara.

Georgescu, M., B. Eisenhower, and I. Mezic. 2012. Creating zoning approximations to building energy models using the Koopman operator. *Proceedings of the IBPSA-USA SimBuild 2012, Madison: WI*, 40-47.

Georgescu, M., and I. Mezić. 2015. Building energy modeling: A systematic approach to zoning and model reduction using Koopman Mode Analysis. *Energy and Buildings* 86:794-802.

Goia, F. 2016. Search for the optimal window-to-wall ratio in office buildings in different European climates and the implications on total energy saving potential. *Solar Energy* 132:467-492.

Goia, F., M. Haase, and M. Perino. 2013. Optimizing the configuration of a façade module for office buildings by means of integrated thermal and lighting simulations in a total energy perspective. *Applied Energy* 108:515-527.

Goldberg, L. 1985. A comparative validation of the long term energy consumption predictions of five residential building energy simulation programs in a heating

climate. *Proceedings of the 1st International Building Simulation Conference, Seattle, WA*, 282-289.

Grondzik, W.T., and A.G. Kwok. 2014. *Mechanical and electrical equipment for buildings,* 12th ed., Hoboken, NJ: John Wiley & Sons, Inc.

Haberl, J., and S. Cho. 2004. *Literature Review of Uncertainty of Analysis Methods: DOE-2 Program.* ESL-TR-04-11-01, College Station, TX:

Heidell, J.A., and Z.T. Taylor. 1985. Comparison of empirically measured end-use metered data with DOE 2.1 simulations. *Proceedings of the 1st International Building Simulation Conference, Seattle, WA*, 290-295.

Heller, J., M. Heater, and M. Frankel. 2011. Sensitivity Analysis: Comparing the impact of design, operation, and tenant behavior on building energy performance. *Report of the New Building Institute*.

Hensen, J., and R. Lamberts. 2011. *Building performance simulation for design and operation. edited by Jan L.M. Hensen and Roberto Lamberts*: London ; New York : Spon Press, 2011.

Hetherington, R., R. Laney, and S. Peake. 2012. Zone modelling and visualisation: Keys to the design of low carbon buildings. *Proceedings of the 16th International Conference on Information Visualisation, Montpellier, France*, 495-503.

Hillier, F.S., and M.M. Connors. 1966. Quadratic assignment problem algorithms and the location of indivisible facilities. *Management Science* 13(1):42-57.

Hinchey, S.B. 1991. Influence of thermal zone assumptions on DOE-2 energy use estimations of a commercial building. Master's thesis, Department of Mechanical Engineering, Texas A&M University.

Hirsch, J.J. 2015. *eQUEST*, Version 3.65.Camarillo, CA: Lawrence Berkeley National Laboratory, James J. Hirsch and Associates.

Huang, J. 1993. *DrawBDL User's Guide*, Joe Huang and Associates.

IBPSA. 2012. Thermal Zoning Determination. IBPSA-USA. Retrieved June 12, 2015, from http://www.bembook.ibpsa.us/index.php?title=Thermal_Zoning_Determination

Jones, N.L., C.J. McCrone, B.J. Walter, K.B. Pratt, and D.P. Greenberg. 2013. Automated translation and thermal zoning of digital building models for energy analysis. *Proceedings of the 14th International Building Simulation Conference, Chambery, France*, 202-209.

Judkoff, R., and J. Neymark. 1995. A Procedure for Testing the Ability of Whole Building Energy Simulation Programs to Thermally Model the Building Fabric. *Journal of Solar Energy Engineering* 117:7-15.

Klein, S.A. 1976. *TRNSYS: A transient simulation program*, Madison, WI: Solar Energy Laboratory, University of Wisconsin-Madison.

Klein, S.A., W.A. Beckman, J.W. Mitchell, J.A. Duffie, N.A. Duffie, T.L. Freeman, J.C. Mitchell, J.E. Braun, B.L. Evans, and J.P. Kummer. 2004. *TRNSYS 16–A TRaNsient system simulation program, user manual*, Madison, WI: Solar Energy Laboratory, University of Wisconsin-Madison.

Klein, S.A., W.A. Beckman, J.W. Mitchell, J.A. Duffie, N.A. Duffie, T.L. Freeman, J.C. Mitchell, J.E. Braun, B.L. Evans, and J.P. Kummer. 2010. *TRNSYS 17-TRaNsient system simulation program, user manual*, Madison, WI: Solar Energy Laboratory, University of Wisconsin-Madison.

Kreider, J.F. 2001. *Handbook of heating, ventilation, and air conditioning*: CRC Press.

Kreider, J.F., T.A. Reddy, P. Curtiss, and A. Rabl. 2017. *Heating and cooling of buildings : principles and practice of energy efficient design. Third edition. T. Agami Reddy, Jan F. Kreider, Peter S. Curtiss, and Ari Rabl*: Boca Raton : Taylor & Francis, CRC Press, 2017.

LBNL. 1982. *DOE-2 Engineers Manual.* Berkeley, CA:

LBNL. 1984. *DOE-2 Reference Manual.* Berkeley, CA:

LBNL. 1993a. *DOE-2*, Version 2.1E.Berkeley, CA: Lawrence Berkeley National Laboratory.

LBNL. 1993b. *DOE-2 Supplement.* Berkeley, CA:

Lee, J.W., H.J. Jung, J.Y. Park, J.B. Lee, and Y. Yoon. 2013. Optimization of building window system in Asian regions by analyzing solar heat gain and daylighting elements. *Renewable Energy* 50:522-531.

Lin, H.W., and T.Z. Hong. 2013. On variations of space-heating energy use in office buildings. *Applied Energy* 111:515-528.

Lokmanhekim, M. 1971. Description of the program and details of the load program. *Proceedings of the USPS symposium: Computer program for analysis of energy utilization, Washinton, DC,* 29-79.

Maile, T., M. Fischer, and V. Bazjanac. 2007. Building energy performance simulation tools-a life-cycle and interoperable perspective. *Center for Integrated Facility Engineering (CIFE) Working Paper* 107:1-49.

McDowall, R. 2006. *Fundamentals of HVAC systems,* 1st ed. Chapter 5, Zone. London: Elsevier.

Medjdoub, B. 2000. Separating topology and geometry in space planning. *Computer aided design* 32(1):39-61.

Michalek, J., R. Choudhary, and P. Papalambros. 2002. Architectural layout design optimization. *Engineering optimization* 34(5):461-484.

Michalek, J., and P. Papalambros. 2002. Interactive design optimization of architectural layouts. *Engineering optimization* 34(5):485-501.

Moss, K. 2007. *Heat and mass transfer in buildings. 2nd ed. Keith Moss*: London ; New York : Taylor & Francis, 2007.

Mottahedi, M., A. Mohammadpour, S.S. Amiri, D. Riley, and S. Asadi. 2015. Multi-linear regression models to predict the annual energy consumption of an office building with different shapes. *Procedia Engineering* 118:622-629.

Musau, F., and K. Steemers. 2007. Space Planning and Energy Efficiency in Laboratory Buildings: The Role of Spatial, Activity and Temporal Diversity. *Architectural Science Review* 50(3):281-292.

Musau, F., and K. Steemers. 2008. Space Planning and Energy Efficiency in Office Buildings: The Role of Spatial and Temporal Diversity. *Architectural Science Review* 51(2):133-145.

Nguyen, A.-T., S. Reiter, and P. Rigo. 2014. Review: A review on simulation-based optimization methods applied to building performance analysis. *Applied Energy* 113:1043-1058.

O'Brien, W., A. Athienitis, and T. Kesik. 2011. Thermal zoning and interzonal airflow in the design and simulation of solar houses: a sensitivity analysis. *Journal of Building Performance Simulation* 4(3):239-256.

Ott, L., and M. Longnecker. 2010. *An introduction to statistical methods and data analysis*: Brooks/Cole Cengage Learning.

Ourghi, R., A. Al Anzi, and M. Krarti. 2007. A simplified analysis method to predict the impact of shape on annual energy use for office buildings. *Energy conversion and management* 48(1):300-305.

Pan, Y., Z. Huang, and G. Wu. 2007. Calibrated building energy simulation and its application in a high-rise commercial building in Shanghai. *Energy and Buildings* 39(6):651-657.

Perez-Lombard, L., J. Ortiz, and C. Pout. 2008. A review on buildings energy consumption information. *Energy and Buildings* 40(3):394-398.

Price. 2011. *Price Engineer's HVAC Handbook: A Comprehensive Guide to HVAC Fundamentals*: Price Industries Limited.

Raftery, P. 2011. Calibrated whole building energy simulation: An evidence-based methodology. Ph.D. dissertation, College of Engineering and Informatics, National University of Ireland.

Rodrigues, E., A.R. Gaspar, and Á . Gomes. 2013. An evolutionary strategy enhanced with a local search technique for the space allocation problem in architecture, Part 1: Methodology. *Computer-Aided Design* 45:887-897.

Samuels, R., J. Ballinger, S. Coldicutt, and T. Williamson. 1993. Thermal zoning in solar efficient design: user experiences and designer preconceptions. *Architectural Science Review* 36(4):151-156.

Shen, H., and A. Tzempelikos. 2012. Daylighting and energy analysis of private offices with automated interior roller shades. *Solar Energy* 86(2):681-704.

Shen, H., and A. Tzempelikos. 2013. Sensitivity analysis on daylighting and energy performance of perimeter offices with automated shading. *Building and Environment* 59:303-314.

Smith, L. 2012. Beyond the Shoebox: Thermal Zoning Approaches for Complex Building Shapes. *ASHRAE Transactions* 118(2):141-148.

Smith, L., K. Bernhardt, and M. Jezyk. 2011. Automated energy model creation for conceptual design. *Proceedings of the 2011 Symposium on Simulation for Architecture and Urban Design,* 13-20.

Tian, Z., and J.A. Love. 2009. Energy performance optimization of radiant slab cooling using building simulation and field measurements. *Energy and Buildings* 41(3):320-330.

USPS. 1971. *US Post Office energy analysis program*, Washington, DC: United States Postal Service.

Winkelmann, F. (2002). Underground surfaces: How to get a better underground surface heat transfer calculation in DOE-2.1E. *Building Energy Simulation User News, 23*.

Wuensch, K.L., K. Wuensch, and J. Evans. 1996. Straightforward Statistics for the Behavioral Sciences. *Journal of the American Statistical Association* 91(436):1750-1751.

Yang, L., J.C. Lam, and C.L. Tsang. 2008. Energy performance of building envelopes in different climate zones in China. *Applied Energy* 85:800-817.

Yi, H. 2015. User-driven automation for optimal thermal-zone layout during space programming phases. *Architectural Science Review*.

Zhu, D.D. 2013. A detailed loads comparison of three building energy modeling programs: EnergyPlus, DeST and DOE-2.1E. *Building Simulation* 6(3):323-335.